Next-generation adhesives: Combining free-radical and ring-opening metathesis polymerisation

Ellen Moscrop

A thesis submitted in partial fulfilment of the requirements for the degree

of Doctor of Philosophy

Declaration:

The work described in this thesis was undertaken at the University of Sheffield under the supervision of Prof. Patrick Fairclough and Dr Sebastian Spain between October 2018 and November 2023 and has not been submitted, either wholly or in part, for this or any other degree. All the work is original work of the author, except where acknowledged.

Signature:

Ellen Moscrop

Abstract

Methacrylate adhesives provide a strong bond between a varied range of substrates with no pre- or post-treatment required and rapid room temperature cures. Despite this, they suffer from a high degree of shrinkage as well as a low onset temperature of thermal degradation which limits their applications.

Norbornene-based polymers can be polymerised through ring-opening metathesis polymerisation (ROMP) to produce unsaturated, elastomeric polymers with high thermal stability. Norbornene monomers functionalised with methacrylate groups were synthesised and polymerised into macromonomers for poly(methacrylate) adhesives. It was found that even addition of 10 weight percentage (wt%) of a poly(norbornene) could significantly improve the thermal stabilities and reduce the shrinkage upon cure of the adhesives although this reduced the adhesive strength. More polar norbornene-methacrylate monomers were synthesised to increase the surface energy. Additionally, an adhesion promoter in the form of methacrylic acid was tested which resulted in a stronger adhesive.

Dicyclopentadiene (DCPD) is a monomer which can polymerise by ROMP through a norbornene group to form crosslinked polymers with high strength and thermal stabilities and has applications in composite materials. On its own, DCPD has a low surface energy which would make it a weak adhesive so more polar copolymers were added. The methacrylate functionalised norbornene monomer was polymerised through controlled radical polymerisation and introduced into the monomer DCPD before cure. Whilst the adhesive strength was improved, the degradation temperatures were reduced. These polymers had low solubility in DCPD and some phase separation was observed upon cure so smaller norbornene-based crosslinkers with polar ester linkages were synthesised. The aim of this work was tp understand if incorporation of these would reduce the temperature of post-cure of DCPD required to achieve a high glass transition temperature (T_g) thermoset, however only a small improvement was noted. Norbornene-based crosslinkers were found to significantly improve the adhesive strength of the DCPD structural adhesives.

Polynorbornene synthesised through ruthenium-based Grubbs initiators caused crosslinking through the methacrylate groups via a radical polymerisation reaction. To overcome this, the polymerisation was carried out using a photoinitiated metal-free ROMP alternative. The polymerisation was found to be light intensity dependent and scaling up in batch was challenging so a continuous ‘droplet-flow’ polymerisation method was developed, and high conversions were achieved in under 10 minutes residence time.

Acknowledgements

Firstly, the former Spain group members, you were the best! In particular, Anna, you were both a great lab friend and flatmate. To Josh and Sam, thank you for putting up with me complaining about polymers and making me laugh and enjoy our lab. I hope we stay in touch!

Seb, thanks for the great advice as well as making me hyperaware when bond angles are drawn wrong.

To Patrick, thank you for your help and support throughout my project.

To Steven and Dean at Scott Bader, thank you for your comments and encouragement. I always left our meetings feeling re-enthused. I also have to thank Tymon for sharing his vast knowledge of lap shear testing and answering all my many questions.

Also, thanks to everyone at Mimetics, (Paul, Alessandra, Jordan, Matt, David, and Ellie) for making me feel part of the team, laugh endlessly, and be inspired by chemistry again.

Thank you to Professor Tanja Junkers for inviting me to Monash University and the whole Polymer Reaction Design group for making my placement so enjoyable. My experience in Melbourne is something that I will never forget and our group trips to the Yarra Valley, Grampians national park and weekly pint at Pixel were definitely highlights.

Thank you to the Slark group for taking me in during the last 6 months. Even though you complained my monomers stunk out the lab, you made me feel like part of the group and I had a lot of fun!

The amazing people I have had the opportunity to live with the past few years, Ellie, Maeve, Chris and Nathan made my time in Sheffield enjoyable and gave me good escapism from the lab.

Eve, Beth and Victoria, your support has truly helped me get to this point and showing me retail therapy does work!

Thank you to my family for their support and for helping me move 8 times in 5 years; I don’t even want to think about the number of carloads of boxes there have been.

Table of Contents

Chapter 1 - Introduction 1

1.1 Adhesives 1

1.1.1 Reasons for using adhesives 1

1.1.2 Types of adhesives 2

1.1.3 Adhesive Testing 4

1.1.4 Adhesive Failures 7

1.1.5 Common structural adhesives 7

1.1.6 Methacrylates 9

1.1.7 Free Radical Polymerisation 10

1.1.8 Curing PMMA based adhesives 12

1.1.9 Shrinkage 13

1.1.10 Thermal degradation of PMMA 15

1.2 Ring-opening metathesis polymerisation 16

1.2.1 Background to olefin metathesis 16

1.2.2 ROMP initiators 18

1.2.3 Mechanism 21

1.3 Poly(dicyclopentadiene) 23

1.3.1 PDCPD in adhesives 25

1.3.2 Diels-Alder [2+4] cycloadditions to form monomers for ROMP 25

1.4 Conclusions 27

Chapter 2 - General Methods Experimental 29

2.1 Materials Used: 29

2.2 Instrumentation 29

2.3 Chapter 3 methods 31

2.3.1 Synthesis of 5-Norbornene-2-Methylene Methacrylate 31

2.3.2 Synthesis of 5-Norbornene-2-Carboxylic Acid (NBOOH) 32

2.3.3 Synthesis of 2-Hydroxypropanyl methacrylate, 5-norborn-2-yl ester (NBGMA) 33

2.3.4 Synthesis of poly(norbornene methylene methacrylate) 33

2.3.5 Synthesis of poly(2-Hydroxypropanyl methacrylate, 5-norborn-2-yl ester) (PNBGMA) 34

2.3.6 Synthesis of poly(norbornene methylene methacrylate-*co*-norbornene carboxylic acid) (P(NBMMA-*co*-NBOOH)) 35

2.3.7 Synthesis of M1X adhesives 35

2.3.8 Determination of gel fraction 36

2.3.9 PVC lap shear testing: 36

2.4 Chapter 4 methods 36

2.4.1 General AGET ATRP reaction 36

2.4.2 Synthesis of PNBMMA by AGET ATRP 37

2.4.3 Synthesis of PEHMA by AGET ATRP 37

2.4.4 Synthesis of P(NBMMA-*co*-EHMA) by AGET ATRP 38

2.4.5 Synthesis of PIBMA by AGET ATRP 39

2.4.6 Synthesis of P(NBMMA-*co*-IBMA) by AGET ATRP 39

2.4.7 Synthesis of 5-Norbornene-2,3-diicaboxylic acid 40

2.4.8 Synthesis of 5-Norbornene,2,3-(di-5-norbornene-2-methanyl) (CL1) 40

2.4.9 Synthesis of Ethylene Glycol Di-1-methyl-1-norbornene (CL2) 41

2.4.10 P2 Acid Etch 42

2.4.11 Curing PDCPD adhesives 42

2.5 Chapter 5 methods 43

2.5.1 Synthesis of 2,4,6-Tris(*para*-methoxyphenyl)pyrylium tetrafluoroborate[108] 43

2.5.2 General Batch Metal-Free Ring Opening Polymerisation (MF-ROMP) Procedure 43

2.5.3 MF-ROMP to synthesise PNB 44

2.5.4 MF-ROMP to synthesise P(NB-*co*-MMA) 44

2.5.5 MF-ROMP to synthesise P(NB-*co*-NBMMA) 45

Chapter 3 – Methacrylate-functionalised ROMP polymers as additives in PMMA adhesives 46

3.1 Introduction 46

3.1.1. Functionalised poly(norbornene) 46

3.1.2 Effect of anchor group on ROMP 48

3.1.3 Chapter Aims 50

3.2 Results and Discussion 51

3.2.1 Methacrylate functionalised norbornene 51

3.2.2 Polymerisation of poly(norbornene methylene methacrylate) 54

3.3.3 Radical reaction between Ru and MMA 58

3.3.4 Removing Ru from PNBMMA 60

3.3.5 Thermal degradation of P(MMA-*co*-NBMMA) 62

3.3.6 Shrinkage 66

3.3.7 Lap Shear Adhesive Testing 68

3.3.8 Effect of MMA on the shrinkage and thermal properties 73

3.3.9 Copolymerising NBMMA with NBOOH 74

3.3.10 Hydroxyl functionalised monomer 79

3.3.3 Conclusions 82

Chapter 4 - Norbornene crosslinkers for PDCPD adhesives 84

4.1 Introduction 84

4.1.1 ATRP 84

4.1.2 AGET ATRP 85

4.1.3 Introducing functional groups into DCPD 86

4.1.4 Chapter aim 89

4.2 Results and discussion 90

4.2.1 Radical polymerisation of A-PNBMMA 90

4.2.2 Effect of methacrylate polymer end group 91

4.2.3 P(DCPD-*co*-A-NBMMA) polymers 93

4.2.4 Synthesis of P(EHMA-*co*-NBMMA) and P(IBMA-*co*-NBMMA) copolymers 94

4.2.5 Curing PDCPD 98

4.2.6 Thermal Degradation Temperatures of the PDCPD Adhesives 100

4.2.7 Lap shear tests to determine the adhesive strength 103

4.2.8 Designing crosslinkers to improve adhesive properties of PDCPD 107

4.2.9 Effect of lap shear preparation 109

4.2.10 Tensile testing for PDCPD adhesives with norbornene crosslinkers 111

4.2.11 Thermal properties of PDCPD adhesives with norbornene crosslinkers 112

4.3 Conclusions 115

Chapter 5 - Combining radical and metal-free ring-opening metathesis polymerisation 117

5.1 Introduction 117

5.1.1 Metal-free ring-opening metathesis polymerisation 117

5.1.2 Incorporating functionality into MF-ROMP 119

5.1.3 Hybrid MF-ROMP 120

5.1.4 Flow polymerisation 122

5.1.5 Chapter Aims 125

5.2 Results and Discussion 125

5.2.1 MF-ROMP to synthesise poly(norbornene) 125

5.2.2 Effect of the photocatalyst and its *para*-substituents 126

5.2.3 Copolymerisation of NB with MMA 131

5.2.4 Copolymerisation of NB with NBMMA 140

5.2.5 Scaling-up MF-ROMP of PNB by droplet-flow polymerisation 145

5.2.6 Copolymerisation of norbornene and MMA by droplet-flow polymerisation 150

5.3 Conclusions 152

Chapter 6 - Future Work 154

7. References 156

8. Appendix 168

List of Figures, Schemes and Tables

Figure 1. 1: Diagrams of composites held together by mechanical fastenings (left) and chemical adhesives (right) 1

Figure 1. 2: Stress-Strain graph of thermoset, thermoplastic and PSA adhesives[2] 2

Figure 1. 3: Schematic of different adhesive tests where the dark blue shows the adhesive layer. (a) Lap shears, (b) T-peel tests, (c) Compressive shear and (d) Tensile tests 6

Figure 1. 4: Three common modes of adhesive failure 7

Figure 1. 5: Figure to show the increase in density during the cure 14

Figure 1. 6: Diagram to show random chain scission leading to 'unzipping' depolymerisation of PMMA 16

Figure 1. 7: Structures of the 1st, 2nd and 3rd generation Grubbs initiators respectively. 19

Table 1. 1: Comparisons of the properties of methacrylate and epoxy adhesives[17] 8

Scheme 1. 1: Step-growth polymerisation of epoxies and crosslinking through secondary amines and etherification from the hydroxyl group[23] 9

Scheme 1. 2: polymerisation of a methacrylate monomer to a poly(methacrylate) 10

Scheme 1. 3: Disproportionation termination mechanism in FRP 11

Scheme 1. 4: Combination FRP termination mechanism 11

Scheme 1. 5: Reaction scheme to show the redox reaction between BPO and a tertiary amine to generate a free-radical.[41] 13

Scheme 1. 6: Original proposed 'pairwise' metathesis mechanism 17

Scheme 1. 7: Chauvin [2+2] cycloaddition metathesis mechanism 17

Scheme 1. 8: Reaction to convert G1 to G2 20

Scheme 1. 9: Conversion of G2 to G3 20

Scheme 1. 10: Initiation, propagation, and termination mechanism of ROMP. 21

Scheme 1. 11: Mechanism of ROMP of norbornene 22

Scheme 1. 12: Reaction of the G3 catalyst with EVE to terminate the polymerisation. 22

Scheme 1. 13: Crosslinking of DCPD through ROMP and radical addition polymerisation 24

Scheme 1. 14: DA of cyclopentadiene to give the *endo* and *exo* DCPD isomers.**Error! Bookmark not defined.**

Scheme 1. 15: Reaction scheme to show how the stability of the diene leads to a different favoured isomer. 26

Figure 3. 1: Grubbs 3rd generation initiator (G3) chelating to the ester group on a functionalised norbornene[77, 110] 49

Figure 3. 2 Intermediate ruthenium-monomer complex showing steric hinderance and chelation effects. 50

Figure 3. 3: Diagram of the crosslinked P(MMA-*co*-NB) polymers where the red dots represent the crosslinks. 51

Figure 3. 4: ^{1}H NMR ($CDCl_3$) of NBMMA 53

Figure 3. 5: ^{1}H NMR spectrum of NBMMA and PNBMMA ($CDCl_3$, 400 Hz) 55

Figure 3. 6: SEC chromatograms of the PNBMMA synthesised using G1 and G3 showing a separated *exo* peak (left) and *endo* peak (right), (THF, PMMA standards) 56

Figure 3. 7: Figure to show G3 coordinating with the incoming monomer and steric hinderance causing a large difference in polymerisation rates. 57

Figure 3. 8: Photo to show that MMA monomer had polymerised due to residual Ru catalyst. 59

Figure 3. 9: Structure of Ru scavenger molecule SnatchCat® 61

Figure 3. 10: Graph to show the effect of the M_w of PNBMMA when 10 wt% is added to the MMA adhesives. 63

Figure 3. 11: The effect of increasing the PNBMMA concentration within a PMMA adhesive 65

Figure 3. 12: Graph to show the decrease in shrinkage as the proportion of PNBMMA in adhesive formulation increases. 68

Figure 3. 13: Diagram of PVC compressive lap shear in the jig with the force applied upwards onto the smaller PVC piece. 70

Figure 3. 14: The effect of the PNBMMA in the PMMA adhesives on the stress of the compressive lap shears 71

Figure 3. 15: Diagram of a lap shear showing plasticisation of the adhesive into the PVC and a photo of 10 wt% PNBMMA adhesive PVC compressive lap shear after testing. 72

Figure 3. 16: Graph to show the effect of increasing the viscosity on the adhesive strength of PVC compressive lap shears with 5 wt% MAA. 73

Figure 3. 17: ^{1}H NMR spectrum (MeOD) of P(NBMMA-*co*-NBOOH) in a 1:1 mol. ratio 76

Figure 3. 18: DSC thermogram of P(NBMMA-*co*-NBOOH) in a 1:1 mol. ratio showing one T_g 77

Figure 3. 19: PVC lap shear results of the 4:1 and 1:1 co-polymers in comparison with the PNBMMA homopolymers with and without the MAA adhesion promoter 78

Figure 3. 20: Photo of PVC compressive lap shear after testing with 1:1 P(NBMMA-*co*-NBOOH) 78

Figure 3. 21: PVC lap compressive lap shears with 10 wt% P(NBMMA-co-NBOOH) copolymers in PMMA 79

Figure 3. 22: ^{1}H NMR spectrum of PNBGMA in $CDCl_3$ and MeOD 81

Figure 3. 23: Comparison of 10 wt% of different functionalised polynorbornenes in PMMA adhesive 82

Table 3. 1: Table to show the M_n and $Đ_M$ of the different isomer peaks and overall isomer mixture... 56

Table 3. 2*: Residual Ruthenium levels determined by ICP-MS. * A – 1 precipitation, B – 2 precipitations, C – 2 precipitations then filtering through silica, 4 – 2 precipitations, 30 minutes with 4.4 eq. SnatchCat® then filtering through silica*. 62

Table 3. 3: The degradation temperatures of the 10 wt% PNBMMA adhesives 64

Table 3. 4: The degradation temperatures of PMMA adhesives containing PNBMMA 66

Table 3. 5: The density of the adhesives before and after curing and the shrinkage between the two. 67

Table 3. 6: Average displacement and force of the aluminium lap shears bonded with the PMMA-NBMMA adhesives. 69

Table 3. 7: Solid and liquid density of P(MMA-*co*-NBMMA) adhesives with 5 wt% MAA. [a]Calculated using diluted solutions in a density meter and extrapolating densities to 100 % adhesive [b]calculated by helium pycnometer. 74

Scheme 3. 1: ROMP to synthesise poly(caryophyllene) from caryophyllene.[117] 47

Scheme 3. 2: Esterification reaction scheme to synthesise NBMMA 52

Scheme 3. 3: Acidic esterification, transesterification and methacryloyl chloride esterification of NBOH to NBMMA 53

Scheme 3. 4: Polymerisation of NBMMA to PNBMMA 54

Scheme 3. 5: Reaction scheme for the synthesis of NBOOH 74

Scheme 3. 6: Copolymerisation of NBOOH and NBMMA 75

Scheme 3. 7: Reaction scheme to form NBGMA through Diels-Alder addition of CPD with acrylic acid and consequent ring opening esterification with GMA 80

Figure 4. 1: Norbornene derived crosslinkers for reducing the M_c of PDCPD[89] 87

Figure 4. 2: ^{1}H NMR spectrum of A-PNBMMA to show that there is a decrease the norbornene olefin resonances with respect to the $-C\mathbf{H}_2NB$ 91

Figure 4. 3: Thermal gravimetric analysis (TGA) analysis showing the effect of the PNBMMA end groups on the degradation temperatures. 92

Figure 4. 4: ^{1}H NMR spectrum to show the fraction of each monomer in the resultant P(EHMA-*co*-NBMMA) copolymer where x = *exo* and n = *endo*. 95

Figure 4. 5: DSC thermograph to show the single T_g resonance of P(EHMA-*co*-NBMMA) 96

Figure 4. 6: ^{1}H NMR spectrum of fraction of NBMMA and IBMA in the resultant copolymer P(IBMA-*co*-NBMMA) 97

Figure 4. 7: DSC thermogram showing the T_g of P(IBMA-*co*-NBMMA) 98

Figure 4. 8: Photos of PDCPD cured with [C]:[M] 1:2000 (top), 1:1000 (middle) and 1:500 (bottom) 99

Figure 4. 9: DSC thermographs to show the T_g of the PDCPD adhesives after a 150 °C post-cure.....100

Figure 4. 10: TGA of P(NBMMA-*co*-EHMA) with a ramp rate of 10 °C min^{-1} 101

Figure 4. 11: Graph to show the mass loss of the PDCPD adhesives containing methacrylate co- and homopolymers in comparison to PMMA as temperature increased. 102

Figure 4. 12: Aluminium lap shears of 10 wt% methacrylate polymers in DCPD. 104

Figure 4. 13: Aluminium lap shears with PDCPD based adhesive formulations containing 10 wt% methacrylate and 5 wt% MAA...105

Figure 4. 14: Bond strengths of PDCPD based adhesives with 25 wt% ENB and 5 wt% MAA 106

Figure 4. 15: Photo to show the cohesive failure during the lap shear test of P(DCPD-ENB-IBMA-NBMMA)...107

Figure 4. 18: Aluminium lap shear results of PDCPD adhesives with norbornene crosslinkers..........109

Figure 4. 19: The effect of the aluminium substrate preparation on the stress of PDCPD adhesives 110

Figure 4. 20: Photo of mould for tensile testing and a PDCPD dog bone containing 30 wt% CL2 after tensile testing 111

Figure 4. 21: Results of tensile testing of PDCPD and crosslinker based adhesives...........................112

Figure 4. 22: Thermal degradation of PDCPD with 10 wt% EGDNB..113

Figure 4. 23: DSC thermographs of PDCPD with and without 10 wt% of crosslinker with no post-cure (exotherm = up and endotherm = down)..115

Table 4. 1: The solubility of methacrylate homopolymers in DCPD with their M_w and $Đ_M$ ^{a}determined by SEC (THF) and their T_gs from literature ^{b}determined by DSC[145] 94

Table 4. 2: Degradation temperatures of PDCPD based adhesive formulations...............................102

Scheme 4. 1: Reaction scheme for traditional ATRP...85

Scheme 4. 2: Reaction scheme to show the mechanism of AGET ATRP...86

Scheme 4. 3 Scheme of the synthesis of PDCPD functionalised a) at C2 by Lemcoff and co-workers[136] and b) at C3 by Wulff and co-workers[135] 89

Scheme 4. 4: AGET ATRP synthesis of A-PNBMMA with the initiator EBiB...90

Scheme 4. 5: Reaction scheme to synthesise crosslinker 1 (CL1) – Dinorbornene methanyl norbornene dicarboxylate ... 107

Scheme 4. 6: Reaction scheme to synthesis crosslinker 2 (CL2) – Ethylene glycol dimethyl norbornene ... 108

Figure 5. 1: Structure of a pyrylium tetrafluoroborate photocatalyst ... 118

Figure 5. 2: Structures of bifunctional vinyl ether initiators synthesised by the Boydston group[159] .. 120

Figure 5. 3: High-resolution MS showing repeating units of the PNB-*co*-MMA copolymer carried out by the Boydston group[152] ... 122

Figure 5. 4: Diagrams to show the direction of flow and outcome on residence time distribution by SEC ... 124

Figure 5. 5: Photo of batch MF-ROMP set-up ... 126

Figure 5. 6: ^{1}H NMR spectroscopy to show the conversion of norbornene to poly(norbornene) ... 127

Figure 5. 7: Graph to show the effect of *p*OMeTPT concentration on the conversion of NB to PNB determined by ^{1}H NMR spectroscopy ... 128

Figure 5. 8: Structure of TPT photocatalyst ... 129

Figure 5. 9: Graph to show the effect of TPT concentration on the conversion of norbornene to PNB ... 130

Figure 5. 10: Graph to show the absorption of wavelengths by *p*OMeTPT (blue --) and TPT (green ···) ... 130

Figure 5. 11: Graph to show the effect of increasing the fraction of MMA and of changing from dry air to an inert N_2 atmosphere. ... 132

Figure 5. 12: ^{1}H NMR spectrum ($CDCl_3$) to show the conversion of norbornene and MMA to poly(norbornene-*co*-methyl methacrylate) ... 133

Figure 5. 13: Photos to show the colour of the NB: MMA (1:1 mol. ratio) reaction mixture at the end of the reaction after being degassed in O_2, N_2 and a mixture. ... 134

Figure 5. 14: Conversion of NB and MMA to P(NB-*co*-MMA) and first-order semi-log plot. ... 135

Figure 5. 15: DSC of P(NB-*co*-MMA) (2.4 wt % MMA) 135

Figure 5. 16: Graph to show the effect on T_g and M_w as the fraction of MMA in the copolymer increases 136

Figure 5. 17: Graphs to show the conversion of total monomer, b) NB and c) MMA over time. The solid lines represent the light being switched on and the grey dotted lines when the light is switched off. 137

Figure 5. 18: Photo to show the LED set-up connected to an Arduino programmed to control the voltage. 138

Figure 5. 19: A) Graph to show the effect of light intensity on the conversion of NB and MMA (determined by ^{1}H NMR spectroscopy) and B) The dispersity and M_w (determined by SEC (THF)) ...139

Figure 5. 20: ^{1}H NMR spectrum to show the overlapping resonances from the P(NB-*co*-NBMMA) copolymer. 141

Figure 5. 21: ^{1}H NMR spectrum of P(NB-*co*-NBMMA) 142

Figure 5. 22: Effect of fraction of NBMMA in monomer feed to show the total norbornene conversion 142

Figure 5. 23: Molar mass distributions of P(NB-*co*-NBMMA) with increasing retention times with increasing NBMMA fraction in the monomer feed 143

Figure 5. 24: Conversion of NB and NBMMA to polymer during MF-ROMP measured by GC 145

Figure 5. 25: Droplet-flow reactor set-up 146

Figure 5. 26: Photo of reaction set-up of reactor and ball-mixer 147

Figure 5. 27: The effect of residence time on % conversion and M_w (left) and a photo to show the flow reactor at a residence time of 24 minutes (right) 148

Figure 5. 28: Diagrams to show how the fluorescence of the pOMeTPT photocatalyst shortens as the light intensity increases. 149

Figure 5. 29: Effect of light intensity on NB conversion during droplet flow polymerisation 150

Figure 5. 30: Graph to show the effect of norbornene and MMA conversion on the fraction of MMA in the monomer mixture. 151

Figure 5. 31: Graph to show the effect of increasing the Target DP on the • monomer conversion (determined by ^{1}H NMR spectroscopy) and ■ M_w (determined by SEC (THF)) 152

Figure 5. 32: Photos to show the colour of the reaction mixture at the end of the flow polymerisation with increasing target DPs 152

Table 5. 1: The effect of the ratio of norbornene (NB) and NBMMA in the monomer feed (^{a}- determined by SEC (THF) and ^{b}- determined by DSC) 144

Scheme 5. 1: Proposed mechanism for MF-ROMP of Norbornene 118

Scheme 5. 2: Mechanism for the hybrid MF-ROMP of norbornene and MMA. 121

Scheme 5. 3: Reaction scheme for the ROMP of 3-methoxycyclopent-2-ene and norbornene[161] 122

Scheme 5. 4: MF-ROMP of norbornene to PNB 125

Scheme 5. 5: Reaction scheme of the synthesis of pOMeTPT[108, 172] 127

Scheme 5. 6: Hybrid MF-ROMP of norbornene and methyl methacrylate 131

Scheme 5. 7: Reaction scheme for the MF-ROMP to form p(NB-*co*-NBMMA) 140

Abbreviations

AGET ATRP = activators generated by electron transfer atom-transfer radical polymerisation

AIBN = azobisisobutyronitrile

AROMP = alternating ring opening metathesis polymerisation

ATRP = atom-transfer radical polymerisation

BPO = dibenzoyl peroxide

CPD = cyclopentadiene

Đ = dispersity

DA = Diels-Alder

DCC = dicyclohexylcarbodiimide

DCPD = dicyclopentadiene

DCU = dicyclohexylurea

DEPT = distortionless enhancement by polarisation transfer

DMAP = 4-dimethylaminopyridine

DP = degree of polymerisation

DSC = differential scanning calorimetry

EGDMA = ethylene glycol dimethacrylate

EHMA = 2-ethylhexyl methacrylate

ENB = 5-ethylidene-2-norbornene

EPE = ethyl propenyl ether

EVE = ethyl vinyl ether

FRP = free radical polymerisation

G1 = Grubbs 1st generation catalyst

G3 = Grubbs 3rd generation catalyst

GMA = glycidyl methacrylate

NB = norbornene

NBCA = 5-norbornene-2-carboxylic acid

NBDCA = 5-norbornene-2-dicarboxylic acid

NBGMA = 2-Hydroxypropanyl methacrylate, 5-norborn-2-yl ester

NBMMA = 5-norbornene-2-methylene methacrylate

NBOH = 5-norbornene-2-methanol

NMR = nuclear magnetic resonance

MF-ROMP = metal free ring-opening metathesis polymerisation

MMA = methyl methacrylate

MS = mass spectrometry

$\boldsymbol{M}_w$ = weight average molecular weight

PTFE = polytetrafluoroethylene

p**MeOTPT** = 2,4,6-*Tris*(*para*-methoxyphenyl)pyrylium tetrafluoroborate

PVC = poly(vinyl chloride)

IBMA = isobornyl methacrylate

ICP = induction coupled plasma

IR = infrared spectroscopy

RIM = reaction injection moulding

ROP = ring-opening polymerisation

ROMP = ring-opening metathesis polymerisation

SEC = size exclusion chromatography

TMA = 4,*N,N*-trimethylaniline

Chapter 1- Introduction

1.1 Adhesives

1.1.1 Reasons for using adhesives

An adhesive is a substance which can hold two surfaces together through chemical bonds and interactions; these can be either reactive or non-reactive. Adhesives are a popular choice over traditional mechanical fastening alternatives which include nuts, bolts, and rivets (Figure 1. 1). Mechanical fastenings have many advantages such as the ability to be visually inspected and replaced without dismantling large components. Despite this, they have flaws such as adding weight to a material, susceptibility to corrosion and weakening of the substrate whilst drilling holes to fit the fastener. This is especially significant for anisotropic composites where forces are distributed along particular axes.[1] Adhesives are lightweight and can be used to bond together dissimilar materials, including steel and organic polymers. The adhesive layer can be distributed evenly across the adherend meaning that stresses are not localised and allowing the bond to maintain flexibility.[1]

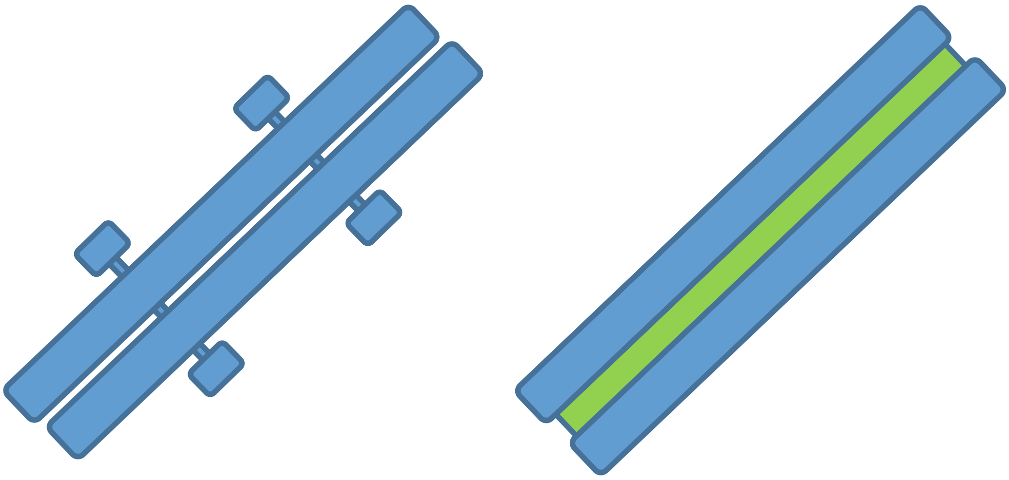

Figure 1. 1: Diagrams of composites held together by mechanical fastenings (left) and chemical adhesives (right)

1.1.2 Types of adhesives

There are three main categories of adhesives: thermoset, thermoplastic and pressure sensitive adhesives (PSA). The gradient of the curves in the stress-strain graph (Figure 1. 2) represents the Young's modulus which is a measure of the stiffness of the polymer. The toughness of the material can be found by integration of the stress-strain curve, this is the amount of energy that can be absorbed before the material breaks.

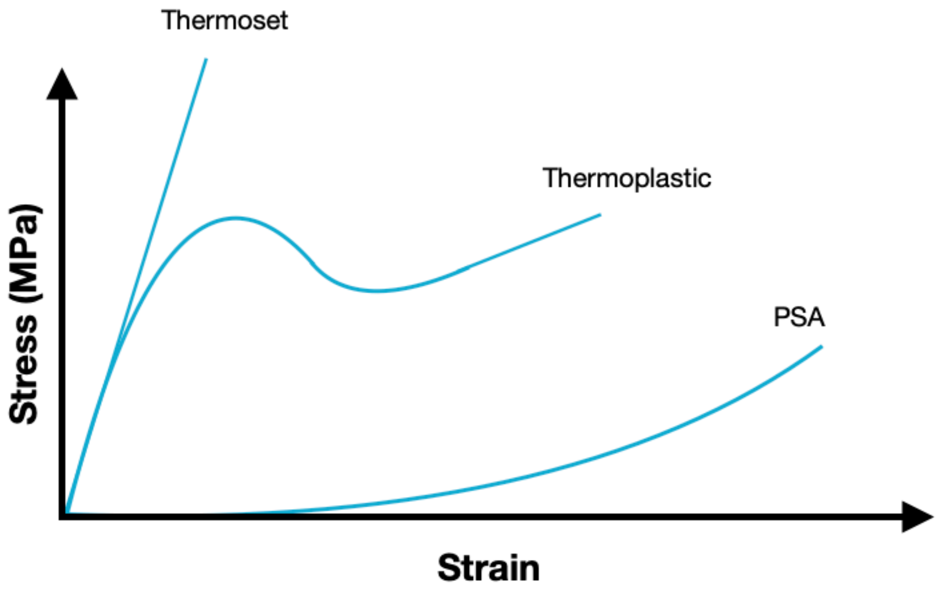

Figure 1. 2: Stress-Strain graph of thermoset, thermoplastic and PSA adhesives[2]

PSAs are non-reactive adhesives which bind to their adherends without undergoing any chemical reactions.[1] Their adhesive ability is due to strong non-covalent van der Waal's and dipole-dipole interactions. When shear is applied, they have low viscosity, allowing them to flow into crevices in the substrate surface and cover a large surface area. When the shear is withdrawn the viscosity increases and the PSA is able to withhold the stress applied.[3] Since no cure is involved, PSAs can form instant adhesion.[4, 5] They are highly elastomeric so can achieve high strain with very little stress however, do break at the lowest levels of stress in comparison to thermosetting and thermoplastic adhesives

(Figure 1. 2).[2] Despite being known as 'pressure-sensitive' there is very little correlation between the amount of pressure applied and the bond strength.[6]

Thermoplastic adhesives also do not undergo a chemical reaction during the cure. They are typically applied as a 'hot melt' in liquid form and harden as they cool to form a solid that adheres to the substrate. They are not crosslinked so have a melting point and can be removed to leave the substrate in the original condition. A limitation is that these adhesives cannot be used for high temperature applications as they lose their mechanical properties. Additionally, the melting temperature (T_m) of the substrate must be higher than the adhesive.[7] As the stress applied to a thermoplastic adhesive is increased, it initially undergoes elastic deformation where the stress is instantaneous, and the polymer is able to return to its original shape as soon as the stress is removed. Above the 'maximum yield strength' the polymer undergoes viscous deformation which is irreversible and lasts until the 'maximum tensile strength' is reached, at which point the polymer breaks (Figure 1. 2).[2]

Thermosetting adhesives undergo an irreversible chemical reaction during their cure from a liquid to a solid.[8] They contain bifunctional (or multifunctional) monomers, which form crosslinks within the material giving them improved strength, chemical resistance and mechanical properties over thermoplastics. This makes them suitable for applications within aerospace, electronics, and construction.[8] The greater the degree of crosslinks the higher the Young's modulus, making the polymers more brittle (Figure 1. 2). The problem with thermosetting polymers is that they are typically non-degradable which renders any composites that they adhere unrecyclable, although alternative methods to reuse these materials such as shredding are possible.[9, 10]

1.1.3 Adhesive Applications

PSAs are used in a wide range of applications where it is desirable to hold two substrates together whilst being able to easily separate on demand.[11] These include resealable food packaging and labels, bandages and electronics.[12, 13]

Thermoplastics are used in applications where a greater strength is required. When using thermally resistant substrates these can be applied in the form of a hot-melt or within a solvent such as ethyl acetate or water. These can be found within cars to adhere textiles, sealed food packaging and electronics. Examples of common thermoplastic adhesives are cyanoacrylates and poly(vinyl acetates).

Thermosetting adhesives are used when a high tensile strength is required or when the bond needs to be able to withstand high temperatures. A common application is in airplane wings where a structural adhesive is used to adhere the wing 'skin' which is the outer layer. This area of a plane is prone to 'buckling' due to the air resistance. A lightweight adhesive covering the entire bonded area is advantageous to rivets which only join the materials in specific spots, leaving unbonded regions between.[14] Similarly, for anisotropic composite materials containing glass or carbon fibres, when mechanical fastenings are used the directional structure gets disrupted and this leads to weaknesses where breakage is more likely to occur under impact or stress.[15]

1.1.4 Adhesive Testing

There are many industry standard tests used to measure the strength of a chemical adhesive, with many being a variation on the four shown in Figure 1. 3. Single lap shear joints (Figure 1. 3 a), are made from two adherends overlapping with a set area. To test the strength of the joints, the ends are clamped into a tensometer and force applied in opposite directions, pulling the adhesive layer until it breaks. Typically, lap shears are prepared in a jig so that the overlap is consistent between samples and glass beads can be added to ensure an even bond thickness.[5, 16, 17] A peel test measures the strength of the adhesive-adherend interface where two substrates are adhered together with an upwards force applied at 90 ° (Figure 1. 3 b).[18] The adhesive either peels away from the substrate or forms a crack which propagates from the tip through the adhesive layer.[19] In compressive lap shears the force is applied directly onto the lap shear until the adhesive breaks (Figure 1. 3).[20] The tensile strength of adhesives are found by moulding the adhesive into a 'dog-bone' shape. The tensometer is clamped to the wider ends and a force is applied, stretching the adhesive until it reaches a maximum elongation where it breaks.[21]

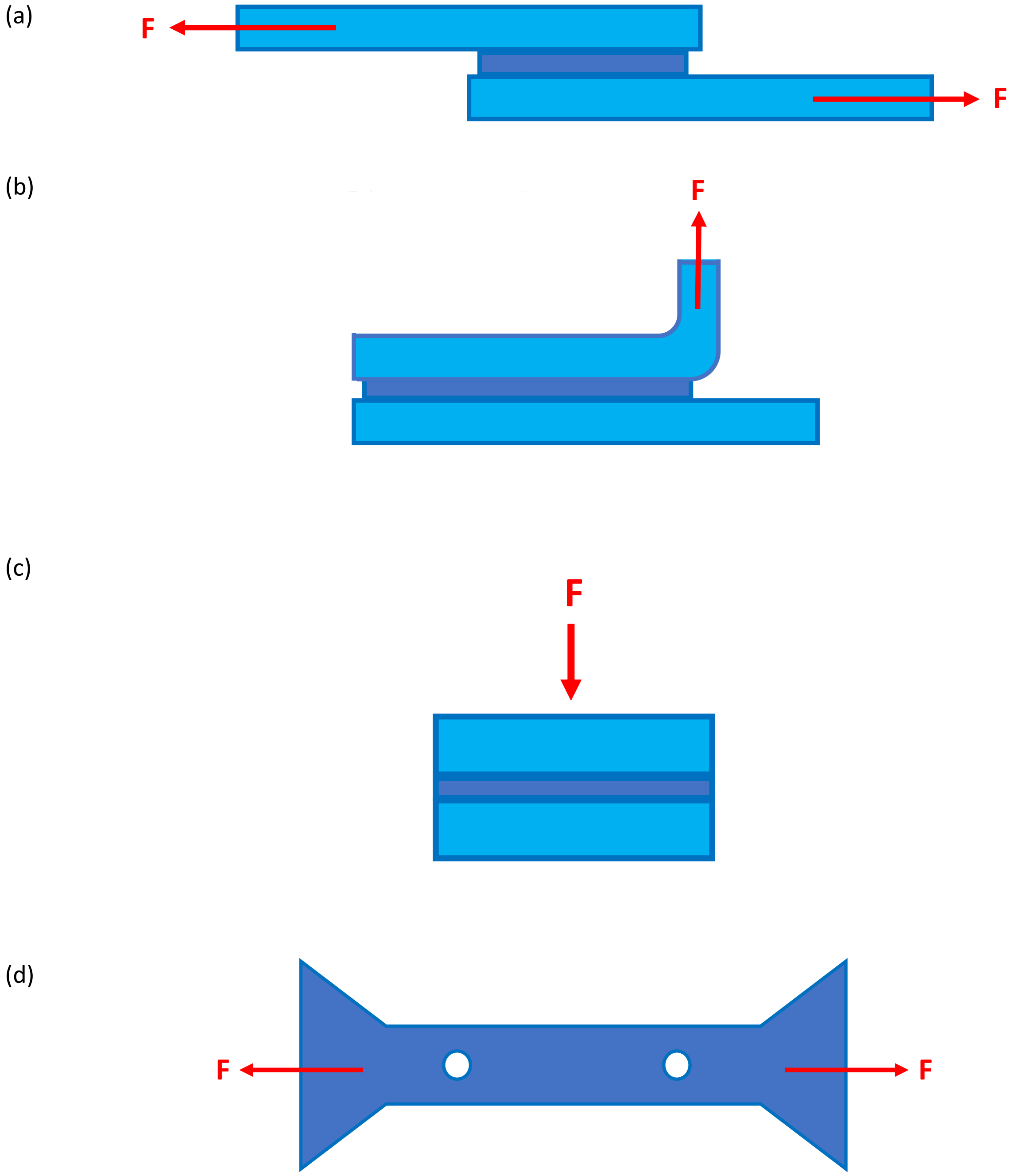

Figure 1. 3: Schematic of different adhesive tests where the dark blue shows the adhesive layer. (a) Lap shears, (b) T-peel tests, (c) Compressive shear and (d) Tensile tests

1.1.5 Adhesive Failures

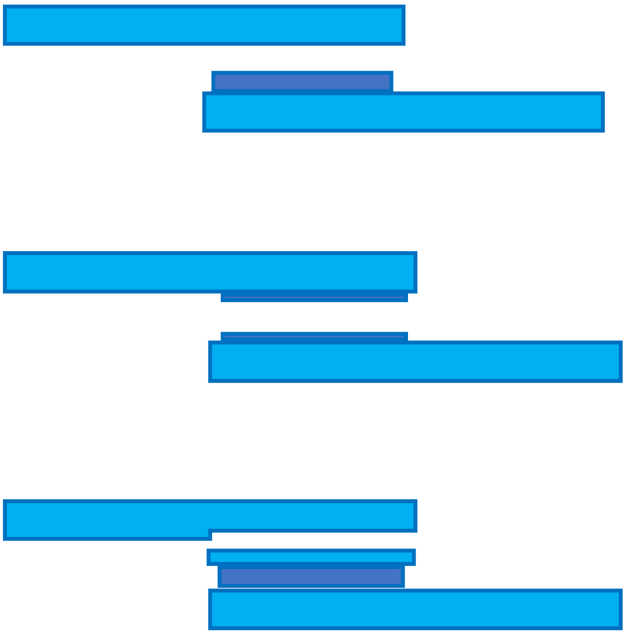

Adhesive Failure
Adhesive failure is where the adhesive peels from one of the substrates due to a weak adhesive-substrate bond.

Cohesive Failure
Cohesive failure is where there is a fracture within the adhesive layer that propagates through, leaving adhesive on both substrate surfaces.

Substrate Failure
When the adhesive layer is stronger than the material being held together, in this case, the substrate either cracks or becomes disfigured.

Figure 1. 4: Three common modes of adhesive failure

1.1.6 Common structural adhesives

Two of the most common structural adhesives used are methacrylates and epoxies. These have very different properties and are chosen depending on the desired requirements for the application (Table 1. 1).

Table 1. 1: Comparisons of the properties of methacrylate and epoxy adhesives[22]

	Methacrylates	**Epoxies**
Speed of cure	Fast (10-60 minutes)	Slow (minutes to hours for sufficient cure and days for full cure)
Cure Temperature	RT	RT (and a post cure heat for optimal performance)
Temperature resistance	Low (100-120°C depending on cure)[23]	High (up to 200 °C depending on cure)[24]
Shrinkage	High (~20% v/v)	Low (~6% v/v)[25]
Pre-treatment needed	No[22]	Sometimes
Compatible with composites	V. Good	Good
Compatible with polymers	V. Good	Poor
Compatible with metal	Good	V. Good (pre-treatment)

Epoxy monomers contain two or more functional groups and are cured by a ring-opening reaction with an equivalent moles of 'hardener'. These are typically bifunctional amines, although diols can also be used.[26] Commonly, aromatic epoxies are used in adhesives since they have upper service temperatures of around 200 °C, whilst aliphatic epoxies only have upper service temperatures of around 100 °C.[27] Bisphenol A diglycidyl ether (DGEBA) is the most common epoxy used in adhesives.[1]

Epoxies are able to polymerise through either step-growth or chain growth polymerisation.[28] Shrinkage during this process is negligible due to the opening of the epoxy ring. Epoxies are able to form highly crosslinked networks by reacting through hydroxyl and secondary amine groups that form during the polymerisation (Scheme 1. 1). At low conversion the adhesive has a low viscosity so that the propagating polymer chains can flow easily, however, at higher conversion the movement becomes restricted so there are a lot of unreacted chain ends. Increasing the temperature increases the flexibility of the polymer and gives the tangled chains more mobility to react. Typically, whilst curing epoxies, the temperature is increased gradually to prevent the loss of volatile monomers, oligomers, and initiators. This has an effect of increasing the performance of the adhesive.[29] Additionally, when exposed to higher temperatures further crosslinking such as etherification and dehydration can occur between the -OH groups.[30, 31]

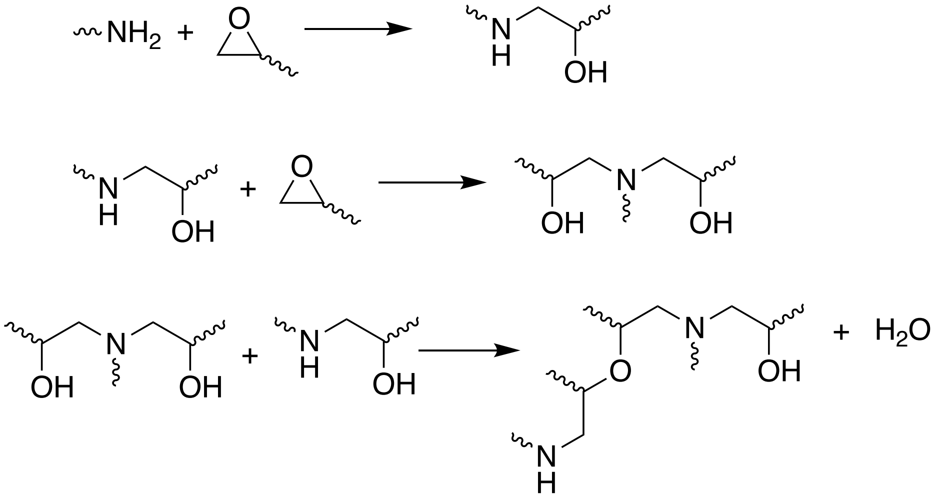

Scheme 1. 1: Step-growth polymerisation of epoxies and crosslinking through secondary amines and etherification from the hydroxyl group[31]

Epoxies have very poor adhesion with composites and polymers since there are no reactive groups at the surface. Metals such as aluminium make better adherends however, pre-treatment is required to increase adhesion by depositing an clean oxide layer to the surface of aluminium substrates.[32]

1.1.7 Methacrylates

Poly(methyl methacrylate) (PMMA) is optically transparent with high impact strength and low density. It is used for an array of applications such as within medicines, dentistry and as a shatter-resistant alternative to glass. The ester linkages within the methacrylate monomer give the polymer high polarity, making it a good adhesive with high surface wetting to polar substates. In methacrylate adhesives, the adhesive itself acts as a solvent which makes it more tolerant to surface contaminants than epoxies.[22] PMMA is regularly cross-linked with di-functional methacrylate monomers, e.g. ethylene glycol dimethacrylate (EGDMA) in order to increase the T_g and improve mechanical properties.[33] The conversion of bifunctional monomer reaches a critical point where they become a 'gel' and are infinitely three-dimensional so no longer soluble.[34]

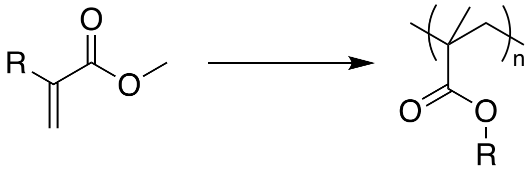

Scheme 1. 2: polymerisation of a methacrylate monomer to a poly(methacrylate)

1.1.8 Free Radical Polymerisation

Methacrylate monomers can be polymerised through free radical polymerisation (FRP). This is a technique where monomers containing an unsaturated carbon-to-carbon bond are converted to a polymer with a saturated carbon backbone through addition of radicals. Initiation begins with generation of a radical by homolysis of the initiator. These typically contain either a peroxide (R-O-O-R) or azo (R-N=N-R) group which is broken by an applied stimulus such as light, heat or through a redox reaction. The free radical is then able to attack the π-bond on the monomer, causing it to break by homolytic fission.[35]

Propagation continues on a millisecond scale with the radical on the terminal carbon of the growing chain attacking a π-bond from a monomer. The addition typically occurs with head-to-tail addition where the R groups are evenly spaced with a -CH_2 between each unit, however head-to-head addition can also occur and causes weak points within the backbone.[36]

The two most common methods of termination are disproportionation and combination. Disproportionation is where the radical on the terminal carbon of a propagating chain abstracts a hydrogen from another propagating chain (Scheme 1. 3). The chain which has lost a hydrogen then has two free radicals which join to form a new π-bond so that both chains have been terminated with one having an unsaturated end group and one having a saturated end group.[36, 37]

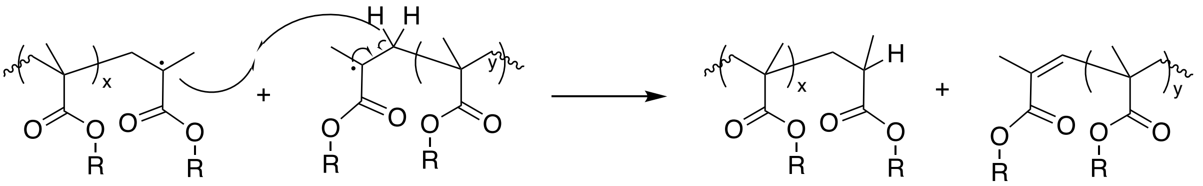

Scheme 1. 3: Disproportionation termination mechanism in FRP

The second common termination mechanism is combination. This is where the free radicals on two terminal carbons on propagating chains react with each other rather than an unsaturated monomer end group (Scheme 1. 4). For methacrylates, the most common termination mechanism is disproportionation whereas for acrylates and vinyl monomers combination can be more favoured.[38]

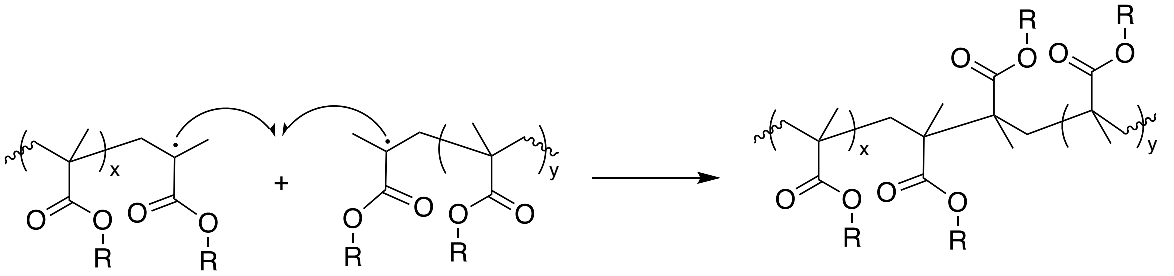

Scheme 1. 4: Combination FRP termination mechanism

During the bulk polymerisation of a methacrylate, the initial propagation stage occurs at a relatively steady rate before undergoing a short period of rapid auto-acceleration known as the Trommsdorff effect. Initially, the viscosity is very low, so it is easy for propagating chains to diffuse through the monomer.[39] During this time the rate of termination from combination of radicals is almost at an equal rate to initiation. Above a critical concentration of polymer, the propagating chains become so entangled that their movement is restricted. This leads to an inefficient heat transfer from the exothermic reaction which increases the rate of diffusion of the relatively small monomer molecules and the rate of polymerisation accelerates and continues until there is no more monomer available.[36, 40-43] The rate of termination by combination is also restricted. Factors such as temperature, solvents and initiator choice and concentration affect the onset of the Trommsdorff effect.[44] In adhesives this dictates the 'working time' of the adhesive since at high viscosities the polymer is not able to flow into crevices into the substrate and has reduced surface wetting leading to a weaker bond.

Controlled radical polymerisations such as reversible addition-fragmentation chain-transfer (RAFT), atom transfer radical polymerisation (ATRP) and nitroxide mediated polymerisation (NMP) have been developed. These are living polymerisation techniques since they protect the radical by keeping it in a state of equilibrium and limiting the opportunities for termination.[45-47]

1.1.9 Curing PMMA based adhesives

PMMA adhesives are cured in bulk by radical polymerisation using the monomer as the solvent and are available in one-part or two-part formulations. In one-part adhesive formulations, the initiator and monomers are stored together. There are usually a small number of radical inhibitors present to prevent any premature polymerisations. To cure the adhesive a stimulus is usually applied such as heat or UV light. The problem with thermally initiated systems is that it is often difficult to evenly heat the surface of a substrate to initiate the polymerisation without damaging the surface. UV or blue light curing adhesives are commonly used in dental applications with recent research into the development of less toxic, amine-free initiators.[48]

Two-part adhesive formulations commonly use redox initiation systems. This is where half of the monomer mixture and an initiator are stored separately from the other half of the monomer mixture and an activator. There is a mixing tube attached to the applicator where the two-parts can be combined, beginning the initiation process.

One of the most common redox initiation systems is between dibenzoyl peroxide (BPO) and a tertiary amine. These two components are typically kept in a stoichiometric ratio. During the redox initiation, the lone pair on the nitrogen of the amine can attack one of oxygens in the peroxide bond, causing the bond to break and abstract a proton from the amine (Scheme 1. 5). The resulting products include a benzoyloxy radical, a *N*-methylene radical and benzoic acid. Both radicals are able to initiate polymerisation.[36, 49]

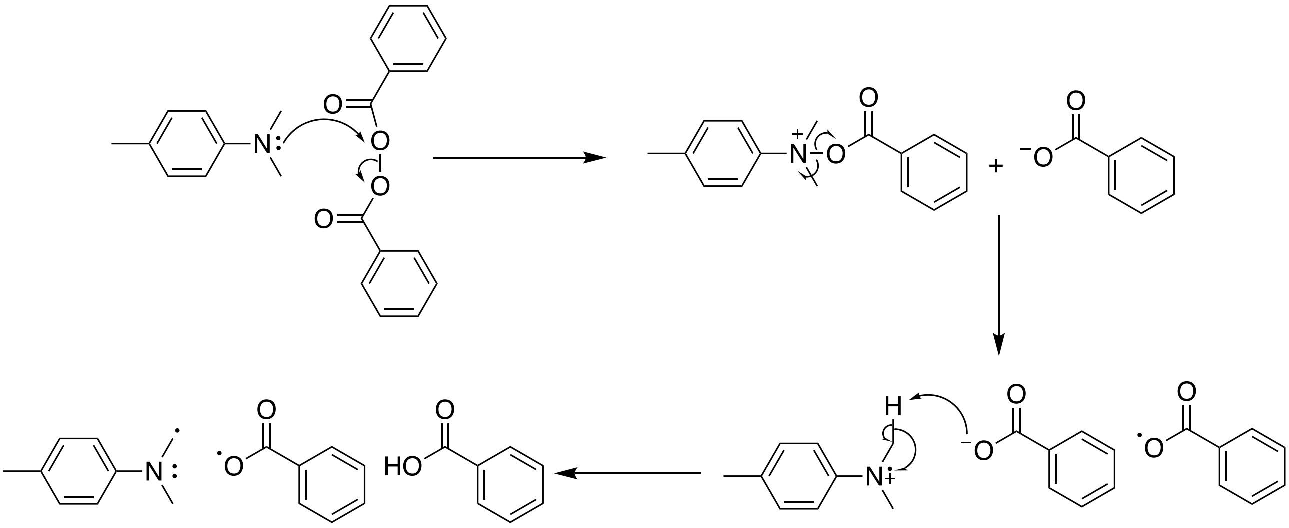

Scheme 1. 5: Reaction scheme to show the redox reaction between BPO and a tertiary amine to generate a free-radical.[50]

1.1.10 Shrinkage

Shrinkage of adhesives is due to the reduction of volume of a material during cure as the longer van der Waals, hydrogen bonding and dipole interactions move closer together to form shorter covalent bonds (Figure 1. 5). Methacrylates have been found to have a volume shrinkage of up to 20 volume % (v/v %).[51]

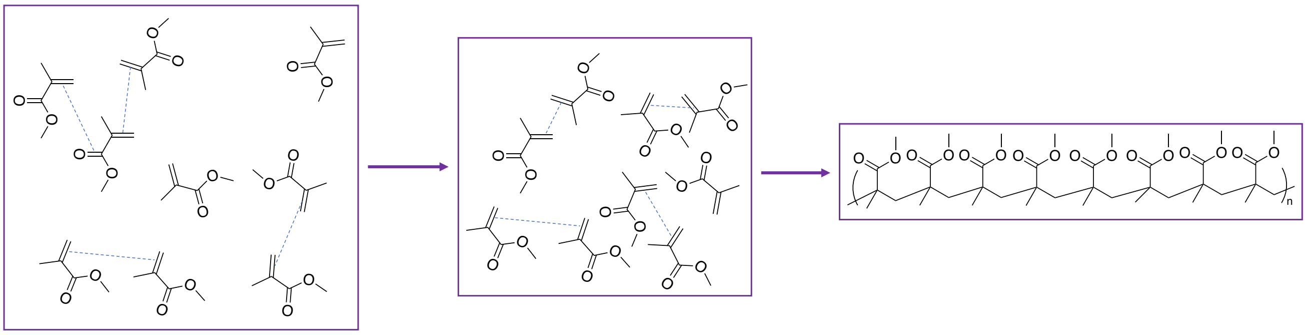

Figure 1. 5: Figure to show the increase in density during the cure

The problem with shrinkage is that it can lead to areas of localised stress and weaken the bond between the adhesive layer and the adherend and can lead to voids within the adhesive layer. The shrinkage of a material can be decreased by reducing the density difference between the liquid and the solid material. Using a methacrylate with a larger side chain increases the volume of the monomer and therefore decreases the % shrinkage.[51] A common method is to start with partially polymerised material as the larger the macromonomer, the fewer covalent bonds would need to form.[52] This is especially true for methacrylate monomers where there is no ring-opening to balance out the shrinkage.

It has been shown that the rate of cure has an effect on the shrinkage stress of methacrylate adhesives. Stansbury and co-workers used thiol a chain-transfer agent (CTA), to delay the onset of gelation of the methacrylates so that the adhesive could flow over the substrate for longer. This showed reduced stress however for a commercial product an odourless, less harmful alternative would need to be discovered.[53] Y. Kinomoto *et al*. found that having an increased porosity in the substrate reduced the stress of the cured adhesive due to the presence of oxygen during the polymerisation which inhibited the reaction, reducing the rate of cure.[54]

1.1.11 Thermal degradation of PMMA

The degradation mechanism of poly(methyl methacrylate) (PMMA) has been extensively studied and it is known that it proceeds through an ‘unzipping’ process, resulting in the regeneration of monomer (Figure 1. 6). This process can begin between 180-230 °C, as the unsaturated chain ends begin to undergo radical depropagation accounting for around 10-20 % of weight loss.[55, 56] The next step, around 300 °C is where random chain scission occurs, generating radicals that can depropagate down the chain, accounting for 80-90 % of weight loss.[55, 57, 58]

Kashiwagi *et al.* were able to prove that the lower temperature degradation step comes from the weaker ‘head-to-head’ linkages formed from recombination and the unsaturated chain ends.[59] This was shown by TGA, where PMMA synthesised through radical combination was found to have much lower thermal degradation temperatures than when synthesised through anionic polymerisation where recombination does not occur.

Addition of crosslinkers increases the thermal degradation temperatures of PMMA. As the molecular weight between crosslinks (M_c) decreases, the amount of depolymerised material from one random chain scission decreases.[57] Polymerising PMMA in the absence of oxygen also increases the thermal degradation temperatures since there is no oxygen inhibition creating a greater number of chain ends.[23]

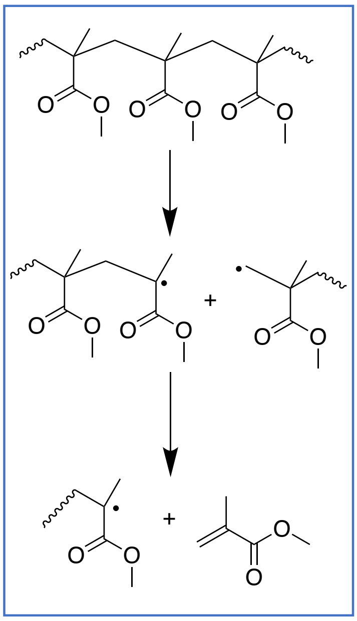

Figure 1. 6: Diagram to show random chain scission leading to ‘unzipping’ depolymerisation of PMMA

Another method that has been used to increase the degradation temperatures of PMMA is to introduce inorganic nanoparticles such as silica dioxide (SiO_2) and magnesium dihydroxide $Mg(OH)_2$ which are able to reduce heat transfer within the material.[60, 61]

1.2 Ring-opening metathesis polymerisation

1.2.1 Background to alkene metathesis

Alkene metathesis was first reported in the 1960s, with one of the first papers published by Calderon *et al.* in 1967.[62] Since then it has become one of the most widely researched, versatile and popular methods of carbon-carbon bond formation. Alkene metathesis involves the rearrangement of C=C double bonds and incudes ring-opening metathesis polymerisation (ROMP), ring-closing metathesis (RCM), ring-opening metathesis (ROM), cross-metathesis (CM) and acyclic diene metathesis (ADMET).[63-65]

It was originally suggested by Chauvin that a "pairwise mechanism" opperated.[66] This involved 2 alkenes coordinating to a metal catalyst centre and exchanging alkylidene groups through a 'quasimetallocyclobutane' intermediate, also known as alkylidentation (Scheme 1. 6).[62] Eventually this mechanism was considered inaccurate since the ratio of possible products did not agree with the predicated ratios. In addition, cross products were also observed at the very beginning of the reaction which would not be expected until higher conversions using this theory.

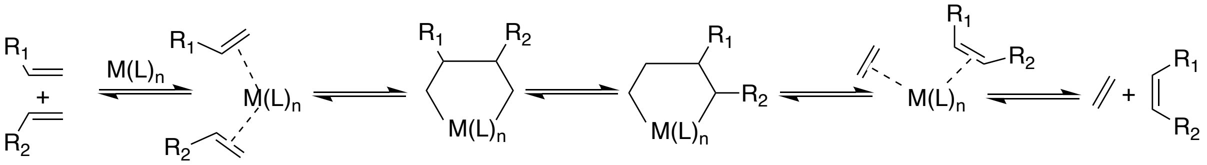

Scheme 1. 6: Original proposed 'pairwise' metathesis mechanism

In 1971, Chauvin proposed that instead, all of the alkene metathesis reactions proceeded through a metallocyclobutane intermediate.[67] A metal alkylidene species acts as an initiator and undergoes a [2 + 2] cycloaddition with the alkene monomer forming the intermediate. This then undergoes a [2 + 2] cycloreversion to give a new metal alkylidene species and product whilst maintaining the total number of carbon-carbon double bonds.

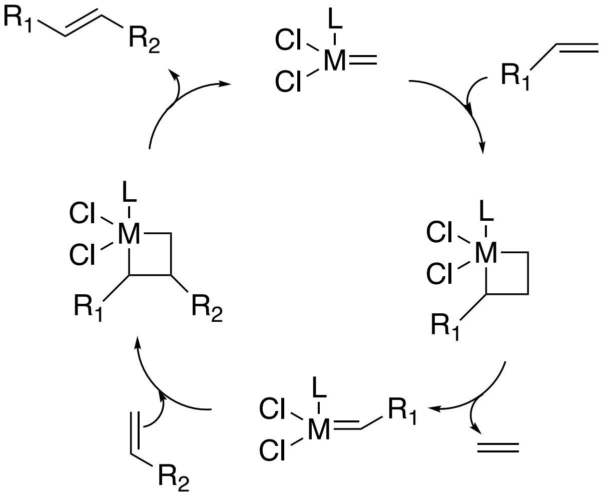

Scheme 1. 7: Chauvin [2+2] cycloaddition metathesis mechanism

1.2.2 ROMP initiators

Initially, catalysts for alkene metathesis were formed *in situ* from a precursor based on a transition metal halide and a main-group-metal cocatalyst. These were cheap and are still used in some industrial applications. Tungsten, molybdenum and rhenium were the three main metals used. Tungsten was the most studied and had very high reactivities however, this meant it was reactive towards common functional groups, especially acidic monomers. It also had short catalyst lifetimes and was uncontrollable during metathesis.[68] An example is $WCl_6/EtAlCl_3$ which was used for the industrial polymerisation of cyclopentadiene by reaction injection moulding (RIM) in the mid-1950s.[69]

Research next focused on molybdenum pre-catalysts since they are less reactive, so more tolerant towards different functional groups.[70] In 1990 Schrock synthesised a molybdenum catalyst which was stabilised by alkoxide and imido ligands that had high activity and was tolerant to phosphines and amines. Whilst molybdenum catalysts are effective at opening ring-strained monomers whilst not reacting with the unsaturated backbone formed during ROMP, they are not air and moisture sensitive so all experiments had to be carried out in a glovebox.[71]

The first Ru based metathesis initiators were reported by Grubbs and co-workers in the 1990s, beginning as a $Ru(Cl)_2(PPh_3)_4$ and diphenylcyclopropenone system that formed the catalyst *in situ*.[72, 73] Whilst this was stable in a range of solvents and tolerant of water, it was only stable for a few minutes when exposed to oxygen. Further research led to the development of the range of Grubbs initiators that are now well known and established. They are Ru-based complexes and are tolerant to oxygen, moisture and a large variety of functional groups and solvents. They are often called catalysts although initiator is a more appropriate term as they are poisoned in order to terminate the reaction.[74]

The 1st generation Grubbs initiator (G1) was based on a $(PPh_3)_2Cl_2RuCHCHCPh_2$ in a square pyramidal orientation (Figure 1. 7).[75] Cl was found to be the most effective halogen due to its small size and strong electron-withdrawing ability. The position of the halogen *trans* to the incoming alkene increased the bond strength between the alkene and the Ru whilst the halogen used had no effect on the phosphine ligand due to the *cis* orientation. The triphenylphosphine groups were soon replaced with the bulkier tricyclohexylphosphine (PCy_3) groups which had a larger cone angle and were more able to stabilise the metal complex, increasing the rate of polymerisation.[76] This catalyst was very non-polar so had poor solubility in solvents. Additionally, the initiation was slow which led to polymers with broad dispersity.

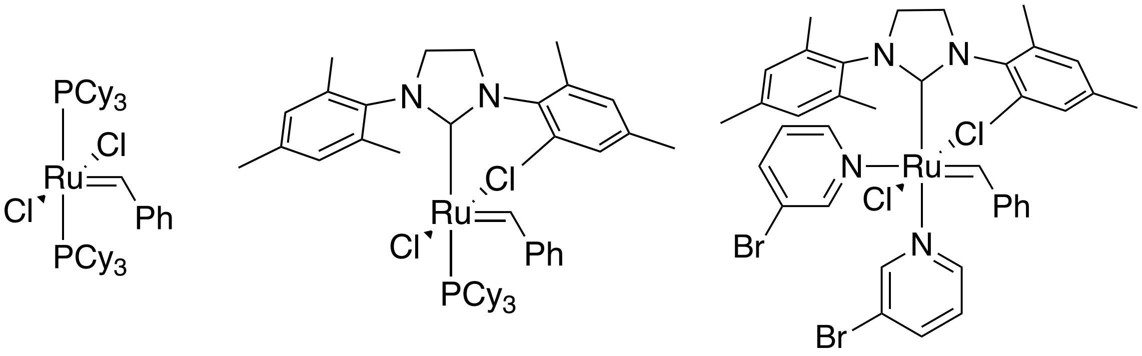

Figure 1. 7: Structures of the 1st, 2nd and 3rd generation Grubbs initiators respectively.

The 2nd generation catalyst was based on the same metal complex however one of the tricyclohexylphosphine ligands was replaced with an *N*-heterocyclic carbene (NHC) ligand.[77-79] The NHC ligand on G2 is commercially available with and without a saturated or unsaturated C-C bond on the heterocyclopentene ring. The initiator is more active when the saturated NHC is used as this is unable to stabilise the carbene and makes the ligand more basic so that the Ru has a greater electron density.[80] The NHC ligand also makes G2 more soluble in a range of solvents than G1 however it still has slow initiation which leads to broad polydispersities. Another advantage was that G2 was shown to be tolerant of nitrile and amine groups which have been shown to poison the G1 initiator.[81]

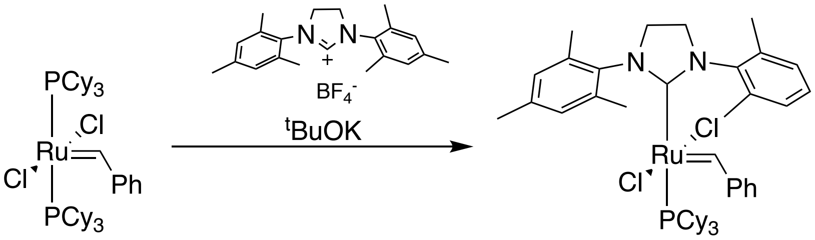

Scheme 1. 8: Reaction to convert G1 to G2[80]

The slow initiation was resolved with the third generation Grubbs initiator (G3) where the phosphine ligands were replaced by more labile pyridine ligands.[82] Pyridine is able to stabilise the electron deficient π-orbitals through conjugation, allowing the ligand to rapidly leave and re-bond with the Ru-centre giving the unsaturated bond from the monomer time to interact.

There are further Grubbs initiators such as the Hoveyda-Grubbs catalysts which have chelating ligands and are phosphine free. Despite being slower to initiate, these initiators are more stable and can be modified easily with water-soluble versions available.[83]

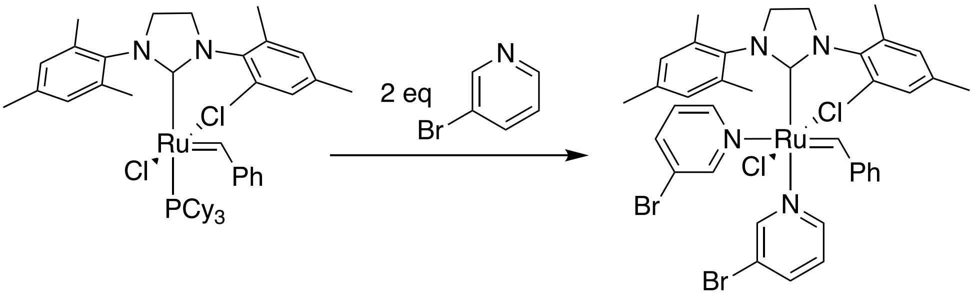

Scheme 1. 9: Conversion of G2 to G3

1.2.3 Mechanism

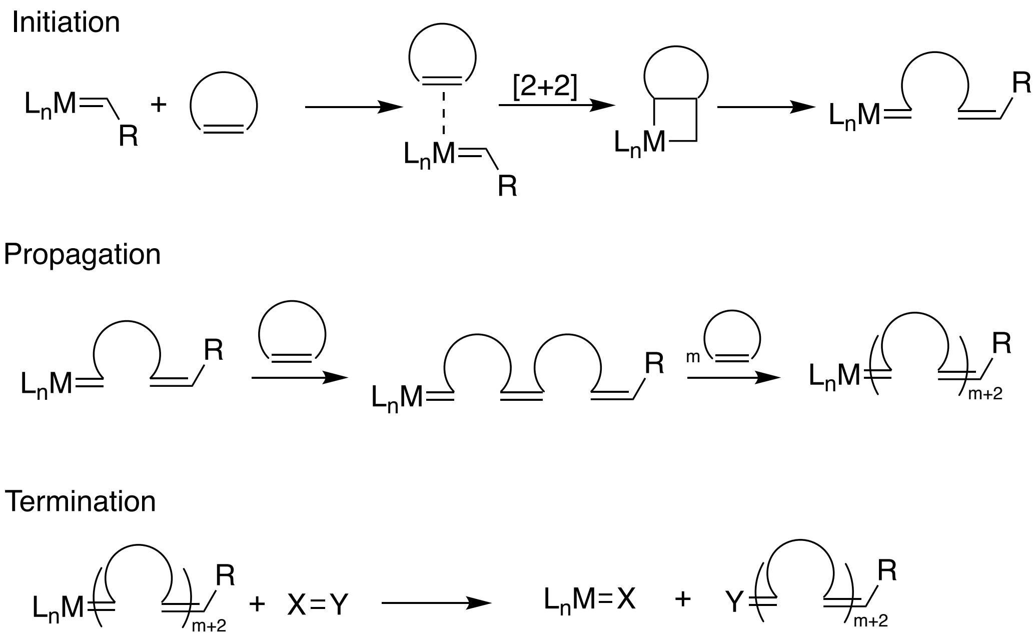

Scheme 1. 10: Initiation, propagation, and termination mechanism of ROMP.

ROMP polymerisation with a Grubbs initiator undergoes a dissociative initiation where the phosphine or pyridine ligands dissociate to reduce the electron-count of the Ru centre to 16 e$^-$. This creates a vacancy where the ruthenium centre can interact with the double bond on the monomer and form a metallacyclobutane intermediate via [2 + 2] cycloaddition.[84] Hyatt *et al.* used density functional theory (DFT) calculations and ^{1}H and ^{13}C NMR spectroscopy with different isotopes to find that this is the rate determining step for the initiation stage.[85] Following the formation, the metallacyclobutane intermediate is highly ring-strained so collapses to ring-open and form two new alkenes. There are two options in the cycloreversion, however this is the favourable route since it gives Ru a 14 e$^-$ count and a more stable product as opposed to a less stable 12 e$^-$ count and a cyclopropane. The dissociated ligands can re-associate with the Ru complex at this point.

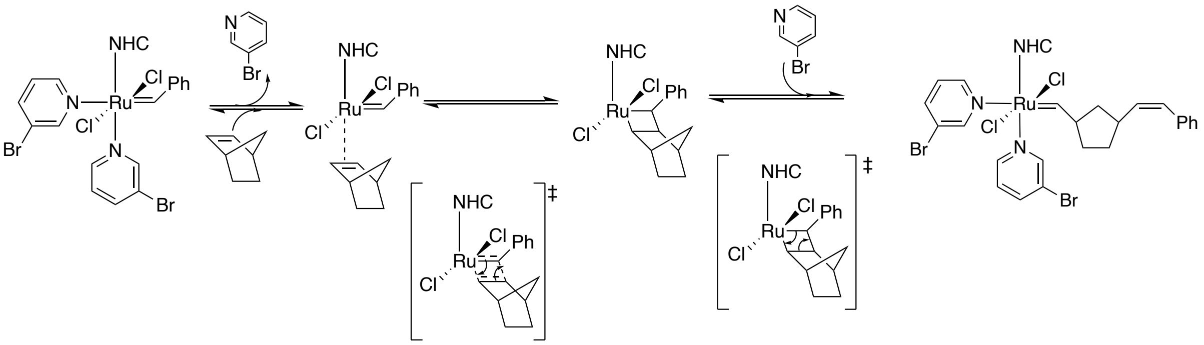

Scheme 1. 11: Mechanism of ROMP of norbornene

This process can continue propagating through the alkene attached to the Ru in the same way until all monomer has been used up. Since this is a living process, more monomer can be added and the polymerisation would continue.[86] All of the stages of ROMP are reversible however when monomers with a high ring-strain are used, this drives the equilibrium strongly in the direction of the polymer.

ROMP is a living polymerisation as it can continue growing until it is ‘poisoned’. Ethyl vinyl ether (EVE) is the most common reactant to quench metathesis reactions using Grubbs initiators. Once the vinyl ether forms the metallacyclobutane intermediate ring-opens to release the growing polymer chain as the EVE is more electronegative. The Ru-complex formed is a Fischer carbene where the two electrons are donated through the σ-bond and the *p*-orbitals are empty to receive back-donation through π-bonds. These Fischer carbenes are more stable than the alkylidene complexes such as the Ru-complex with the propagating polymer chain, hence they are unreactive in metathesis and the polymerisation is quenched.[87]

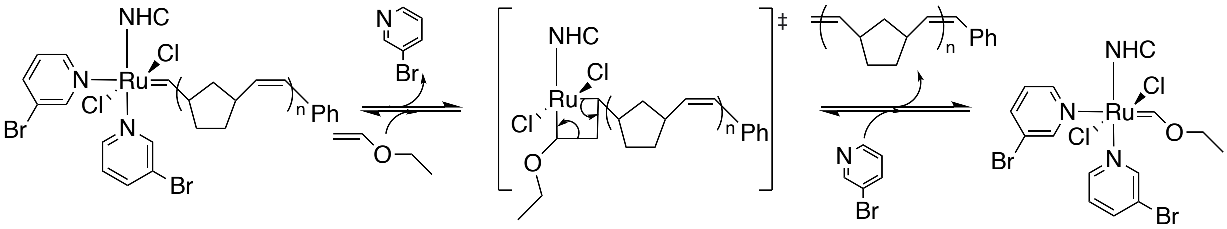

Scheme 1. 12: Reaction of the G3 catalyst with EVE to terminate the polymerisation.

The driving force for ROMP is the release of the ring strain; norbornenes are commonly used as monomers because they have a ring strain of 27.2 kcal mol^{-1}.[88] A. Hejl *et al*. showed that the ring strain for ROMP should be at minimum between 3.4 and 4.4 kcal mol^{-1}. This means that cyclopentene rings are not strained enough however substitution with an electron withdrawing group, such as a ketone, on C-3, opposite the double bond, the strain is sufficiently increased for ROMP to be favourable.[89]

1.3 Poly(dicyclopentadiene)

Dicyclopentadiene (DCPD) is a dimer of cyclopentadiene (CPD) that is formed through [2 + 4] Diels-Alder (DA) cycloaddition. DCPD has a norbornene ring with a high ring strain (26.2 kcal mol^{-1}) and a cyclopentene ring with much lower ring (4.5-6.8 kcal mol^{-1}).[90] The norbornene ring is known to undergo ROMP readily whilst the crosslinking through the cyclopentene ring is able to crosslink through ROMP and radical addition polymerisation (Scheme 1. 13). Davidson *et al*. monitored the disappearance of alkene peaks of DCPD during the polymerisation to form short oligomers using tungsten and molybdenum based catalytic systems and found that the crosslinking through the cyclopentene ring was by radical addition.[91, 92] Ruthenium has been shown to be capable of polymerising cyclopentene in certain conditions however it is less favourable and low temperatures are favoured.[89, 93]

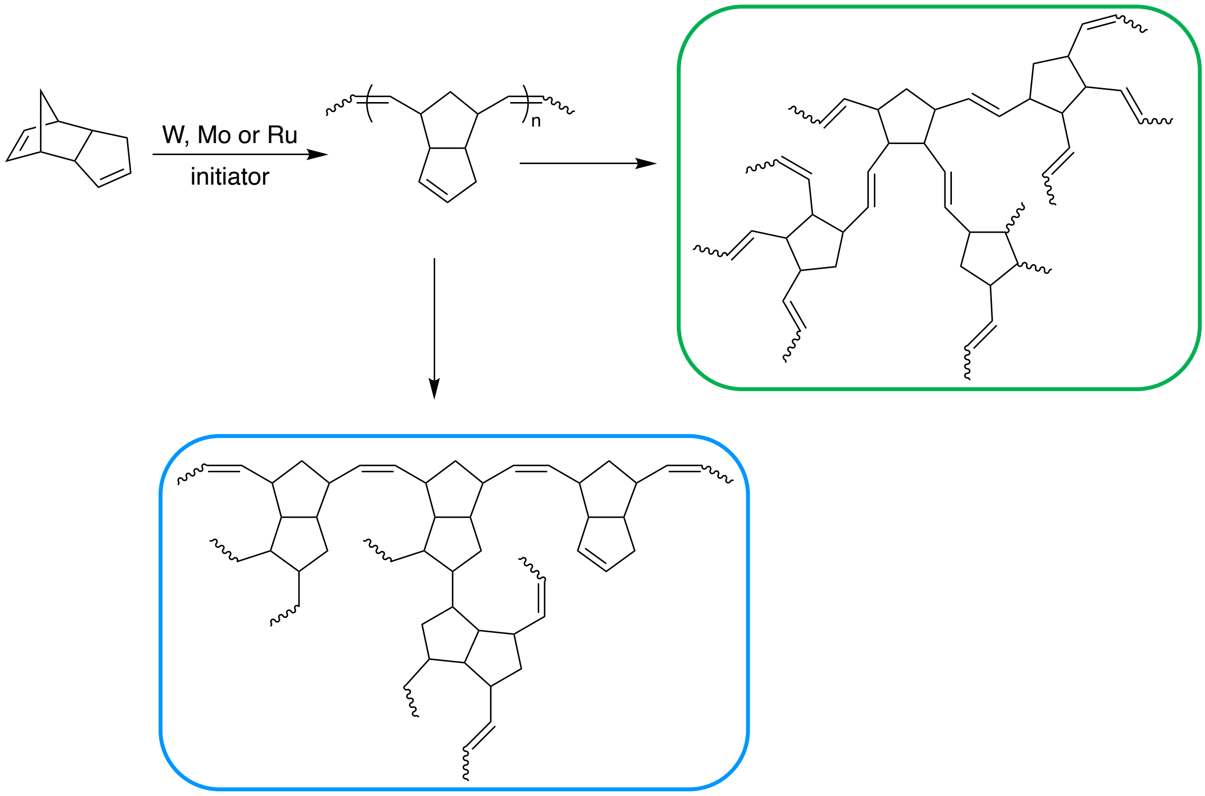

Scheme 1. 13: Crosslinking of DCPD through ROMP (green) and radical addition (blue) polymerisation

The properties of PDCPD can vary significantly depending on the conditions of the cure. The greater the catalyst loading, the greater the glass transition temperature (T_g) of the polymer since there is more crosslinking between chains. This reduces the elasticity of the polymer.[94, 95,96] Kessler and co-workers investigated the effect of cure temperature on the T_g and conversion of PDCPD. It was shown that curing at 25 °C produced PDCPD with a T_g between -25 °C and 30 °C depending on the length of cure whereas a higher temperature cure of 120 °C, a T_g between 120-140 °C can be achieved in just a few minutes.[97] The T_g of PDCPD varies and is proportional to the average molecular weight between crosslinks (M_c).[98] One way to decrease the M_c is to increase the monomer to initiator ratio or change to a more active catalyst.[96] Alternatively, high temperature post-curing can cause crosslinking through radical addition reactions.[91, 97, 99] RIM has been used to manufacture PDCPD where the reactor can control the exotherm released through heating/cooling to produce a consistent product as a strong thermoset.[100-102]

1.3.1 PDCPD in adhesives

PDCPD has been used in a lot of research into self-healing epoxy adhesives. In these systems the ROMP-able monomer is typically encapsulated in a vesicle which can rupture when a force is applied with the ruthenium-based Grubbs catalyst free within the material (although this can be the opposite way round). When the vesicle is ruptured, the catalyst and monomer mix and polymerise filling any crack and preventing it from propagating along the adhesive.[103-105] Whilst DCPD gave promising results, Wilson and co-workers found that copolymerising DCPD with a norbornene dimethyl ester monomer increased the strength by forming non-covalent interactions from the ester bond to the epoxy amine and alcohol groups.[103]

The report of PDCPD being tested as a structural adhesive was published by Knorr and co-workers. They deposited silanes on the surface of aluminium lap shear substrates and applied DCPD cured with a range of G2 catalyst concentrations. They subjected each lap shear to post-cures of 140 °C. The T_gs of all the adhesives were above 120 °C and were the same regardless of the catalyst concentration. It was shown that with a suitable silane substrate preparation, PDCPD adhesives can reach equivalent lap shear strength as epoxies.[106]

1.3.2 Diels-Alder [2+4] cycloadditions to form monomers for ROMP

DA cycloadditions were first reported in 1928 by Otto Diels and Kurt Alder. They allow a conjugated diene and a dienophile to undergo a [2 + 4] cycloaddition where the bonds break in a concerted single cyclic transition, often yielding a cyclohexene structure. During this transition three π-bonds break to form two σ-bonds and a new π-bond. Products of DA reactions are reversible and dissociate back into their starting reactants when exposed to heat.[107] DA is a way of forming carbon to carbon bonds that allow the formation of bicyclic compounds, such as norbornene and dicyclopentadiene.

Dicyclopentadiene is an example of a product of a DA reaction. At elevated temperatures around the boiling point above 170 °C, the dimer undergoes retro-DA to give two cyclopentadiene molecules.[108] Two different isomers, the *endo* and *exo*, of the product can form during a DA reaction. The ratio of these isomers produced can be changed through changing the reaction conditions such as temperature or solvent. During the dimerisation of DCPD, the *endo* product is the kinetically favoured product since there are bonding interactions between the non-reacting orbitals which stabilise the intermediate. This also means that the product is less stable and is more able to go through retro-DA.[109]

It is not always the *endo* product that is the major isomer as seen during the DA reaction between furan and maleic anhydride (Scheme 1. 14). When furan and cyclopentadiene undergo DA with maleic anhydride, there is an opportunity for both the *endo* and *exo* isomer to form. For cyclopentadiene, the kinetically favoured *endo* product is the major isomer. Furan is a more stable diene due to the polar oxygen atom withdrawing some of the electron density, so it is able to form the thermodynamically favoured *exo* isomer driven by the steric hinderance from the maleic anhydride (Scheme 1. 14).[109, 110]

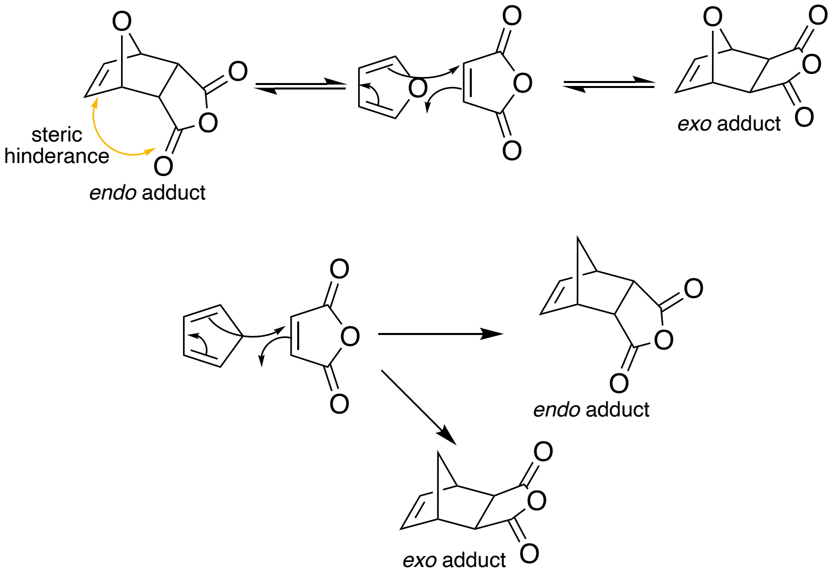

Scheme 1. 14: Reaction scheme to show how the stability of the diene leads to a different favoured isomer.

Diels-Alder reactions to form products with cyclopentadiene have been synthesised in a one-pot reaction where DCPD is cracked into CPD at 180 °C, which can rapidly react with the dienophile. In order to achieve a high yield, an electron-withdrawing group must be conjugated to the double bond. This group makes the product more stable and less likely to undergo retro-DA and therefore can be synthesised in high yield and isolated.[111]

The *endo* to *exo* ratio of a norbornene-type monomer has been found to be important in the kinetics of ROMP. M. Suzuki and co-workers synthesised norbornene-lactones, as more polar alternatives to DCPD, and found that the *exo*-isomer could be polymerised to full conversion using either G1, G2 or G3. The *endo* isomer reacted complete conversion with G3 in 10 minutes however G1 gave low conversion and G2 took 4 hours.[112] This is due to steric and electronic effects of incoming monomer as it interacts with the initiator.[113]

The T_g of the ROMP polymers is also dependent on the *endo*/*exo* ratio of the isomers. Takagi and co-workers polymerised norbornene functionalised with a cyano and an ester group and found that when 100 % *endo* was used the T_g was 151 °C, 40 °C higher than the T_g of 111 °C for 100 % *exo*. The proposed reason for this was more steric hindrance in the chain, reducing the flexibility.[114]

1.4 Conclusions

Adhesives are an essential method of forming bonds between dissimilar materials, such as composites and metals. They are found in a vast array of applications within the medical, transport and electronic industries. A range of commercially available adhesives are available however each has to be selected depending on the desired properties. Epoxies are thermally stable at temperatures above 200 °C however with little shrinkage however cure slowly and typically require high temperature post-cures to achieve maximum tensile strength. Methacrylates are prone to high levels of shrinkage upon cure however cure rapidly at room temperature with little to no post-cure.

Poly(norbornenes) can be polymerised through ROMP at room temperature to produce polymers with high thermal stability, excellent mechanical properties and elasticity and a room temperature cure with no deoxygenation required. Due to the low polarity of poly(norbornene), there has been little research into their application within adhesives since they are expected to have low surface energy.

Dicyclopentadiene is a bifunctional 'ROMPable' monomer which has excellent impact resistance, rapid curing, high T_g and low shrinkage. Currently, it has been used in self-healing epoxy adhesives however there has been no research published using it as the main component. In order to get optimum properties a high temperature post-cure is required in order to crosslink through the cyclopentene alkene and heteroatoms would need to be introduced in order to increase the non-covalent bonds to the substrate. Functionalised norbornene monomers can readily be synthesised through DA of a diene and dienophile.

1.5 Thesis aims

The aims of this thesis are to design a next-generation structural adhesive which can combine the beneficial properties of current commercially available products. An adhesive that can cure at room temperature without a high temperature post-cure would be preferred since it saves the end-user a step in there manufacturing process and also is more energy efficient. In addition, this allows the fastening of lower T_g and non-temperature resistant materials. An adhesive with negligible shrinkage will reduce localised regions of stress and lead to a higher strength product. The thesis will also targe an adhesive that can be used at temperatures above 200 °C, greater than currently available PMMA adhesive

Chapter 2- General Methods Experimental

2.1 Materials Used:

Acrylic acid (99 %), boron trifluoride methyl etherate (≥ 61 %), α-bromoisobutyrate (≥ 99 %), 2-bromopyridine (99 %), copper (II) bromide (99 %), dibenzoyl peroxide (Luperox, 25 % H_2O), dicyclopentadiene (≥ 96 %), Dichloro[[5-[(dimethylamino)sulfonyl]-2-(1-methylethoxy-O)phenyl]methylene-C](tricyclohexylphosphine)ruthenium(IV) (90 %), ethylene glycol dimethacrylate (98 %), 2-ethylhexyl methacrylate (98 %), ethyl propenyl ether (98 %), ethyl vinyl ether (99 %), glycidyl methacrylate (97 %), Grubbs 1st generation catalyst (97 %), Grubbs 2nd generation catalyst, Grubbs 3rd generation catalyst, 4,*N,N*-trimethylaniline (99 %), isobornyl methacrylate (≥ 80 %), maleic acid (99 %), maleic anhydride (98.5 %), 4-methoxyacetophenone (99 %), methacrylic acid (≥ 98.5 %), 4-methoxybenzaldehyde (≥ 98 %), ruthenium (III) chloride hydrate (≥ 99.9 % trace metal basis), 3 Å molecular sieves, SnatchCat® (≥ 95 %), tin (II) 2-ethylhexanoate (≥ 92.5 %), tributyltin hydride (97 %), *p*-toluenesulfonic acid monohydrate (≥ 98.5 %) and 2,4,6-tris(*para*-methoxyphenol)pyrylium tetrafluoroborate (≥ 90 %) were purchased from Sigma Aldrich. Methyl methacrylate (99 %) was purchased from Acros Organics, 5-norbornene-2-methanol (≥ 95 %) was purchased from Fluorochem, magnesium sulfate anhydrous was purchased from Fisher and silica gel (40-60 µm), pentamethyldiethylenetriamine (≥ 98 %) and aluminium oxide (basic) was purchased from VWR.

All reagents were used as supplied unless otherwise stated.

2.2 Instrumentation

All NMR spectra were recorded using a Bruker Avance spectrometer at 25 °C. ^{1}H NMR spectra were recorded at 400 MHz taking 64 scans per second. All DEPT ^{13}C NMR spectra were measured at 100 MHz taking 2048 scans per spectrum. $CDCl_3$ (Merck) and CH_3OD (Merck) were used as deuterated solvents and the protonated solvent was used as the reference. Samples were analysed using MestReNova software. Infrared spectroscopy was carried out using a Perkin-Elmer Spectrum Two FTIR spectrometer equipped with a diamond ATR attachment. Size exclusion chromatography (SEC) was carried out using an Agilent PL-GPC50 with a reflective index detector and a PLgel Mixed-C (7.8. x 300 mm. 5 μm guard column. The flow rate was set to 1.0 mL min^{-1} and the eluent system was THF with 0.025 wt% butylated hydroxytoluene. The samples were measured relative to poly(methyl methacrylate) (PMMA) standards with molecular weights ranging from 550 to 1568000 Da (Agilent). Inductively coupled plasma mass spectroscopy (ICP-MS) was performed on an Agilent 7500ce instrument after samples were digested in nitric acid. Differential scanning calorimetery (DSC) was carried out using a TA DSC 25 instrument. Samples (5-10 mg) was placed in an aluminium Tzero pan and sealed with a Tzero Hermetic lid. Two heating ramps were performed at 10 °C min^{-1} with a cooling ramp in between at 30 °C min^{-1}. TA instruments Trios software was used to determine the glass transition temperature (T_g). Thermogravimetric analysis (TGA) was carried out using TA TGA Q500 instrument with TA Instrument Explorer software. GraphPad Prism 7 was used to analyse the data. Unless otherwise stated, samples were measured under air with a temperature ramp of 10 °C min^{-1} up to 800 °C. Solid densities were measured using a Micrometrics AccuPyc II 1340 helium pycnometer and data was analysed using FoamPyc V2 Software. The liquid densities were measured using an AntonPaar DMA 4200 M density meter. Lap shears were tested using an Instron 6800 tensometer. UV-vis spectroscopy was carried out using a Varian Cary50 Probe spectrometer and measured wavelengths between 750 – 200 nm. The spectra were analysed using Cary WinUV software.

2.3 Chapter 3 methods

2.3.1 Synthesis of 5-Norbornene-2-methylene methacrylate (NBMMA)[115]

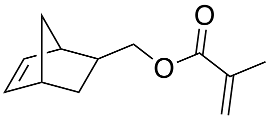

5-Norbornene-2-methanol (1 eq., 201 mmol, 25 g), methacrylic acid (1 eq., 201 mmol, 17.1 mL) and 4-(Dimethylamino)pyridine (5 wt%, 2.1 g) were dissolved in dry DCM (approx. 50 mL), degassed with N_2 for 30 minutes and left at -20 °C for 1 hour. *N*,*N*′-dicyclohexylcarbodiimide (1 eq., 201 mmol, 41.4 g) was dissolved in dry DCM, degassed with N_2 and left at -20 °C for 1 hour. The *N*,*N*′-dicyclohexylcarbodiimide solution was added slowly to the alcohol solution in an ice bath and the reaction was left for up to 16 hours. The dicyclohexylurea was filtered twice and the product was washed with 1 M HCl (3 x 50 mL), 10 wt% NaOH (3 x 50 mL), brine (50 mL), dried with $MgSO_4$ and reduced under vacuum to yield a pale brown oil. The crude product was then purified by column chromatography with a silica stationary phase and an eluent system of ethyl acetate:hexane (1:9 v/v) (yield = 84 %, 33.4 g)

^{1}H NMR (400 MHz, $CDCl_3$): 6.16 (1H, dd, *endo* NB C=C**H**, *J* = 5.8, 3.2 Hz), 6.10 (3H, m, *exo* NB C=C, MMA **H**C=C), 5.95 (1H, dd, *endo* NB C=C**H**, *J* = 5.8, 2.9 Hz), 5.55 (1H, s, MMA **H**C=C), 4.22 (1H, ddd, *exo* -C**H₂**O, *J* = 10.9, 6.5, 1.3 Hz), 4.05 (1H, ddd, *exo* -C**H₂**O, *J* = 10.9, 6.5, 1.3 Hz), 3.95 (1H, ddd, *endo* -C**H₂**O, *J* = 10.9, 6.7, 1.4 Hz), 3.70 (1H, ddt, *endo* -C**H₂**O, *J* = 10.7, 9.4, 1.9 Hz), 2.90 (1H, s, *exo* -C**H**CH=CH), 2.84 (2H, s, *endo* and *exo* -C**H**CH=CH), 2.73 (1H, s, *endo* -C**H**CH=CH), 2.43 (m, 1 H, C**H**CH_2O), 1.94 (s, 3H, -C**H**$_3$) 1.91-1.82 (1 H,m, -C**H**$_2$ from NB ring), 1.76 (1 H, m, -C**H**$_2$ from NB ring), 1.47 (2H, m, -C**H**$_2$ from NB ring), 1.30 (2 H, m, bridgehead C**H**$_2$), 0.59 (1 H, dt, -C**H**$_2$ from NB ring, *J* = 11.7, 4.1), *endo:exo*: 0.57:0.43.

^{13}C NMR (101 MHz, $CDCl_3$): 18.40 (-**C**H_3), 28.91 (-**C**H_2 in NB), 37.80 (-**C**H-CH_2O), 41.62 (-**C**H in NB ring), 49.38 (bridgehead -CH_2-), 68.26 (-**C**H_2-O-C-O), 125.33 (=**C**H_2 in MMA), 137.60 (**C**=C in NB), 136.27 (**C**=C in NB), 136.97 (**C**=CH_2 in MMA), 164.32 (-O-**C**-O) FTIR: 2953 (C-H), 1715 (C=O), 1634 (C=C), 1289 (C-H), 1157 (C-O), FTIR: v_{max}/cm^{-1} (ATR): 2955 (C-H), 1708 (C=O), 1633 (C=C), 1170 (ester C-O), 725 (C-H)

2.3.2 Synthesis of 5-Norbornene-2-carboxylic acid (NBCA)[116]

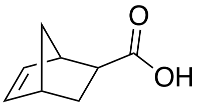

Dicyclopentadiene (DCPD) (0.5 eq., 0.15 mol, 20 g) was cracked by heating to 170 °C and cyclopentadiene (CPD) (1 eq., 0.3 mol, 20 g) was collected by distillation and quickly added to acrylic acid (1 eq., 0.3 mol, 10.32 mL) with stirring. The product was collected by vacuum distillation at 120 °C to yield transparent, viscous liquid with a strong odour (yield = 36.4 g, 87 %), *endo:exo*: 1:0.79

^{1}H NMR (400 MHz, $CDCl_3$): 11.24 (broad s, 1H, -COO**H**) 6.20 (dd, 1H, *endo* **H**C=C, *J* = 5.8, 3.1 Hz), 6.13 (qd, 2H, *exo* **H**C=C *J* = 5.6, 2.7 Hz), 5.99 (dd, 1H, *endo* **H**C=C, *J* = 5.7, 2.9 Hz), 3.27 (s, 1H, *endo* **H**C-CO), 3.14 (s,1H, *exo* **H**C-CO), 2.29 (ddd, 1H, *exo* CH-C**H**$_2$-CH, *J* = 8.8, 4.5, 1.7 Hz), 1.97 (m, 3H, *endo* CH-C**H**$_2$-CH), 1.80-1.27 (m, 4H, -C**H**-CH_2 and bridgehead -C**H**$_2$)

^{13}C NMR (101 MHz, $CDCl_3$): 181.2 (-**C**(=O)-OH), 138.3 (-**C**=C), 136.02 (-**C**=C), 132.7 (-**C**=C), 116.1 (**C**H-C=O), 115.2 (**C**H-C=O), 46.2 (cyclohexane -**C**H_2),45.6 (cyclohexene -**C**H_2) 43.6 (cyclohexene -**C**H_2), 41.6 (cyclohexene -**C**H_2), 29.0 (bridgehead -**C**H_2), 28.6 (bridgehead -**C**H_2)

FTIR: v_{max}/cm^{-1} (ATR): 2949 (C-O), 2673 (C-H), 1697 (C=O), 1170 (C-O), 682 (C-H)

2.3.3 Synthesis of 2-Hydroxypropanyl methacrylate, 5-norborn-2-yl ester (NBGMA)

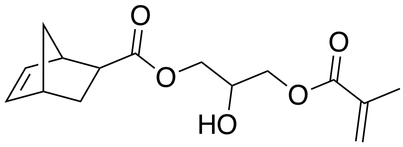

NBCA (1 eq., 72.4 mmol, 10 g) and glycidyl methacrylate (GMA) (1 eq., 72 mmol, 9.2 mL) were dissolved in dry THF (15 mL) with cetyltrimethylammonium bromide (CTAB) (5 wt%, 2.78 mmol, 1.01 g) and MEHQ (5 wt%, 8.17 mmol, 1.01 g). The solution was heated to reflux at 80 °C for 4 hours. The product was washed with EtOAc, 1 M HCl, brine and dried with MgSO$_4$ before the solvent was removed in vacuo. The product was purified by column chromatography in an eluent of EtOAc:hexane (2:8 v/v) to yield a light yellow oil (yield = 14.8 g, 52.9 mmol 73.5 %)

^{1}H NMR (400 MHz, CDCl$_3$): 6.24-6.09 (m, 2 H, *endo* and *exo* NB -HC=C**H**, -COC=C**H**), 5.95 (m, 1 H, *endo* -HC=C**H**), 5.62 (m, 1 H, -COC=C**H**), 5.18 (broad s, 1 H, -O**H**), 4.49-3.58 (m, 4 H, -C**H**$_2$CHOH), 3.40-3.12 (m, 1 H, -C**H**OH), 3.09-2.48 (m, 2 H, -C**H**-), 1.95 (s, 3 H, -C**H**$_3$), 1.50-1.10 (m, 4 H, bridgehead -C**H**$_2$ and NB ring -C**H**$_2$), ^{13}C NMR (100 Hz, CDCl$_3$): 138.2 (**C**=C), 137.2 (**C**=C), 135.5 (**C**=C), 132.2 (**C**=C), 126.1 (H**C**-C=O), 65.9 (H$_2$**C**-OH), 63.4 (H$_2$**C**-OH), 50.0 (H$_2$**C**-CH-C=O), 46.6 (H$_2$**C**-CH-C=O), 43.3 (H$_2$**C**-C-OH), 42.1 (**C**H-CH=CR), 29.3 (bridgehead **C**H$_2$) 18.1 (-**C**H$_3$) FTIR: ν_{max}/cm^{-1} (ATR): 3430 (broad OH), 2940 (CH), 1710 (C=O), 1150 (CO), MS: $C_{15}H_{20}O_5$, [M+] theoretical 280.13 Da, found 121.05 Da, 211.09 Da, 233.07 Da, 335.2 Da, melting point = -51- -44°C

2.3.4 Synthesis of poly(norbornene methylene methacrylate)[117]

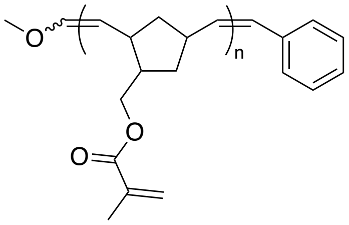

NBMMA (320 eq., 5.04 mmol, 1 g) was dissolved in DCM (10 mL) and cooled in an ice bath. Grubbs third generation initiator (1 eq., 0.016 mmol, 0.014 g) in DCM (1 mL) was added with rapid stirring. After 5 minutes an excess of ethyl vinyl ether (EVE) (0.5 mL) was added to quench the reaction. The reaction mixture was precipitated in cold methanol twice to yield PNBMMA as a tacky, dark brown gel.

^{1}H NMR (400 MHz, CDCl$_3$): 6.10 (1 H, s, -CH=C**H**$_2$), 5.56 (1 H, s, -C=C**H**$_2$), 5.43-5.08 (2 H, m, *trans* and *cis* -C**H**-C**H**), 4.14 (1 H, *exo* -C**H**$_2$O), 3.98 (1 H, m, *endo* -C**H**$_2$O), 2.99-2.79 (2 H, m, *endo* NB -C**H**, 2 x *exo* NB -C**H**), 2.80-2.69 (1 H, m, *endo* NB -C**H**), 2.49-2.32 (1 H, m, *exo* -CHC**H**$_2$CH), 2.18-1.17 (5 H, m, backbone -CH$_2$, bridgehead -C**H**$_2$, *endo* -CHC**H**$_2$CH), 1.14-1.05 (1 H, m, *exo* C**H**CH$_3$O-), 0.91 (3 H, m, backbone -C**H**$_3$), T_g = 18 °C

2.3.5 Synthesis of poly(2-Hydroxypropanyl methacrylate, 5-norborn-2-yl ester) (PNBGMA)

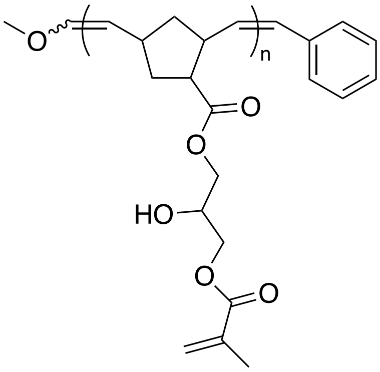

NBGMA (300 eq., 3.57 mmol, 1 g) was dissolved in DCM (80 wt%, 4 g, 5.32 mL) and G3 (1 eq., 0.011 mmol, 0.010 g) was added with rapid stirring. The reaction was left for 1 hour before being quenched with an excess of EVE (0.5 mL). After 15 minutes the polymer was precipitated in cold hexane (150 mL) and partially dried under vacuum to leave a low viscosity, sticky brown polymer.

^{1}H NMR (400 MHz, CDCl$_3$): 5.94 (1 H, s, MMA **H**C=C), 5.42 (1 H, s, MMA **H**C=C), 5.32-4.83 (2 H, m, backbone **H**C=C), 4.21-3.18 (4 H, s, **-CH**$_2$CHOH), 2.89-2.11 (3 H, m, -C**H**OH and -C**H**CH=C)

1..73-1.58 (3 H, s, C**H**$_3$), 1.30-0.73 (4 H, m, norbornene -C**H**$_2$)

2.3.6 Synthesis of poly(norbornene methylene methacrylate-*co*-norbornene carboxylic acid) (P(NBMMA-*co*-NBCA))

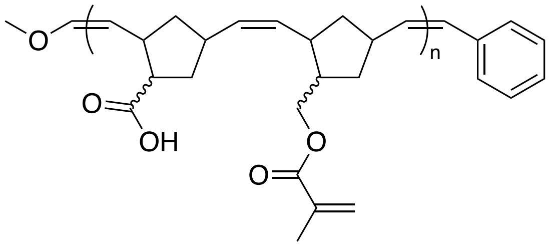

NBMMA (160 eq., 5.04 mmol, 1 g) and NBCA (160 eq., 5.04 mmol, 0.70 g) were dissolved in DCM (50 wt%, 4.25 g, 5.65 mL) and methanol (30 wt%, 2.55 g, 2 mL). G3, (1 eq., 0.032 mmol, 0.027 g) was added with rapid stirring and the reaction was left for 45 minutes. An excess of EVE (0.75 mL) was added to quench the reaction and after 15 minutes the polymer was precipitated into cold hexane (150 mL) and partially dried under vacuum to leave a sticky, light brown polymer (conversion = 100 % (^{1}H NMR)).

^{1}H NMR (400 MHz, CDCl$_3$): 6.08 (s, 1 H, MMA =C**H**), 5.60 (s, 1 H, MMA = C**H**), 5.52-5.09 (4 H, m, backbone =C**H**), 4.50-4.19 (s, 2 H, -OC**H**$_2$), 2.95-1.44 (m, 14 H, norbornene -C**H**), 1.32-1.09 (m, 3 H, -C**H**$_3$), T_g = -13 °C

2.3.7 Synthesis of M1X adhesives

Monomer mixture, M1, was prepared by mixing MMA (90 wt%, 17.26 mmol, 1.85 mL) and EGDMA (10 wt%, 0.97 mmol, 0.19 mL). Both monomers had been passed through basic alumina to remove inhibitor before use. The adhesives were made up of M1 (100-50 wt%) and poly(norbornene) derivative (0-50 wt%). BPO (4 wt%, 0.33 mmol, 0.08 g) and TMA (0.33 mmol, 0.04 g, 0.05 mL) were added with rapid mixing and the adhesive was poured onto lap shear/ into mould before gelling took place.

Prior to TGA, DSC and IR analysis the lap shears were held at 40 °C *under vacuo* for 16 hours.

2.3.8 Determination of gel fraction

Sample was dried in a vacuum oven at 40 °C for 24 hours and then weighed in a thimble and refluxed with DCM (300 mL) in soxhlet glassware for 24 hours. The thimble was removed and dried in a vacuum oven at 40 °C for 24 hours.

$$Gel\ fraction\ \% = \frac{initial\ mass - final\ mass}{initial\ mass} \times 100$$

Equation 1: Calculation for the gel fraction of a thermoset

2.3.9 PVC lap shear testing:

PVC rectangles (dimensions: 5 cm x 2.5 cm x 0.4 cm) and squares (dimensions: 2.5 cm x 2.5 cm x 0.4 cm) were washed with deionised water. The adhesive was poured into the centre of the rectangle and acid-washed glass beads (212-300 μm) were sprinkled on. The smaller piece on top so that there was full contact with the adhesive and the lap shear was left for 24 hours at room temperature to cure.

2.4 Chapter 4 methods

2.4.1 General AGET ATRP reaction

$CuBr_2$ (1 eq., 0.078 mmol, 1.4 mg) and PMDETA (1.5 eq., 0.117 mmol, 0.024 mL) were dissolved in 2-butanone (3 mL) and left to form a metal-ligand complex for 10 minutes. EBiB (1 eq., 0.078 mmol, 0.013 mL) and monomer was added, and the reaction was purged with N_2 for 30 minutes. $Sn(EH)_2$ (0.5 eq., 0.031 mmol, 0.13) was dissolved in 2-butanone (to make 20 wt%) and purged with N_2 for 30 minutes. $Sn(EH)_2$ was added to the monomer solution and the reaction was placed in a preheated heating mantle at 65 °C and left for at least 8 hours. Bu_3SnH (3 eq, 0.234 mmol, 0.063 mL) was added and left for a further 2 hours. Conversion was determined through ^1H NMR. The reaction was quenched by exposing to air and removing from the heat. The polymer was purified by passing through aluminium oxide and reprecipitating in methanol.

2.4.2 Synthesis of PNBMMA by AGET ATRP[117]

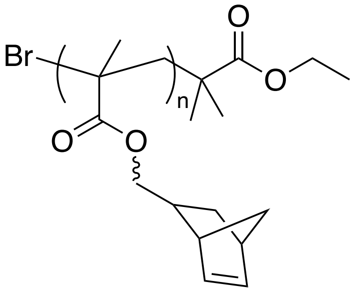

NBMMA was polymerised following the general AGET ATRP procedure. The polymerisation was quenched after 2 hours before 45 % gelation.[117] PNBMMA was collected as a white powder (0.41 g, 41 %).

^{1}H NMR (400 MHz, CDCl$_3$): 6.25-6.07 (2 s, 2 H, *endo* and 2 *exo* **H**C=C), 5.95 (s, 1 H, *endo* **H**C=C), 4.09 (s, 1 H, *exo* -C**H**O), 3.80 (2 s, 2 H, *endo* and *exo* -C**H**O), 3.53 (s, 1 H, *endo* -C**H**O), 2.87 (s, 1 H, *exo* -C**H**-HC=C), 2.78-2.69 (2 s, 1 H, *exo* and *endo* -C**H**-HC=C), 2.43 (s, 1 H, *endo* -C**H**-HC=C), 2.13-1.18 (3H, -C**H**$_2$ on bridgehead, -C**H**CH$_2$O), 1.82-1.78 (7H, -C**H**$_3$, -CHC**H**$_2$CH, backbone -C**H**$_2$) 0.97-0.79 (1H, -C**H**$_2$ from NB ring) FTIR: ν_{max}/cm^{-1} (ATR): 2969 cm^{-1} (C-H), 1725 cm^{-1} (C=O), 1449 cm^{-1} (CH$_3$), 1235 cm^{-1} (C-O), 1140 cm^{-1} (secondary C-O), T_g = 88 °C

2.4.3 Synthesis of PEHMA by AGET ATRP[118]

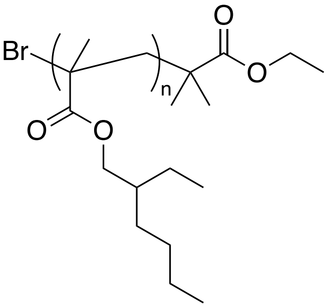

2-ethylhexyl methacrylate (EHMA) (100 eq., 5.04 mmol, 1 g) was polymerised using the general AGET ATRP procedure to give poly(2-ethylhexyl methacrylate) as a sticky white solid (0.84 g, 84 % conversion).

^{1}H NMR (400 MHz, $CDCl_3$): 4.01-3.68 (2H, -C**H**$_2$O), 2.7-1.78 (1H, -C**H**), 1.71-1.01 (11H, -C**H**$_2$ from ethyl and hexyl groups, -C**H**$_2$ from backbone), 0.99-0.82 (8H, -C**H**$_3$ from ethyl group, - C**H**$_3$ from hexyl group, -C**H**$_2$CH), FTIR: ν_{max}/cm^{-1} (ATR): 2923 cm^{-1} (C-H), 1702 cm^{-1} (C=O), 1456 cm^{-1} (CH_3), 1140 cm^{-1} (C-O) T_g = 108.0 °C

2.4.4 Synthesis of P(NBMMA-*co*-EHMA) by AGET ATRP

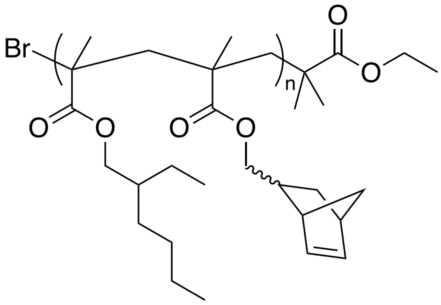

NBMMA (50 eq., 2.52 mmol, 0.5 g) and EHMA (50 eq., 2.52 mmol, 0.5 g) were polymerised following the general AGET ATRP procedure. The polymerisation was stopped after 2 hours before crosslinking to give poly(2-ethylhexyl methacrylate) as a white solid. (Yield = 0.48 g, 48 %)

^{1}H NMR (400 MHz; $CDCl_3$): 6.24-6.07 (3H, m, *endo* C=C**H** and 2 x *exo* C=C**H**), 5.93 (1H, s, *endo* C=C**H** on NB), 3.99-3.66 (4H, *exo*-C**H**$_2$, *endo*-C**H**$_2$O and EHMA -C**H**$_2$O), 3.55 (1H, s, *exo*-C**H**$_2$O), 2.94 (1H, s, *endo*-C**H** on NB), 2.89-2.78 (2H, m, *exo*-C**H** and *endo*-C**H** on NB), 2.73 (1H, s, *exo*-C**H** on NB), 2.39 (1H, s, *endo*-C**H** on NB), 2.11 – 1.79 (2H, m, -C**H** on hexyl group, *exo*-C**H** on NB), 1.78-1.00 (18H, m, -C**H**$_2$ on ethyl and hexyl groups, -C**H**$_2$ on backbone, -C**H**$_3$ on backbone, -C**H**$_2$ from bridgehead), 0.89 (10H, *exo*-C**H** from NB, -C**H**$_3$ from ethyl group, -C**H**$_3$ from hexyl group, -C**H**$_2$CH from hexyl group), 0.62-0.51 (1H, s, *endo*-C**H** from NB), FTIR: ν_{max}/cm^{-1} (ATR): 2930 cm^{-1} (C-H), 1725 cm^{-1} (C=O), 1464 cm^{-1} (C-H, methylene group), 1239 cm^{-1} (C-O), 740 (C=C, disubstituted *cis*), T_g = 41.6 °C

2.4.5 Synthesis of PIBMA by AGET ATRP[119]

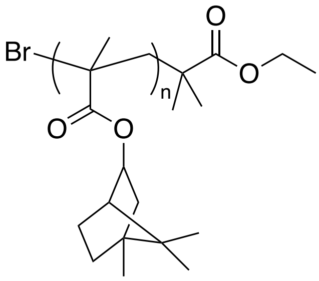

Isobornyl methacrylate (IBMA) (100 eq., 4.31 mmol, 1 g) was polymerised using the general AGET ATRP procedure to yield poly(isobornyl methacrylate) as a white powder (0.87 g, 87 %)

^{1}H NMR (400 MHz; CDCl$_3$): 4.6-4.24 (1H, m, -C**H**O), 2.15-1.64 (7H, m, *exo*-H from -C**H**$_2$, -CHC**H**$_2$CH- from IB ring, -C**H** from IB ring, -C**H**$_2$ from backbone), 1.27-0.66 (14 H, m, bridgehead -C**H**$_3$, -C**H**$_3$ *endo*-H from -C**H**$_2$ and backbone -C**H**$_3$), FTIR: ν$_{max}$/cm^{-1} (ATR) 2929 (C-H), 1723 (C=O), 1449 (C-H), 986 (C-O), 671 (C-Br)

2.4.6 Synthesis of P(NBMMA-*co*-IBMA) by AGET ATRP

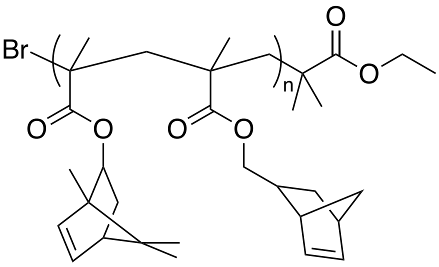

P(NBMMA-*co*-IBMA) was polymerised following general the AGET ATRP procedure and quenched after 2 hours before gelation. The product was collected as a white powder (0.39 g, 39 %)

^{1}H NMR: (400 MHz; CDCl$_3$): 6.21-6.04 (3H, m, *endo* **H**C=C and 2 x *exo* **H**C=C), 5.90 (1H, s, *endo* **H**C=C), 4.56-4.25 (1H, s, -C**H**O on IBMA), 3.74 (2H, s, *endo* -C**H**$_2$O on NB and *exo* -C**H**$_2$O on NB), 3.60-3.37 (1H, s, *endo* -C**H**$_2$O on NB), 2.93 (1H, m, *exo* -C**H** on NB), 2.87-2.79 (2 H, m, *endo* -C**H** and *exo* -C**H** on NB), 2.70 (1H, m, *endo* -C**H** on NB), 2.35 (1H, m, *exo*-C**H**$_2$ on NB), 2.13-1.20 (16H, m, C**H**$_2$ on IB, *endo*-C**H**$_2$ on NB, C**H**$_3$ on IB, C**H**$_2$ on backbone), 1.21-0.78 (13H, m, C**H**$_3$ on backbone, C**H**$_3$ on bridgehead, *exo*-C**H**CH$_2$O on NB), 0.55 (1H, m, *endo*-C**H**CH$_2$O on NB), FTIR: ν$_{max}$/cm^{-1} (ATR): 2921 (C-H), 1731 (C=O), 1667 (C=O), 1424 (C-H), 704 (C-Br), T_g = 106 °C

2.4.7 Synthesis of 5-Norbornene-2,3-dicaboxylic acid (NBDCA)[120]

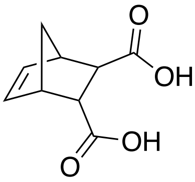

DCPD (1 eq., 75.6 mmol, 10 g) was cracked into CPD by heating to 180 °C and collected by distillation. Maleic acid (2 eq., 151 mmol, 17.6 g) was dissolved in acetone and CPD was added directly and left to crystallise. The white crystals were washed with hexane and deionised water and then freeze dried for 48 hours. (Yield = 89 %, 0.134 mol, 24.4 g).

^{1}H NMR (400 MHz, CH$_3$OD): 6.20 (s, 2 H, **H**C=C), 3.30 (dt, 2 H, -C**H**CH=CH, *J* = 3.2, 1.7 Hz), 3.11 (m, 2 H, -C**H**COOH), 1.41 (qt, 2 H, bridgehead C**H$_2$** *J* = 8.4, 1.7 Hz), ^{13}C NMR (101 MHz, CH$_3$OH): 175.15 (**C**=O), 135.46 (**C**=C) , 47.1 (**C**H$_2$), 46.3 (**C**H), 45.2 (**C**H), FTIR: ν$_{max}$/cm^{-1} (ATR): 2250 (C=O), 1646 (C=O), 1230 (C-O), 800 (CH)

2.4.8 Synthesis of 5-Norbornene,2,3-(di-5-norbornene-2-methanyl) (CL1)[121]

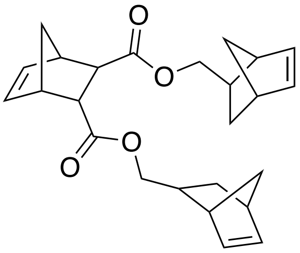

NBDCA (1 eq., 27 mmol, 5 g) and 5-Norbornene-2-methanol (2 eq., 55 mmol, 6.83 g) were heated to 100 °C with *p*-toluenesulfonic acid (5 wt%, 0.59 g) and *N,N*-dimethyl-3,5-di-tert-butyl-4-

hydroxybenzylamine (5 wt%, 0.59 g) for 4 hours. The product was washed with 10 wt% NaOH (3 x 100 mL), saturated NaCl solution (100 mL). The organic layer was dried over $MgSO_4$ and reduced under vacuum to yield a golden-brown liquid. The crude product was purified by column chromatography on a silica stationary phase with the eluent mixture ethyl acetate:hexane (1:9 v/v) to yield a pale yellow viscous liquid (Yield = 57 %, 15 mmol, 6.07 g)

^{1}H NMR (400 MHz, $CDCl_3$): 6.37-5.83 (6 H, m, **H**C=C), 4.22-3.51 (4 H, m, O-C**H**$_2$), 3.44-3.11 (4 H, m, -OCH$_2$C**H**), 2.98-2.03 (4 H, m, -CHC**H**$_2$CH), 1.88-1.03 (9 H, m, bridgehead -C**H**$_2$, -C**H**), 0.60-0.48 (1 H, m, -C**H**), ^{13}C NMR (101 MHz, $CDCl_3$): 136.27 (**C**=C), 135.07 (**C**=C), 129.87 (**C**=C), 127.63 (**C**=C), 68.51 (**C**-O), 68.12 (**C**-O), 68.5 (**C**-O), 66.44 (**C**-O), 48.47 (bridgehead **C**-C), 45.19 (bridgehead **C**-C), 48.04 (**C**-C=O-), 46.41 (**C**-C=O-), 43.7 (**C**-C=C), 41.85 (**C**-C=C), 46.62 (**C**-C=C), 37.72 (**C**-R$_3$), 29.92 (**C**H$_2$-CH), 29.03 (**C**H$_2$CH), FTIR: ν_{max}/cm^{-1}(ATR): 2930 (alkene C-H), 1736 (C=O), 1186 (ester C-O), 710 (C-H), $C_{25}H_{30}O_4$ $[M]^+$ theoretical 394.81 Da, found 395.22 Da, Melting point = -66 - -61 °C

2.4.9 Synthesis of Ethylene Glycol Di-1-methyl-1-norbornene (CL2)

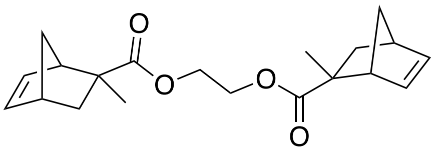

In a one-pot synthesis EGDMA (1 eq., 0.1 mol, 18.9 mL), DCPD (0.75 eq., 0.076 mol, 10 g) and MEHQ (2.5 wt%, 0.75 g) was heated to 170 °C to yield an excess of CPD (1.5 eq., 0.152 mol, 10 g) which reacted with EGDMA by a [2 + 4] Diels-Alder cycloaddition. The product was filtered through silica with hexane to remove excess DCPD and then collected with (1:1 v/v) hexane:EtOAc and the solvent was removed under reduced pressure. (Yield: 0.077 mol, 77 %, 25.6 g)

^{1}H NMR (400 MHz, $CDCl_3$): 6.27-6.19 (1 H, s, *endo* **H**C=C), 6.17-6.00 (3 H, m, *exo* and *endo* **H**C=C), 4.42-4.16 (4 H, m, O-C**H**$_2$-R), 3.08-2.98 (4 H, m, *endo* -C**H**-CH=CH), 2.98-2.76 (4 H, m, *exo* -C**H**-CH=CH), 2.49-

2.36 (2 H, m, bridgehead -C**H**$_2$), 1.97-1.89 (2 H, m, bridgehead -C**H**$_2$), 1.51-1.34 (6 H, s, -C**H**$_3$), 1.18-1.07 (2 H, m, *endo* -C**H**$_2$-C), 0.87 (2 H, m, *exo* -C**H**$_2$-C)

^{13}C NMR (101 MHz, $CDCl_3$): 178.52 (**C**(=O)-O), 177.21(**C**(=O)-O), 138.73 (**C**=C), 137.92 (**C**=C), 133.44 (**C**=C), 126.00 (**C**=C), 62.44 (-O-**C**), 62.05 (-O-**C**), 50.83, 50.47, 49.05, 46.85, 42.73, 42.56, 38.00, 37.83, 29.30, 24.16, MS: $C_{20}H_{26}O_4$ $[M]^+$ theoretical: 330.18 not found, C_5H_6 $[M]^+$ theoretical: 66.05, found: 69.03, $C_{10}H_{14}O_4$ $[M]^+$: theoretical: 198.09, found: 197.19, FTIR: ν_{max}/cm^{-1} (ATR): 2920 (CH), 1724 (C=O), 1410 (CH), 1210 (C-O), 670 (C=C), Melting point = -30- -25 °C

2.4.10 P2 Acid Etch

Sulfuric acid (28.7 wt%) was slowly added to deionised water (59.7 wt%) followed by Iron (III) sulfate hydrate (11.6 wt%) and stirred at 60-68 °C for 30 minutes. Aluminium substrates were degreased with propan-2-ol then submersed in the P2 solution for 12 minutes. They were submersed in a beaker of deionised water for 5 minutes then a second beaker of deionised water for a further 5 minutes. The substrates were then left in a preheated oven at 40 °C to dry.

2.4.11 Curing PDCPD adhesives

DCPD (2000 eq., 15.13 mmol, 2 g) was heated up to 35-40 °C then G1 (1 eq., 0.0076 mmol, 0.0062 g) in DCM (0.1 mL) was added with rapid mixing then poured onto the substrate within 5-10 seconds within the lap shear jig. The second substrate was placed to give a bond area of 25 x 12 mm. The lap shears were cured at 40 °C for 30 minutes then placed in a preheated oven at 100 °C overnight.

2.5 Chapter 5 methods

2.5.1 Synthesis of 2,4,6-Tris(*para*-methoxyphenyl)pyrylium tetrafluoroborate[122]

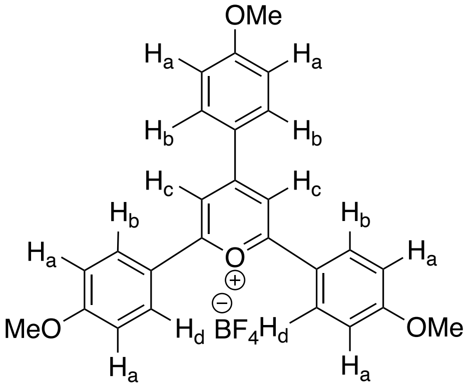

4-Methoxybenzaldehyde (1 eq., 0.035 mol, 4.2 mL) and 4-methoxyacetophenone (2 eq., 0.07 mol, 10.5 g) were degassed with N_2 for 20 minutes. Boron trifluoride methyl etherate (2.5 eq., 0.0875 mol, 11.08 mL) was added slowly. The mixture was heated at 100 °C for 100 minutes and was accompanied by a colour change from colourless to orange to dark brown. The product was a viscous oil that was washed with diethyl ether and recrystallised from acetone to yield a bright orange powder (8.17 g, 48 %)

^{1}H NMR (400 MHz, DMSO): 8.77 (2 H, s, $\mathbf{H}_c$), 8.63-8.53 (m, 2 H, $\mathbf{H}_d$), 8.52-8.42 (m, 4 H, $\mathbf{H}_b$), 7.32-7.20 (m, 6 H, $\mathbf{H}_a$), 3.95 (s, 9 H, O-C$\mathbf{H}_3$), ^{13}C NMR (101 MHz, DMSO): 167.9 (O=**C**) , 165.1 (**C**-PhOMe) , 164.4 (**C**-O-CH$_3$), 161.4 (**C**-O-CH$_3$), 132.3 (**C**H$_b$), 130.7 (**C**H$_d$), 124.5 (**C**H$_a$) , 121.5 (**C**-OCH$_3$), 115.4 (**C**H$_a$), 111.0 (**C**H$_c$), 55.9 (O-**C**H$_3$), UV/ vis: peak at 432 nm

2.5.2 General Batch Metal-Free Ring Opening Polymerisation (MF-ROMP) Procedure

Norbornene (100 eq., 10.6 mmol, 1 g), 2,4,6-tris(*para*-methoxyphenyl)pyrylium tetrafluoroborate (*p*-OMeTPT) (0.05 eq., 0.0053 mmol, 0.0026 g) and ethyl propenyl ether (EPE) (1 eq., 0.106 mmol, 0.0071 mL) were dissolved in DCM (5.3 mL, 2 mM) which had been dried over alumina columns. Compressed air that had been passed through a short column of phosphorus pentoxide was bubbled through the mixture for 20 minutes in an ice bath. The reaction was then exposed to blue LED light (λ = 465 nm, 3.54 mW cm^{-2}) for 1 hour. The reaction mixture was poured through basic alumina and precipitated in methanol followed by 3 reprecipitations to yield a white solid.

2.5.3 MF-ROMP to synthesise PNB[123]

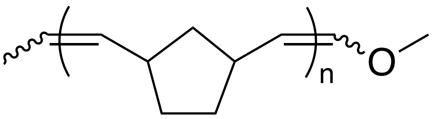

Norbornene (NB) (100 eq., 10.6 mmol, 1 g), was polymerised using the general MF-ROMP procedure and yielded PNB as a white solid (0.95 g, 95 %)

^{1}H NMR (400 MHz, $CDCl_3$): 5.37 (s, 2H, *trans* -C**H**$_2$-, J = 4.3, 2.1 Hz), 5.22 (s, 2H, *cis* -C**H$_2$**-, J = 6.0, 1.9 Hz), 2.81 (s, 1H, *cis* -C**H**-), 2.45 (s, 1H, *trans* -C**H**-), 1.83 (m, 2H, -C**H**$_2$ and -CHC**H**$_2$CH-), 1.36 (m, 2 H, --CHC**H**$_2$CH), 1.09 (m, 2 H, -C**H**$_2$), *trans:cis* = 1:0.34, T_g = 40 °C

2.5.4 MF-ROMP to synthesise P(NB-*co*-MMA)[124]

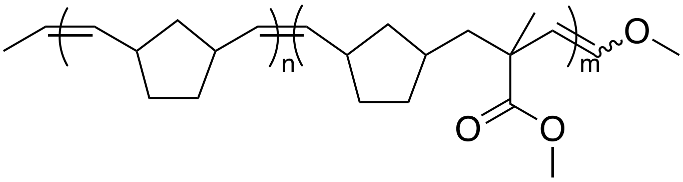

NB (90-30 eq.) and methyl methacrylate (MMA) (10-70 eq.) to give total monomer (10.6 mmol) concentration of 2 mM in dry DCM.

^{1}H NMR (400 MHz, $CDCl_3$): 5.38 (2H, s, *trans* -C**H**-C), 5.23 (2 H, s, *cis* -C**H**-C), 3.62 (3H, s, -O-C**H**$_3$), 2.79 (2H, s, *cis* -C**H**-CH$_2$), 2.43 (2H, s, *trans* -C**H**-CH$_2$), 1.89 (2H, m, -CH-C**H**$_2$-CH), 1.76 (2H, m, -CH-C**H**$_2$-CH$_2$), 1.66 (2H, m, -C**H**$_3$), 1.36 (2H, m, -CH-C**H**$_2$-CH$_2$), 1.08 (2H, m, -CH-C**H**$_2$-CH) *trans:cis* = 1:0.32, T_g - 19 – 40 °C

2.5.5 MF-ROMP to synthesise P(NB-*co*-NBMMA)

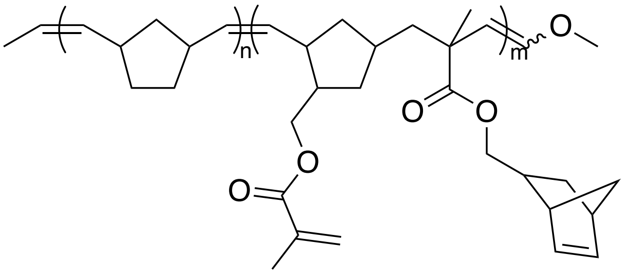

NB (90-30 eq) and methyl methacrylate (MMA) (10-70 eq) to give total monomer (10.6 mmol) concentration of 2 mM in dry DCM.

^{1}H NMR (400 MHz, CDCl$_3$): 6.18 (1H, s, *exo* NBMMA **H**C=C), 6.08 (3H, m, *endo* NBMMA **H**C=C and MMA **H**C=C), 5.52 (1H, m, MMA **H**C=C), 5.19 (1H, s, NB backbone *cis* **H**C=C), 4.05 (3H, m, MMA backbone *exo* -C**H**$_2$O- and NBMMA backbone -C**H**$_2$O-), 3.75 (2H, m, MMA backbone *endo* -C**H**$_2$O-), 3.52 (1H, m, MMA backbone *exo* -C**H**$_2$O-), 2.96-2.64 (3H, m,-C**H**CH= in NBMMA and -C**H**- in backbone), 2.51-2.28 (2H, m, *trans* NB -C**H**- and -C**H**-CHO$_2$), 2.10-1.68 (7H, m, NBMMA -C**H**$_3$, NB -C**H**$_2$, backbone -C**H**$_2$), 1.74-1.60 (2H, m, MMA -C**H**$_2$-), 1.50-0.97 (4H, m, *endo* -C**H**$_2$ in norbornene backbone and *exo* -C**H**$_2$ in cyclopentene ring), 0.79-0.97 (3H, MMA *trans* C**H**$_3$), 0.62-0.50 (3 H, MMA *cis* -C**H**$_3$), T_g = 15-40 °C

Chapter 3 – Methacrylate-functionalised ROMP polymers as additives in PMMA adhesives

3.1 Introduction

3.1.1. Functionalised poly(norbornene)

The first commercially available poly(norbornene) (PNB), Norsorex®, was produced in 1978 and was sold for applications such as a sound barrier, dampening and oil spill recovery. The linear polymer has an unsaturated backbone which can undergo post-polymerisation modifications such as vulcanising with sulfur to form a crosslinked higher T_g thermoset.[125,68] Since then, a variety of PNB derivatives functionalised with a range of groups including ester, cyano and alcohol have been developed.[112, 114, 126, 127]

Grubbs and co-workers demonstrated that unlike earlier transition metal alkylidene catalysts, the ruthenium-carbene based alternatives are tolerant towards functional groups that can undergo further polymerisation such as methacrylates and epoxies. These remain intact after ring-opening metathesis polymerisation (ROMP).[128, 129] Several research groups have shown that norbornene monomers with pendant methacrylates are able to undergo ROMP with the methacrylate functionality completely intact at the end of the reaction.[117, 130, 131]

Wooley and co-workers synthesised norbornene monomers with pendant methacrylate groups that are able to undergo both radical polymerisation and ROMP. It was demonstrated that a Ru-Grubbs initiator was very selective for the norbornene and ROMP was the only polymerisation mechanism observed. When the monomer was polymerised by ATRP, there was a greater affinity towards the methacrylate alkene, however as the reaction progressed, crosslinking with the norbornene alkene lead to gelation.[117]

Norbornene methylene acrylate bifunctional monomers have been used to synthesise polymer coatings. The acrylate group was used to bond to the steel substrate and the Ru catalyst is added with norbornene so that the polymer chain can propagate forming a protective layer around the substrate. The properties of this layer can easily be tuned by varying the DP or length of anchor group.[132] Grau and co-workers showed that the naturally produced monomer, caryophyllene, could be polymerised by ROMP to produce a linear polymer capable of crosslinking through radical polymerisation (Scheme 3. 1). This produced a polymer with a high thermal stability where the temperature at which there was 10 % mass loss ($T_{10\%}$) was 200 °C for the linear polymer and between 310-340 °C for the cross-linked polymer.[133]

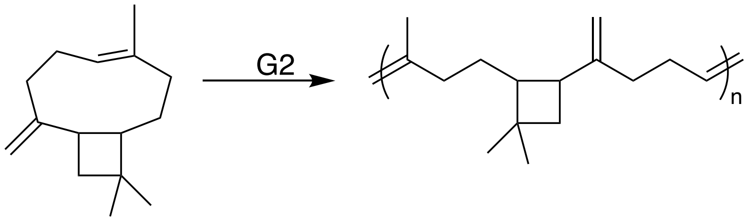

Scheme 3. 1: ROMP to synthesise poly(caryophyllene) from caryophyllene.[133]

Grubbs and co-workers noticed that cyclooctene functionalised with a methacrylate pendant group could be polymerised by ROMP using Grubbs first generation catalyst (G1) to form an unsaturated chain with pendant methacrylate's intact. Whilst there was no immediate reaction with the methacrylate group, after 12 hours the polymer had formed an insoluble gel. The addition of a radical inhibitor prevented crosslinking, showing that it is a radical reaction rather than metathesis.[129] Despite other groups researching the effect of acrylate and methacrylate functionalised monomers, other papers have not reported this phenomenon.[117, 130, 134] Before crosslinking occurred, these linear polymers were dissolved in MMA then cured into a thermoset. This material had a greater thermal degradation temperature, measured by thermal gravimetric analysis (TGA) in comparison to PMMA.

3.1.2 Effect of anchor group on ROMP

Recently there has been considerable research into the effect of the anchor groups of norbornenes polymerised by ROMP, particularly with large macromonomers for the formation of bottlebrush polymers.[135-137] As the length of the anchor group increases, the control of the polymerisation decreases due to a slower rate of propagation (k_p). This can make the polymerisation begin to exceed the lifetime of the catalyst so that full conversion cannot take place.[138, 139]

Matson and co-workers used computational experiments to find the highest occupied molecular orbital (HOMO) of a variety of functional groups on *exo*-norbornene and the effect on k_p. They found that the higher energy level the HOMO, the faster the k_p and the greater the control of the polymerisation. This was true until a limit, where increasing the HOMO energy had no further effect on k_p.[126, 135] It was proved that monomers that can chelate to the ruthenium have a slower k_p since the intermediate is stabilised, although the effect was shown to be smaller than that of the HOMO energy. Hyatt *et al.* showed the presence of an ester group adjacent to the norbornene ring causes stabilisation, so any ester functionalised monomer reacts slower through ROMP (Figure 3. 1).[85]

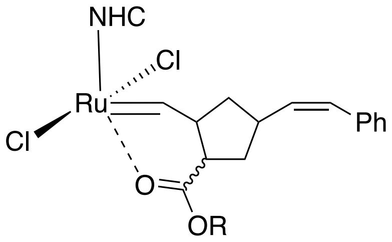

Figure 3. 1: Grubbs 3rd generation initiator (G3) chelating to the ester group on a functionalised norbornene[85, 126]

J. Moore and co-workers showed that *exo*-dicyclopentadiene (DCPD) has higher reactivity rates than *endo*-DCPD due to steric hindrance from the incoming ligand. Coordination from the ruthenium to the second alkene group was also observed, stabilising the intermediate for the *endo*-isomer (Figure 3. 2).[113] This has since been found to be true for a range of norbornene functionalised monomers.[112, 140] Other groups have published papers with a range of 'ROMPable' monomers confirming these observations.[112, 114]

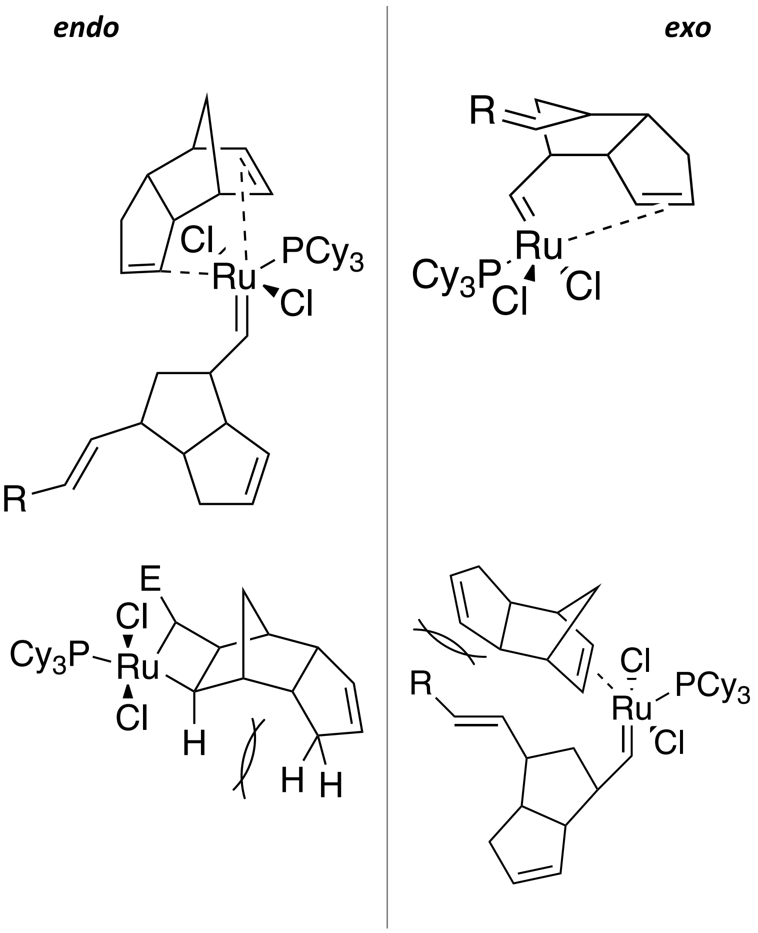

Figure 3. 2 Intermediate ruthenium-monomer complex showing steric hindrance and chelation effects.

3.1.3 Chapter Aims

The aims of the research is to increase the thermal degradation temperatures and reduce the shrinkage of poly(methyl methacrylate) (PMMA) adhesives. To do this PNB chains, which degrade at higher temperatures than PMMA, will be synthesised and added to the PMMA adhesive formulation. Addition of macromonomers such as linear polymers decreases the shrinkage since there are fewer non-covalent interactions to chemically react to form shorter covalent bonds.

In order to make the non-polar, hydrocarbon PNB soluble in methyl methacrylate (MMA), the norbornene monomers will be functionalised with MMA groups which contain polar oxygen atoms and also are able to crosslink into the material (Figure 3. 3).

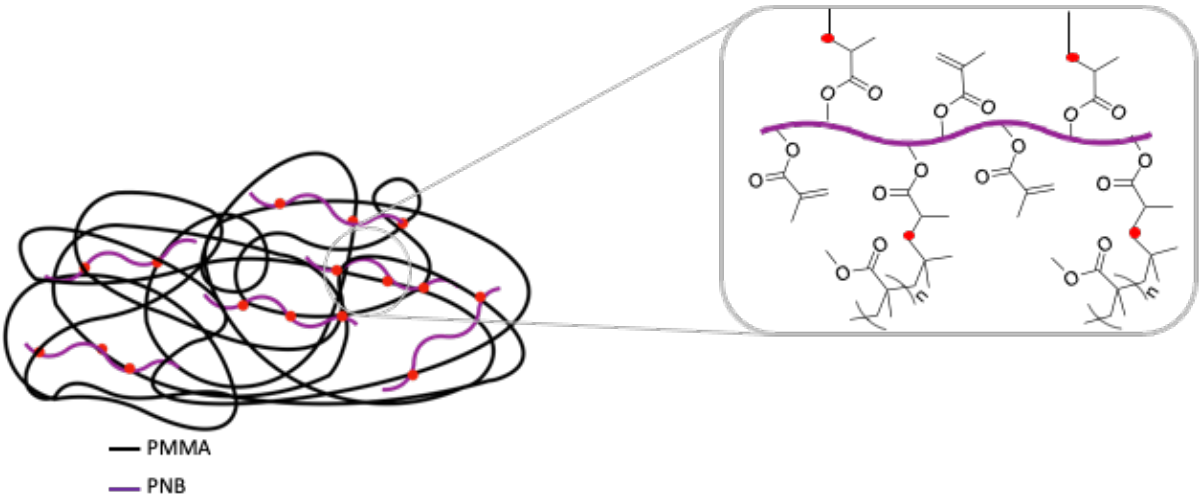

Figure 3. 3: Diagram of the crosslinked P(MMA-*co*-NB) polymers where the red dots represent the crosslinks.

3.2 Results and Discussion

3.2.1 Methacrylate functionalised norbornene

The base for the adhesive formulation is MMA which is quite polar since it contains two oxygen molecules in an ester functional group. This means that additives need to be quite polar in order to be soluble within MMA and not lead to phase separation when they cure.

PNB is formed from only carbon and hydrogen which makes it non-polar and therefore insoluble in MMA adhesives. A norbornene monomer, norbornene methylene methacrylate (NBMMA), with an MMA anchor group was synthesised from a commercially available hydroxy functionalised norbornene starting material (Scheme 3. 2). This monomer contained two oxygen molecules which increased the polarity, making the polymer MMA soluble and additionally forming a group to crosslink the norbornene into the adhesive. Steglich esterification between 5-norbornene-2-methanol (NBOH) and methacrylic acid (MAA) was chosen as the method of synthesis since it is low temperature and high yielding (84 %) (Scheme 3. 2). Dicyclohexylcarbodiimide (DCC) was used as a coupling agent and 4-dimethylaminopyridine (DMAP) was used as a base. Industrial synthesis would not use this method since it has a low atom efficiency with dicyclohexylurea (DCU) being produced as a biproduct.

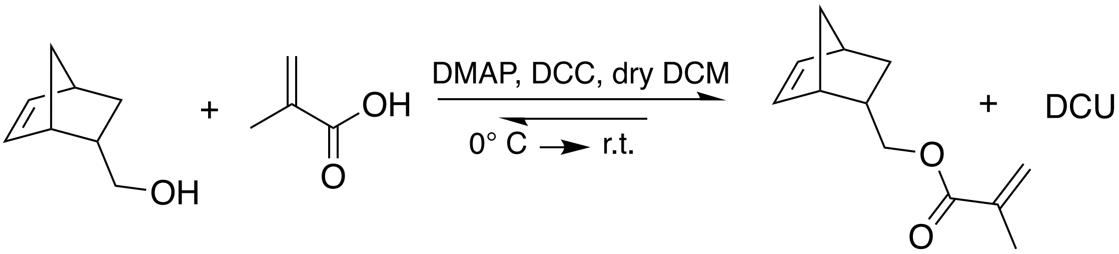

Scheme 3. 2: Esterification reaction scheme to synthesise NBMMA

Other methods such as high temperature acidic esterification with *p*-toluenesulfonic acid and transesterification with MMA were also tried, however they were prone to radical polymerisation through one of two alkenes resulting in lower yields. Methacryloyl chloride was also used as a more reactive alternative to MMA to give yields of > 90% conversion, however this was only carried out during smaller scale syntheses due to the hazard since HCl is produced as a biproduct and relative cost of the reagents (Scheme 3. 3).

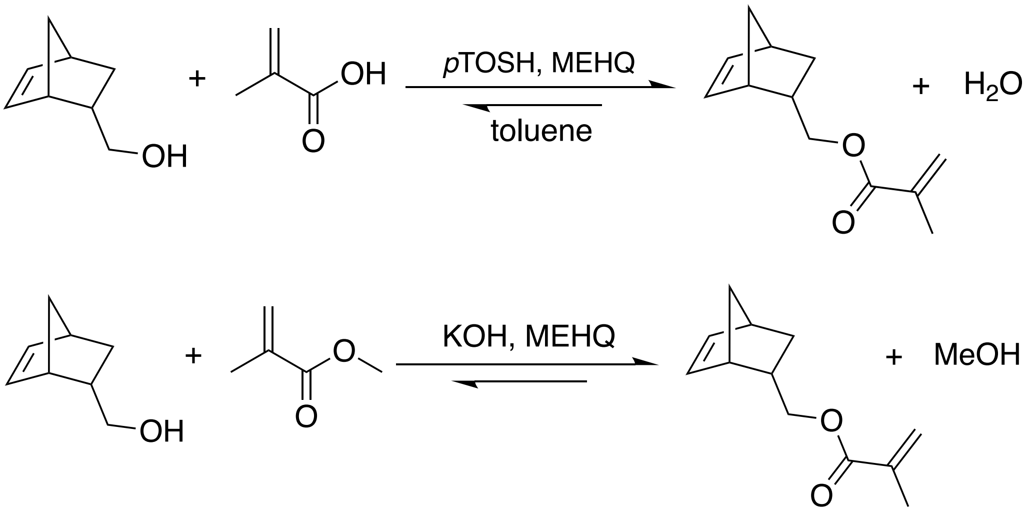

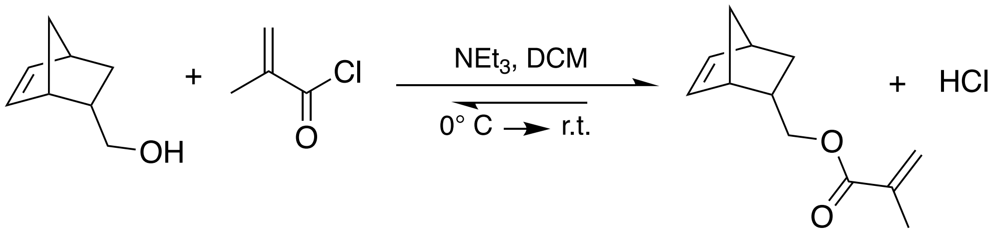

Scheme 3. 3: Acidic esterification, transesterification and methacryloyl chloride esterification of NBOH to NBMMA

The NBMMA monomer was synthesised from a starting material that had a ratio of *endo: exo* isomers of 0.57:0.43 (determined by ^{1}H NMR). The ratio of *endo*: *exo* isomers of the product was found to be the same by comparing the -C**H**$_2$-O resonances of the ^{1}H NMR where the two *exo* protons have resonances at δ= 4.24 and 4.05 ppm and the *endo* protons have resonances at δ= 3.95 and 3.70 ppm (Figure 3. 4).

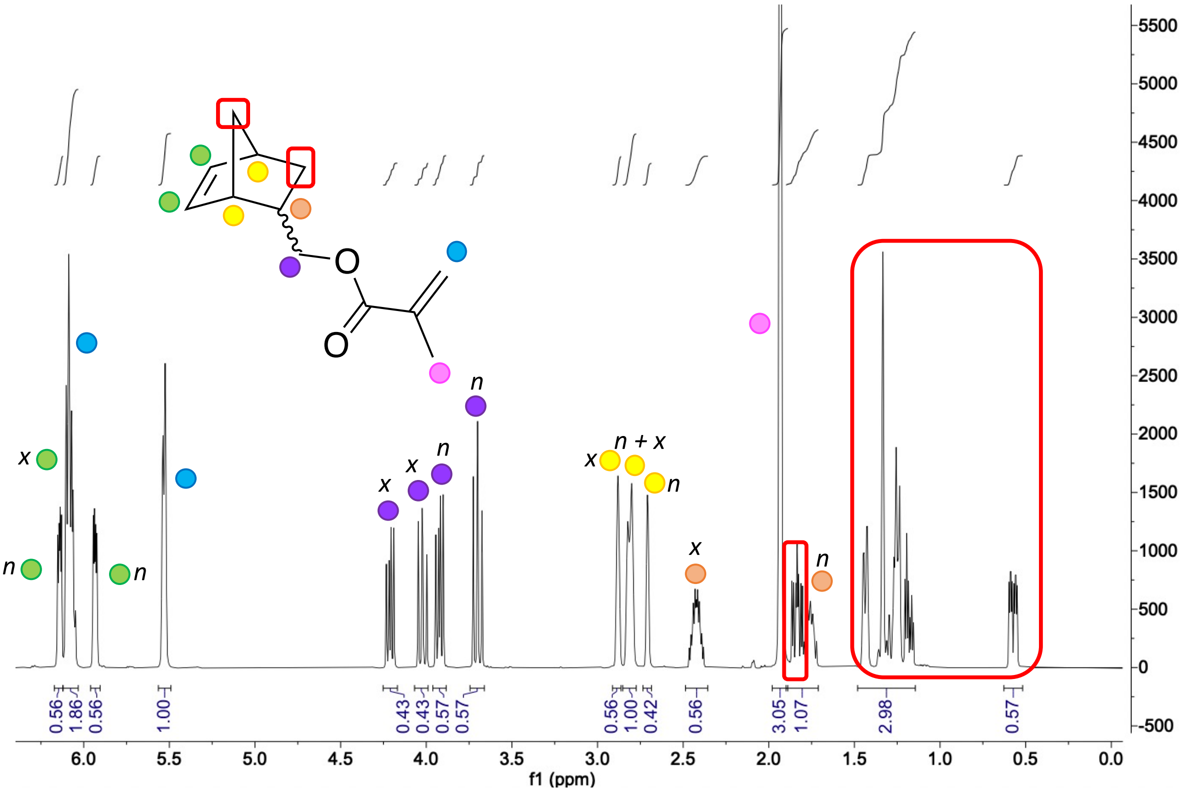

Figure 3. 4: ^{1}H NMR spectrum ($CDCl_3$) of NBMMA

3.2.2 Polymerisation of PNBMMA

G3 was chosen as the ROMP initiator due to its rapid rate of initiation it gives well controlled polymerisations with low dispersity ($Đ_M$).[141] This allows the effect of the chain length of the PNBMMA within an adhesive to be compared. Dichloromethane (DCM) was chosen as a solvent since it solubilises the catalyst, monomer and polymer, is non-coordinating so does not affect k_p and has a low boiling point so is easy to remove. The reaction was carried out with a monomer concentration of 0.45 M and at a temperature of 0 °C since this has been shown to give better control and lower $Đ_M$s of poly(norbornenes) by reducing chain transfer reactions.[141, 142] Even in an ice bath, monomer concentrations greater than 0.5 M showed exotherms which lead to gelation of the reaction. No degassing was carried out prior to polymerisation since G3 is oxygen tolerant.[86]

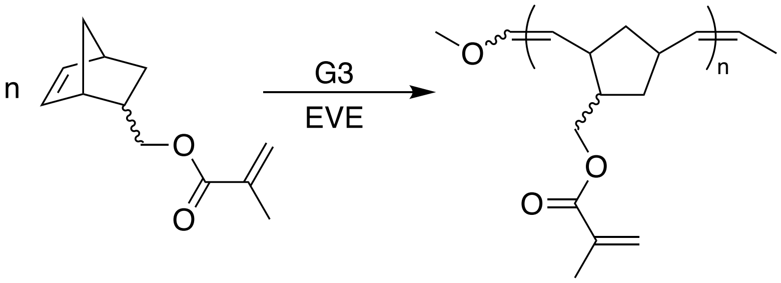

Scheme 3. 4: Polymerisation of NBMMA to PNBMMA

The beginning of the ROMP reaction could be seen by the colour change of the ruthenium from dark green to a golden-brown colour representing the change in electron density around the metal core. The reaction solution quickly increased in viscosity and was quenched after a few minutes by adding an excess of ethyl vinyl ether (EVE) to cleave the polymer from the Ru-complex (1.1.4)

As previously discussed, when polymerised using a Grubbs initiator, the highly ring-strained norbornene is the only functional group that is seen to react.[117] This was demonstrated by ^{1}H nuclear magnetic resonance (NMR) spectroscopy whereby the norbornene alkene resonances at δ = 6.15, 6.10 and 5.94 ppm (Figure 3. 4) completely disappeared in the polymer ^{1}H NMR spectrum (Figure 3. 5). Meanwhile, the methacrylate alkene resonances at δ= 6.10 and 5.20 ppm in the monomer (Figure 3. 4) were unaffected and still present in the polymer ^{1}H NMR spectrum (Figure 3. 5).

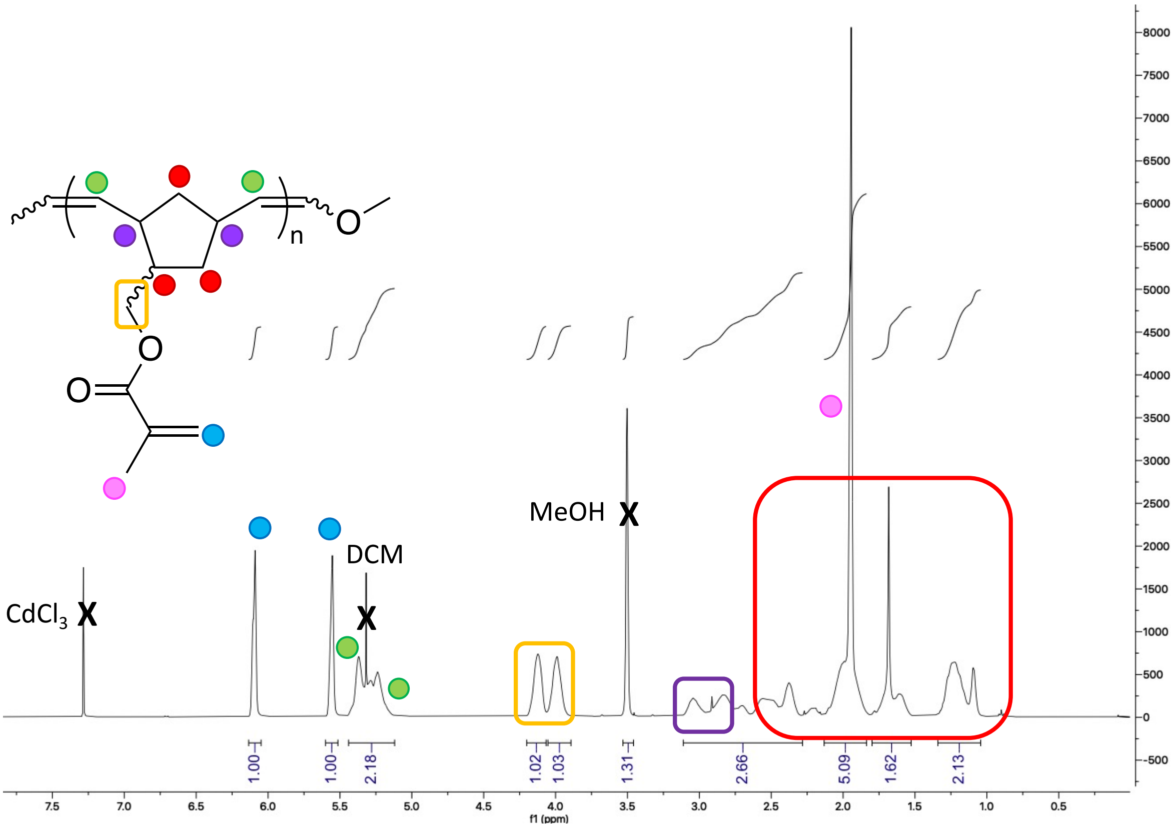

Figure 3. 5: ^{1}H NMR spectrum of NBMMA and PNBMMA (CDCl$_3$)

The size exclusion chromatography (SEC) chromatagrams in tetrahydrofuran (THF) of PNBMMA synthesised using G3 showed two peaks rather than one. This is the consequence of the low dispersities allowing the difference in the rate of polymerisation of *endo* and *exo* monomers to be observed (Figure 3. 6). The polymerisation of NBMMA was also carried out with G1 to see if this was tolerant to the methacrylate functional group and able to polymerise the bifunctional monomer. As with G3, only the norbornene group polymerised ROMP however, due to the slower initiation of G1, the SEC chromatogram showed one, broader distribution as opposed to two. The overall $Đ_M$ of the isomer mixture is 1.3 for G3 and 1.79 for G1 (Table 3. 1) showing that G3 still gives a lot more control over weight-average molecular weight (M_w).

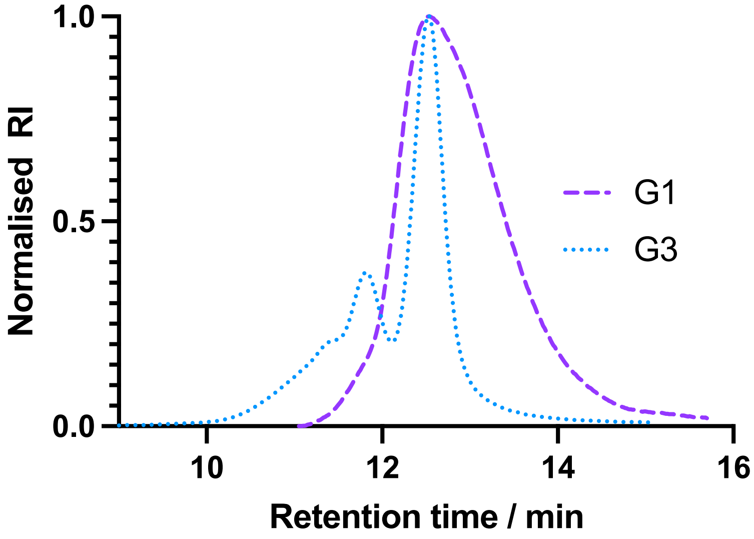

Figure 3. 6: SEC chromatograms of the PNBMMA synthesised using G1 and G3 showing a separated *exo* peak (left) and *endo* peak (right), (THF, PMMA standards)

Table 3. 1: Table to show the M_w and $Đ_M$ of the different isomer peaks and overall isomer mixture.

Initiator	**Peak**	**M_w / g mol^{-1}**	**$Đ_M$**
G3	*exo*	65 000	1.04
	endo	31 000	1.03
	Overall	40 000	1.30
G1	-	91 000	1.79

The differences in reactivity rates comes from the interactions between the Ru-centre and the methacrylate anchor group. *Exo*-NBMMA has the methacrylate anchor group away from the Ru-centre whereas the *endo* isomer has an orientation whereby the Ru can chelate to the methacrylate alkene, stabilising the intermediate and slowing the reaction down.[113] Additionally, there is steric hindrance between the methacrylate anchor and the propagating polymer chain of the *endo* isomer (Figure 3.

7). Since the reactions were carried out on a 1 g scale, G3 was used as the initiator for the remained of the work mentioned, however, G1 was also used to demonstrate the methacrylate functional group tolerance.

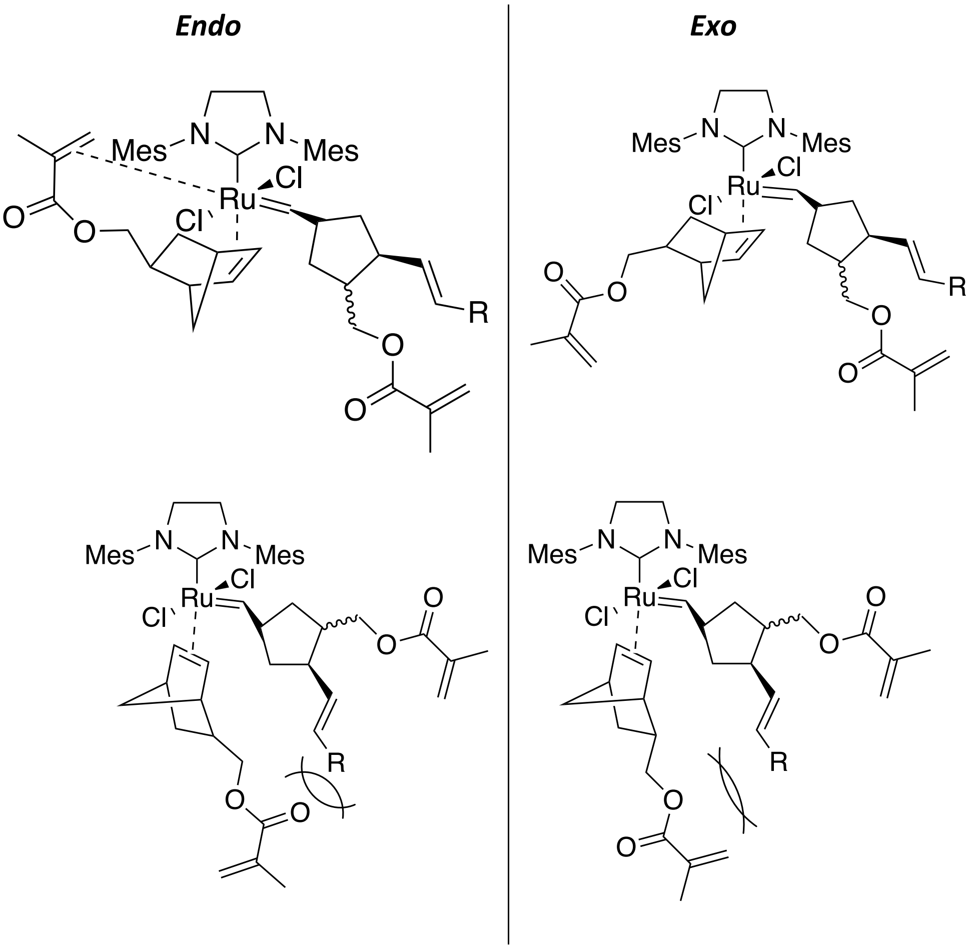

Figure 3. 7: Figure to show G3 coordinating with the incoming monomer and steric hindrance causing a large difference in polymerisation rates.

Even after 3 reprecipitations, the resulting polymer remained a dark brown colour due to residual ruthenium. It is challenging to remove residual ruthenium from the polymer due to its ability to form bonds with the unsaturated backbone and methacrylate alkene.[143] When the polymer was dried under vacuum to remove solvent a crosslinking reaction took place producing a brittle and insoluble network.

This was the same for PNBMMA polymerised by both G1 and G3 initiators and was demonstrated by measuring the gel fractions. The polymer was allowed to dry under vacuum for 24-hours before a 24-hour Soxhlet extraction in DCM. The resulting product broke apart into a powder and had lost its colour. The gel fraction of PNBMMA synthesised by G3 was 89 % and by G1, 87 % which could have been within error and therefore, showed little differences between the two.

3.3.3 Radical reaction between Ru and MMA

A series of experiments were carried out to understand the mechanism behind the crosslinking. The hypothesis being, that this was due to a radical reaction of the MMA initiated by Ru (Experiment 1). MMA and G3 (1000:1 mol. ratio) were mixed and left for a week at room temperature. The colour of the solution darkened from green to a dark brown/ black suggesting that there was some oxidation or destabilisation of initiator. However, ^{1}H NMR spectroscopy showed no loss of methacrylate resonance demonstrating that G3 did not cause a cross-metathesis or radical reaction. Within this time G3 is expected to have decomposed, which is likely the reason for the observed colour change.[86]

Experiment 2 was to synthesise PNB using G3 and diluting the mixture in MMA to see if a reaction takes place. Attempts to remove G3 were made by 3 reprecipitations in methanol after quenching with EVE. The polymer appeared mostly white, suggesting that the Ru had been removed. 1 g of PNB was added to 4 g of MMA and was insoluble due to the polarity difference. However, after 2 hours there was a significant viscosity increase in the solution and a colour change to light brown. By the following day the MMA had completely polymerised to form a brown solid block (Figure 3. 8). The same experiment was repeated using G1 where the polymer crosslinking was observed to be slower. In this instance, there was an obvious viscosity increase after 6 hours. After 24 hours the solution was a thick gel and after 48 hours appeared to be completely solid.

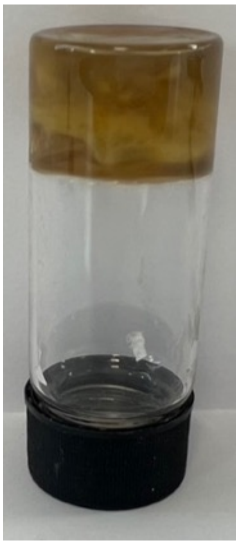

Figure 3. 8: Photo to show that MMA monomer had polymerised due to residual Ru catalyst.

Experiment 3 was carried out to prove that the Ru is the initiator of the polymerisation. A metal-free ROMP (MF-ROMP) alternative was used to synthesise PNB with a pyrylium photocatalyst, enol ether initiator and blue LED light (Chapter 2.5.2). Even after several weeks with 1 g of PNB in 4 mL of MMA there was no viscosity increase and ^{1}H NMR spectroscopy showed no polymerisation.

As experiment 1 showed that G3 does not cause MMA to undergo a radical or ROMP polymerisation alone, the possibility that EVE had an effect was investigated. At the end of the ROMP to form PNB, no EVE was added to cleave the Ru from the propagating polymer chain, however, PNB still was able to polymerise MMA within 24 hours.

In order to understand whether this is a radical polymerisation, a surplus of radical inhibitor (10 wt% 4-methoxyphenol (MEHQ)) was added to the PNB in MMA solution. The MMA remained unreacted even after one week which suggests that this must be a radical mechanism. MEHQ has been shown to have no effect on ROMP.[128] Additionally, when MMA was replaced with EVE which undergoes cationic polymerisation, no viscosity change was seen. The mechanism behind this radical initiation is unknown, Ruthenium (II) complexes have been used as radical initiators however, typically with an haloalkane or haloketone co-initiator and at an elevated temperature around 80 °C.[144, 145]

A final experiment compared the effect of the oxidation state of the Ru on the ability to initiate radical polymerisation of MMA. Ruthenium (III) trichloride and Dichloro[[5-[(dimethylamino)sulfonyl]-2-(1-methylethoxy-O)phenyl]methylene-C](tricyclohexylphosphine)ruthenium(IV) were added to MMA to form a brown and dark green solution respectively. After 1 week at ambient temperature there was no viscosity increase however both were a dark brown colour. This demonstrated that a degradation of G1 and G3 to these oxidation states following ROMP was not responsible for the observed radical polymerisation.

3.3.4 Removing Ru from PNBMMA

An isocyanide scavenger molecule, SnatchCat® (Figure 3. 9), has been shown to be able to remove Ru from reaction mixtures after ring-closing metathesis and to achieve low ppm levels if added at the end of the reaction.[146] A small excess of SnatchCat® in comparison to the Ru (4.4 mol. eq.) is needed and there is a short binding time of about 30 minutes. The chelated isocyanide-Ru complex can then be filtered out of the solution by passing through silica. Since the application is intended for an industrial purpose and it is not economical to add extra steps, simpler methods of Ru removal were tested first, such as the effect of reprecipitations and filtering through silica with no scavenger. Inductively coupled plasma (ICP) was used to measure the quantity of Ru remaining.

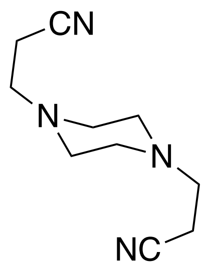

Figure 3. 9: Structure of Ru scavenger molecule SnatchCat®

The target degree of polymerisation (DP) for the polymers was 320 and ^{1}H NMR spectroscopy was used to show 100 % conversion of monomer. The total amount of Ru present if no purification had taken place was calculated to be 1590 ppm.

Reprecipitating the polymer had a significant impact on reducing the levels of Ru in the product. This would be the Ru that is non-chelated to the polymer backbone and has been cleaved from the chain by EVE. Filtering through a short column of silica had a negligible impact on the Ru levels however a significant decrease in yield was observed. A sticky brown layer of polymer formed on top of the silica and began crosslinking and becoming insoluble showing that either the polymer crosslinked before it could be filtered, or the ruthenium-SnatchCat-polymer complex all bound to the silica although this must have been strong since addition of DCM did not dissolve this.

The addition of SnatchCat® led to a decrease of ruthenium levels to 28 ppm however, there was also a decrease in yield of the polymer. This was due to passing the polymer through silica gel to collect the SnatchCat® complex and even with excess solvent passed through, a brown, thick polymer layer sat on top of the gel (Table 3. 2). Even with levels this low the methacrylate functional group still crosslinked and became an insoluble solid.

Table 3. 2*:* Residual Ruthenium levels determined by ICP-MS. * A – 1 precipitation, B – 2 precipitations, C – 2 precipitations then filtering through silica, 4 – 2 precipitations, 30 minutes with 4.4 eq. SnatchCat® then filtering through silica.

Ruthenium Removal Method	Ruthenium Remaining / ppm	S.D.	Yield / %
1	209	21	92
2	49	24	81
3	48	4.1	69
4	28	2.2	55

The results show these methods do not allow the complete removal of Ru from PNBMMA. In the rest of the chapter the polymer was used quickly after synthesis and the remaining solvent from synthesis and precipitation was calculated by ^{1}H NMR spectroscopy and taken into consideration in the adhesive formulation.

3.3.5 Thermal degradation of P(MMA-*co*-NBMMA)

The PMMA adhesives were formulated using a 9:1 mol. ratio of MMA: ethylene glycol dimethacrylate (EGDMA), this will be termed “M1” before crosslinking and “M1X” after. Free radical polymerisation (FRP) was used to cure the adhesive using a benzoyl peroxide (BPO) and 4,*N,N*-trimethylaniline (TMA) redox initiation system, creating M1X. PNBMMA was added to the M1 mixture quickly after the ROMP synthesise. A small amount of drying had taken place to purify the polymer, however this had to be balanced with maintaining the solubility before crosslinking. The M1-PNBMMA liquid adhesives were a light brown colour due to the presence of Ru and had increased viscosity with increased levels of PNBMMA.

Due to the rapid initiation and propagation using G3, it was easy to control the DP of the ROMP polymers. Hence, the effect of the chain length on the degradation temperatures of the resultant polymers were compared to the adhesives with and without 10 wt% of monomer (Figure 3. 10).

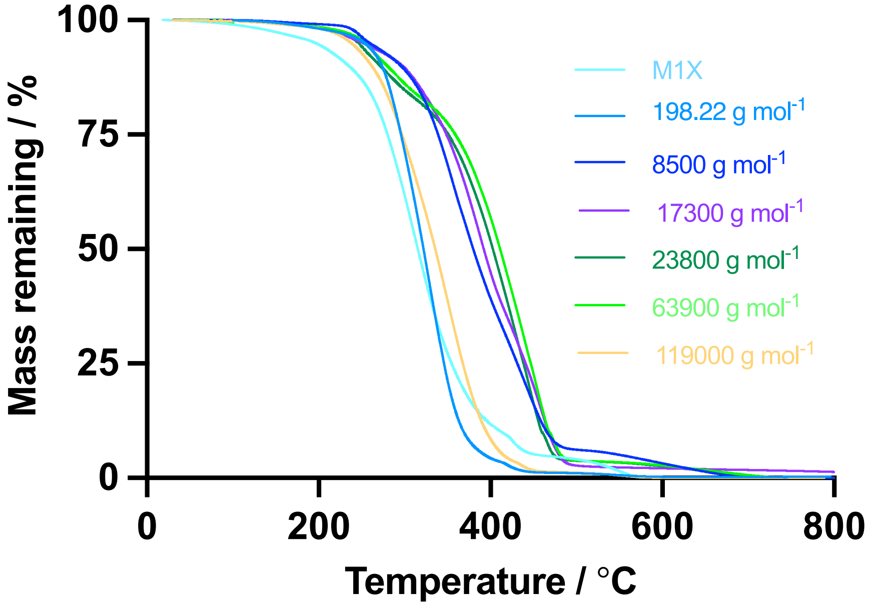

Figure 3. 10: Graph to show the effect of the M_w of PNBMMA when 10 wt% is added to the MMA adhesives.

The thermal degradation of M1X began at a low temperature of around 100 °C and the temperature where 5 % of mass had been lost, $T_{5\%}$, was 196.2 °C (Table 3. 3). The $T_{5\%}$ of the M1X adhesives containing PNBMMA were similar around 250-260 °C with the 119 000 g mol^{-1} being slightly lower than lower M_w PNBMMA.

Table 3. 3: The degradation temperatures of the 10 wt% PNBMMA adhesives

M_w / g mol^{-1}	$T_{5\%}$ / °C	$T_{10\%}$ / °C	$T_{50\%}$ / °C
M1X	196	235	315
198	253	274	322
8500	259	296	380
17300	252	297	392
23800	246	272	403
63900	254	280	411
119000	238	262	336

The M_w had a bigger impact on the $T_{50\%}$ where 50 % of the mass had been lost. This increased with an increase in M_w until the 119 000 g mol^{-1} polymer where phase separation was more likely to have occurred.

In a radical polymerisation, NBMMA reacts primarily through the more reactive MMA functional group however, the NB alkene is also able to participate in the polymerisation.[117] Thus, statistical copolymers would be formed with MMA as the predominant bond. Since PMMA depolymerises through an 'unzipping' mechanism the incorporation of these norbornene groups might disrupt the linear chain, blocking the 'unzipping' and making the polymer more thermally stable. The samples with PNBMMA do not have norbornene alkenes but still have accessible unsaturated carbon bonds on the PNBMMA backbone.

Reasons for the increase in chain length improving the $T_{10\%}$ and $T_{50\%}$ could be that the 'unzipping' process takes longer due to the lengthening chains. The proximity of the non-methacrylate radical bonds might lead to more temperature resistant areas of adhesive.

The effect of increasing the amount of PNBMMA within the adhesive was tested with the greater the amount of PNBMMA promoting the greater thermal stability of the material (Figure 3. 11). The reason for this might be that there is more disruption to the PMMA chain meaning that the 'unzipping' depolymerisation process is much slower.

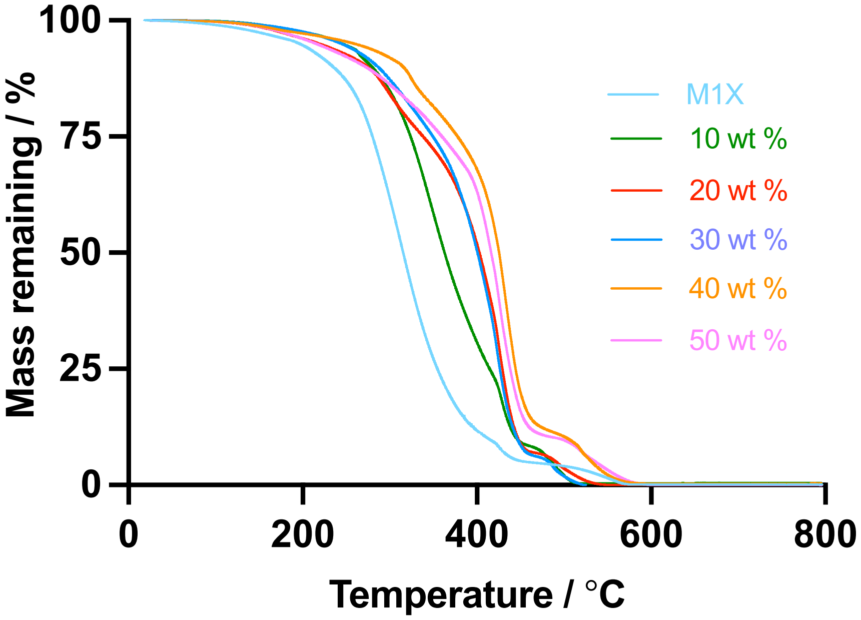

Figure 3. 11: The effect of increasing the PNBMMA concentration within a PMMA adhesive

All three degradation points, $T_{5\%}$, $T_{10\%}$ and $T_{50\%}$ increase as the amount of PNBMMA in the adhesive increases until 50 wt% (Table 3. 4). As the amount of PNBMMA in the starting adhesive formulation increases the viscosity increased significantly, meaning that it would be more difficult for the methacrylate groups to move through the material during the cure, which leads to a greater number of MMA end groups for initiating depolymerisation.

Table 3. 4: The degradation temperatures of PMMA adhesives containing PNBMMA

Wt% PNBMMA	$T_{5\%}$ / °C	$T_{10\%}$ / °C	$T_{50\%}$ / °C
0	196	235	315
10	245	279	363
20	219	274	403
30	244	286	401
40	259	315	426
50	215	272	416

3.3.6 Shrinkage

To measure the shrinkage of the methacrylate adhesives, the density of the uncured liquid and cured solid adhesive was determined and the percentage difference calculated. To calculate the solid density a helium pycnometer was used to find the volume by the displacement of helium gas compared to the weight. For each sample, 10 cycles were carried out and the mean calculated. This method was found to be not suitable for the liquid density since MMA is volatile so was displaced from the first chamber to the second, extension chamber, making it appear as though the volume decreases over cycles.

A density meter was used to find the density of the liquid adhesive. Some of the adhesives had a high viscosity and the capillary of the density meter was narrow, so dilutions were made and then extrapolated to 100% adhesive. ^{1}H NMR spectroscopy had shown that 16.1 wt% methanol was remaining in the PNBMMA homopolymer which could not be removed without crosslinking and losing solubility, so this was included in the density calculations.

The density of the adhesive after cure is greater than before curing because more monomers are held together by shorter covalent bonds rather than longer van der Waals' and dipole-dipole interactions (Table 3. 5). The solid density however decreases as the proportion of PNBMMA increases. This could be due to a reduction in crosslinking due to the viscous solution preventing radicals and monomers flowing through the solution.

Table 3. 5: The density of the adhesives before and after curing and the shrinkage between the two.

Wt% PNBMMA in M1	**Liquid Density / g cm^{-3}**	**Solid Density / g cm^{-3}**	**Shrinkage / %**
0	0.95	1.19	26
10	0.98	1.19	21
20	1.01	1.18	16
30	1.09	1.17	7.3
40	1.10	1.16	5.6
50	1.13	1.15	1.9

As the amount of pre-polymerised material within the adhesive increases the shrinkage decreases (Figure 3. 12). Low shrinkage is considered beneficial in an adhesive as it can reduce the internal stresses and leave an even distribution across the substrate.

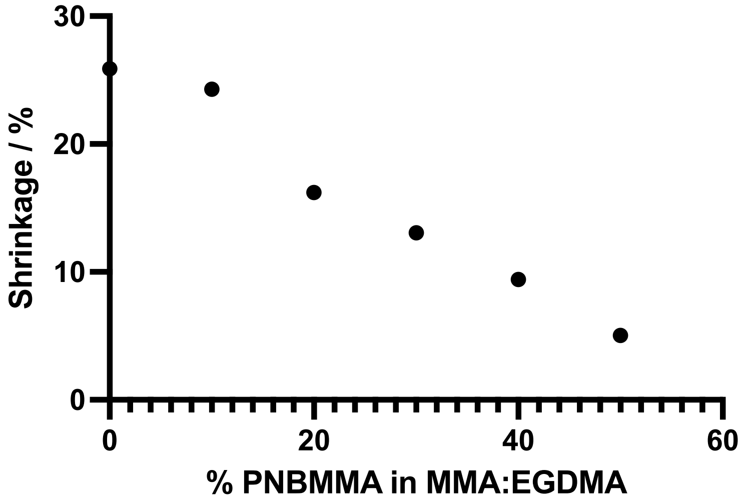

Figure 3. 12: Graph to show the decrease in shrinkage as the proportion of PNBMMA in adhesive formulation increases.

3.3.7 Lap Shear Adhesive Testing

Aluminium lap shears were first prepared by acid-etching using a ferric sulfate and sulfuric acid mix known as P2 (2.4.2). This pre-treatment forms a fresh oxide layer on the aluminium substrate which improves bonding to the adhesive and creates pores which increase the surface area of the bond.[17, 147] A small amount of glass beads, 230-300 μm, were added to give the bond a consistent width.

The M1X adhesives on aluminium substrates were unable to withhold significant stress (Table 3. 6). The adhesives with no PNBMMA had very low viscosity, allowing the adhesive to flow out of the join before curing, resulting in the bonding becoming thinner and weaker. This could be improved by adding some pre-polymerised PMMA to increase the viscosity. The sample with 10 wt% PNBMMA could hold a higher stress since it was slightly more viscous. However, this could not be defined as a structural adhesive, which is typically considered to have a strength around 20 MPa.[5] The 20 wt% PNBMMA lap shears were very weak and all samples broke during transport to the tensometer. The 30-50 wt% samples were not strong enough to be removed from the jig after preparation.

Table 3. 6: Average displacement and force of the aluminium lap shears bonded with the PMMA-NBMMA adhesives.

Wt% of PNBMMA in adhesive	**Av. Displacement / mm**	**Av. Bond Strength / MPa**	**S.D.**
0 wt%	0.646	0.53	0.163
10 wt%	1.33	1.73	0.551
20 wt%*	-	-	-

Compressive lap shears using poly(vinyl chloride) (PVC) substrates which are also used as a standard within industry were used as an alternative to aluminium. The lap shears are formed from a larger rectangular piece and a smaller square piece with the adhesive in between. Glass beads with a diameter of 212-300 μm were used to maintain a fixed bond diameter and no post-cure was used however the adhesives were left for at least 24 hours in ambient conditions before testing. The strength of the bond was tested by holding the lap shear in a jig and applying a force upwards on the smaller piece (Figure 3. 13).

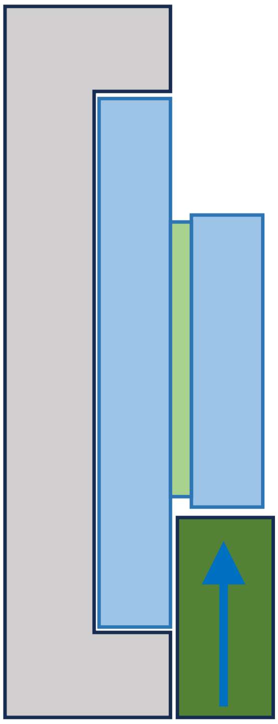

Figure 3. 13: Diagram of PVC compressive lap shear in the jig with the force applied upwards onto the smaller PVC piece.

An adhesion promoter in the form of 5 wt% of methacrylic acid (MAA) was also added to increase polarity and form non-covalent hydrogen bonding. Small organic acids such as MAA and maleic acid are commonly used additives in adhesive formulations.

Initially the 0 and 10 wt% PNBMMA adhesives were tested without the addition of the MAA-adhesion promoter (Figure 3. 14). The 0 wt% adhesive with no MAA had a stronger bond than the 10 wt% with MAA. This could be due to the lower viscosity making it able to permeate the PVC better. Additionally, it is a more polar adhesive as it lacks the non-polar norbornene, this increases the number of non-covalent interactions.

After 5 wt% MAA was added the bond strength of all of the adhesive mixtures improved with the 0 % having the smallest increase. As before, with the amount of non-polar PNBMMA increasing beyond 10 wt%, the bond strength of the lap shears decreased. As well as the polarity decreasing, the viscosity of the adhesive increased so there could be less plasticisation as the adhesive filled pores in the substrate.

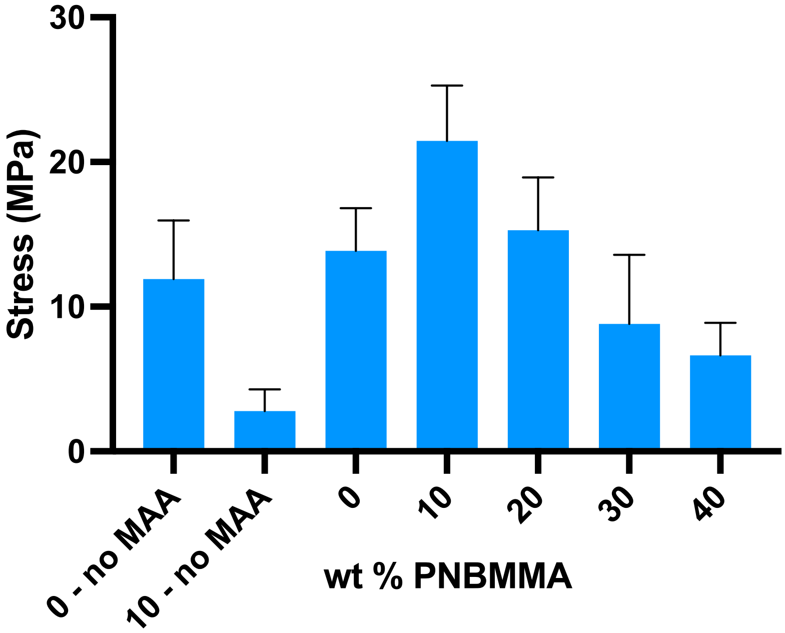

Figure 3. 14: The effect of the PNBMMA in the PMMA adhesives on the stress of the compressive lap shears

The main failure of the lap shears was substrate failure. For the 0, 10 and 20 wt% adhesives with MAA, as the displacement increased, the stress increased linearly until it began to either level off or drop. At this point the PVC substrate began to deform and bend (Figure 3. 15). For the 30 and 40 wt% adhesives, rather than the PVC changing shape, it shattered after reaching its peak stress.

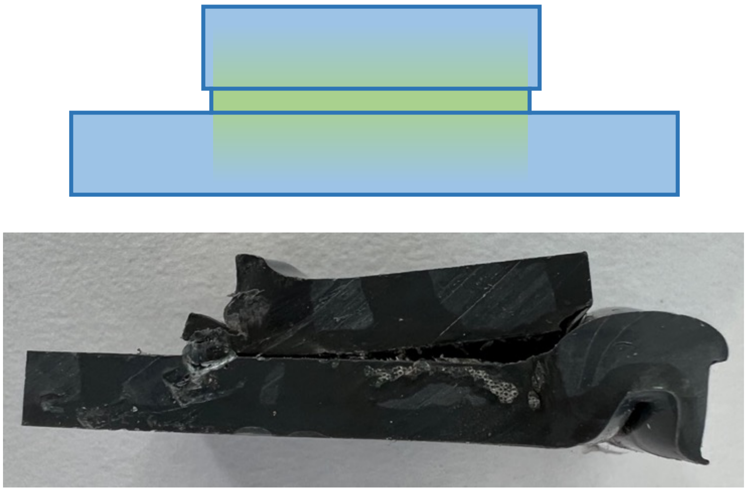

Figure 3. 15: Diagram of a lap shear showing plasticisation of the adhesive into the PVC and a photo of 10 wt% PNBMMA adhesive PVC compressive lap shear after testing.

To test how the viscosity of the adhesive influences the maximum strength it can withstand, some of the monomer MMA was removed and replaced with PMMA synthesised by FRP (M_w = 30 000 g mol^{-1}, $Đ_M$ = 1.74).

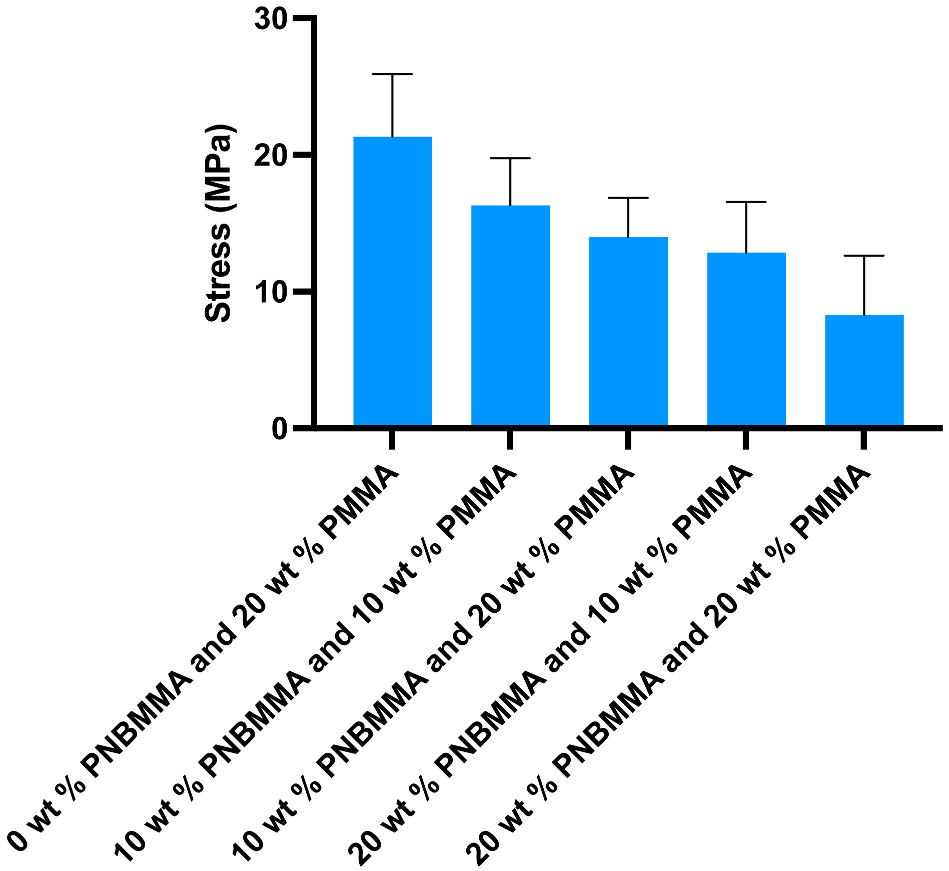

Figure 3. 16: Graph to show the effect of increasing the viscosity on the adhesive strength of PVC compressive lap shears with 5 wt% MAA.

3.3.8 Effect of MMA on the shrinkage and thermal properties

The shrinkage of the 0 – 20 wt% adhesives containing the MAA were measured to determine how the MAA altered the shrinkage given that it has high polarity so can form stronger non-covalent bonds, pulling the monomers closer together (Table 3. 7). Five repeats of the measurements were taken, and the shrinkage was found to decrease compared to samples without MAA since the density of the starting material was higher than without the MAA.

Table 3. 7: Solid and liquid density of P(MMA-*co*-NBMMA) adhesives with 5 wt% MAA. [a]Calculated using diluted solutions in a density meter and extrapolating densities to 100 % adhesive [b]calculated by helium pycnometer.

Wt% PNBMMA	**Liquid Density /g cm^{-3} [a]**	**Solid Density g cm^{-3} [b]**	**Shrinkage / %**
0	0.967	1.182	22
10	1.023	1.183	15
20	1.037	1.189	14

3.3.9 Copolymerising NBMMA with NBCA

PNBMMA has a low polarity which means that it reduces the polarity and surface wetting mixtures with PMMA adhesives. To improve surface wetting but maintain the high thermal stability from the unsaturated norbornene backbone, NBMMA was copolymerised with a carboxylic acid functionalised norbornene.

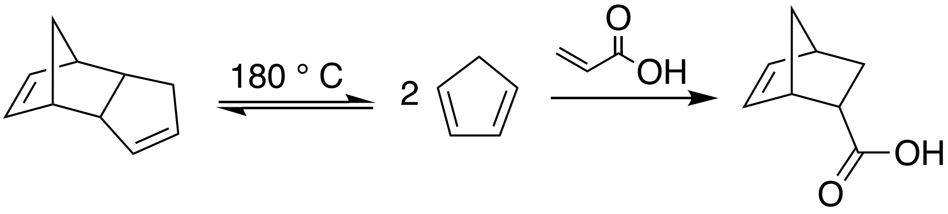

Scheme 3. 5: Reaction scheme for the synthesis of NBCA

5-Norbornene-2-carboxylic acid (NBCA) can be synthesised by cracking DCPD to form CPD and then adding it directly to acrylic acid where it undergoes a [2 + 4] Diels-Alder (DA) reaction to give a majority *exo* isomer product at room temperature (Scheme 3. 5). Due to the proximity of the ester group to the norbornene, the Ru initiator can interact with the C=O bond, stabilising the intermediate and thus ROMP is much slower than for the PNBMMA homopolymer.[85]

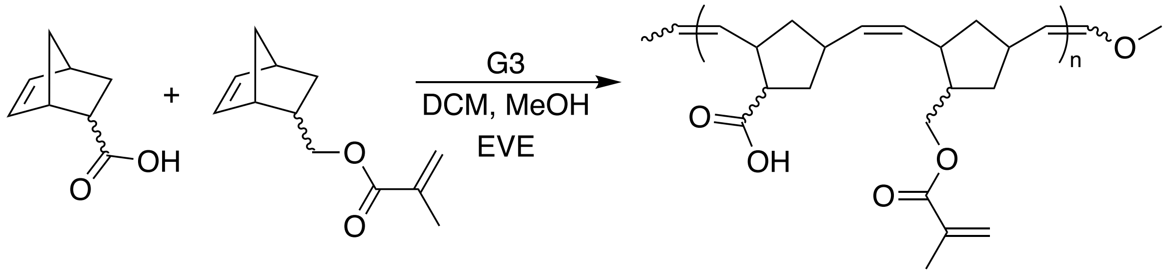

Scheme 3. 6: Copolymerisation of NBCA and NBMMA

Copolymers were synthesised in a 1:1 and 4:1 molar ratio of NBMMA to NBCA using G3. The ROMP polymerisation was significantly slower than for PNBMMA. Hyatt *et al*. suggested that the double bond in the ester is in close proximity to the ruthenium centre in the initiator and so chelates, stabilising the intermediate and slowing k_p.[85]

^{1}H NMR spectroscopy showed that there was 100 % conversion of both monomers after 45 minutes with a target DP of 320. Similar to the PNBMMA homopolymer, the residual ruthenium-complex is difficult to remove, and the polymer crosslinked before all solvent could be removed and therefore, some hexane from the precipitation remained in the ^{1}H NMR spectrum (MeOD). The methacrylate resonance integrals compared to unsaturated backbone resonance integrals were 1:2 as expected (Figure 3. 17).

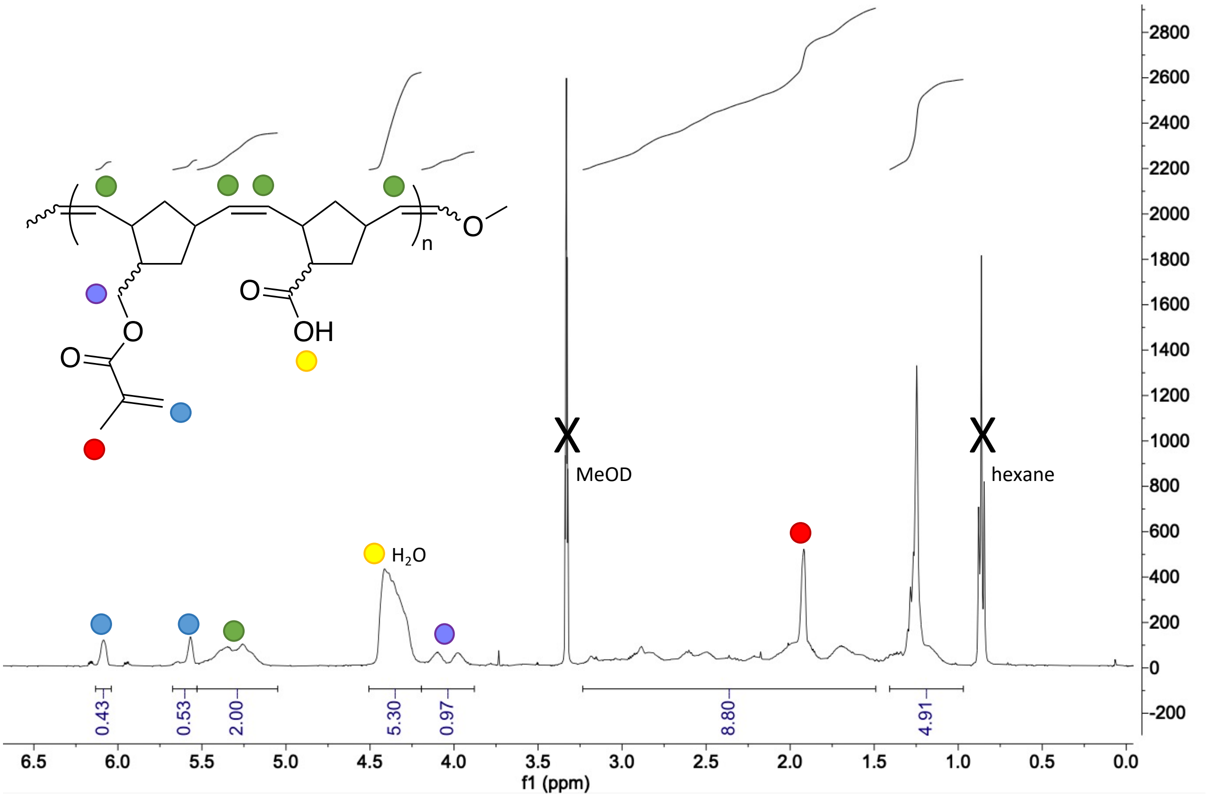

Figure 3. 17: ^{1}H NMR spectrum (MeOD) of P(NBMMA-*co*-NBCA) in a 1:1 mol. ratio

SEC could not be carried out on these polymers since the acid groups would mean that they would adsorb to the column. It was not possible to methylate the polymer since it is unstable and cannot be purified. Differential scanning calorimetry (DSC) analysis was used to find the T_g of the 1:1 mol. ratio copolymer and found one transition at -13 °C which is lower than the PNBMMA homopolymer (18 °C) (Figure 3. 18).[148] The blockiness of the statistical copolymers was not determined.

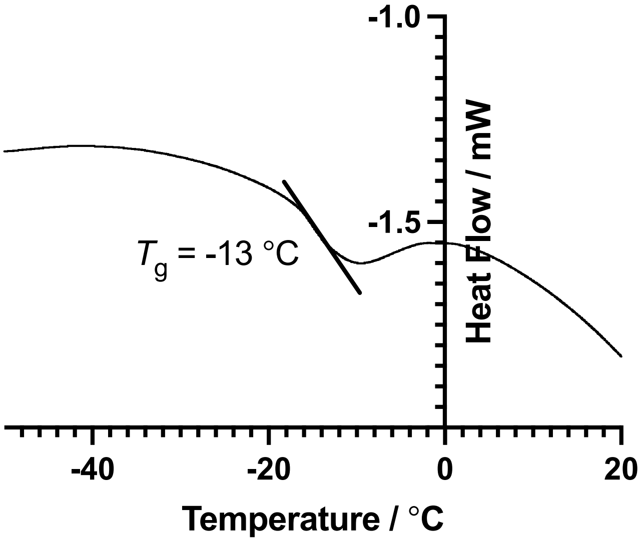

Figure 3. 18: DSC thermogram of P(NBMMA-*co*-NBCA) in a 1:1 mol. ratio showing one T_g

PVC compressive lap shears were made up with 10 wt% of copolymers of NBMMA and NBCA in a 1:1 and 1:4 ratio. No MAA was added since the acid group was introduced within the NBCA. The adhesive was cured using the same BPO and TMA redox reaction and the addition of glass beads with a diameter of 212-300 μm to maintain the bond width.

It was shown that incorporating the carboxylic acid into the polynorbornene had a significant improvement on the adhesive strength of the PMMA adhesive in comparison to the NBMMA homopolymer although not as much as the homopolymer with 5 wt% MAA (Figure 3. 19). The 1:1 mol ratio NBMMA and NBCA copolymer cured within PMMA to form a cloudy solid suggesting there was phase separation, yet still showed good adhesive strength.

Unlike the 10 wt% PNBMMA with 5 wt% MAA which underwent substrate failure where the PVC was deformed, both of the copolymers had substrate failure with the PVC fracturing into many pieces.

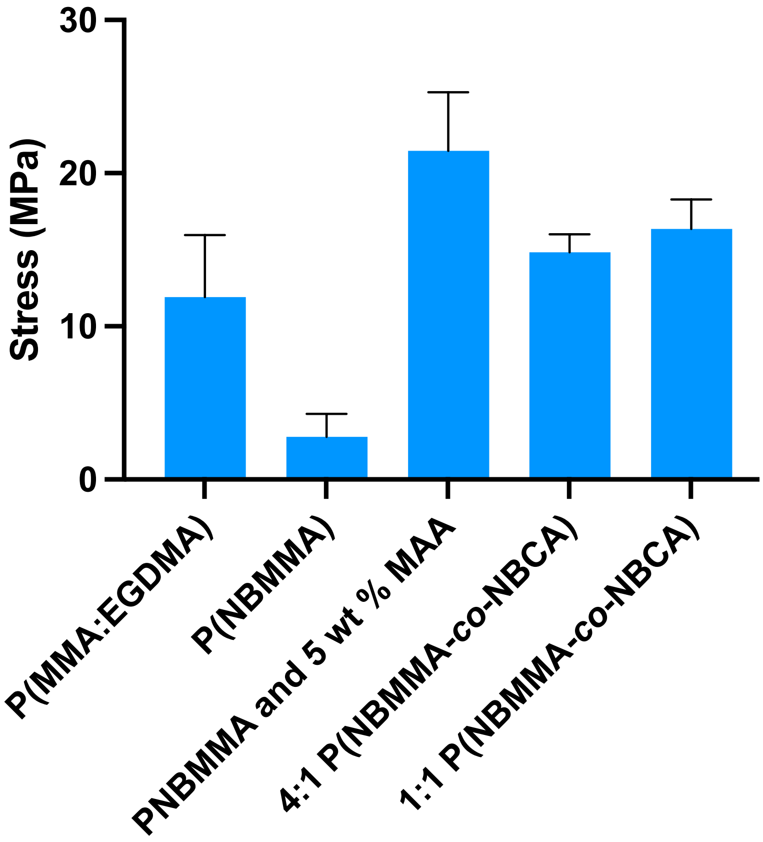

Figure 3. 19: PVC lap shear results of the 4:1 and 1:1 copolymers in comparison with the PNBMMA homopolymers with and without the MAA adhesion promoter

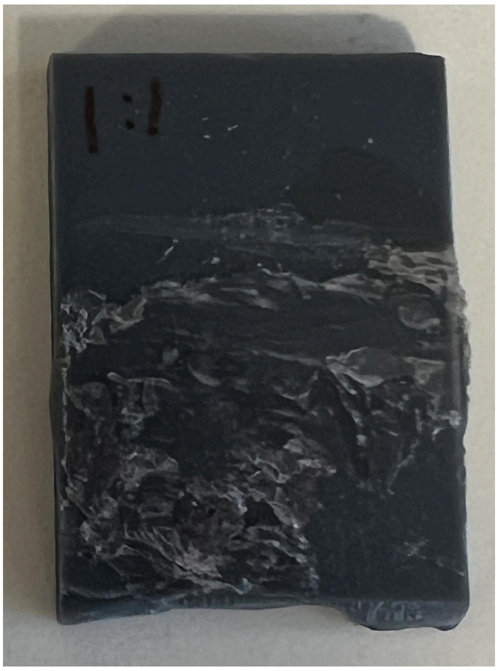

Figure 3. 20: Photo of PVC compressive lap shear after testing with 1:1 P(NBMMA-*co*-NBCA)

The levels of carboxylic acid in the M1X-poly(norbornene) are still relatively high at 4 and 1 wt% NBCA content in comparison to commercially available adhesives. The NBCA: NBMMA molar ratio was reduced to three new mixtures of 1:10, 1:20 and 1:30 and PVC compressive lap shears were prepared (Figure 3. 21). The stress that was achieved by the 4:1 ratio and 10:1 molar ratios were similar but there was a big decrease reducing from 20:1 to 30:1 (Figure 3. 19). The failure mechanism for the 10:1 was substrate failure whilst it was adhesive failure for the 20:1 and 30:1. This shows that addition of NBCA at even very small levels has a slight improvement on the strength although an additional adhesive promoter would be needed to meet the requirements for a structural adhesive.

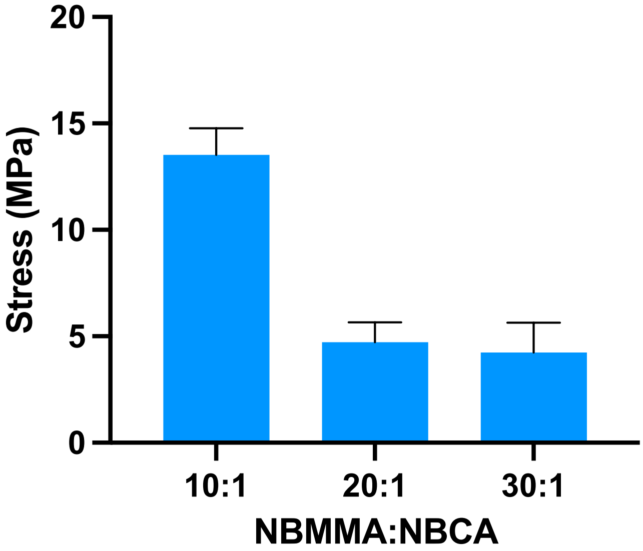

Figure 3. 21: PVC lap compressive lap shears with 10 wt% P(NBMMA-co-NBCA) copolymers in PMMA

3.3.10 Hydroxyl functionalised monomer

As an alternative to copolymerising with NBCA, a more polar methacrylate functionalised norbornene monomer was synthesised. 2-Hydroxy-3-[(2-methyl-1-oxo-2-propen-1-yl)oxy]propyl bicyclo[2.2.1]hept-5-ene-2-carboxylate (NBGMA) was synthesised through epoxy ring-opening of glycidyl methacrylate (GMA) with NBCA (Scheme 3. 7). This monomer has two ester bonds and a hydroxyl group which can promote polar intermolecular interactions and hydrogen bonding, improving substrate wetting.

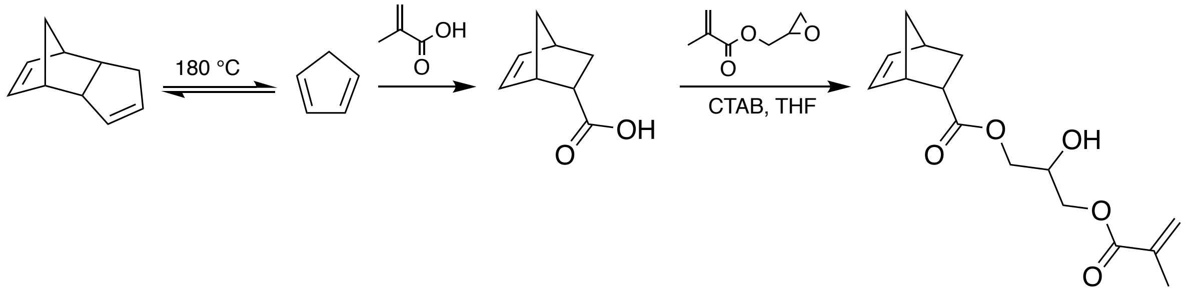

Scheme 3. 7: Reaction scheme to form NBGMA through Diels-Alder addition of CPD with acrylic acid and consequent ring opening esterification with GMA

NBGMA was polymerised with G3 to form PNBGMA with a target DP of 300. The polymerisation appeared to take longer to reach a high viscosity so was left for 1 hour before being quenched with EVE. Similarly, to the NBCA copolymers, the M_w could not be determined through SEC since the polar groups would adsorb to the column.

PNBGMA was a sticky, low viscosity, polymer that appeared to have a low T_g and similarly to PNBMMA, rapidly crosslinked at room temperature when the solvent was evaporated. This meant that DSC analysis could not be used to determine the T_g of the base polymer. ^{1}H NMR spectroscopy showed the shift in resonance of the norbornene alkenes from δ=6.24-5.90 ppm

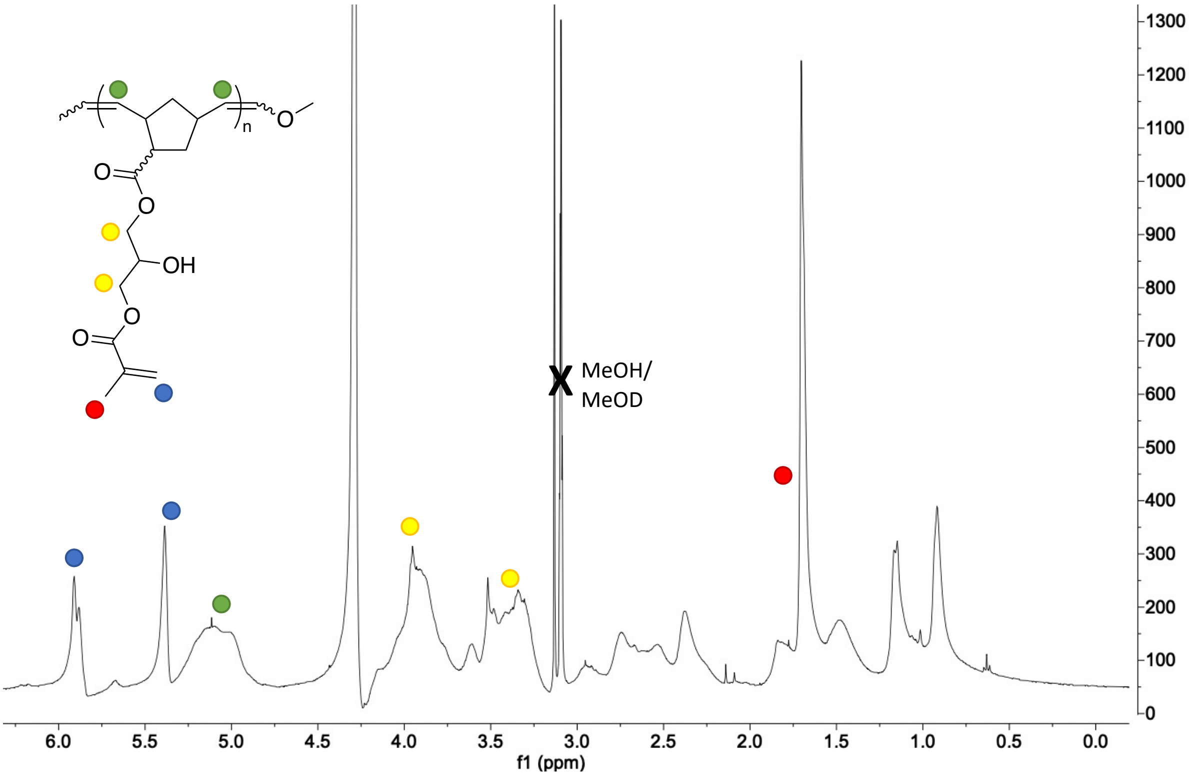

Figure 3. 22: ^{1}H NMR spectrum of PNBGMA in $CDCl_3$ and MeOD

10 wt% of PNBGMA was added to the PMMA adhesives and PVC compressive lap shear tests were carried out to determine the effect on the adhesive strength. The polymer appeared to fully dissolve into the MMA but, upon curing the product appeared cloudy suggesting that there was some precipitation and phase separation. A copolymer of NBMMA and NBGMA using a 1:1 molar ratio of each monomer was also synthesised and used for adhesive testing. This showed no visible phase separation after curing.

10 wt% of the new polymers were added to M1 and crosslinked to form M1X. Lap shear tests were made to see if they could withstand higher stress than the original PNBMMA polymer (Figure 3. 23). The presence of the hydroxyl group and second ester group increased the polarity and thus, increased the non-covalent interactions to improve the bond strength. If 5 wt% of MAA was added as an

adhesion promoter, the maximum stress could be increased and potentially exceed the 20 MPa requirement to be classed as a structural adhesive.

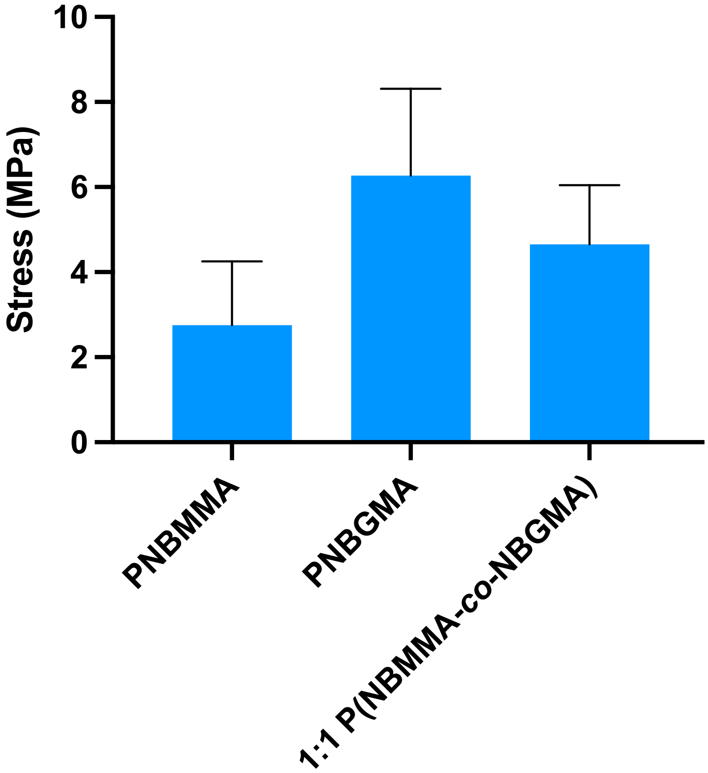

Figure 3. 23: Comparison of 10 wt% of different functionalised polynorbornenes in PMMA adhesive

3.3.3 Conclusions

A methacrylate functionalised polynorbornene was polymerised using a Ru Grubbs initiator with 100% conversion of monomer, as determined by ^{1}H NMR spectroscopy, producing a polymer with an unsaturated polynorbornene backbone and intact methacrylate groups. The high concentration of alkenes in the polymer made Ru removal challenging and the initiator caused radical crosslinking between the remaining alkene groups making the polymer insoluble. This meant that the methacrylate functionalised polymers produced could not be dried and completely isolated.

PMMA thermosets typically begin degrading at low temperatures through an ‘unzipping’ mechanism however incorporation of 10 wt% of either monomer or polymer form of NBMMA leads to a significant increase in this temperature stability. The longer the polymer chain the higher the $T_{50\%}$ of the adhesives until the DPs of the polymer exceeded 500.

The shrinkage of the PMMA adhesives decreased as the percentage of PNBMMA increased due to a smaller quantity of short covalent bond formation. This remained true for adhesives containing a MAA adhesion promoter despite the increased dipole-dipole and hydrogen bonding.

To compare the strength of the adhesive, PVC compressive lap shear tests were carried out. It was shown that addition of PNBMMA has a negative effect on the adhesive strength of the PMMA since it reduces the polarity and therefore the surface wetting. Addition of 5 wt% MAA compensates for this and increases the stress the bond can withstand although this also decreases with increasing PNBMMA concentration.

NBMMA was then copolymerised with a carboxylic acid functionalised norbornene monomer which gave improved adhesive properties over PNBMMA despite there being less than 5 wt% acid groups. Phase separation meant that there could be regions of higher concentrations of polar acid groups which lead to an increase the bond strength.

A more polar methacrylate polymer was synthesised containing two ester groups and a hydroxyl. This was observed to polymerise slower due to chelation of an ester group with the Ru but, it also crosslinked slower with a larger amount of solvent remaining. The polymer was soluble in MMA, although there was visible phase separation after curing as the sample turned cloudy. The increased polarity increased the adhesive strength of PVC compressive lap shears.

Chapter 4 - Norbornene crosslinkers for PDCPD adhesives

4.1 Introduction

4.1.1 ATRP

Atom transfer radical polymerisation (ATRP) is a controlled radical polymerisation (CRP) technique that was developed by Matyjaszewski and co-workers in the mid-1990s. It can allow high molecular weights and narrow dispersities of polymers by minimising the chain termination reactions through repeated activation and deactivation (Figure 4. 1).[149]

Standard ATRP begins with a transition metal catalyst (commonly Cu) which can exist in two oxidation states. At the beginning of the polymerisation, the catalyst is in the lower oxidation state before reacting with an initiator in the form of an alkyl halide.[46] This leads to an increase in oxidation number and creates an alkyl radical. This is the activated state, with a rate constant for its formation, k_{act}. Whilst in this state, the alkyl radical can react with monomers causing propagation of the polymer. The transition metal rapidly transfers the halide back to the alkyl group, deactivating the catalyst, with a rate constant, k_{deact}. K_{ATRP} is the ratio between k_{act} and k_{deact}. To ensure a small dispersity, at any time there should be a high concentration of dormant chains and the reaction should remain in the active state for as short a time as possible, i.e. K_{ATRP} should be low.[35]

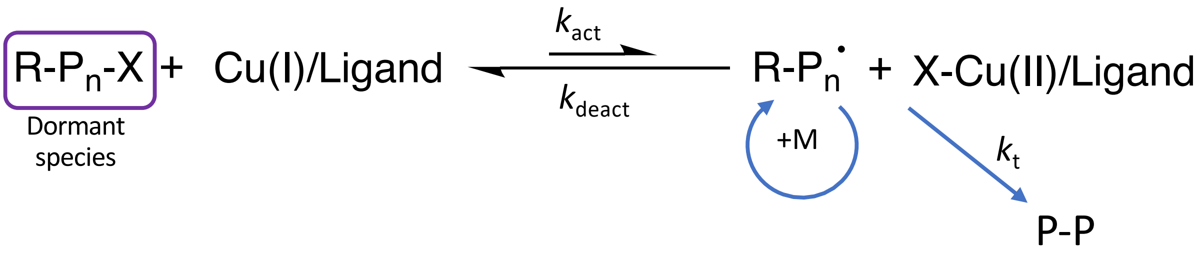

Scheme 4. 1: Reaction scheme for traditional ATRP

Control over an ATRP reaction can be achieved by selecting appropriate ligands and initiators. The greater the ability of the ligand to stabilise the halogen onto the metal catalyst, the smaller k_{deact} and the longer the duration of propagation. This results in a quicker yield but a greater dispersity as the chance for chain termination is higher. Similarly, the alkyl halide bond strength can be varied to gain control of the reaction, with the C-Br bond strength lower than the C-Cl bond strength, allowing for easier cleavage of the halide and therefore, a higher k_{act} and K_{ATRP}. Br is less electronegative than Cl so forms a more stable complex with the metal catalyst. This means that alkyl bromides have a greater K_{ATRP} than alkyl chlorides. Similarly, the more stable the radical is on the alkyl halide the greater K_{ATRP} tertiary alkyl halides stabilise radicals significantly better than secondary and primary alkyl halides which have similar K_{ATRP}.

4.1.2 AGET ATRP

The problem with standard ATRP is that it is very oxygen sensitive and requires careful preparation prior to the polymerisation to get the Cu into the lower oxidation state. Activator generated by electron transfer (AGET) ATRP was designed so that higher oxidation number catalysts could be used, avoiding the need to carefully prepare and store the catalysts under an inert atmosphere. It works by starting with a higher oxidation number catalyst and adding a reducing agent such as tin (II) 2-ethylhexanoate or ascorbic acid. This produces the active catalyst *in situ* and the polymerisation can propagate as with standard ATRP (Figure 4. 2).[150]

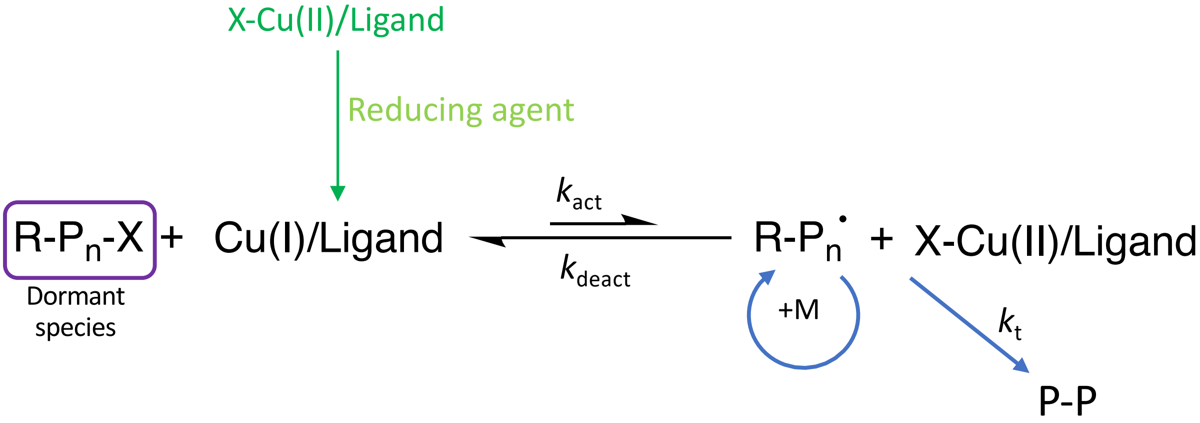

Scheme 4. 2: Reaction scheme to show the mechanism of AGET ATRP

4.1.3 Introducing functional groups into DCPD

DCPD contains only carbon and hydrogen atoms which makes it non-polar with a low surface energy and therefore would not be a good adhesive for polar adherends. This also reduces the opportunities for tunability and varying the properties such as the glass transition temperature (T_g), Young's modulus and tensile strength.[94, 126, 148, 151] The DCPD monomer also has a strong odour which is not desirable in a commercial product.[152]

Crosslinkers containing multiple norbornene groups are commonly used to increase the density and reduce the molecular weight between crosslinks (M_c) since norbornene has a much greater ring-strain (26.2 kcal mol^{-1}) compared to the cyclopentene moiety (4.5-6.8 kcal mol^{-1}).[90]

Caster and co-workers tried synthesising norbornene-based crosslinkers for DCPD adhesives to increase polarity. The structure of their crosslinkers were initially derivatives of anthraquinones and were polar solids. The solubility of these polar crosslinkers within the non-polar DCPD was a challenge. They then used benzonorbornadienes with methyl and ethyl groups on the norbornene bridgeheads to reduce polarity. They found that there was no benefit to the bond strength of steel substrates at room temperature but did improve performance at elevated temperatures.[153]

Norbornene based crosslinkers have been used to decrease the M_c, by reducing the need for the less-ring strained cyclopentene ring to undergo metathesis.[94, 153, 154] Moore and co-workers used crosslinkers with two and three norbornene groups and cured DCPD through frontal polymerisation with G2 (Figure 4. 1). Three of the crosslinkers contained ester linkages and the fourth contained an amide linkage. The M_c decreased with respect to poly(dicyclopentadiene) (PDCPD) for all 4 of the crosslinkers. The T_g of the PDCPD with the amide increased the most however this was not investigated much further in the study as a result of the lower solubility reducing the rate of frontal polymerisation. The yield strength with all crosslinkers improved by 12 % with respect to PDCPD homopolymer.[94] The group also showed that copolymerising DCPD with di-norbornene monomers has a non-monotonic increase in the rate of polymerisation. This is since there are more norbornene moieties in close-proximity with each other that can undergo ROMP more efficiently than the less ring-strained cyclopentene groups of DCPD. At very high crosslinker concentration this reaction rate decreases since the crosslinkers have a lower enthalpy of polymerisation (ΔH_p) so less heat is released.[155]

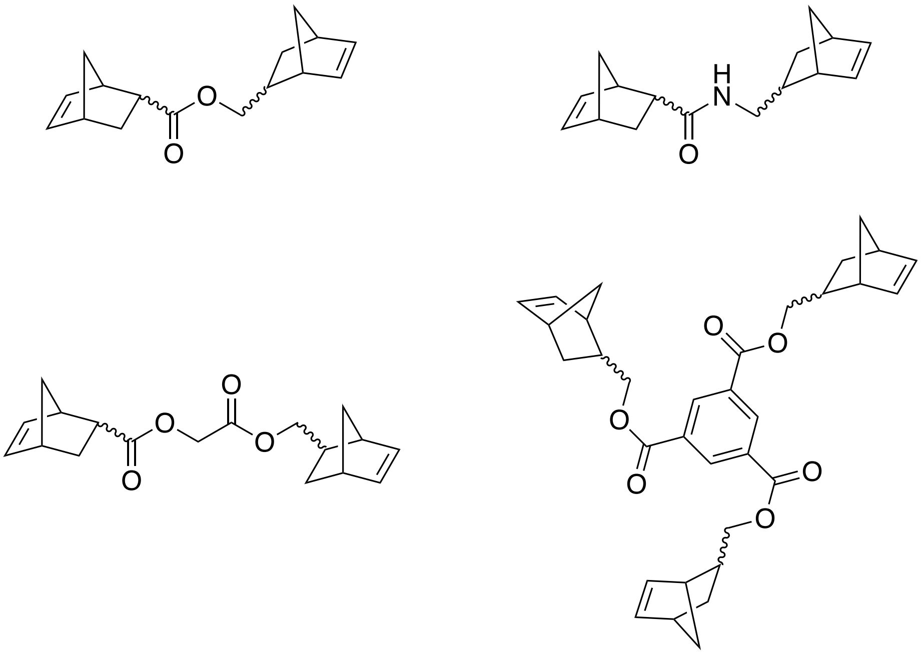

Figure 4. 1: Norbornene derived crosslinkers for reducing the M_c of PDCPD[94]

Further DCPD crosslinkers developed by Sheng *et al*. were analysed by differential scanning calorimetry (DSC). Norbornadiene was shown to be a bad crosslinker since only one of the alkene groups reacted. Addition of a crosslinker formed from joining two norbornene groups together was shown to have no effect on the cure kinetics however the T_g did increase with crosslinker concentration.[154]

Two methods to functionalise DCPD with heteroatoms have been reported. Lemcoff and co-workers reacted *endo*-DCPD with SeO_2 in an allylic oxidation to produce *endo*-hydroxydicyclopentadiene with the functional group at the C2-position on the cyclopentene ring which could further be modified through esterification and etherification (Scheme 4. 3. a). The functionalised monomers were still able to undergo crosslinking through ROMP but showed a significant reduction in the temperature at which thermal decomposition occurred and the T_g were found.[96, 152] Wulff and co-workers synthesised DCPD functionalised with ester and alcohol groups at the C3-position (Scheme 4. 3. b). These were unable to undergo crosslinking through ROMP allowing the production of linear PDCPD, however at high temperatures, around 180 °C, they crosslinked through radical addition to produce PDCPD with T_gs above 200 °C.[151, 156, 157]

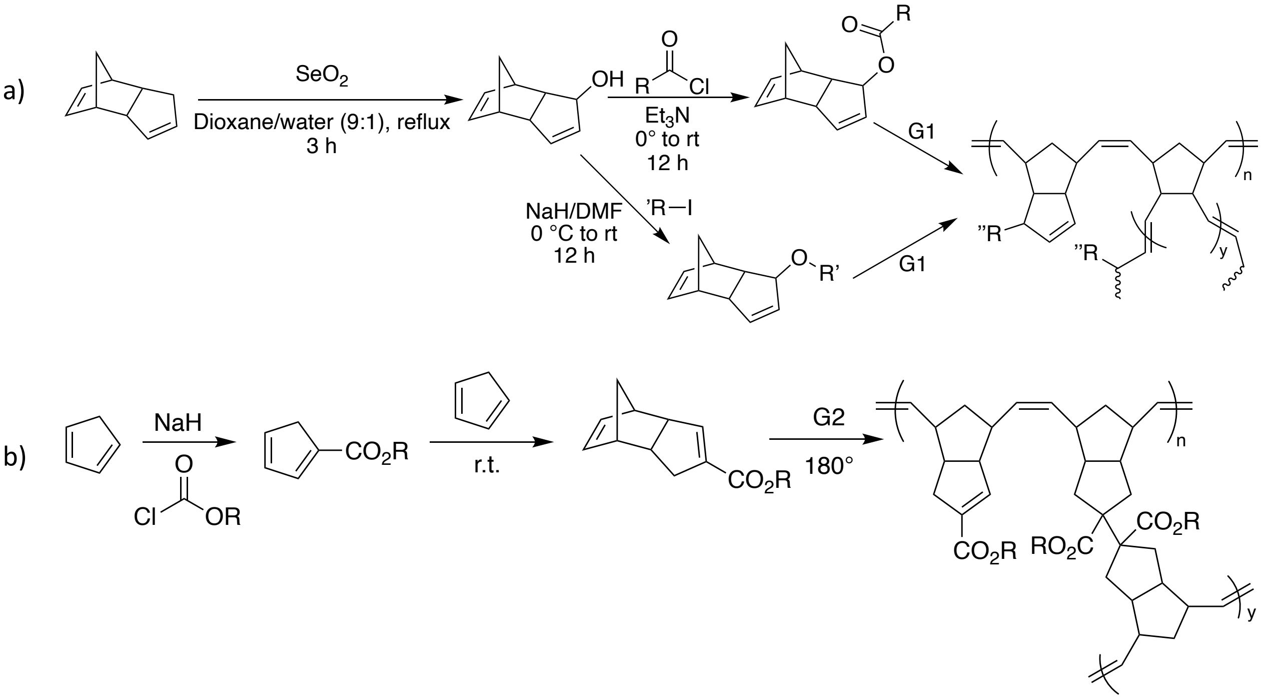
a)
SeO2
Dioxane/water (9:1), reflux
3 h
OH
R
Cl
O
Et3N
0° to rt
12 h
NaH/DMF
0 °C to rt
12 h
'R—I
O
R'
G1
G1
n
y
"R
"R
b)
NaH
O
Cl
OR
CO2R
r.t.
CO2R
G2
180°
n
CO2R
RO2C
CO2R
y

Scheme 4. 3: Scheme of the synthesis of PDCPD functionalised a) at C2 by Lemcoff and co-workers[152] and b) at C3 by Wulff and co-workers[151]

4.1.4 Chapter aims

The aims of this chapter are to formulate PDCPD adhesives which can withstand high levels of stress, high temperatures and cure at room temperature with low shrinkage. In order to do this 5-norbornene-2-methylene methacrylate will be polymerised through AGET ATRP and used as an additive within DCPD adhesives. The ester groups will increase the polarity of PDCPD to increase the non-covalent interactions with the adhesive and the norbornene groups will decrease the molecular weight between crosslinks (M_c) since they ring-open metathesise through ROMP more readily than cyclopentene. Additionally small molecule norbornene crosslinkers will be synthesised to increase the polarity and reduce M_c.

4.2 Results and discussion

4.2.1 Radical polymerisation of A-PNBMMA

The bifunctional methacrylate functionalised norbornene monomer, norbornene methylene methacrylate (NBMMA), was polymerised through AGET ATRP. This CRP was chosen over reversible addition fragmentation chain-transfer (RAFT) polymerisation as it does not depend on the rate of initiator degradation, therefore the polymerisation is in equilibrium from the start, giving low dispersities for small polymer chains. The resultant polymer was named A-PNBMMA to show that it has been synthesised through ATRP as opposed to ROMP in the previous chapter.

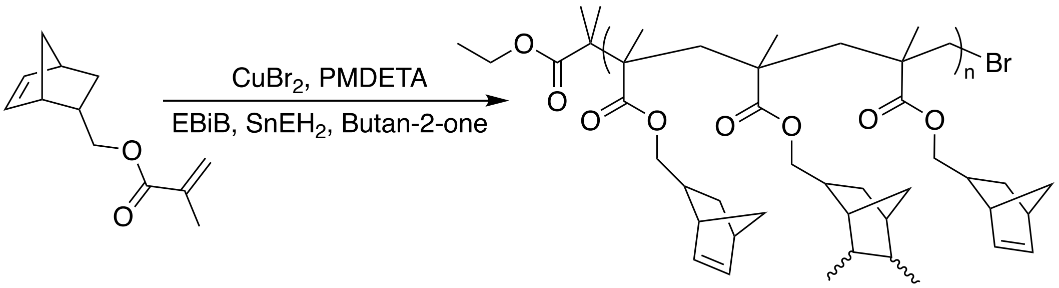

Scheme 4. 4: AGET ATRP synthesis of A-PNBMMA with the initiator EBiB

As previously reported, radical polymerisation has a high preference for the methacrylate functional group on NBMMA. Unlike ROMP, radical polymerisation also has some reactivity towards the norbornene alkene, particularly as the concentration of MMA decreases during the polymerisation.[115, 117] The reactivity ratios for the norbornene and MMA double bonds have been calculated to be r = 0.006 and r = 20 respectively.[117] During the polymerisation the monomer conversion was kept below 50 % to prevent hyperbranching and crosslinking. The resulting polymer was soluble in a range of organic solvents despite ^{1}H nuclear magnetic resonance (NMR) spectroscopy showing some crosslinking (Figure 4. 2). This can be seen through the reduction in norbornene alkene resonances, δ

= 6.2-5.8 ppm, from an integration of 2 to 1.77 with respect to the O-C$\mathbf{H}_2$ resonances between δ = 4.19-3.47 ppm. There are no remaining methacrylate alkene resonances at δ = 6.10 and 5.55 ppm.

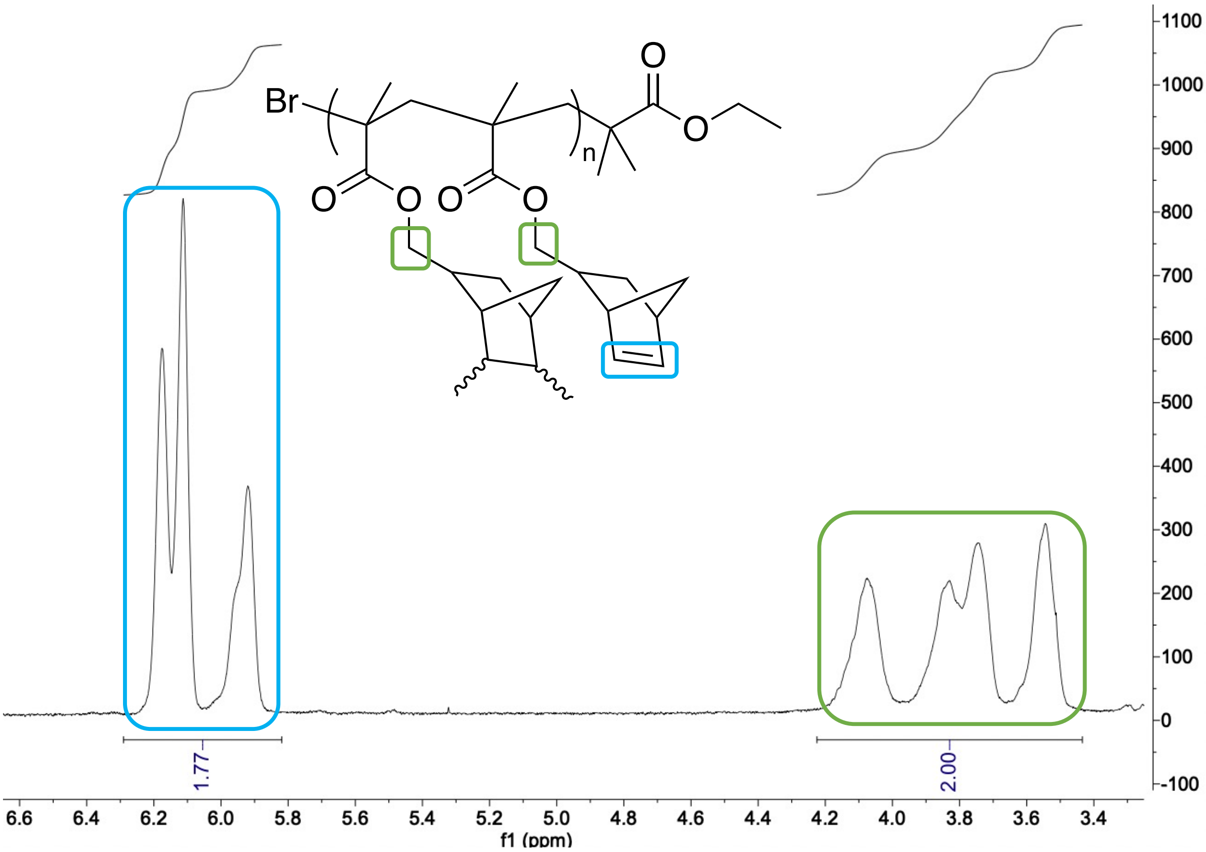

Figure 4. 2: ^{1}H NMR spectrum of A-PNBMMA to show that there is a decrease the norbornene alkene resonances with respect to the -C$\mathbf{H}_2$NB

DSC was used to determine the T_g to be 88 °C which is lower than the T_g of PMMA (Appendix 11). The branching through the norbornene alkene may be partly responsible as well as the large pendent groups, reducing the alignment of chains.

4.2.2 Effect of methacrylate polymer end group

The initiator used was ethyl α-bromoisobutyrate (EBiB) which leaves a bromine atom on the chain end of the polymer. Methacrylate polymers decompose through an 'unzipping' mechanism (1.1.10) so the terminal end groups have a large effect on the rate and temperature at which this process occurs.[158] The effect of the bromine was investigated by comparing the degradation of A-PNBMMA synthesised through free radical polymerisation (FRP) using azobisisobutyronitrile (AIBN) as an initiator with PNBMMA synthesised through AGET ATRP. A comparison was also made using AGET ATRP followed by end group substitution using Bu_3SnH to cleave the Br end group and replace it with a hydrogen.[159]

The polymer capped with the Br end group had the highest thermal degradation temperature followed by the AGET ATRP with the methacrylate groups capped on one end (Figure 4. 3). The FRP synthesised polymer had the lowest temperature onset of degradation because depolymerisation was able to be initiated from the end groups rather than from chain fission.

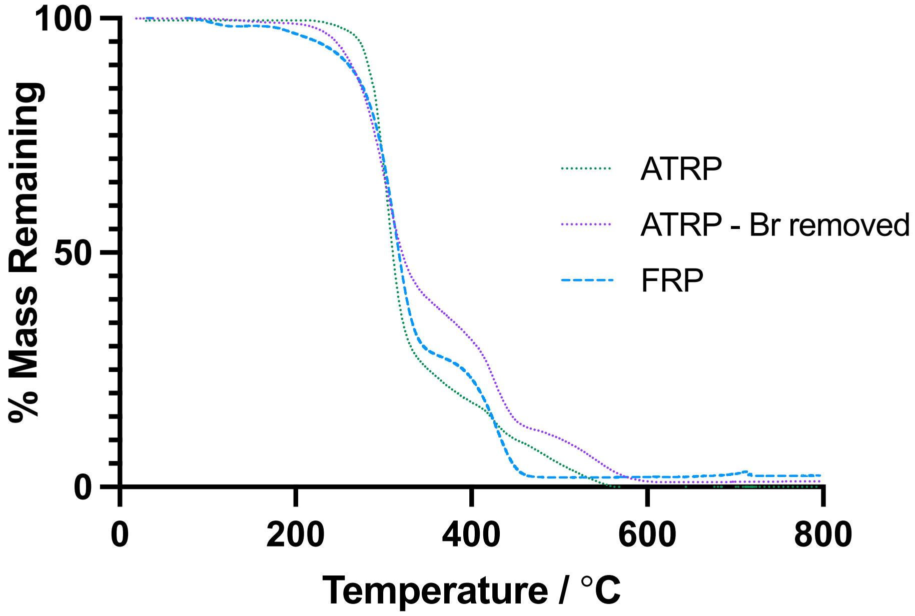

Figure 4. 3: Thermal gravimetric analysis (TGA) analysis showing the effect of the PNBMMA end groups on the degradation temperatures.

4.2.3 P(DCPD-*co*-A-NBMMA) polymers

A-PNBMMA was found to be insoluble in DCPD even after heating and leaving for 24 hours to dissolve. The poor solubility is due to the large polarity difference between the polymer and the DCPD monomer which contains only carbon and hydrogen atoms. In order to make a DCPD based adhesive some heteroatoms are required to have a higher polarity than pure DCPD leading to greater surface wetting and intermolecular bonding. In order to control the polarity of the polymer, NBMMA was copolymerised with a less polar methacrylate. The solubility of a series of methacrylate homopolymers in DCPD were tested (Table 4. 1). A low M_w was targeted in order to increase the potential for good solubility.

The smaller poly(methacrylate)s, such as PMMA and poly(*tert*-butyl methacrylate) (PBMA), were also insoluble in DCPD. However, when the pendent chain length was increased further such in poly(2-ethylhexyl methacrylate) PEHMA and poly(isobornyl methacrylate) (PIBMA) the polymers became sufficiently non-polar to be soluble in DCPD. Both of these were chosen to copolymerise with NBMMA as a consequence of their very different T_gs (-10 °C to 110 °C for PEHMA and PIBMA respectively) so would result in different properties. Poly(ethylene glycol dicyclopentenyl ether methacrylate) was also found to have good solubility in DCPD however this is less commercially available and more expensive so would not be a viable option for a commercially produced adhesive.

Table 4. 1: The solubility of methacrylate homopolymers in DCPD with their M_w and $Đ_M$ ^{a}determined by SEC (THF) and their T_gs from literature ^{b}determined by DSC[160]

Polymer	Structure of monomer	M_w / g mol^{-1a}	$Đ_M^a$	Soluble in DCPD?	T_g of homopolymer / °C^b
PMMA	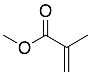	7000	1.18	✗	105
PEGDEMA	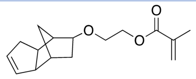	6700	1.12	✓	25-35[161]
PIBMA	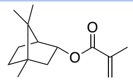	5100	1.21	✓	110
PBMA	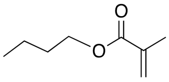	7600	1.20	✗	20
P^{t}BMA	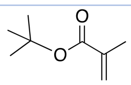	5600	1.22	✗	115
PEHMA	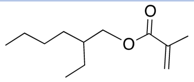	5100	1.14	✓	-10

4.2.4 Synthesis of P(EHMA-*co*-NBMMA) and P(IBMA-*co*-NBMMA) copolymers

Both EHMA and IBMA were copolymerised with NBMMA, targeting a 1:1 molar ratio although the ATRP reaction was quenched at approximately 50 % monomer conversion, determined by ^{1}H NMR spectroscopy, by exposing to oxygen and removing from the heat to prevent gelation through crosslinking of the unsaturated norbornene group.

^{1}H NMR spectroscopy showed that the methacrylate alkene resonances from both NBMMA and EHMA around δ = 5.5 and 6 ppm were completely consumed whilst the norbornene alkene resonances remained. In radical polymerisation, monomers have different preferences to react with themselves or other monomers so despite a 1:1 molar ratio being used in the polymerisation, an equal amount of each monomer was not expected in the copolymer. The amount of each monomer converted to polymer was determined ^{1}H NMR spectroscopy using the region between δ = 4.4 and 3.4 ppm (Figure

4. 4). The integrals for the NBMMA **H**C=C bond can be subtracted from the EHMA resonance to give the amount of EHMA in the polymer (Equation 4. 1).

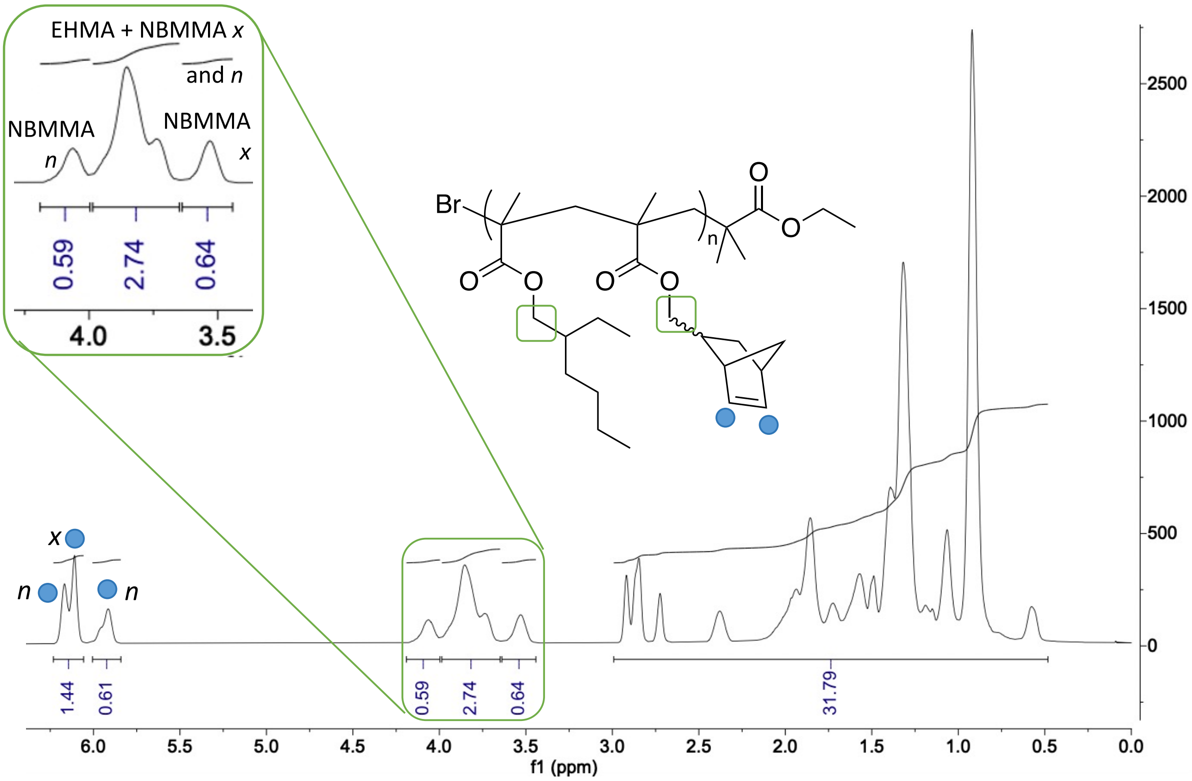

Figure 4. 4: ^{1}H NMR spectrum to show the fraction of each monomer in the resultant P(EHMA-*co*-NBMMA) copolymer where *x* = *exo* and *n* = *endo*.

$$\% \, EHMA = \frac{total\ peak\ integral - n\ NBMMA - x\ NBMMA}{total\ peak\ integral} \times 100$$

$$\% \, EHMA = \frac{2.74 - 0.59 - 0.64}{2.74} \times 100 = 55$$

$$\% \, NBMMA = 100 - \% \, EHMA = 100 - 55 = 45$$

Equation 4. 1: Calculations to show how mol % of each monomer in the resultant polymer.

DSC analysis was used to find the T_g of the copolymers. Two heating cycles were performed and the T_g was taken from the second to ensure that there is no further curing from the first heat ramp.

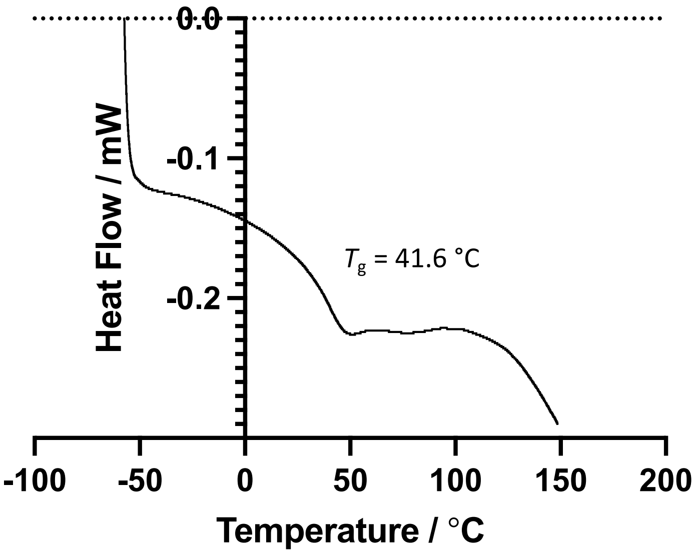

Figure 4. 5: DSC thermograph to show the single T_g resonance of P(EHMA-*co*-NBMMA)

The molecular weights of both monomers were the same, so the mol. fraction was the same as the weight fraction and the Fox equation was used to calculate the theoretical T_g for the copolymer as 36 °C (Equation 4. 2). This is within error of the experimental value.

$$\frac{1}{T_g} = \frac{w_1}{T_{g1}} + \frac{w_2}{T_{g2}}$$

$$\frac{1}{T_g} = \frac{0.55}{361} + \frac{0.45}{263} = 0.00323$$

$$T_g = 309 \text{ K} = 36 \text{ °C}$$

Equation 4. 2: Fox equation to calculate the theoretical T_g of P(NBMMA-*co*-EHMA)

Similar, to the EHMA copolymer, P(NBMMA-*co*-IBMA) showed complete removal of the MMA alkene resonance which can be identified by a singlet at δ = 5.5 ppm whilst a lot of the norbornene alkene remained unreacted since the polymerisation was not allowed to continue until full conversion (Figure 4. 6). The C**H**O from IBMA did not overlap the -C**H**$_2$O from NBMMA so the percentage of each monomer could be calculated from the ^{1}H NMR spectrum (Equation 4. 3).

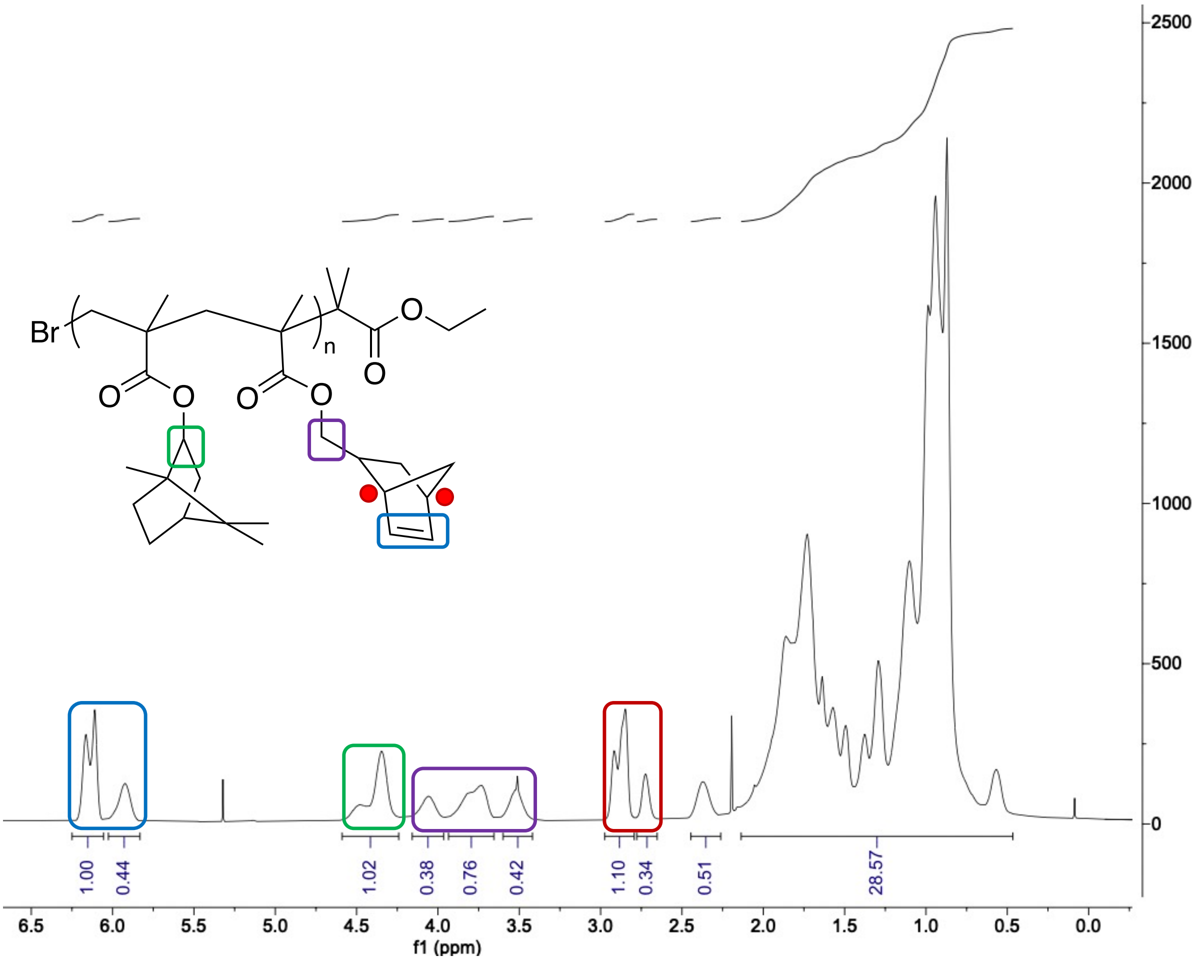

Figure 4. 6: ^{1}H NMR spectrum of fraction of NBMMA and IBMA in the resultant copolymer P(IBMA-*co*-NBMMA)

$$\% \, IBMA = \frac{1.16}{\frac{0.68 + 1.31 + 0.73}{2} + 1.16} \times \, 100 = 46 \, \%$$

$$\% \, NBMMA = 100 - 46 = 54 \, \%$$

Equation 4. 3: Relative ratios of IBMA and NBMMA in P(NBMMA-*co*-IBMA)

The experimental T_g was determined by DSC to be 106 °C by taking the mid-point of an endothermic change in heat flow (Figure 4. 7). The change in heat flow around 85-95 °C was an artifact within the DSC seen for all samples ran during this period of time. The theoretical T_g was calculated by the Flory-Fox equation to be 98 °C, based on the ratio of comonomers by ^{1}H NMR spectroscopy.

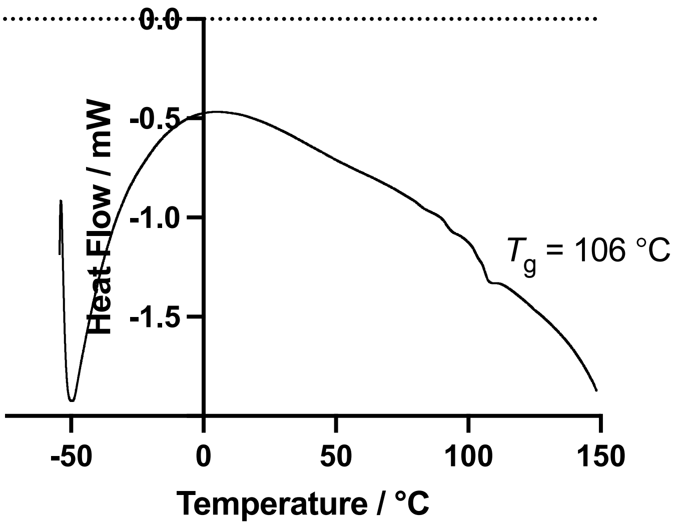

Figure 4. 7: DSC thermogram showing the T_g of P(IBMA-*co*-NBMMA)

$$\frac{1}{T_g} = \frac{0.46}{383} + \frac{0.54}{361} = 0.00270$$

$$T_g = 371\ K = 98\ °\mathrm{C}$$

Equation 4. 4: Flory-Fox equation to calculate the theoretical T_g of P(NBMMA-*co*-IBMA)

4.2.5 Curing PDCPD

G1 was used to cure the adhesive by ROMP rather than G3 since slower initiation gives the adhesive a greater working time and the lower dispersities achieved with G3 are irrelevant in bulk polymerisation. High purity DCPD with a melting point of 33 °C was used so the adhesives were heated to 40 °C to ensure good dissolution and even distribution.

Having a consistent cure of PDCPD was challenging since the degree of crosslinking is dependent upon a range of factors. A higher catalyst loading has been shown to have an effect on the crosslinking density of PDCPD.[96] Since the adhesive formulations were made on a 1 or 2 g scale with a 1:2000 mol. ratio of G1 to DCPD, there was a high degree of error. To reduce this a more dilute stock solution of G1 in DCM was used, although this led to bubble formation upon cure and caused weaknesses in the adhesive. Toluene was used as a higher boiling point alternative as it would evaporate slower, but some remained in the samples after post-cure and appeared as a loss of mass in TGA. Furthermore, the DCPD was heated on a heating mantle on a hotplate which can vary between a couple of degrees. This affected the initial polymerisation rate, which affected the exotherm of the reaction and therefore, the amount of radical crosslinking.

Different ratios of catalyst-to-monomer ([C]: [M]) were used to compare the effect on the resultant polymer (Figure 4. 9). Initially, a 1: 5000 G1 to monomer ratio was used with minimal conversion of DCPD causing the mixture to remain as a liquid and not undergo post-curing. When a 1: 2000 ratio of G1 to monomer was used the polymer crosslinked to form a solid, which remained flexible, suggesting the T_g was below room temperature. When a 1: 500 ratio was used the polymer had such a large enough exotherm that DCM from the catalyst solution and remaining DCPD monomer evaporated causing bubbles and weakening the adhesive (Figure 4. 8).

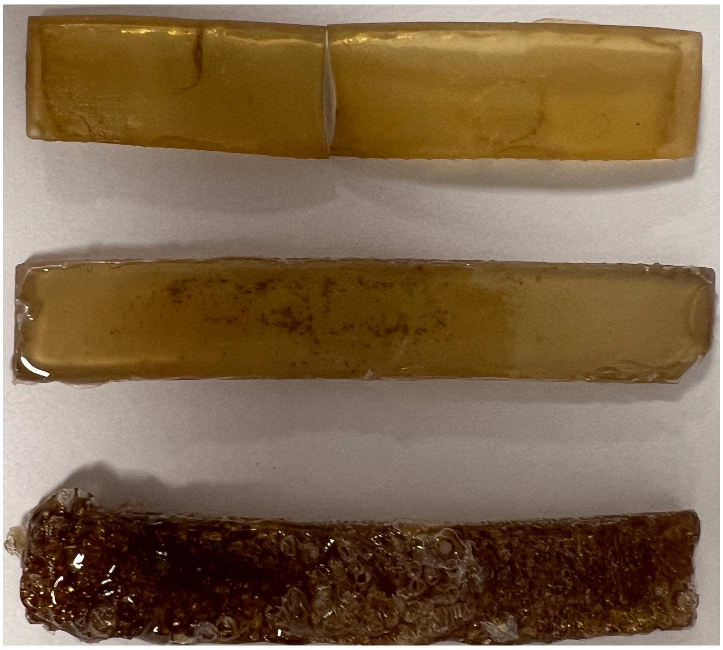

Figure 4. 8: Photos of PDCPD cured with [C]:[M] 1:2000 (top), 1:1000 (middle) and 1:500 (bottom)

The PDCPD was post-cured under vacuum at 60 °C for 1 hour then 150 °C for 16 hours to achieve optimum cure and the T_gs of were determined by DSC. The T_g was shown to increase slightly with increasing catalyst loading. This is in agreement with work by Knorr and co-workers.[162]

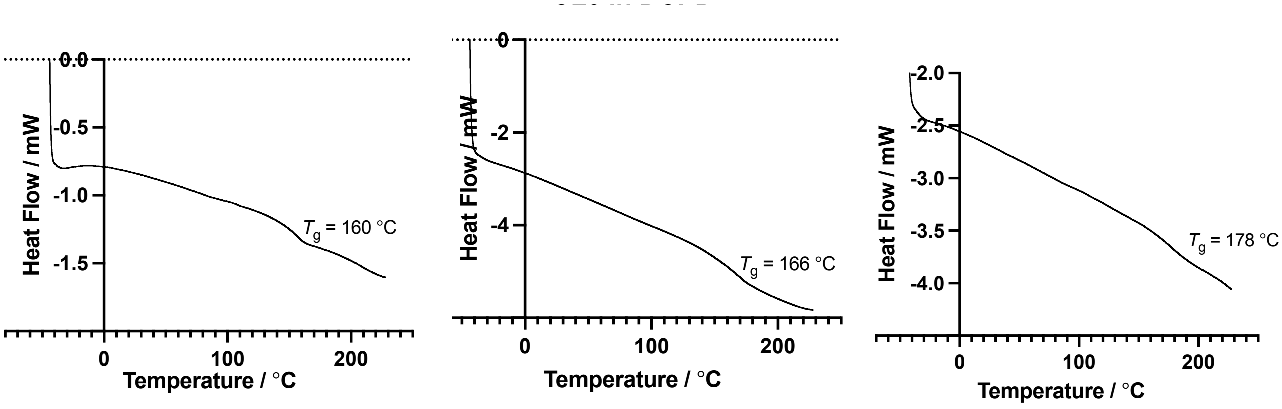

1:2000 1: 1000 1:500

Figure 4. 9: DSC thermographs to show the T_g of the PDCPD adhesives after a 150 °C post-cure.

4.2.6 Thermal Degradation Temperatures of the PDCPD Adhesives

The attribute of PDCPD that makes it desirable as a structural adhesive is its high degradation temperature. TGA was used to ensure that this remained high even after the addition of the methacrylate copolymers. 10 wt% of the copolymers were added to PDCPD and the homopolymers of PEHMA and PIBMA were also compared to see whether there was an effect from crosslinking of the norbornene into the PDCPD network (Figure 4. 11). The polymers were stirred within the DCPD monomer at 40 °C for up to 2 hours to ensure they had dissolved well and been dispersed evenly within the monomer mixture.

The TGA was originally run at 10 °C min^{-1} as had been run with the PMMA adhesives, however, at the point the adhesive began to rapidly decompose, the balance began to jump up to over 1000 % mass to under -200 % mass. This was thought to be due to a sudden rapid degradation and mass loss causing the TGA pan to 'bounce'.

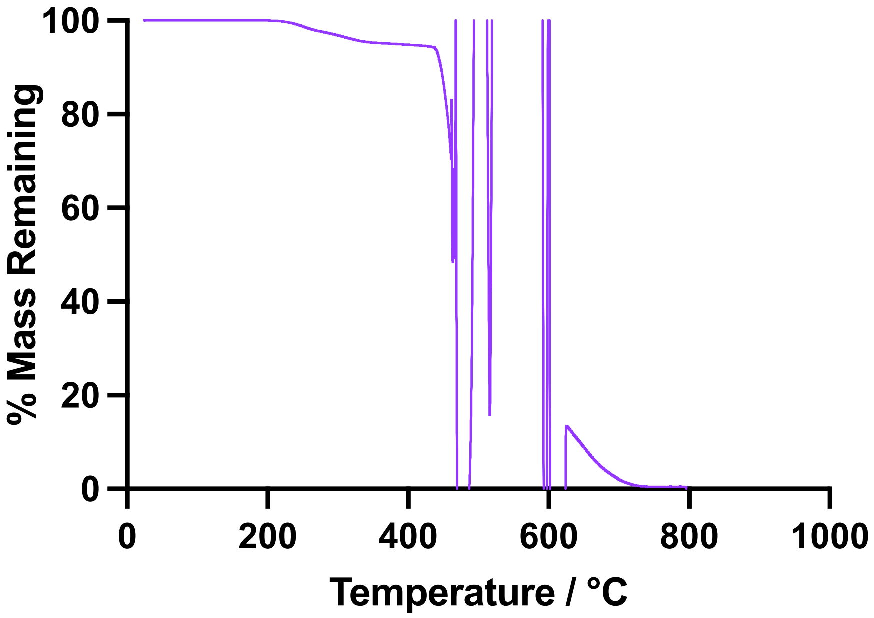

Figure 4. 10: TGA of P(NBMMA-*co*-EHMA) with a ramp rate of 10 °C min^{-1}

The ramp rate was slowed down and a rate of 0.25 °C min^{-1} appeared to give a stable measurement however, this meant the TGA took 38 hours per sample to get to 600 °C. This significant reduction in ramp rate might have led to further post-curing which can increase the degradation temperatures (Figure 4. 11). The initial mass loss at 10 °C min^{-1} heating (Figure 4. 10), around 220 °C was not seen during the slower ramp rate after the sample had been exposed to a high temperature for longer.

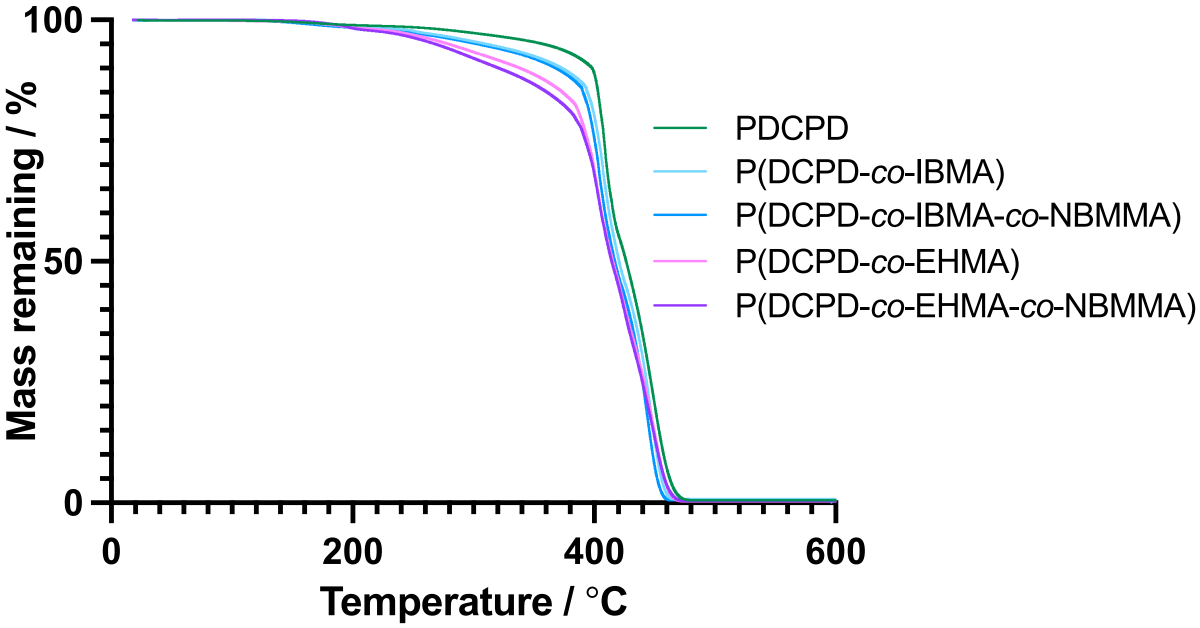

Figure 4. 11: Graph to show the mass loss of the PDCPD adhesives containing methacrylate co- and homopolymers in comparison to PMMA as temperature increased.

As shown in Figure 4. 11, pure DCPD has the highest degradation temperature with the T_{10} being 399 °C in comparison to PMMA where the $T_{10\,\%}$ is only 235 °C (Table 4. 2). The $T_{5\,\%}$ and $T_{10\,\%}$ decreases in order of decreasing T_gs of the methacrylate polymers. The $T_{50\,\%}$ for all of the PDCPD based adhesives are similar and unaffected by the methacrylate polymer as this might have already degraded.

Table 4. 2: Degradation temperatures of PDCPD based adhesive formulations

Polymer	$T_{5\,\%}$ / °C	$T_{10\,\%}$ / °C	$T_{50\,\%}$ / °C
PDCPD	358	399	429
P(DCPD-*co*-IBMA)	311	368	418
P(DCPD-*co*-IBMA-*co*-NBMMA)	303	367	421
P(DCPD-*co*-EHMA)	279	337	426
P(DCPD-*co*-EHMA-*co*-NBMMA)	268	311	420

4.2.7 Lap shear tests to determine the adhesive strength

Aluminium lap shear specimens were prepared with a P2 acid etch which is a solution of sulfuric acid and iron (II) sulfate hydrate. This solution creates a fresh oxide layer on the outside of the aluminium for the adhesive to bond and also etches small pores in the surface to increase the surface area-to-volume ratio and introduce roughness.

After the adhesive solutions were cured using G1 ([M]/[C] = 2000), the viscosity of the adhesives began increasing within seconds and the working time was between 10-15 seconds. A longer working time could be achieved by reducing the concentration of the catalyst. However, the reduction in exotherm during the polymerisation reduces the crosslinking density and therefore strength. The adhesives were post-cured in a vacuum oven at 40 °C for 2 hours and then 12 hours at 100 °C.

None of the lap shears cured were strong enough to be considered as structural adhesives which typically have strengths greater than 20 MPa (Figure 4. 12).[5, 8] PDCPD exhibited a low strength which was slightly improved by addition of the PIBMA polymers, with the P(IBMA-*co*-NBMMA) copolymer having the largest stress. This could have been because it was able to crosslink into the material. The EHMA polymers had lower T_gs and some phase separation was seen during the cure as the polymer precipitated out. This could be due to the polymer being more soluble in monomer DCPD than the polymer. In both cases the adhesives containing NBMMA were stronger than the controls which were unable to crosslink within the material.

The main failure mechanism for these samples was adhesive where, in some cases, the adhesive layer could be peeled away from the aluminium surface leaving it in its original condition. This could partially be due to the surface preparation of the aluminium and partly to do with the adhesive having a lower polarity so only weak intermolecular forces held the substrate together.

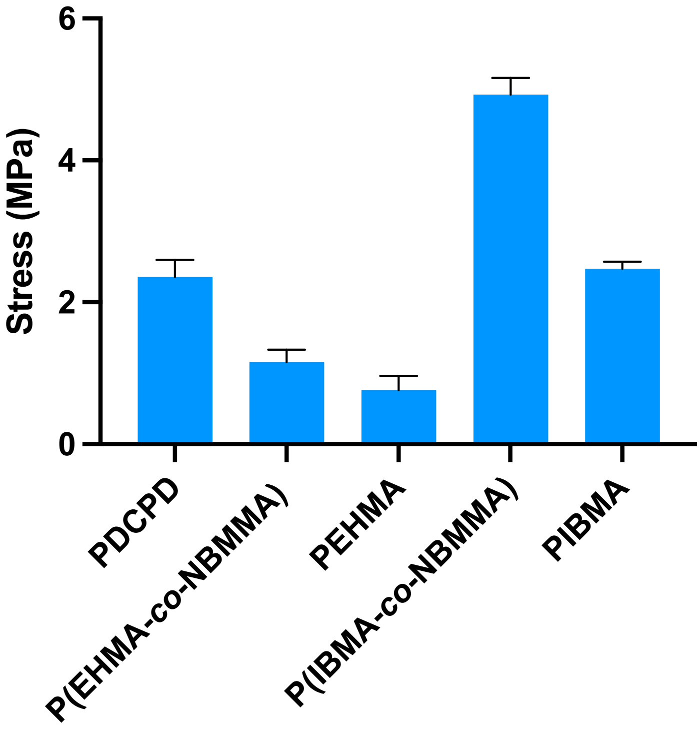

Figure 4. 12: Aluminium lap shears of 10 wt% methacrylate polymers in DCPD.

5 wt% MAA was added as an adhesion promoter since the carboxylates can form strong hydrogen bonds with the oxide layer.[5] Addition of MAA appeared to increase the solubility of the poly(methacrylate)s which did not need to be mixed for as long periods of time. Addition of 5 wt% MAA as monomer increased the rate of ROMP and reduced the working time of the adhesive to around 5 seconds. The same effect was observed by Matson and co-workers when they carried out ROMP using G3 in ethyl acetate which has a small concentration of acetic acid present. The cause of this is the protonation of the labile ligand, PCy_3, making it less able to rebind to the Ru so that the initiator is more active.[86]

The strength of all the lap shears reduced with the addition of MAA as a consequence of the rapid rate of cure leaving not enough time for there to be sufficient surface wetting and for the adhesive to get full contact into the pores before the viscosity increases (Figure 4. 13). PDCPD had the greatest strength, despite having the least intermolecular bonding with the substrates, which could be because it had the lowest viscosity and therefore, the longest working time to get a strong bond.

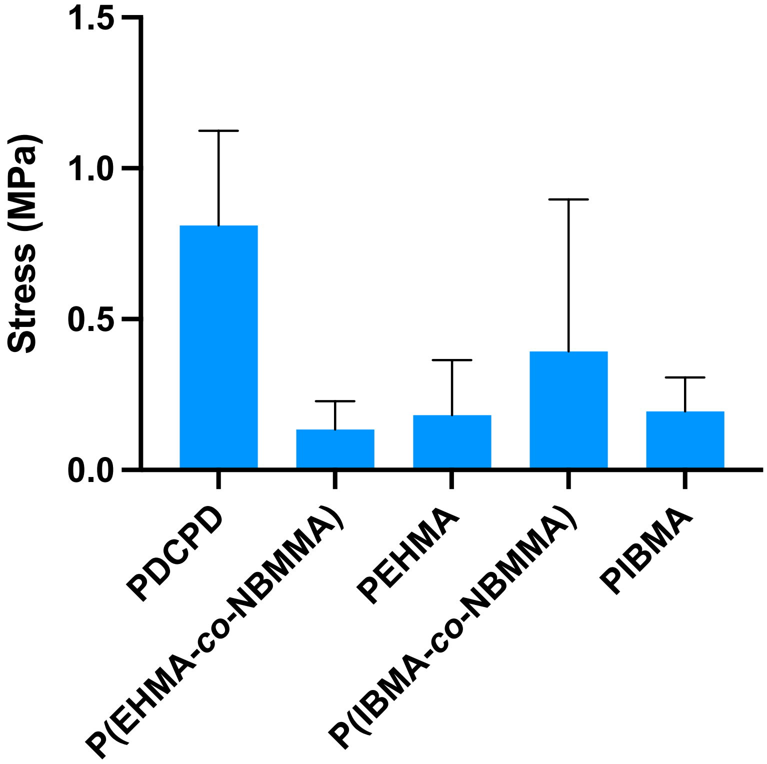

Figure 4. 13: Aluminium lap shears with PDCPD based adhesive formulations containing 10 wt% methacrylate and 5 wt% MAA.

One method of reducing the rate of polymerisation caused by using the Grubbs initiator is to add an excess of phosphine ligands which are able to shift the equilibrium of the ligand dissociation. This means that there is less opportunity for the DCPD monomer to fit around the central Ru metal. Alternatively, the polymerisation could be carried out at a lower temperature.

5-ethylidene-2-norbornene (ENB) is a monomer with a melting point of -80 °C. It is often added to DCPD within industry to decrease the melting point so that it is a liquid at room temperature.[163, 164] By adding 25 wt%, the monomer mixture was liquid at room temperature so no preheating was required and the working time of the adhesive would be longer since the initiator has less energy.

Addition of ENB increased the strength of the DCPD but decreased the strength of the adhesives containing methacrylate polymers (Figure 4. 14). All the adhesives broke through cohesive failure due to the brittle nature (Figure 4. 15). The adhesion was also weak as the adhesive could be scrapped off easily leaving no mark on the aluminium surface. This might be because the polymerisation was carried out at a lower temperature and the slower initiation resulted in a smaller exotherm and therefore, less radical crosslinking through the less ring-strained cyclopentene groups.

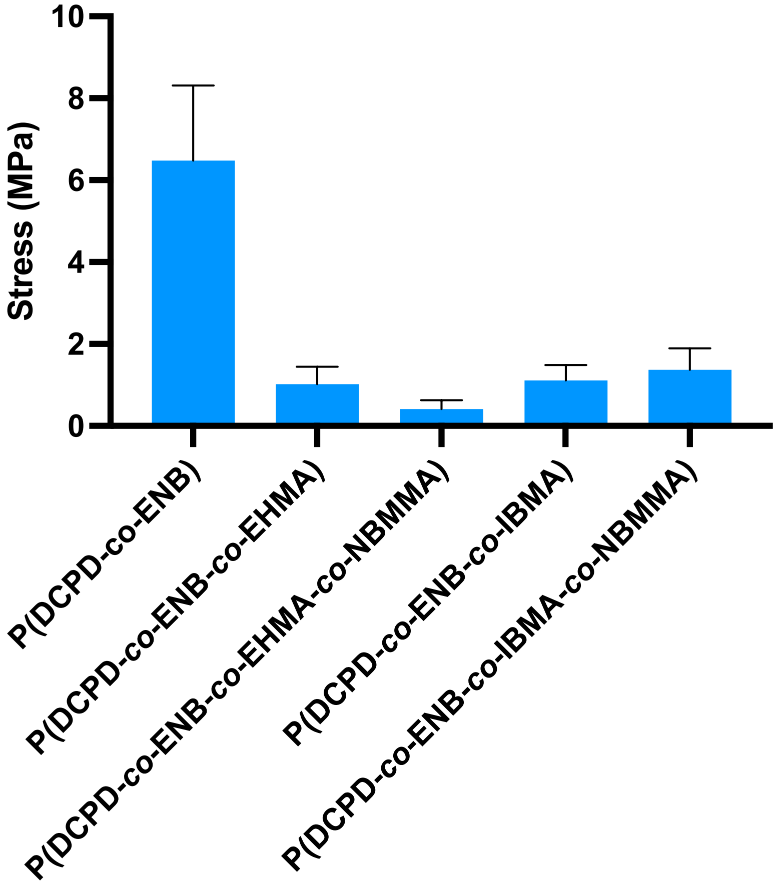

Figure 4. 14: Bond strengths of PDCPD based adhesives with 25 wt% ENB and 5 wt% MAA

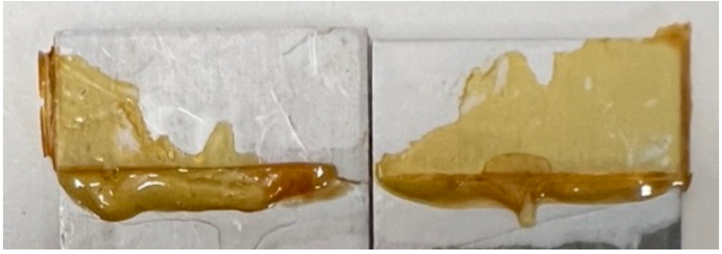

Figure 4. 15: Photo to show the cohesive failure during the lap shear test of P(DCPD-ENB-IBMA-NBMMA)

4.2.8 Designing crosslinkers to improve adhesive properties of PDCPD

To overcome the solubility challenges from the poly(methacrylate)s in DCPD, crosslinkers containing two and three norbornene groups were synthesised. Crosslinker 1 (CL1) was synthesised through Diels-Alder (DA) [2 + 4] cycloaddition between cyclopentadiene (CPD), which was formed from the cracking of DCPD, and maleic acid. Two 5-norbornene-2-methanol molecules were reacted through an esterification reaction to the 5-norbornene-2,3-dicarboxylic acid (NBDCA) to yield a very viscous oil (Scheme 4. 5). NBDCA is formed with the *endo* isomer being the major product. 5-Norbornene-2-methanol (NBOH) is purchased as a 0.57: 0.43 ratio of *endo: exo* isomer mixture which produces the same ratio in the resultant crosslinker. There is also a possible rearrangement of some *endo* NBDCA to *exo* due to the high temperatures during the esterification.

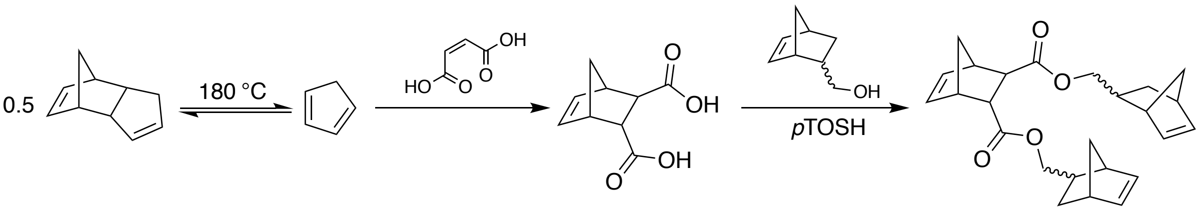

Scheme 4. 5: Reaction scheme to synthesise crosslinker 1 (CL1) – Dinorbornene methanyl norbornene dicarboxylate

Crosslinker 2 (CL2) was synthesised by cracking DCPD to give 2 CPD molecules and then reacting with EGDMA with heating (Scheme 4. 6). Heating was required for this DA reaction due to the steric hindrance from the methyl on the vinyl group. This product also gave 6 stereo- and regioisomers due to the combination of *endo* and *exo* arrangements of the norbornene group and arrangement on C2 and C3 of the norbornene.

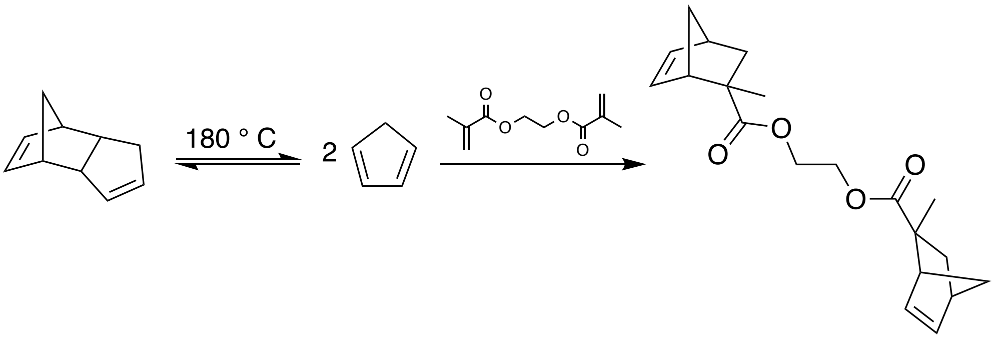

Scheme 4. 6: Reaction scheme to synthesis crosslinker 2 (CL2) – Ethylene glycol dimethyl norbornene

Aluminium lap shears containing the crosslinkers were prepared and tested against pure PDCPD adhesives. Addition of the crosslinkers significantly improved the adhesive strength of PDCPD with only 10 wt% of CL1 doubling the strength (Figure 4. 16). This monomer has 3 norbornenes which can ring-open during ROMP as opposed to two on CL2. Increasing the amount of CL2 increased the bond strength of the adhesives since there would be a greater crosslinking and more polar oxygen molecules to help bond to the surface.

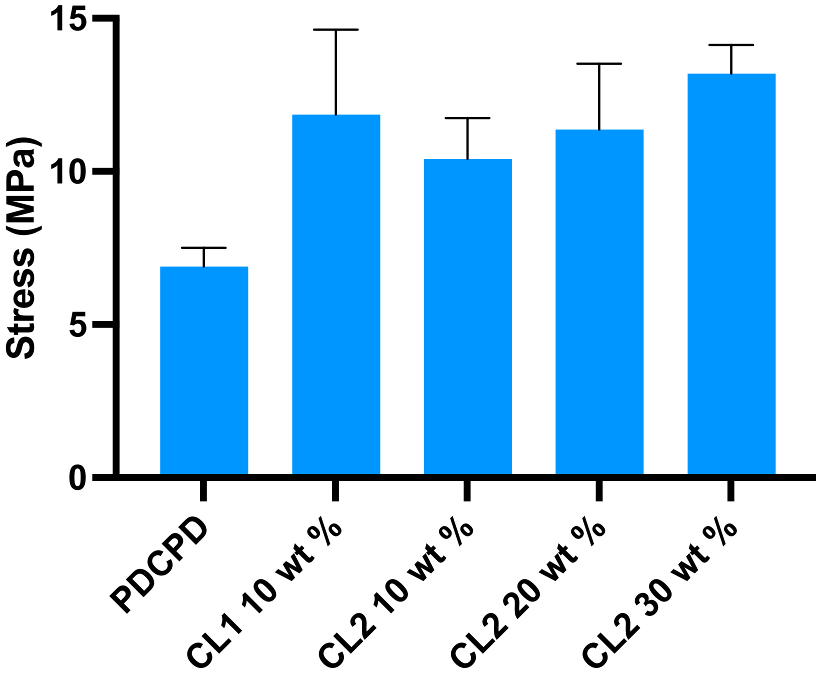

Figure 4. 16: Aluminium lap shear results of PDCPD adhesives with norbornene crosslinkers

4.2.9 Effect of lap shear preparation

The results for the lap shears using a PDCPD adhesive in Figure 4. 16 showed a maximum stress about 6 times greater than in Figure 4. 13. This was thought to be due to subtle improvements in substrate preparation since the lap shears were prepared over a year apart. Initially, the process of acid etching was slower with the aluminium lap shears being left for up to 2 hours before the adhesives were added. This process was improved and the time between acid etching and adhesion was reduced to less than 30 minutes.

The effect of the substrate preparation was tested by comparing aluminium that had been cleaned with acetone, roughened with sandpaper and acid etched with P2 solution (2.4.10) leaving for under 30 minutes and 24 hours between tests (Figure 4. 17). None of the samples that were prepared with aluminium that had only been wiped with acetone were strong enough to survive removing from the lap shear jig and transporting to the tensiometer. The aluminium that had been prepared using sandpaper had improved bonding since it had a greater surface area so more contact between the adhesive and adherend. These samples also had the greatest standard deviation since it is difficult to control the degree of abrasion applied. There was a large difference between the samples that had been prepared using the P2 acid etching solution and those represented in the results previously. When prepared quickly the samples had a much greater strength than samples left for 24 hours. The reason for this is that during the P2 treatment the aluminium surface develops a rough surface with large pores and a thick oxide layer, over time this oxide layer reacts with the air to form a less stable version that is typically found on the surface of aluminium.[165]

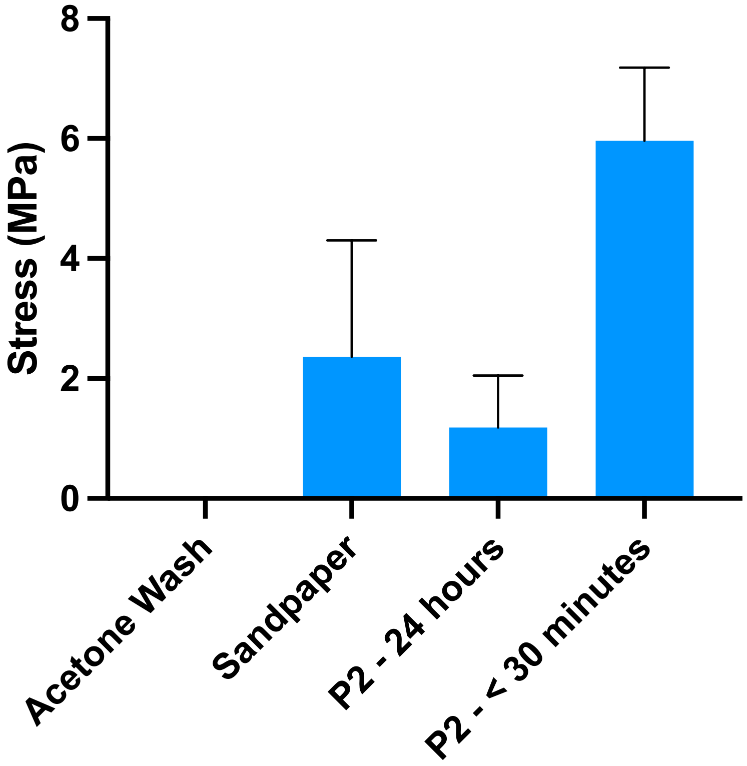

Figure 4. 17: The effect of the aluminium substrate preparation on the stress of PDCPD adhesives

4.2.10 Tensile testing for PDCPD adhesives with norbornene crosslinkers

Tensile testing was carried out to find if there is an improvement in elasticity and reduction in brittleness when using the crosslinkers in PDCPD. Moulds were made from silicone using a 3D printed specimen (Figure 4. 18). G1 was added and the mixture was rapidly poured into the mould. After 30 minutes the polymer was transferred to a vacuum oven at 100 °C for 12 hours. The narrow section of the dog bone was coloured black with a permanent marker and two white dots were drawn so that the camera on the Instron® tensometer could follow during the experiment.

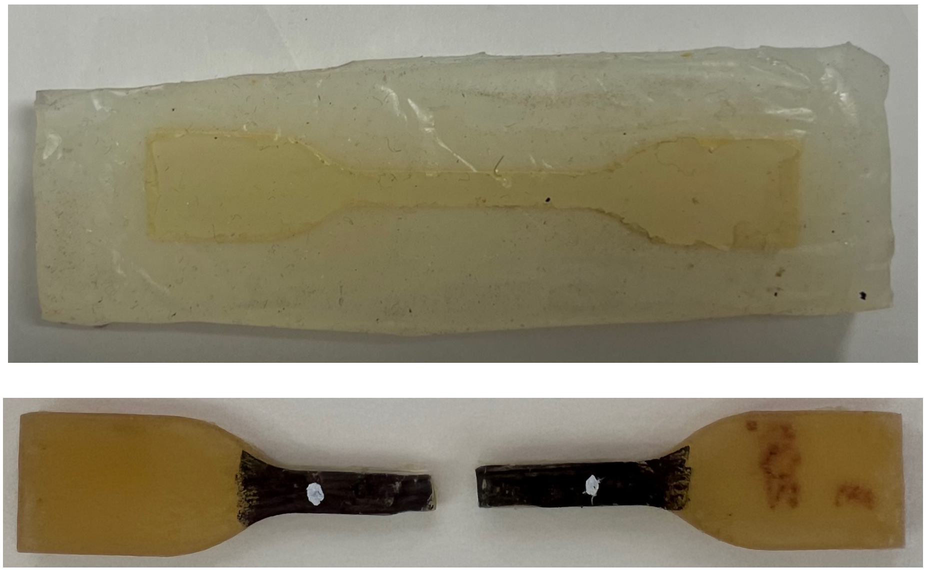

Figure 4. 18: Photo of mould for tensile testing and a PDCPD dog bone containing 30 wt% CL2 after tensile testing

Adding ENB and MAA to PDCPD was shown to reduce the tensile stress with respect to the quantity of PDCPD present. CL1 had less of an improvement on tensile strength than CL2 which increased the maximum stress the greater the percentage added.

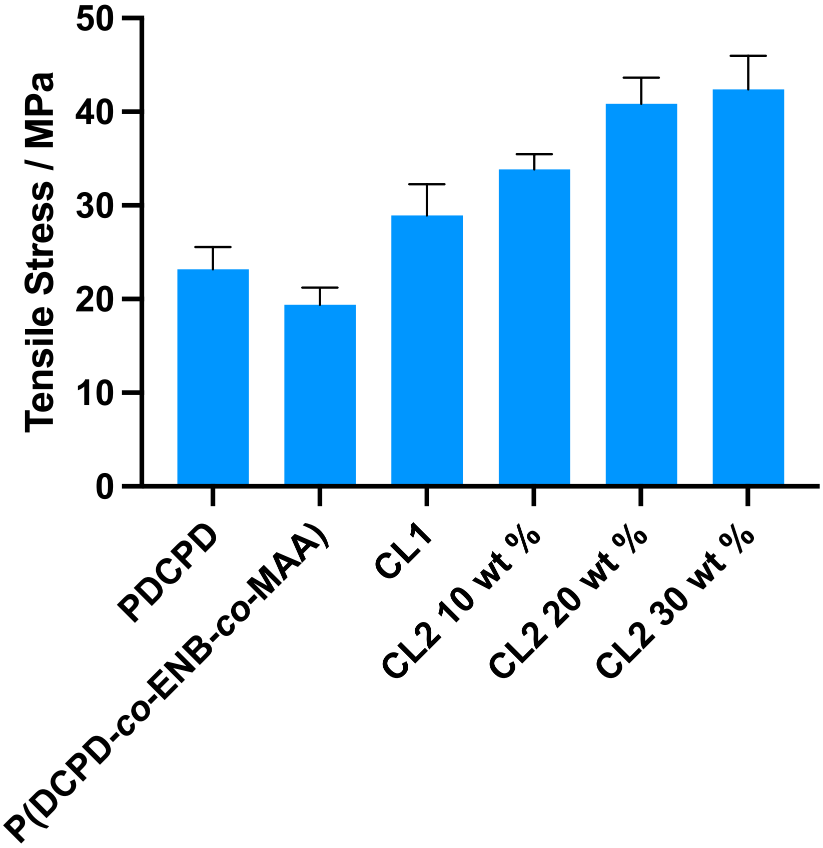

Figure 4. 19: Results of tensile testing of PDCPD and crosslinker based adhesives.

4.2.11 Thermal properties of PDCPD adhesives with norbornene crosslinkers

The effect of the crosslinkers on the thermal degradation of the PDCPD adhesives were tested using TGA. The heat ramp was set to the slower rate of 0.25 °C min^{-1} however, even at this rate the TGA pan ‘bounced’ (Figure 4. 20). Thermal degradation began at around 150 °C with the $T_{10\,\%}$ at 371 °C, just before the main degradation. These degradation temperatures are around 50 °C lower than the PDCPD adhesives with methacrylates (Figure 4. 11).

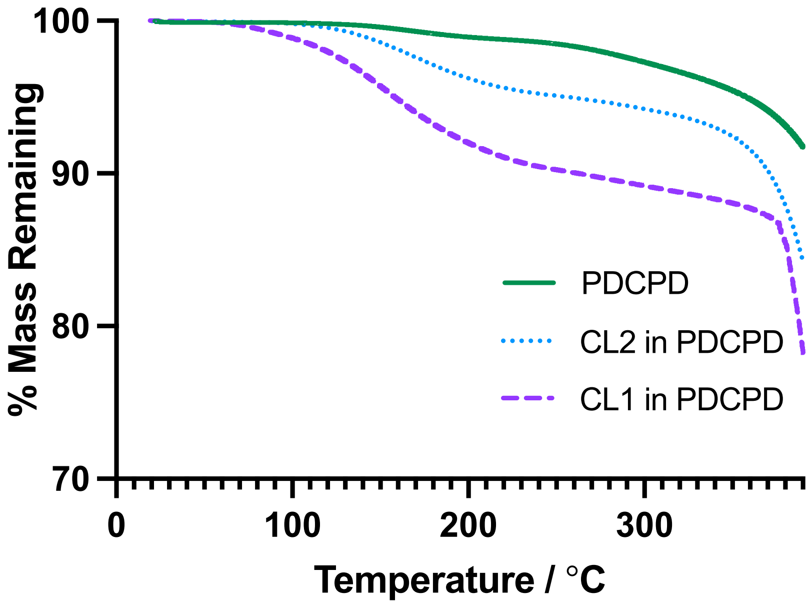

Figure 4. 20: Thermal degradation of PDCPD with 10 wt% EGDNB

The reason for the lower degradation temperatures of the adhesives is unknown. One possibility could be that the crosslinkers have not bonded into the PDCPD and this is what is causing the lower temperature mass loss. If this was the case, then visible phase separation would be expected which would make the product cloudy and opaque however, the polymer was completely transparent. Additionally, due to their large size at atmospheric pressure the boiling point of crosslinkers is higher than the temperature of retro-DA which would be expected above 170 °C.

DSC was used to find the T_g of PDCPD with and without 10 wt% of the crosslinkers with no high temperature post-cure (Figure 4. 21). Two temperature ramps were carried out and for all three samples further curing was observed on the first ramp. This shows that a room temperature cure is not sufficient for the adhesive.

Initially, the T_g is of the adhesives was found to be low, between -10 and 21 °C. However, further curing was seen during the temperature ramp. Only the first temperature ramp was used since no transitions were seen during the second run. This could be due to additional crosslinking during the heat ramp. During the first run the curing began at a higher temperature for the PDCPD with crosslinkers in than without, suggesting that the crosslinkers enabled a greater amount of room temperature cure. After heating to a high temperature during the first ramp, the unsaturated PDCPD could have oxidised, broadening the T_g of the adhesives were not heated above the temperature that the adhesive was shown to degrade during TGA. The T_gs of similar systems with norbornene-based ester crosslinkers have been found to be around 180 °C.[94]

DCPD

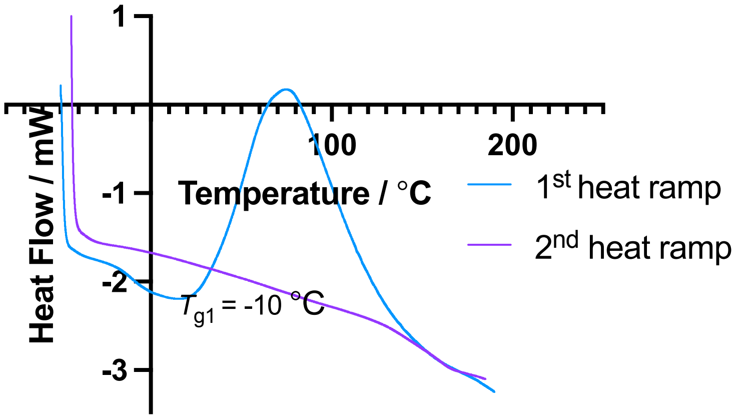

CL1 in DCPD

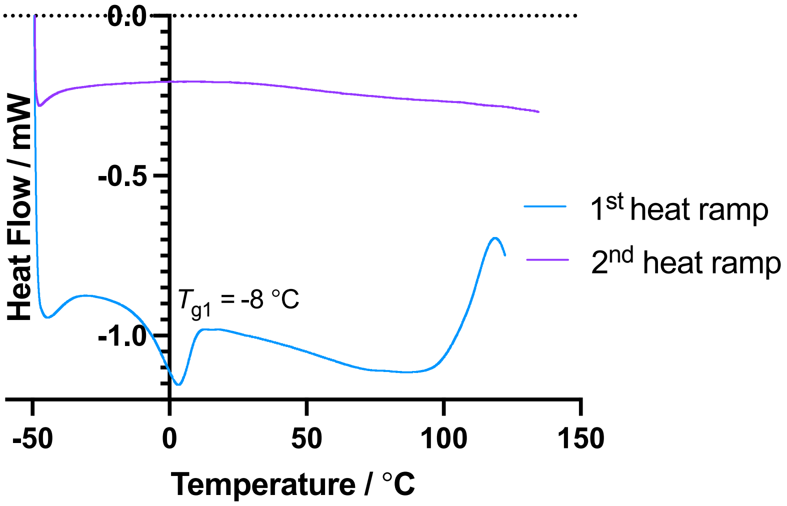

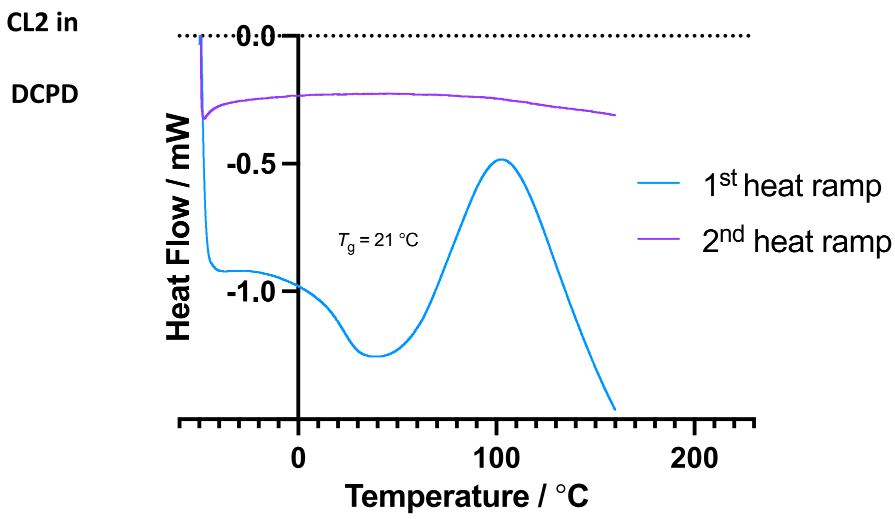

Figure 4. 21: DSC thermographs of PDCPD with and without 10 wt% of crosslinker with no post-cure.

4.3 Conclusions

PDCPD was found to be a thermoset with a high degradation temperature that could be cured without deoxygenated conditions. The low polarity meant that macromonomers or polymer additives must be relatively non-polar to be soluble and did not lead to phase separation during the cure. A-PNBMMA was too polar to be soluble in DCPD but copolymerising NBMMA with EHMA and IBMA by AGET ATRP in a 1:1 molar ratio formed a DCPD soluble polymer. The conversion of NBMMA by radical polymerisation had to be kept low due to branching and crosslinking through the norbornene alkene.

The thermal degradation temperatures of PDCPD were found to be significantly higher than PMMA with the onset of degradation decreasing with addition of the poly(methacrylate)s. This could be due to a radical 'unzipping' through the unsaturated methacrylate backbone into volatile monomers.

None of the PDCPD formulations reached a strength of over 20 MPa in order to be classed as a structural adhesive. Addition of the IBMA into the copolymers increased the maximum stress of the lap shears with respect to PDCPD whilst the EHMA copolymers decreased in strength and experienced visible phase separation whilst curing. The copolymers were stronger than the methacrylate homopolymers which could be due to crosslinking through the norbornene into the DCPD. Addition of MAA as an adhesion promoter reduced the working time of the adhesive, limiting the surface wettability, causing a weaker bond formation.

2 and 3-norbornene containing crosslinkers were synthesised. These had good solubility within DCPD due to their small size and were shown to improve the strength of the bond. They also increased the elasticity of PDCPD during tensile tests. The thermal stability of PDCPD was significantly reduced by introduction of the crosslinkers due to weak ester linkages.

Despite the presence of high ring-strain norbornene groups in the crosslinkers, to get optimal properties of the DCPD a high temperature post-cure was still required. This was shown in DSC analysis where the T_gs of the first temperature ramp were below room temperature and still showed additional curing when heated.

Chapter 5 - Combining radical and metal-free ring-opening metathesis polymerisation

5.1 Introduction

5.1.1 Metal-free ring-opening metathesis polymerisation

In chapter 3, it was shown that incorporating functionalised poly(norbornene)s into methyl methacrylate-based adhesives increases thermal stability and reduces shrinkage. The functionalisation is important with increasing the concentration of polar groups as well as introducing a group that can crosslink the polymer with poly(methyl methacrylate) (PMMA) to strengthen the material. Despite this, the technique has downsides as it is difficult to completely remove the ruthenium catalyst and even small residual quantities creates free radicals which leads to crosslinking and turns the polymer insoluble.

A metal-free ring-opening metathesis polymerisation (MF-ROMP) synthesis has been reported by the Boydston group in the past decade which has been further developed to allow a hybrid polymerisation with methyl methacrylate.[123, 124] The MF-ROMP approach uses a pyrylium tetrafluoroborate catalyst (Figure 5. 1) which gets excited by blue light and can transfer an electron from the photoexcited state to oxidise an enol ether, initiating polymerisation. All three of these components are required for the polymerisation and when one component, such as the light source, is taken away the reaction stops, allowing for finer control over the polymerisation than traditional metal-mediated ROMP.

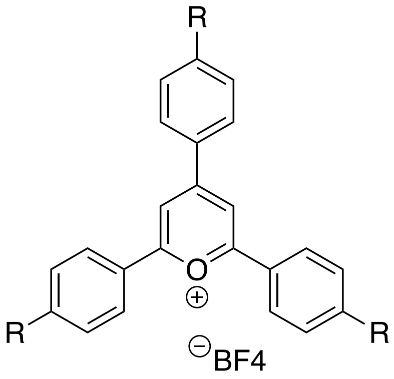

Figure 5. 1: Structure of a pyrylium tetrafluoroborate photocatalyst

The mechanism that has been proposed involves a radical cation that is formed on the enol ether and can interact with a cycloalkene monomer through a [2+2] cycloaddition (Scheme 5. 1). When the cycloalkene monomer has a high enough ring-strain the reaction is driven to ring-open the cyclobutane intermediate. The propagation continues until all the monomer has been consumed and is a 'living' mechanism so can be restarted when more monomer is added. When the light is removed the redox reaction between the photocatalyst and the initiator stops and the propagation appears to stop since there is rapid termination. Oxygen is required as a terminal oxidant in order to regenerate the resting state of the photocatalyst from the photogenerated positively charged state.[166-168] Despite this, purging the headspace of the reaction vial with 100% oxygen had a negative effect on the overall conversion compared to using air.[169]

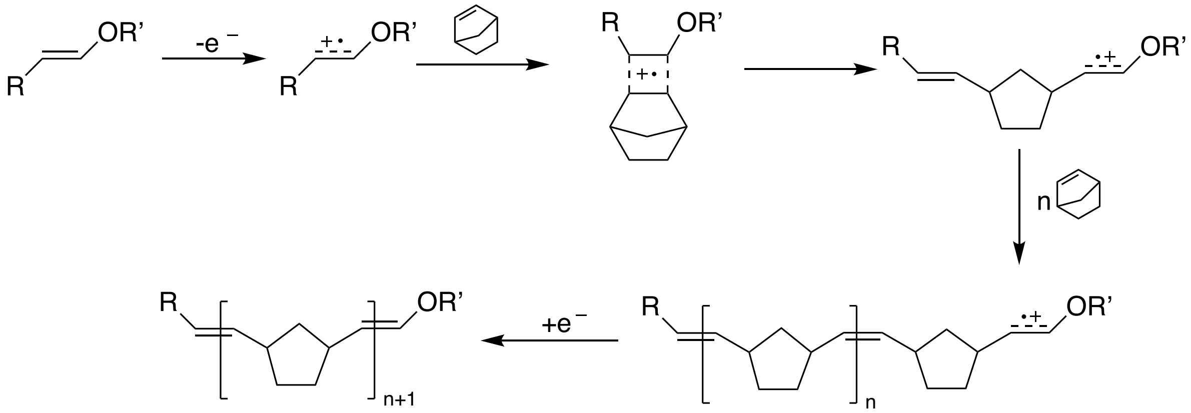

Scheme 5. 1: Proposed mechanism for MF-ROMP of Norbornene

The photostability of pyrylium salts depends on the substituents. Over time they undergo degradation by a process known as photobleaching whereby a molecule is removed from the 'absorption/emission' cycle through a side reaction. The intensity of visible light given to the pyrylium salts is proportional with the rate of photobleaching.[170]

5.1.2 Incorporating functionality into MF-ROMP

The MF-ROMP reaction has been expanded to incorporate a variety of functional groups. One use has been to synthesise linear poly(dicyclopentadiene) (PDCPD) as more common metal-mediated routes are less easy to control and leads to a crosslinked, insoluble polymer. Boydston and co-workers showed that MF-ROMP is selective to the norbornene ring in DCPD and observed no reactivity with the lower ring strain cyclopentene. As the molar ratio of DCPD to norbornene in the reaction mixture increased the conversion decreased. They considered that this was either due to steric hindrance or the presence of a second alkene but concluded that this must be due to the cyclopentene ring since dihydroDCPD showed high conversions.[171]

Boydston and co-workers also tested the tolerance of MF-ROMP towards alcohol functional groups. Initially, they added equimolar amounts of additive, starting with water and methanol and increasing the steric hindrance of the alcohol. They found that water and methanol both significantly reduced the conversion of norbornene but sterically hindered *tert*-butanol had no effect. It was suggested that the reason for this is that radical cations are susceptible to nucleophilic attack by alcohols, quenching the reaction. They next copolymerised norbornene with an alcohol-functionalised norbornene and found the same pattern whereby primary alcohols had the largest reduction in conversion whilst increasing the steric hindrance of the alcohol reduced the quenching effect, restoring conversion.[169]

To show that this technique can be used for bidirectional chain growth for applications such as brush and star polymers, two bifunctional vinyl ether initiators were synthesised (Figure 5. 2). Each initiator had the vinyl group placed on the other side of the ether showing that propagation could take place on the chain ends or within the initiator, growing outwards. Whilst both techniques afforded PNB in a high yield, due to the steric hindrance of initiator 1, the initiator efficiency was lower.[172]

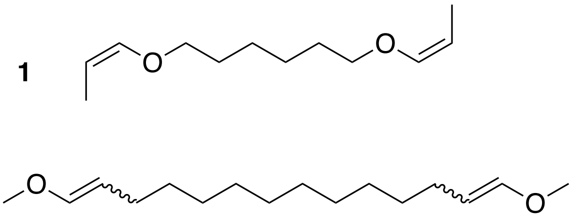

1

2

Figure 5. 2: Structures of bifunctional vinyl ether initiators synthesised by the Boydston group[172]

5.1.3 Hybrid MF-ROMP

In the presence of a pyrylium photocatalyst and an enol ether initiator, norbornene and MMA can copolymerise through a hybrid MF-ROMP and radical mechanism. It is suggested that the polymerisation is initiated by the MF-ROMP mechanism generating a short PNB chain with the ether chain end. This chain end can then form a cyclobutane intermediate which leads to the MMA group attaching to the polymer chain and releasing the vinyl ether. The vinyl ether group reattaches to the polymer chain through nucleophilic addition with the cation and the propagation can continue. Vinyl ethers are able to undergo nucleophilic addition to a radical cation (Scheme 5. 2).[173]

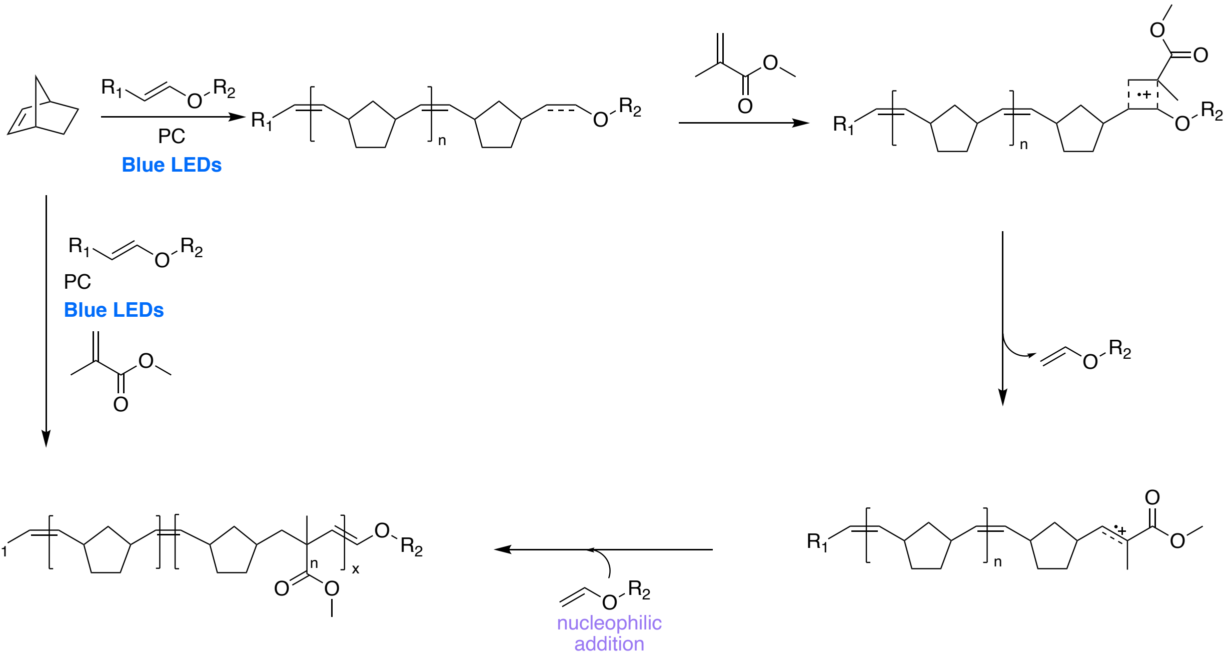

Scheme 5. 2: Mechanism for the hybrid MF-ROMP of norbornene and MMA.

To show that it was a copolymerisation occurred as opposed to two separate polymers forming in parallel, the Boydston group carried out high-resolution mass spectrometry (MS) (Figure 5. 3). The repeat unit with a spacing of 94.08 Da corresponds to the norbornene and the repeat unit spacing with 100.05 Da corresponds to the methyl methacrylate. The charge difference of 5.97 corresponds to the difference in mass between the two monomers.[124] If two separate polymers had formed, then the mass differences from the two polymers would not add up.

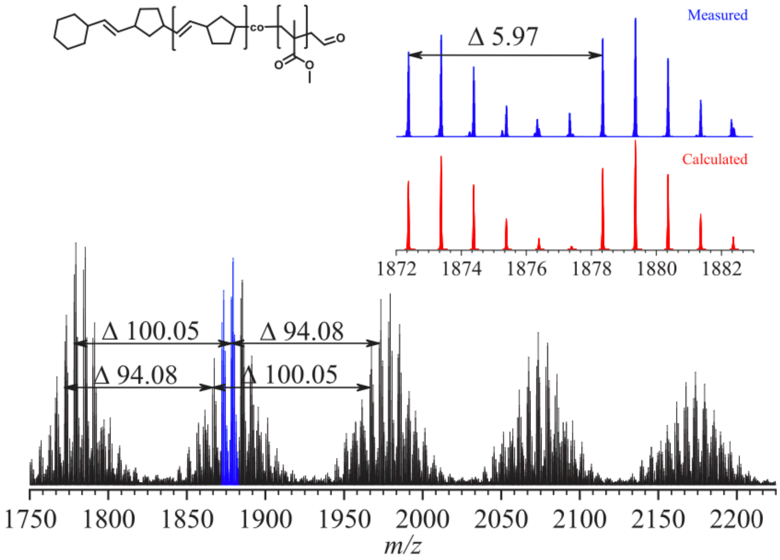

Figure 5. 3: High-resolution MS showing repeating units of the PNB-*co*-MMA copolymer carried out by the Boydston group[124]

Similar materials have been synthesised by Fan and co-workers, who copolymerised norbornene methoxycarbonyl functionalised cyclopentene to introduce a polar group. This copolymerisation reached almost 100 % conversion of NB, yet only 30-45 % conversion of the functionalised cyclopentene depending on the feed ratios used due to the lower ring strain of cyclopentene.[174]

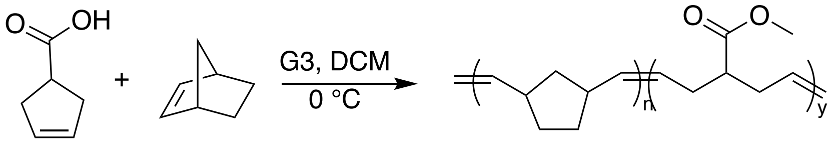

Scheme 5. 3: Reaction scheme for the ROMP of 3-methoxycyclopent-2-ene and norbornene[174]

The effect of the methyl methacrylate on the mechanical properties such as the glass transition temperature (T_g) and thermal degradation temperatures of P(NB-*co*-MMA) from MF-ROMP have not been investigated.

5.1.4 Flow polymerisation

Continuous flow techniques have been used to scale up several different polymerisation techniques such as reversible addition-fragmentation chain-transfer (RAFT), atom transfer radical polymerisation

(ATRP) and ring opening polymerisation (ROP) with great success. The proportionally large surface area-to-volume ratio of the narrow tubing allows better heat transfer, controlled dispersities and optimal light penetration in comparison to polymerisations in batch.[175, 176] Furthermore, computer software can be used to control syringe pumps, hot plates and light sources to make the process automated. Photo-polymerisations benefit in particular as reducing the path length to a mm scale reduces the effect of attenuation of light waves as they pass through a reaction medium as shown in the Beer-Lambert law.[177]

Kinetic experiments can be carried out using flow by using time sweeps where the retention time is increased in increments. Using inline techniques such as nuclear magnetic resonance (NMR) spectroscopy or MS and assuming ideal droplet flow theory, all of the retention times in between can be sampled.[178]

Typical flow reactions depend on laminar flow where there is a continuous flow of reaction mixture which forms layers due to friction at the interface of the liquid-tubing leading to much shorter residence times in the middle of the tube relative to the sides. Over long distances these can lead to a large dispersity (*Đ*). The greater the diameter of the tube, the greater these *Đ*. Increased viscosities, caused by higher weight-average molecular weight (M_w) polymers and high reaction concentrations can also affect the flow rate and lead to blockages and poor reproducibility in laminar flow (Figure 5. 4).[179, 180]

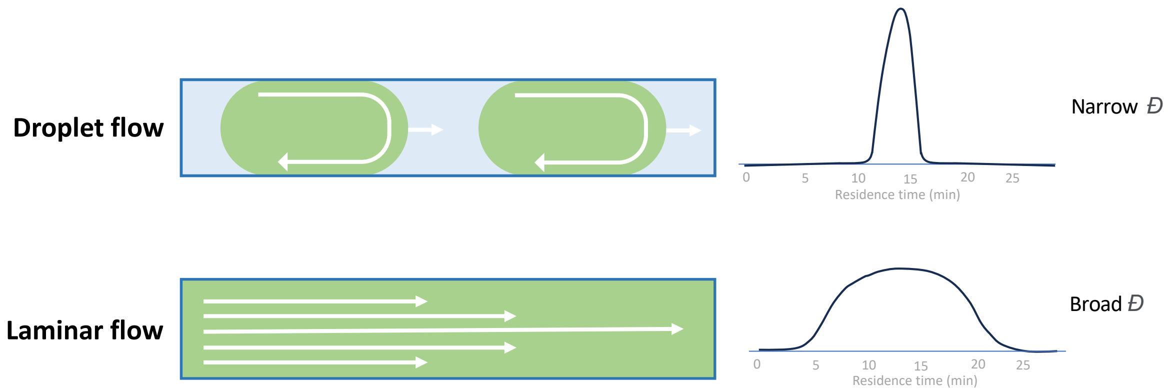

Figure 5. 4: Diagrams to show the direction of flow and outcome on residence time distribution by SEC

Droplet-flow is an alternative process where a typically inert carrier gas is introduced forming regions of liquid separated by gaseous sections. This means that the reactants are captured within liquid bubbles and cannot mix with nearby bubbles therefore reducing the *Đ*.[181] The disadvantages of using droplet flow is that inline monitoring becomes more challenging as NMR, Infrared (IR) spectroscopy and size exclusion chromatography (SEC) cannot be used to give reproducible results due to the presence of the gas bubbles.

Droplet (liquid-gas slug) continuous flow polymerisations have been demonstrated with a variety of polymerisation techniques.[179, 181, 182] Another advantage of droplet continuous flow systems is that it allows for high viscosities of products to be formed. In a regular continuous flow microreactor, an increase in viscosity during the polymerisation can lead to either blockages in the reactor or a broad range in residence times and therefore *Đ*. Interrupting the flow with a gas phase reduces these problems.[181] Additionally, liquid-liquid slug systems have been used to allow polymers with a M_w of 1 000 000 g mol^{-1} to be synthesised.[183]

5.1.5 Chapter Aims

The aim of this chapter is to find a method of synthesising functionalised norbornene polymers as additives for poly(methyl methacrylate) (PMMA) adhesives where the polymerisation can be controlled so that they can be purified without risk of crosslinking. A new photoinitiated MF-ROMP technique will be used and optimised to copolymerise norbornene and norbornene methylene methacrylate (NBMMA). After optimising the reaction in batch, it will be shown that this method can be scaled up by using continuous flow.

5.2 Results and Discussion

5.2.1 MF-ROMP to synthesise poly(norbornene)

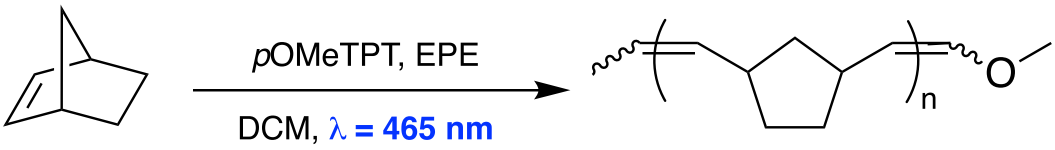

Scheme 5. 4: MF-ROMP of norbornene to PNB

Initially the set-up of the MF-ROMP was tested using the synthesis of poly(norbornene) (PNB) (Scheme 5. 4). A strip of blue LEDs were wrapped around a 300 mL glass beaker and the reaction was carried out in a sample vial placed in the middle (Figure 5. 5). The light intensity was 3.54 mW cm^{-2}. Placing the lights on the outside of the glass helped to insulate the reaction from the increase in temperature throughout the experiment (Figure 5. 5).

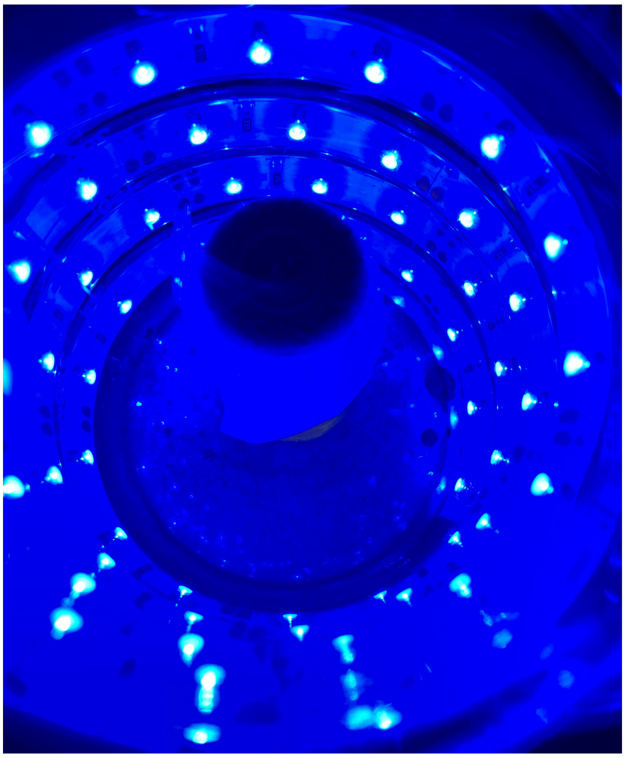

Figure 5. 5: Photo of batch MF-ROMP set-up

To begin with, runs were carried out in air, but the results were not reproducible and resulted in a lower-than-expected yield ranging from 50 – 60 %. Despite using dry DCM, water present in the air is able to quench the radical cation by nucleophilic attack.[169] Following this, all the experiments carried out using compressed air which had been passed through a short column of phosphorus pentoxide to dry. The removal of water was seen by a gradual change of the phosphorus pentoxide from a white powder to a light pink gel.

5.2.2 Effect of the photocatalyst and its *para*-substituents

2,4,6-*Tris*(*para*-methoxyphenyl)pyrylium tetrafluoroborate (*p*OMeTPT) was used as a photocatalyst (PC) for MF-ROMP following the experimental method from the Boydston group.[123] Whilst many pyrylium salt photocatalysts are available, this was selected as the electron-donating -OMe substituents can stabilise the cation whilst the BF_4^- anion gives the salt reasonable solubility in organic solvents. Whilst being expensive to buy it is relatively cheap and easy to synthesise on a large scale.

The synthesis proceeds via a condensation-dehydrogenation mechanism with the BF_3•OEt_2 initiating as a Lewis acid (Scheme 5. 5).[184]

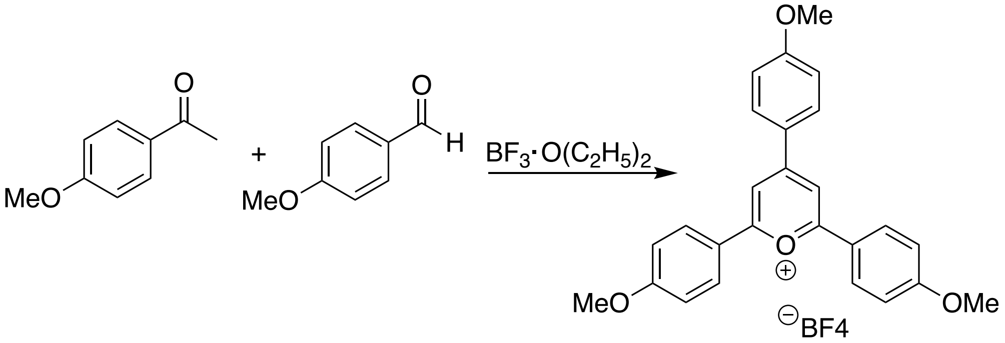

Scheme 5. 5: Reaction scheme of the synthesis of *p*OMeTPT[185, 186]

The conversion of NB to PNB was determined by ^{1}H NMR spectroscopy by using the -C**H**= resonance at δ=5.99 ppm of the monomer and the tertiary -C**H**- protons on the polymer chain at δ=2.22 ppm for the *trans* product respectively. The *cis* resonance was hidden by the monomer -C**H**- resonances but this could be found from the *cis:trans* ratio of the final purified polymer (1:3) (Figure 5. 6).[187]

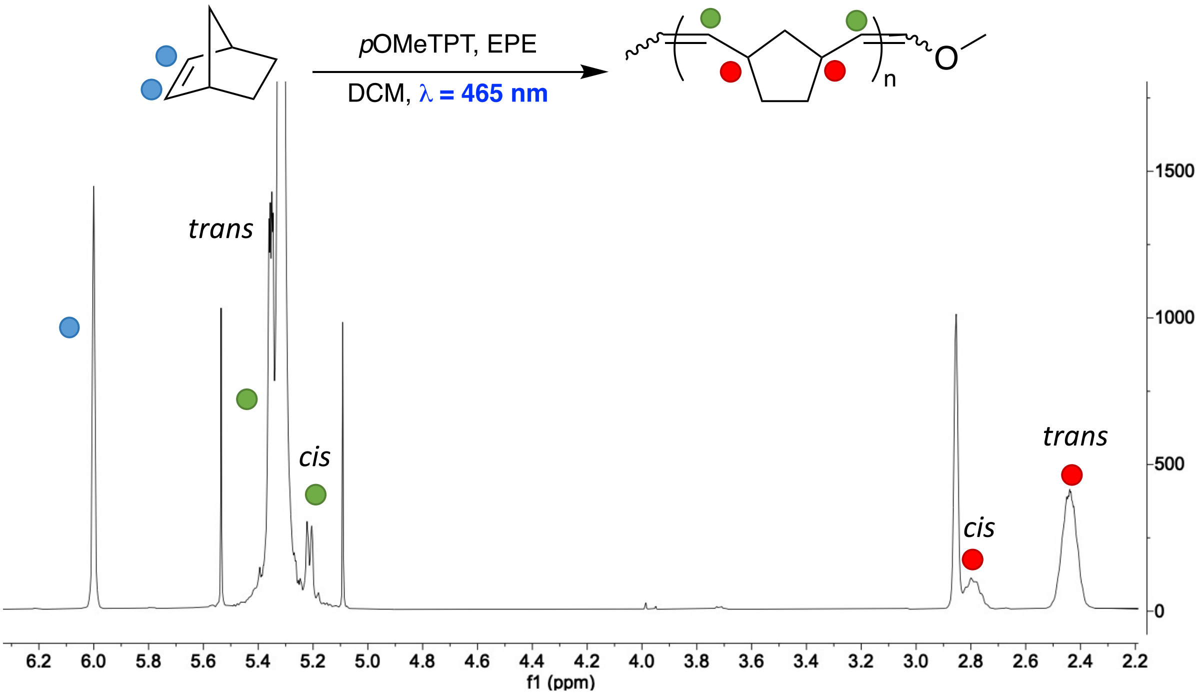

Figure 5. 6: ^{1}H NMR spectroscopy to show the conversion of norbornene to poly(norbornene)

As the concentration of PC was increased, the monomer conversion also increased until 1 mM when the conversion reaches at 95 %. After this the conversion falls, even if the reaction is left running for longer. One reason is that the PC is a very vibrant yellow colour so this might be absorbing too much of the colour preventing it getting into the centre of the sample vial.

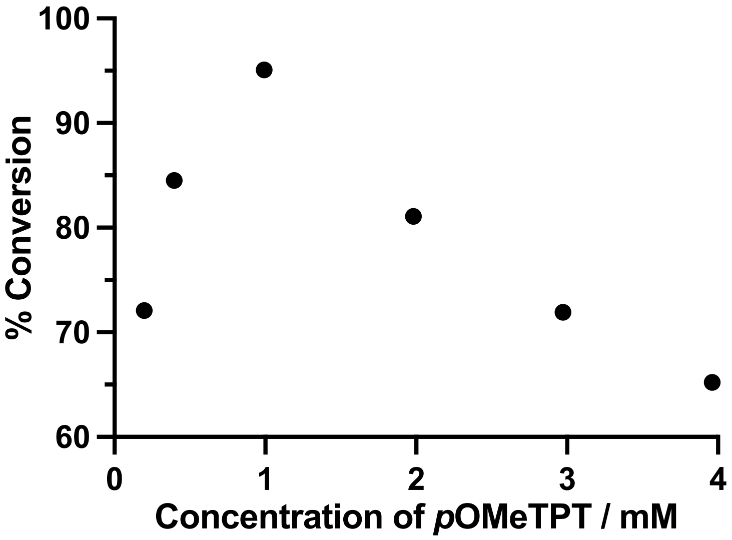

Figure 5. 7: Graph to show the effect of *p*OMeTPT concentration on the conversion of NB to PNB determined by ^{1}H NMR spectroscopy

The molar absorption coefficient (ε) of the photocatalyst was calculated by measuring the absorption at 465 nm, which is the dominant wavelength of the blue LEDs used and using the Beer-Lambert law (Equation 5. 1Equation 5. 1:) with a path length of 1 cm. The molar absorption coefficient was found to be high at 34400 dm^3 mol^{-1} cm^{-1}. This shows that it is a high absorbance which shows that at the wavelength used there is a large excitation and is consistent with similar photocatalysts.

$$\varepsilon = \frac{A}{cl}$$

Equation 5. 1: Beer-Lambert law where ε is the molar absorption coefficient (dm^3 mol^{-1}cm^{-1}), c is the concentration (mol dm^{-3}), A is the absorbance and l is the pathlength (cm).

2,4,6-Triphenylpyrylium tetrafluoroborate (TPT) is a cheaper, more readily available pyrylium catalyst that can also be used for MF-ROMP (Figure 5. 8). Since it does not have the electron donating *para*-OMe substituents, the cation is less stabilised and the photocatalyst is more prone to intramolecular and side reactions. Despite this, this photocatalyst is much cheaper and more readily commercially available which is an important consideration in industrial processes therefore was tested for its ability in MF-ROMP.

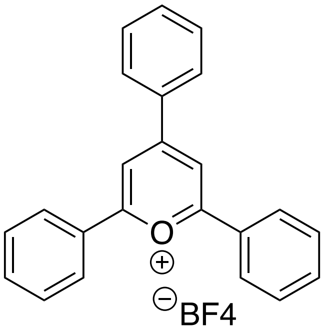

Figure 5. 8: Structure of TPT photocatalyst

The effect of concentration of TPT on the conversion of norbornene was tested and found to follow the same pattern as its methoxyphenol analogue. Initially, increasing the concentration increased the conversion increased until a maximum was reached, following which the conversion decreased and plateaued (Figure 5. 9).

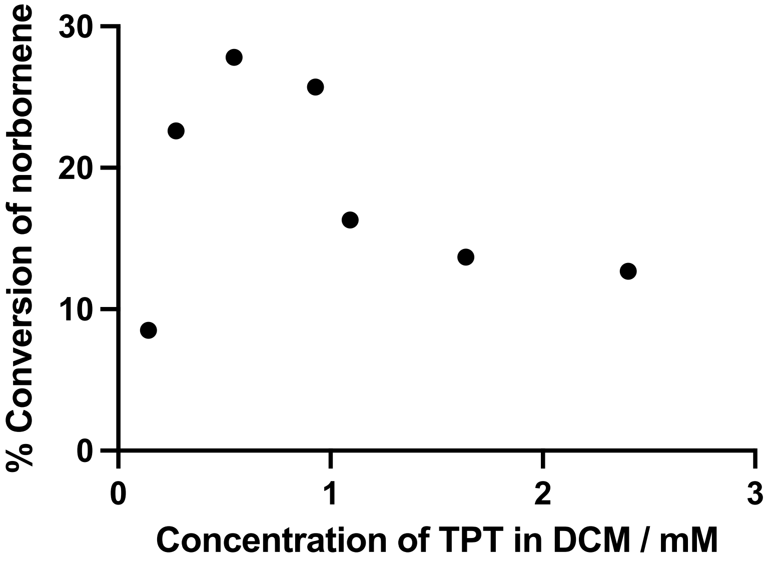

Figure 5. 9: Graph to show the effect of TPT concentration on the conversion of norbornene to PNB

The conversion of PNB was significantly lower for TPT than for *p*OMeTPT. This is partly a consequence this could be the lower oxidation potential and lower stability of the cation in TPT but it could also be that the 470 nm wavelength used was too large. The absorption spectra for TPT and *p*OMeTPT show that the *para* substituents have a large impact on the wavelengths of the energy gaps (Figure 5. 10).

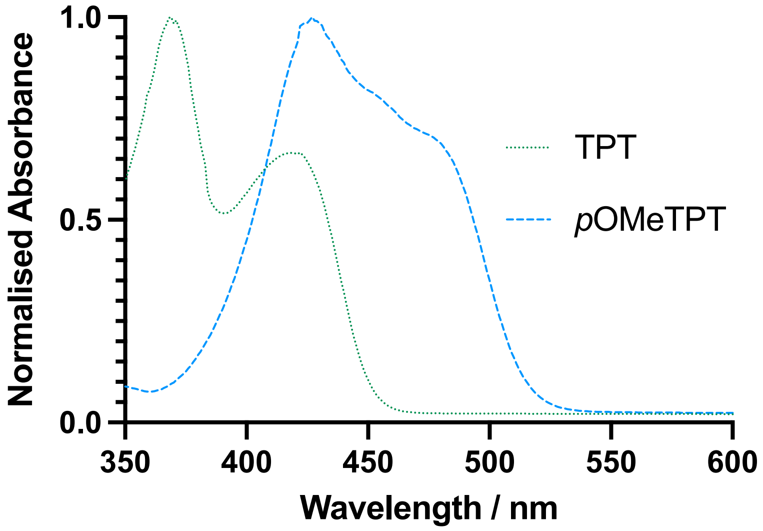

Figure 5. 10: Graph to show the absorption of wavelengths by *p*OMeTPT (blue --) and TPT (green ···)

5.2.3 Copolymerisation of NB with MMA

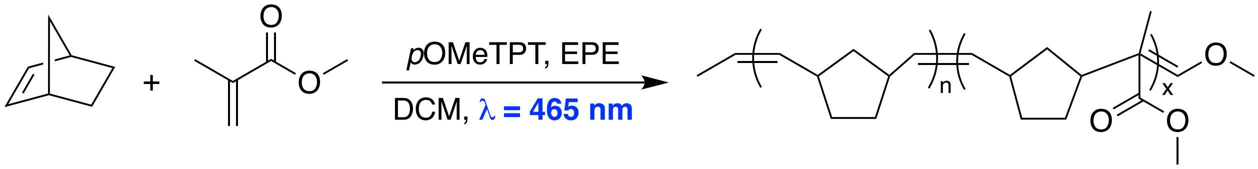

Scheme 5. 6: Hybrid MF-ROMP of norbornene and methyl methacrylate

Before copolymerising NB with NBMMA to get an unsaturated PNB chain with functional methacrylate groups, NB was polymerised with MMA to understand the mechanism and the copolymer properties. Previous work by Krappitz *et al*. claimed that when exposed to oxygen the polymerisation of MMA was inhibited whilst the overall conversion of norbornene increases.[124] This is because oxygen is used to regenerate the PC from its excited state.

The effect of increasing the fraction of MMA in the monomer feed and the effect of polymerising under dry air and N_2 were compared (Figure 5. 11). As the fraction of MMA increases in the polymer the monomer conversion decreases as well as the overall M_w of the polymer (Appendix). Work by Barner-Kowollik and co-workers also noticed that there was a lower overall monomer conversion when MMA was used however, they did not provide a suggestion as to why. They found that when adding additional pyrylium photocatalyst they could restart the polymerisation.[124] In these experiments, carried out in air, there appeared to be remaining photocatalyst at the end of the polymerisation observed by the reaction mixture remaining bright yellow and not having undergone photobleaching. Additionally, after purifying and restarting with additional photocatalyst there was no growth in the polymer chain. This shows that it must be a problem with quenching of the radical cation which could be due to MMA being prone to oxidation which is a competing reaction.[188]

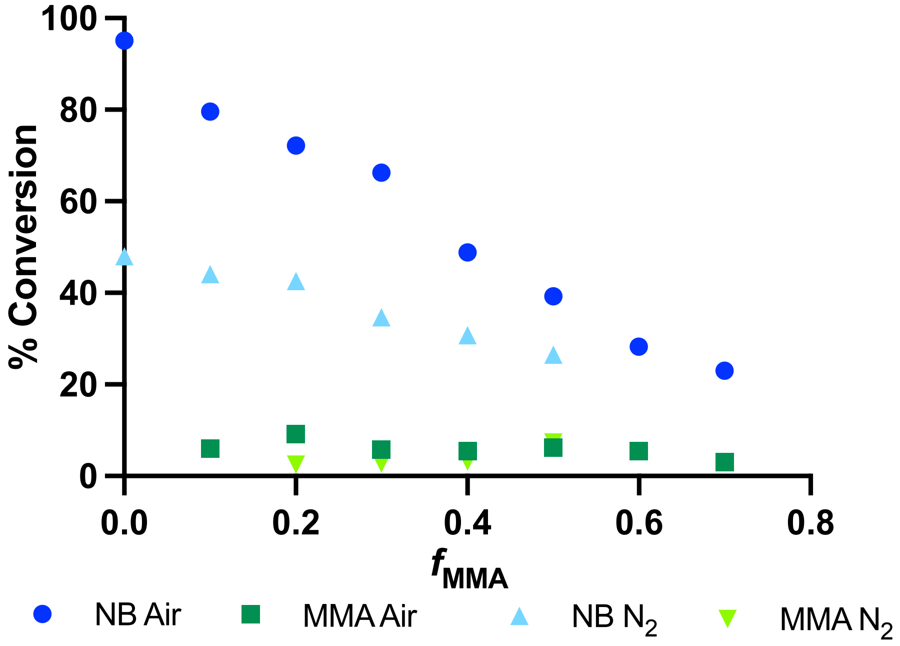

Figure 5. 11: Graph to show the effect of increasing the fraction of MMA and of changing from dry air to an inert N_2 atmosphere.

Conversion was determined by ^{1}H NMR spectroscopy where conversion of NB to PNB was as calculated as described above and the conversion of MMA was determined using the -C**H**$_2$ resonances at δ=6.1 and 5.56 ppm in the monomer and the -C**H**$_3$ resonances in the polymer at δ=3.61 ppm.

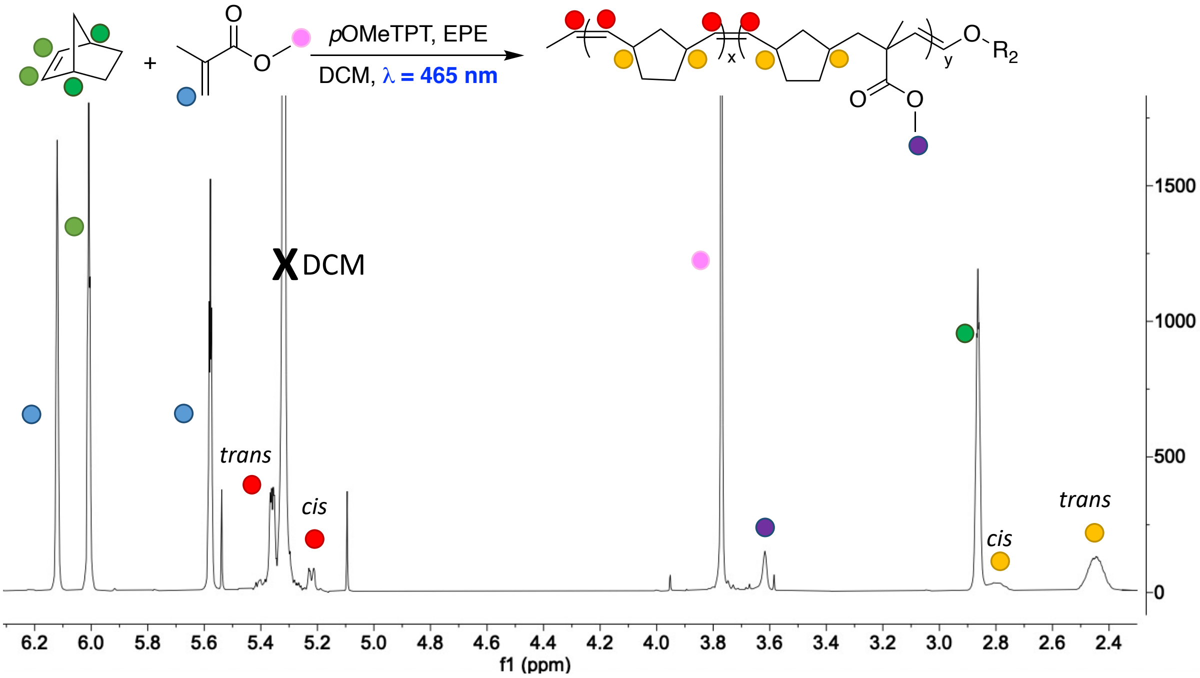

Figure 5. 12: ^{1}H NMR spectrum ($CDCl_3$) to show the conversion of norbornene and MMA to poly(norbornene-*co*-methyl methacrylate)

A colour change to dark red was observed at the end of the NB: MMA (1:1 mol. ratio) copolymerisation when deoxygenated with N_2. This is due to the photocatalyst not being regenerated by oxygen Figure 5. 13). Oxygen acts as a terminal oxidant to convert the photocatalyst into its active state in order to undergo another redox reaction.[167] This explains why the conversions are lower for the deoxygenated reactions. This is in contrast with the PNB homopolymerisation where the colour is completely quenched by the end of the reaction and the polymerisation can be initiated by adding further pyrylium salt.

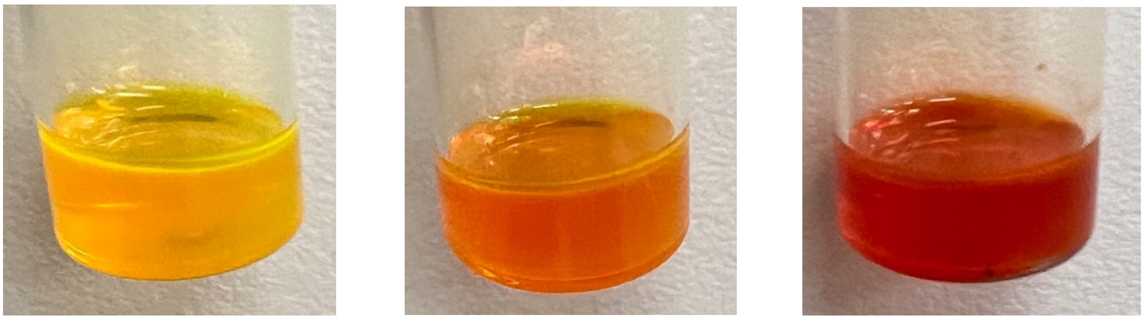

100 % O_2

O_2 and N_2 mixture

100 % N_2

Figure 5. 13: Photos to show the colour of the NB: MMA (1:1 mol. ratio) reaction mixture at the end of the reaction after being degassed in O_2, N_2 and a mixture.

The kinetics of the copolymerisation was measured using ^{1}H NMR spectroscopy with a 1:1 mol ratio of NB and MMA under a dry air atmosphere. Early in the reaction the polymerisation was shown to be predominantly NB, this is expected as the reaction is driven by the high ring strain (Figure 5. 14).

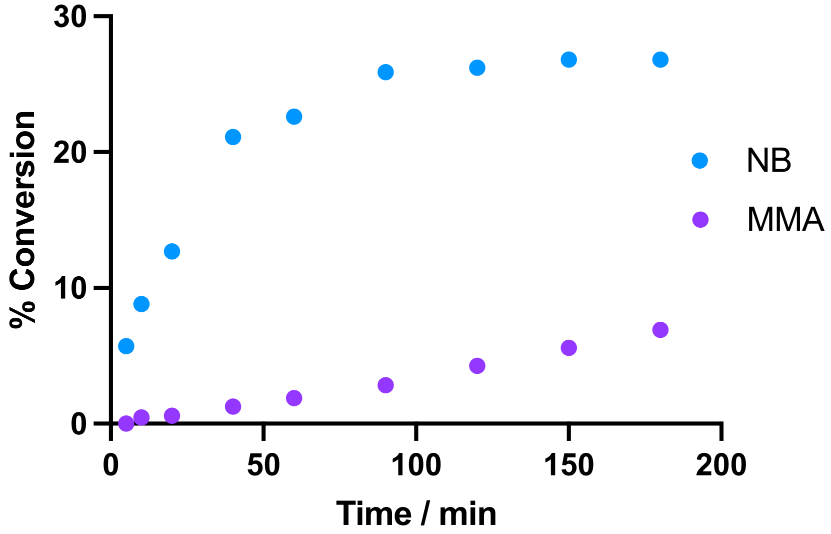

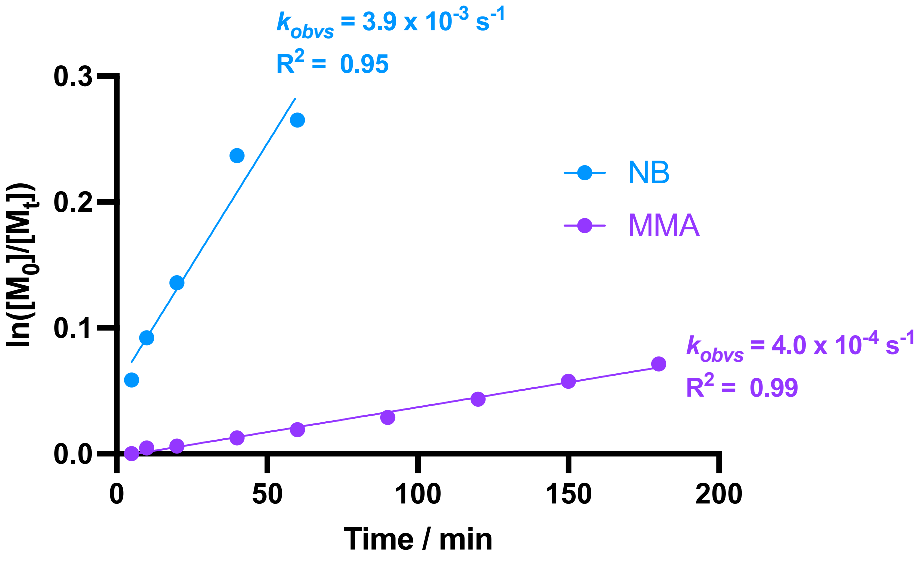

Figure 5. 14: Conversion of NB and MMA to P(NB-*co*-MMA) and first-order semi-log plot.

Differential scanning calorimetry (DSC) was used to determine the T_g of the polymers. This is the temperature at which a polymer undergoes a physical transition from a brittle, glassy state to a rubbery state and were determined by the mid-point of a change in slope of the DSC thermograph (Figure 5. 15). If there were two separate homopolymers forming parallel rather than one copolymer or if the polymer was more block than statistical in sequencing, two different T_gs would be observed.

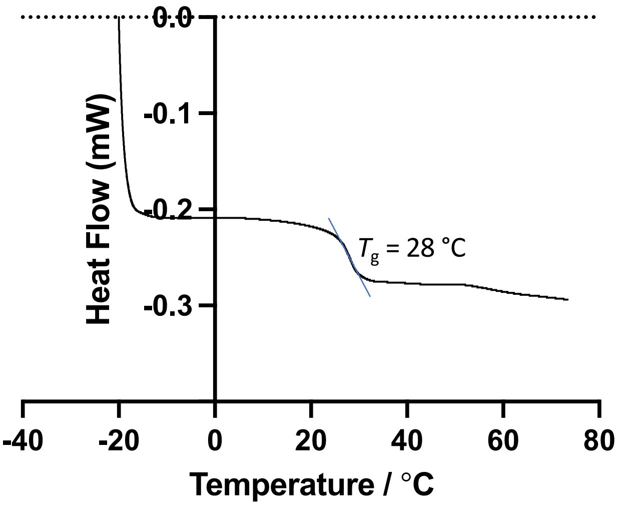

Figure 5. 15: DSC of P(NB-*co*-MMA) (2.4 wt % MMA)

As the fraction of MMA increased the T_g decreased (Figure 5. 16). The T_g of 40 °C is consistent with PNB that is majority *trans* isomer which has a lower T_g than the *cis* isomer.[189] The decrease in T_g could be partly due to increased flexibility caused by less unsaturation in the backbone of the PNB and partly since the molecular weight is decreasing.

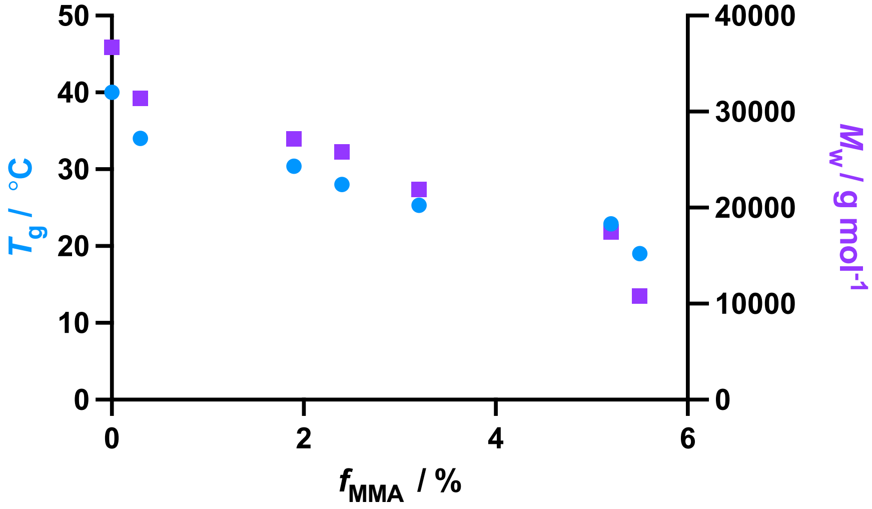

Figure 5. 16: Graph to show the effect on T_g and M_w as the fraction of MMA in the copolymer increases

An experiment was carried out to confirm that both the NB and MMA monomers stopped reacting when the light was switched off (Figure 5. 17). This was shown by running the polymerisation for 10 minutes then leaving it switched off for 5 minutes before repeating. Samples were taken for NMR spectroscopy at the end of each step and the results showed that lights were required for both mechanisms in the polymerisation allowing for a high degree of control of the polymerisation.

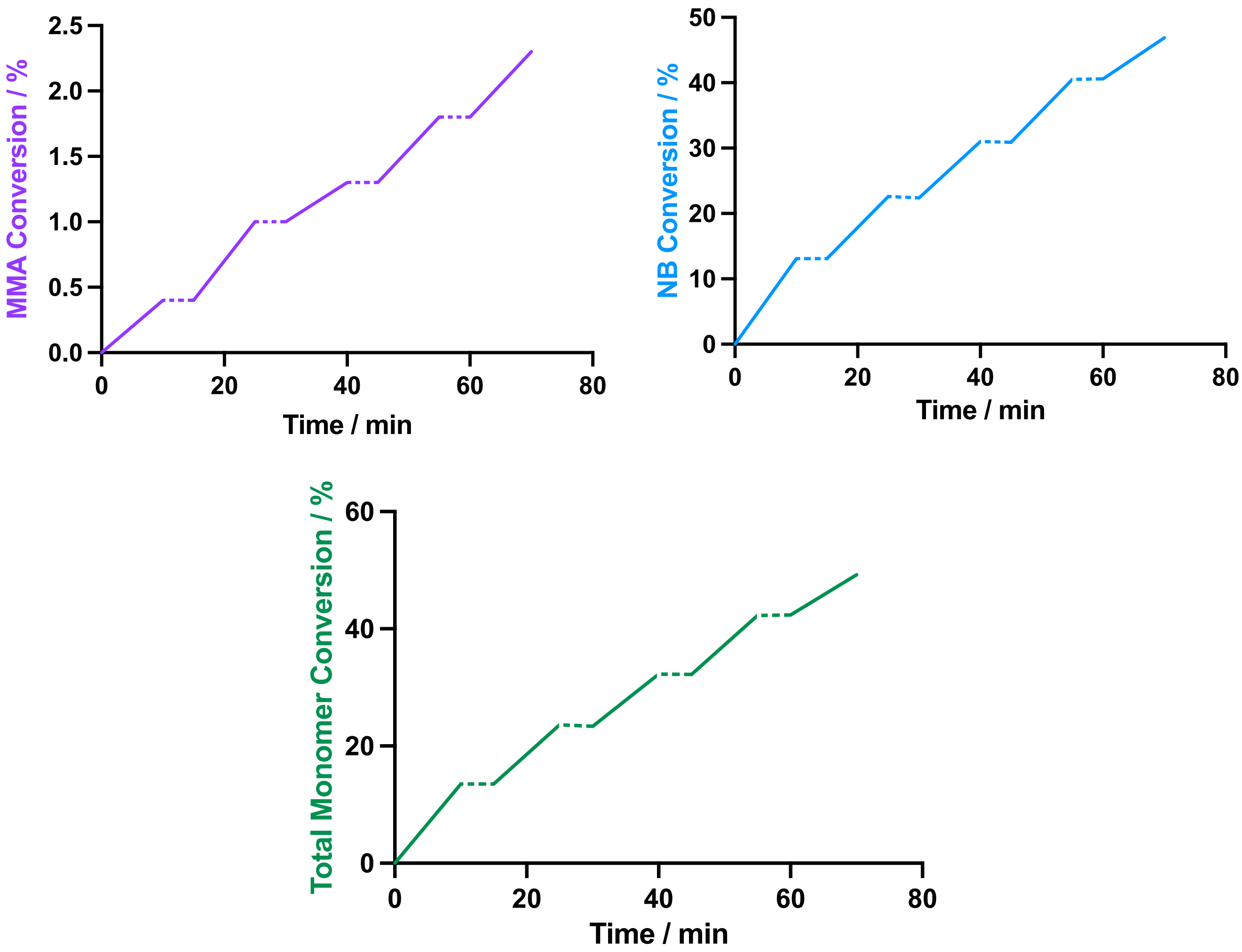

Figure 5. 17: Graphs to show the conversion of total monomer, b) NB and c) MMA over time. The solid lines represent the light being switched on and the grey dotted lines when the light is switched off.

A further experiment was carried out to determine the effect of light intensity on the reaction. An Arduino was programmed to work as a voltmeter which was used to alter the intensity of LED lights by switching them on and off rapidly to make them appear more or less intense. The reaction mixture was exposed to light for 60 minutes with stirring and the concentrations of reagents were kept the same (Figure 5. 18).

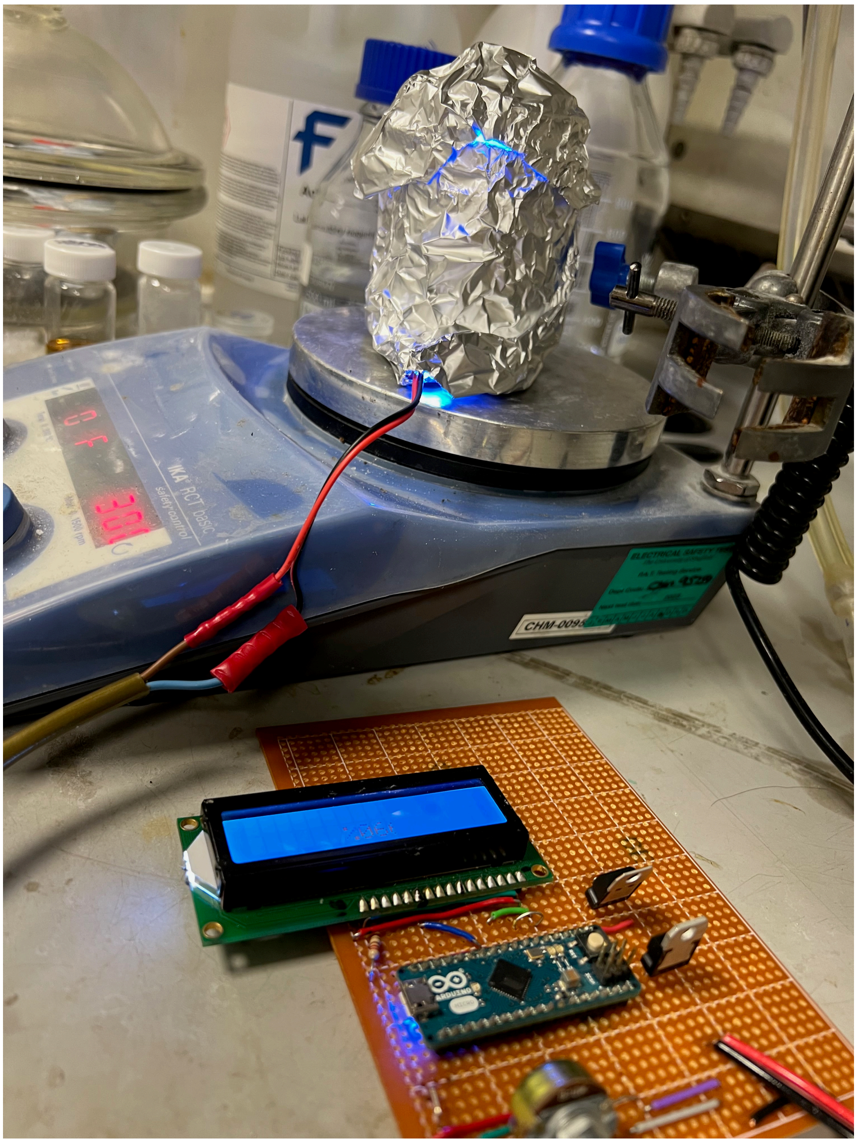

Figure 5. 18: Photo to show the LED set-up connected to an Arduino programmed to control the voltage.

As the intensity of light increases the conversion of NB increases linearly, reaching a maximum conversion around 40 %. The MMA also increases linearly initially but has a greater effect at higher intensities (Figure 5. 19).

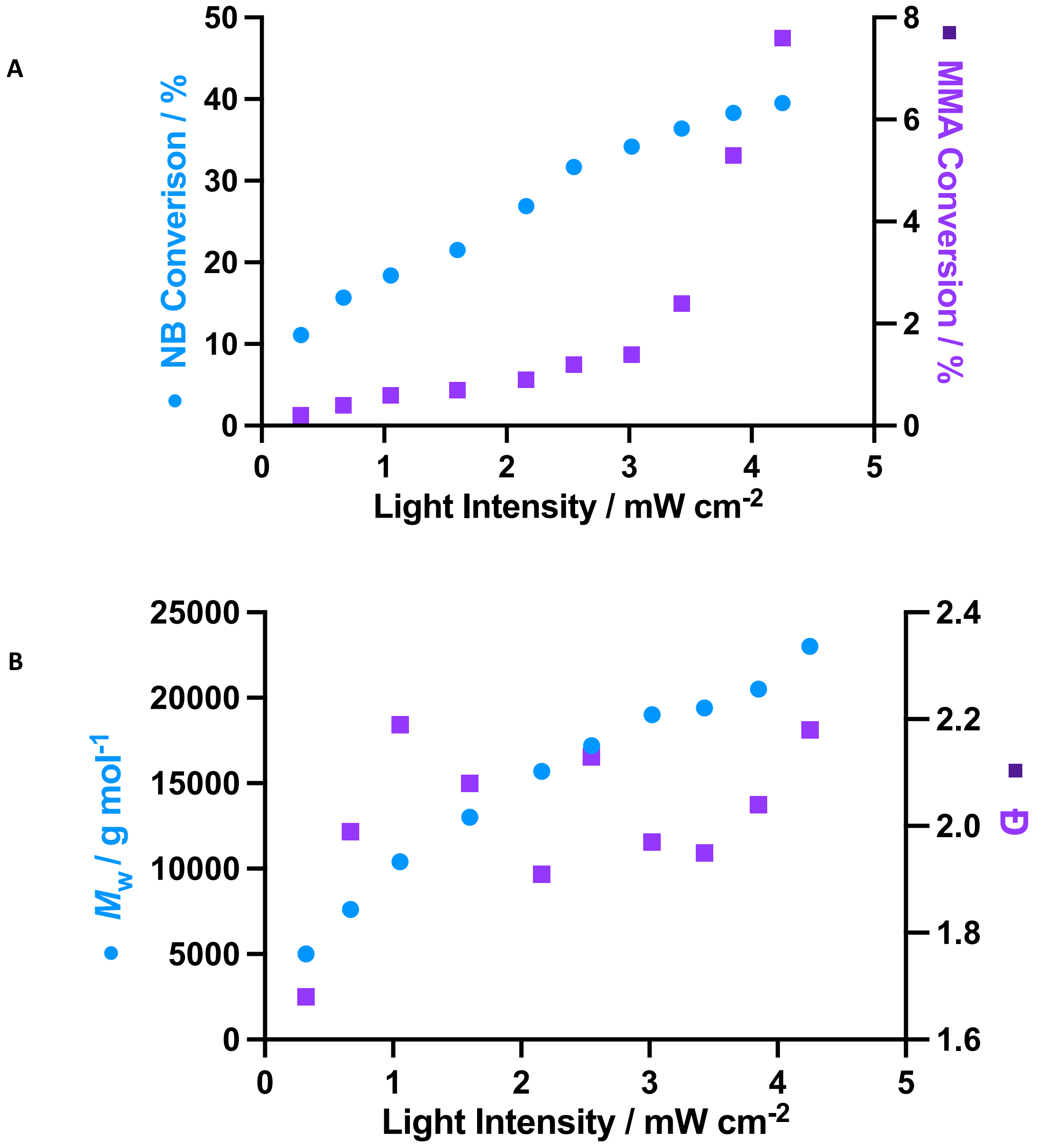

Figure 5. 19: A) Graph to show the effect of light intensity on the conversion of NB and MMA (determined by ^{1}H NMR spectroscopy) and B) The dispersity and M_w (determined by SEC (THF))

5.2.4 Copolymerisation of NB with NBMMA

Next, the monomer 5-norbornene-2-methylene methacrylate (NBMMA) was copolymerised with norbornene where the norbornene group on the bifunctional monomer should react quicker leaving the methacrylate groups available for crosslinking with the MMA adhesive (Scheme 5. 7).

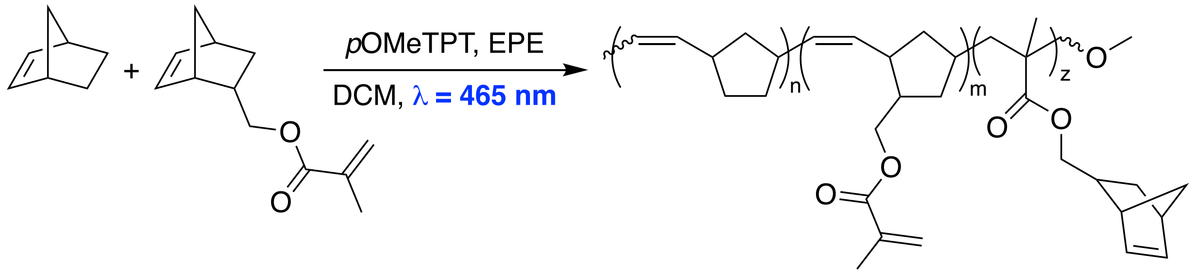

Scheme 5. 7: Reaction scheme for the MF-ROMP to form p(NB-*co*-NBMMA)

Calculating the conversion of the two separate monomers by ^{1}H NMR spectroscopy was challenging since there are overlapping resonances (Figure 5. 20). The NBMMA has the same resonances as norbornene with only a slight change in chemical shift plus both polymerise to form *cis* and *trans* configuration. The NBMMA also begins as a mixture of *exo* and *endo* isomers which both get polymerised. Additionally, the bifunctionality meant that there is some crosslinking where the alkene in both functional groups are consumed since MF-ROMP is preferential to norbornene but reactive with MMA groups.

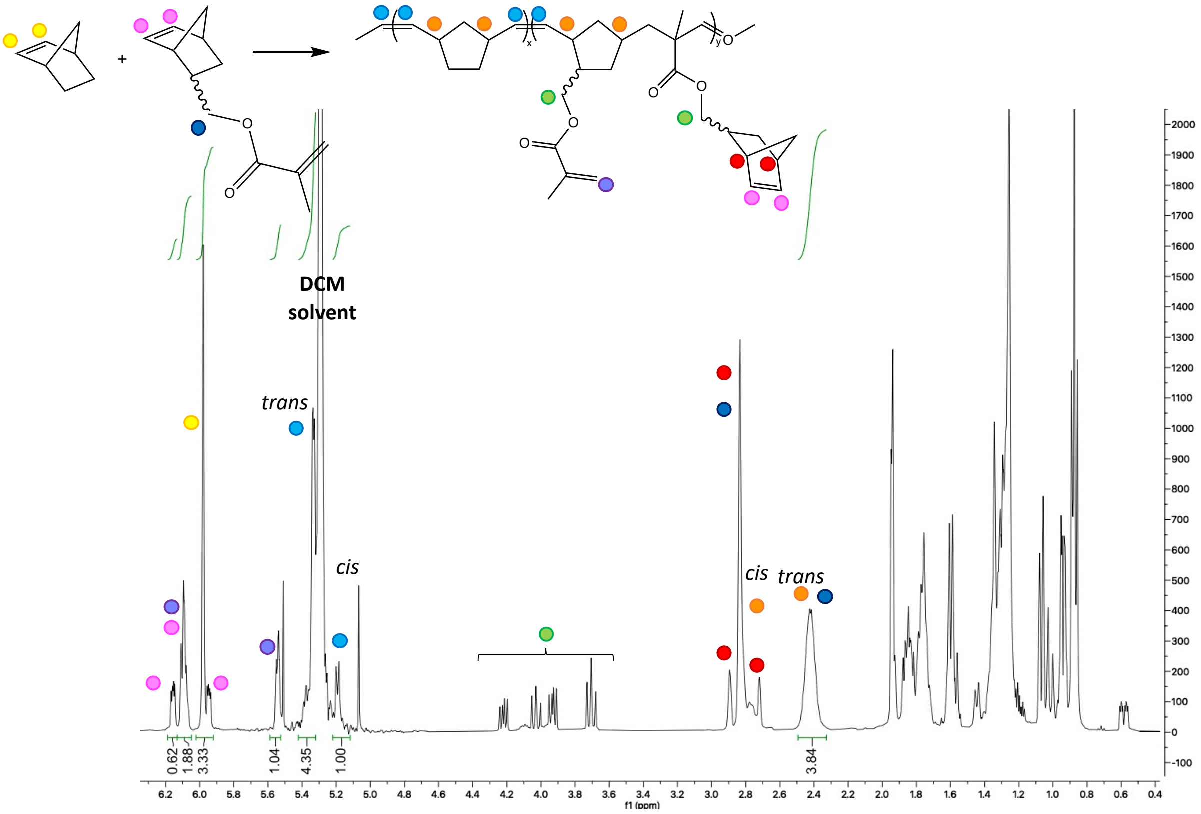

Figure 5. 20: ^{1}H NMR spectrum to show the overlapping resonances from the P(NB-*co*-NBMMA) copolymer.

The conversion was calculated by integrating the norbornene resonance at δ=6.01 ppm and the NBMMA norbornene resonances (*endo* δ=5.94 ppm and δ=6.17 ppm and both *exo* H δ=6.13-6.05). The *exo* norbornene resonance from NBMMA also contains an MMA resonance so needs to be subtracted using the δ=5.55 ppm MMA resonance. The tertiary -C**H**- protons on the norbornene polymer backbone were used to calculate the amount of polymer. The *trans* resonance at δ=2.4 ppm was used since the *cis* resonance was on a shoulder.

The *cis:trans* ratio was found from the purified polymer to be approximately 1:3 for all monomer ratios (Figure 5. 21). This method of measuring conversion is limited as it does not take into consideration NBMMA that has polymerised only through the MMA group however from results in Chapter 5.2 this is expected to be small.

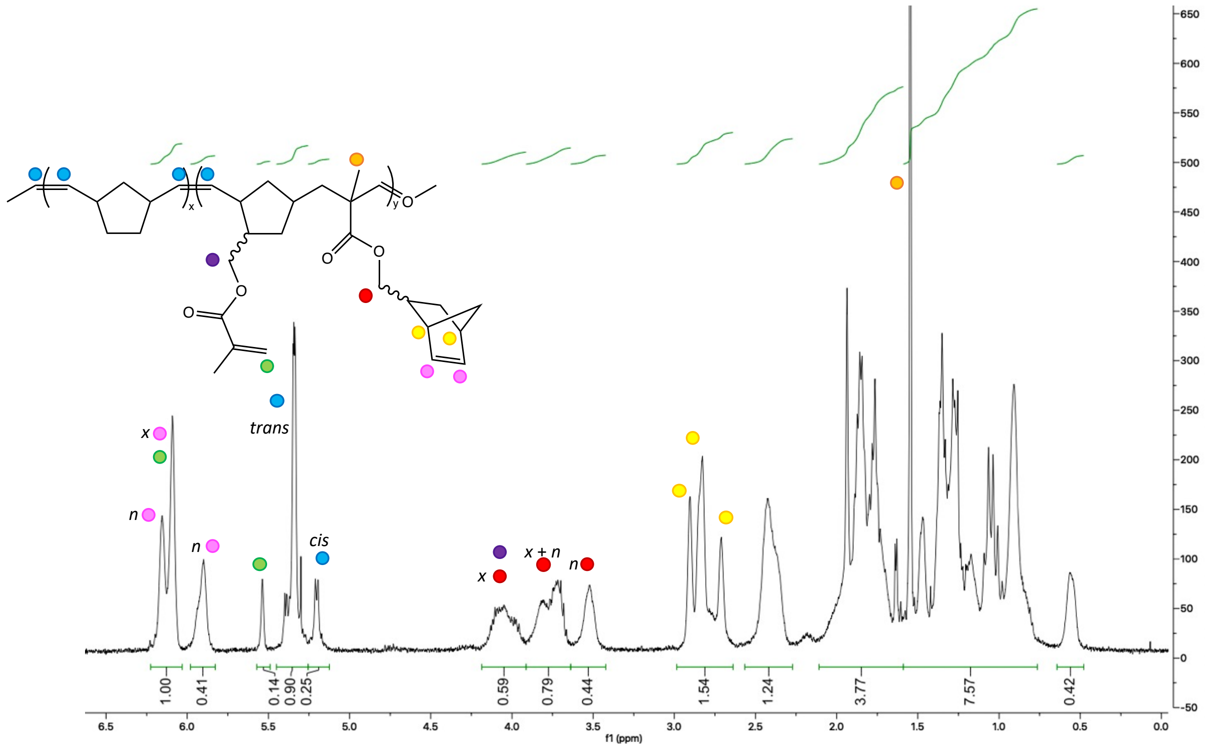

Figure 5. 21: ^{1}H NMR spectrum of P(NB-*co*-NBMMA)

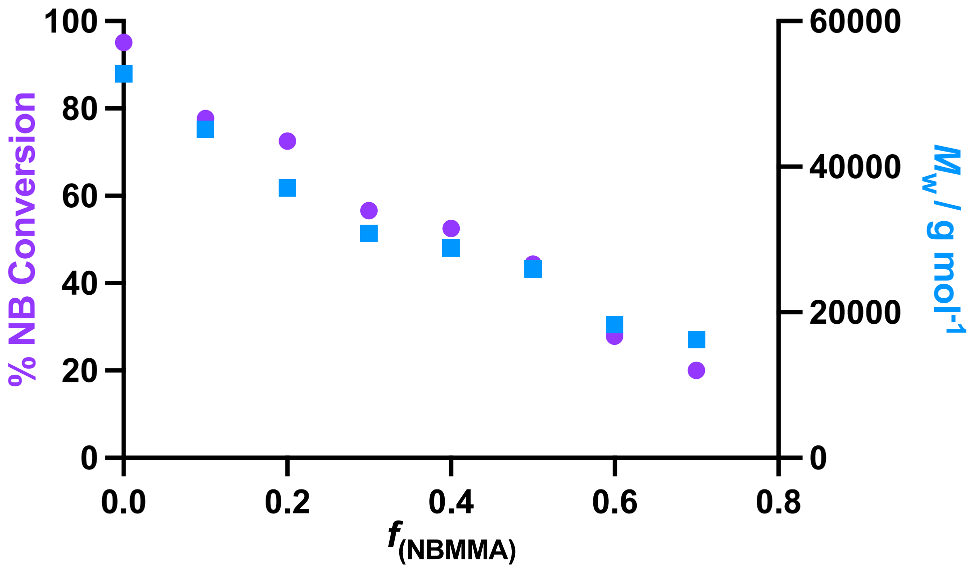

Figure 5. 22: Effect of fraction of NBMMA in monomer feed to show the total norbornene conversion

Since NBMMA is a bifunctional monomer as the fraction in the monomer feed increased the dispersity of the polymer product increased as a result of a small degree of branching/crosslinking. SEC (THF) was used to show this with the higher norbornene content polymers having narrower distributions and the lower norbornene content having a small shoulder at a shorter retention time (Figure 5. 23).

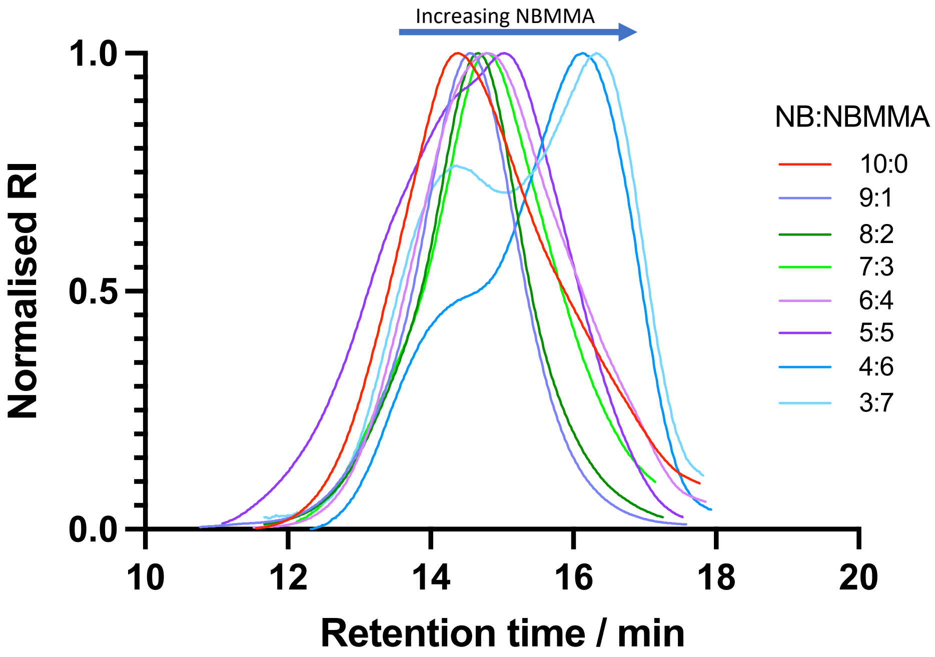

Figure 5. 23: Molar mass distributions of P(NB-*co*-NBMMA) with increasing retention times with increasing NBMMA fraction in the monomer feed

As the content of functionalised norbornene increased the T_g of the polymers decreased (Table 5. 1). Part of the reason for this could be that the molecular weights decreased although it could also be due to the incorporation of MMA groups into the backbone, breaking the rigid, unsaturated structure and introducing more flexibility.

Table 5. 1: The effect of the ratio of norbornene (NB) and NBMMA in the monomer feed on the molecular weight and T_g (^{a}- determined by SEC (THF) and ^{b}- determined by DSC)

f_1 (NB)	**f_2 (NBMMA)**	**NB conversion / %**	**M_w / g mol^{-1} ^{a}**	**$Đ_M$^{a}**	**T_g^{b} / °C**
1.0	0.0	95	52600	3.09	40.8
0.9	0.1	78	45100	2.38	30.2
0.8	0.2	73	37000	2.19	26.5
0.7	0.3	57	30800	2.41	24.5
0.6	0.4	53	28900	3.07	22.6
0.5	0.5	44	25900	3.15	19.6
0.4	0.6	28	18300	3.98	16.5
0.3	0.7	20	16300	4.25	15.4

Both monomers were found to have different retention times in gas chromatography (GC) which meant that the relative kinetics of the two monomers could be measured. Samples were taken regularly during the reaction for GC analysis (Figure 5. 24). The limitation of this method is that there is no way of being able to tell whether the norbornene or MMA group on NBMMA was reacting and any crosslinking would also not be detected.

It was shown that initially the non-functionalised norbornene monomer reacted faster which could be due to steric hindrance although there was only a small overall difference in conversion between the two monomers after 60 minutes. From early experiments using MMA it was assumed that NBMMA reacted predominantly through the norbornene.

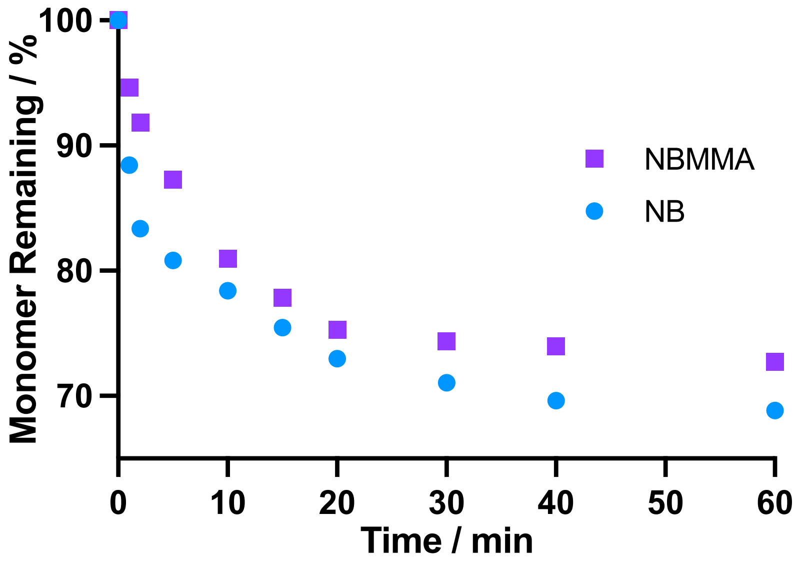

Figure 5. 24: Conversion of NB and NBMMA to polymer during MF-ROMP measured by GC

5.2.5 Scaling-up MF-ROMP of PNB by droplet-flow polymerisation

Carrying out MF-ROMP on a 5 mL scale in a sample vial with a diameter of 2.5 cm did not produce enough product to prepare adhesive samples for mechanical testing. Due to the attenuation of light decreasing with distance from the light source increasing the sample vial the reaction is carried out in would not give good yields. Flow polymerisation was used as an alternative since it gives the reaction a large surface area to volume ratio.

A flow reactor was set-up to show that MF-ROMP of norbornene and MMA could be scaled up. PTFE tubing with a diameter of 1 mm and length of 2 m were wrapped around a glass beaker and blue LED lights were fixed above (Figure 5. 25, Figure 5. 26). The wavelength of the blue LEDs used was 465 nm. The reaction mixture was stored in a gas-tight syringe and introduced to the reactor from a syringe pump.

Since MF-ROMP requires the presence of oxygen and whilst degassing with 100 % oxygen has been shown to decrease the yield, droplet-flow was used as opposed to laminar to control the rate of O_2

introduced. A peristaltic pump was used to pump the gas from a flask with a balloon of O_2 keeping a positive pressure (Figure 5. 25). Initially a ball mixer was used to connect the two phases however this was found to be too turbulent, so a T-mixer was used instead (Appendix 32). The wavelength of light used for the flow polymerisations was 450 nm. For the reactor, tubing with a diameter of 1 mm and a length of 2 m was wrapped around a glass beaker with the LEDs held above. Using a smaller tubing diameter was shown to build too much pressure within the reactor and pushed the liquid phase towards the peristaltic pump.

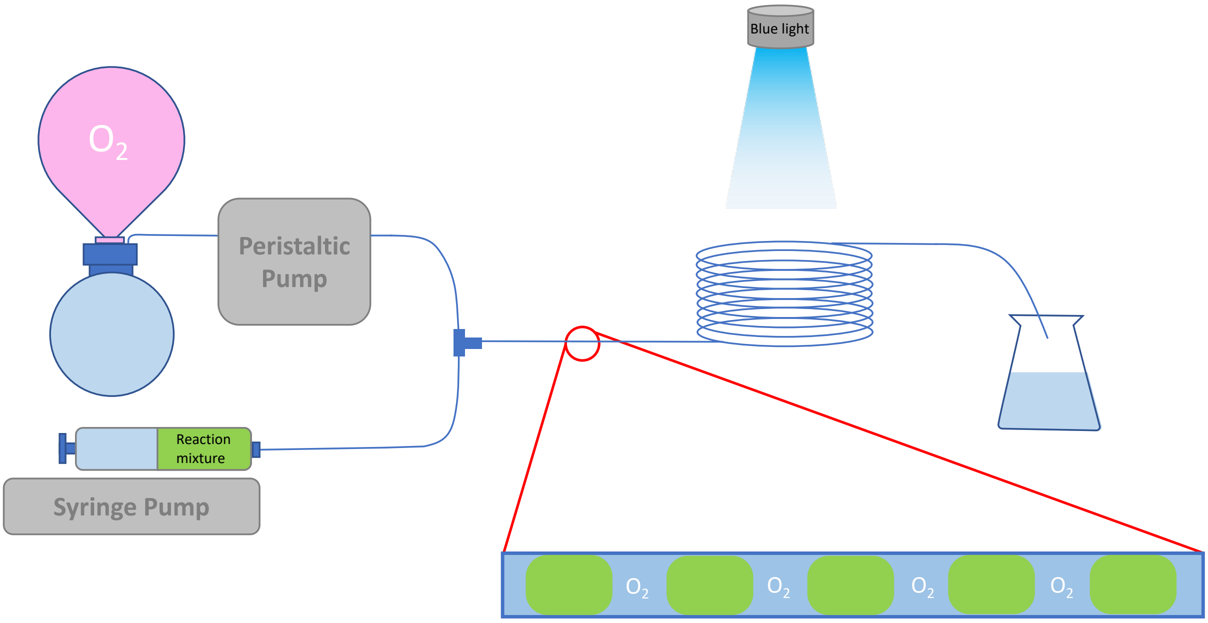
Blue light
O2
Peristaltic Pump
Reaction mixture
Syringe Pump
O2
O2
O2
O2

Figure 5. 25: Droplet-flow reactor set-up

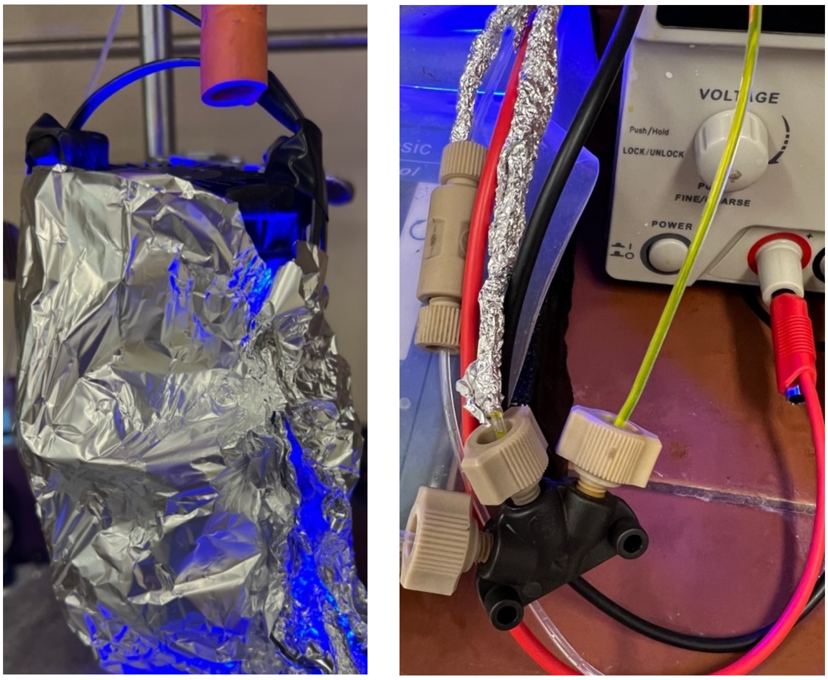

Figure 5. 26: Photo of reaction set-up of reactor and ball-mixer

Kinetic experiments were carried out by using time sweeps where the flow rate is reduced so that the residence time increases and assuming ideal droplet flow all of the residence times between can be sampled.[178, 190] This was tested using inline ^{1}H NMR spectroscopy though, this was not successful for droplet-flow reactions as a consequence of the gas bubbles preventing good NMR spectra and gave incoherent results.

A manual kinetic experiment was carried out by increasing the residence time. The flow was allowed to equilibrate for 1.3 times the residence time before samples were collected and analysed by ^{1}H NMR spectroscopy and SEC (THF).[178] The ratio of gas bubbles to reaction mixture was 1:3 and 0.05 mol. eq. of PC and 1 mol. eq. of initiator was used as in the batch reactions. After 12 minutes there was no further polymerisation with the conversion not reaching 50 %. This was the time taken for the colour of the reaction mixture to become colourless (Figure 5. 27).

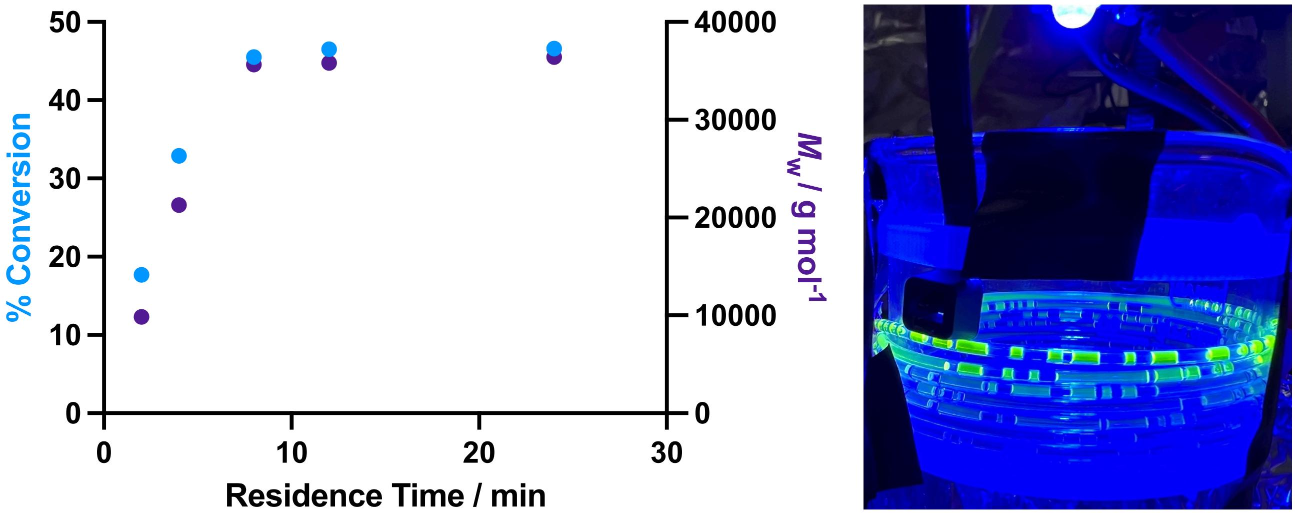

Figure 5. 27: The effect of residence time on % conversion and M_w (left) and a photo to show the flow reactor at a residence time of 24 minutes (right)

The effect of the light intensity on the conversion was investigated by reducing the voltage to the LEDs (Figure 5. 28). The residence time was kept constant at 12 minutes and the length of time before reaction became colourless reduced as the light intensity increased. The reduction in the length of time until photobleaching occurred is due to the increase in rate of unfavourable energy gap transitions.

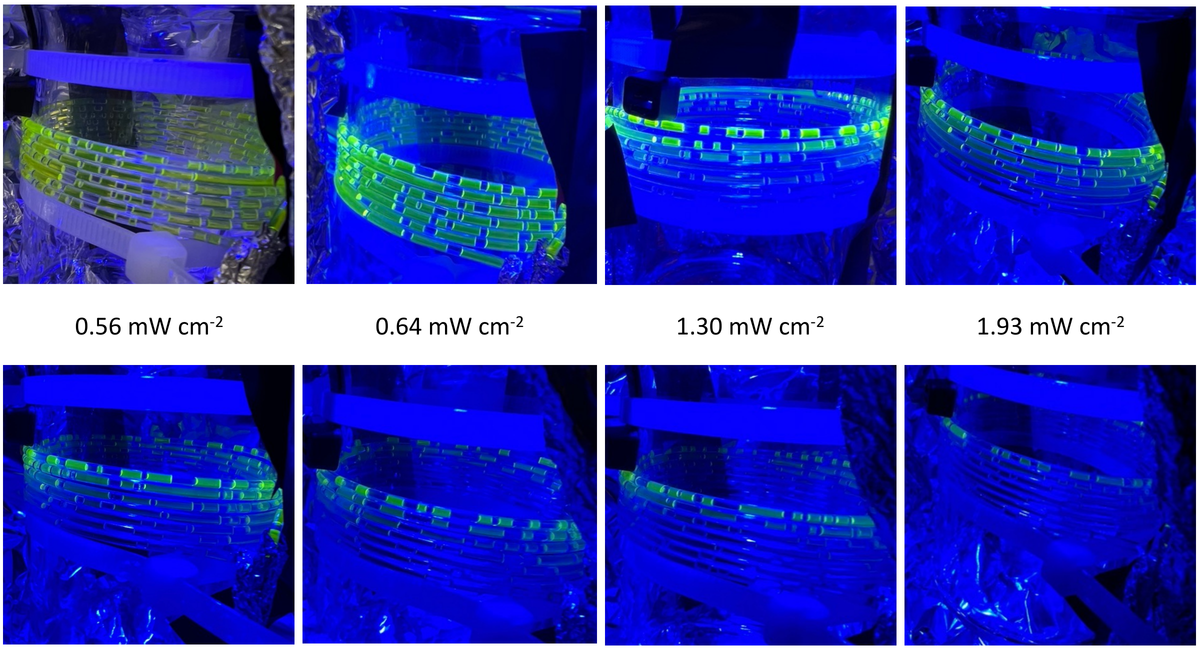

0.56 mW cm^{-2} 0.64 mW cm^{-2} 1.30 mW cm^{-2} 1.93 mW cm^{-2}

2.61 mW cm^{-2} 3.23 mW cm^{-2} 3.98 mW cm^{-2} 7.27 mW cm^{-2}

Figure 5. 28: Diagrams to show how the fluorescence of the *p*OMeTPT photocatalyst shortens as the light intensity increases.

Despite the photocatalyst being active for a shorter period of time, the monomer conversion increased as the light intensity increased until it almost reached 80 % conversion (Figure 5. 29). Even at the highest light intensity, the conversion is a lot lower than conversions that had been reached in batch, potentially as a consequence of the oxygen concentration being higher (Future work). The dispersities for all polymerisations ranged from between 1.8-2.4 which is significantly smaller than $Đ_M$ = 3.65 that was achieved in batch.

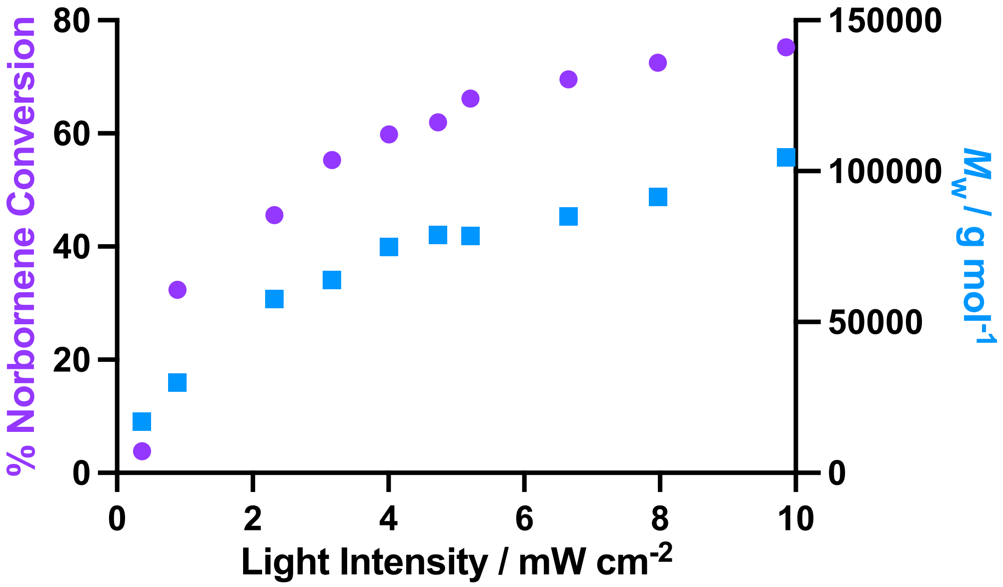

Figure 5. 29: Effect of light intensity on NB conversion during droplet flow polymerisation

5.2.6 Copolymerisation of norbornene and MMA by droplet-flow polymerisation

Next, norbornene was copolymerised with MMA using the same conditions with a light intensity of approximately 6.6 mW cm^{-2} and a residence time of 10 minutes (Figure 5. 30). As in batch reactions, the conversion of both monomers decreased as the fraction of MMA in the monomer mixture increased. Far less MMA was converted into polymer than had during batch polymerisations. A key difference is the light intensity being higher, leading to the reaction rapidly reaching completion in this set-up whilst it was seen in batch of the MMA reacted towards the end of the polymerisation. As was observed in batch polymerisation, photobleaching did not occur and the reaction mixture retained its bright yellow colour.

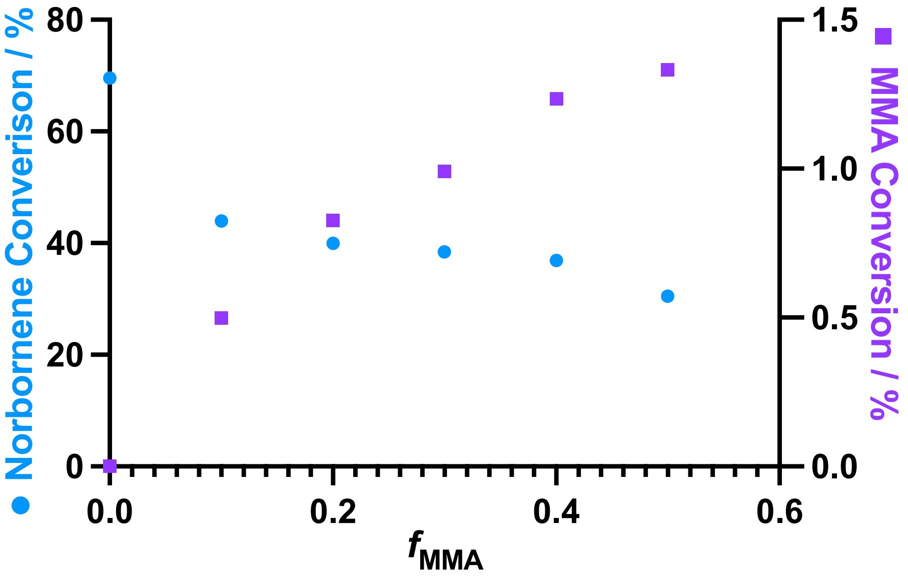

Figure 5. 30: Graph to show the effect of norbornene and MMA conversion on the fraction of MMA in the monomer mixture.

The concentration of initiator in the polymer was varied next, with the monomer and photocatalyst were kept in one syringe and the initiator solution kept in another syringe and the flow rates were varied (Figure 5. 31). When a low degree of polymerisation (DP) was targeted the monomer conversion was lower than expected. There was also a loss of colour due to photobleaching, which suggests that because the equivalents of photocatalyst to monomer were kept the same, it was this that lead to termination (Figure 5. 32). For the higher targeted DPs, the instability of the initiator was the reason for termination.

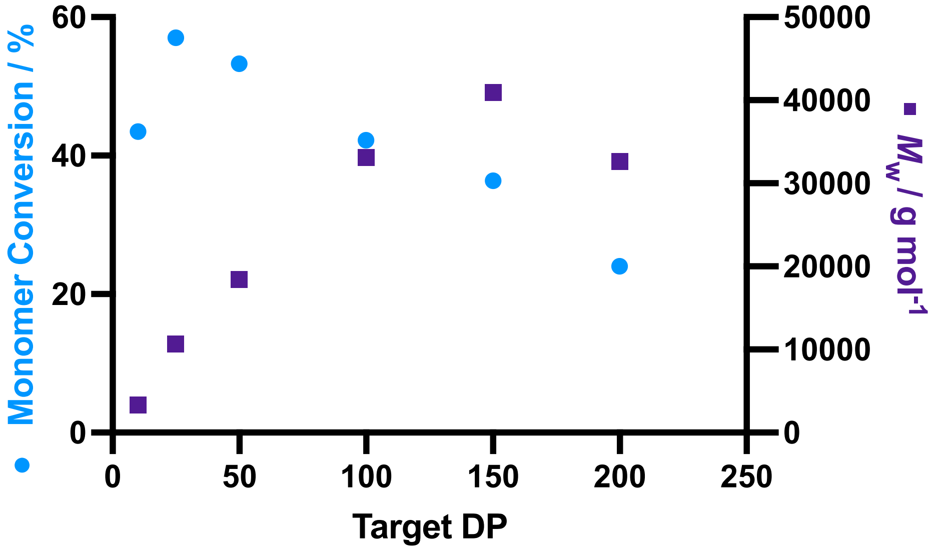

Figure 5. 31: Graph to show the effect of increasing the Target DP on the ● monomer conversion (determined by ^{1}H NMR spectroscopy) and ■ M_w (determined by SEC (THF))

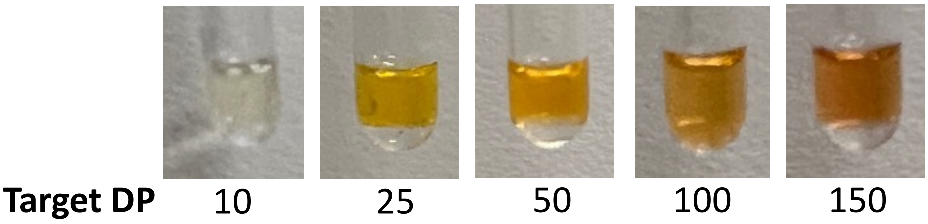

Figure 5. 32: Photos to show the colour of the reaction mixture at the end of the flow polymerisation with increasing target DPs

5.3 Conclusions

MF-ROMP has been shown to be a method of synthesising polynorbornenes with MMA functional groups that is MMA soluble. The reaction can easily be terminated, and the polymers purified without risk of further radical reaction as a high intensity blue light is used to control both the initiation and propagation.

MF-ROMP can be used to create novel poly(norbornene-*co*-methyl methacrylate) copolymers which have higher polarity and better solubility in polar organic solvents. The polymerisation works best when carried out in the presence of oxygen in order to regenerate the photocatalyst. Despite this, it is difficult to increase the amount of MMA in the polymer as it is less reactive than norbornene because the reaction is driven by the release of high ring-strain. Additionally, the greater the fraction of MMA in the starting monomer mixture, the lower the overall monomer conversion due to side reactions and quenching that the MMA can cause.

Similar amounts of NBMMA and norbornene monomers are converted to polymer during MF-ROMP when a 1:1 mol ratio is used however the more NBMMA present the lower the overall monomer conversion is. The monomer conversions are higher when NBMMA is used as a copolymer compared with MMA.

Scaling up MF-ROMP in batch is difficult due to the greater distance the light photons need to travel through the reaction mixture. However, flow polymerisation has been shown to be a successful alternative. Using droplet-flow polymers with lower DPs were achieved than in batch polymerisation. It was also shown that high conversions could be achieved with a retention time of minutes and that the greater the light intensity, the polymerisation proceeds quicker and to a higher conversion.

Chapter 6 - Future Work

It has been shown that poly(norbornene)s with pendant methylene methacrylate groups are polymerisable by ROMP with G3 and form polymers soluble in MMA. Addition of only 10 wt % can increase the thermal degradation temperatures although the adhesive strength decreased. Adding 5 wt % methacrylic acid counteracted the loss of polarity from the poly(norbornene) and improved the strength of the adhesive. Further work could be carried out to find the T_gs of the copolymers and the effect on the elasticity of the methacrylate-based adhesive by the presence of poly(norbornene) through tensile tests. Since the ROMP polymers cannot be isolated and stored due to crosslinking an alternative synthesis could be found such as using a W or Mo based catalyst. These are also cheaper so used more often for ROMP on an industrial scale. These polymers could then be added into a fully formulated adhesive containing further additives such as rubber to prevent crack propagation to compare to current commercially available structural adhesives.

It was shown that the viscosity of the adhesive is important on the strength of the lap shears however the viscosities were not found. Rheology had been carried out using a cone however the viscosity of the MMA: EGDMA mixture (M1) was too low and leaked out. The adhesives would need to be prepared on a 20 g scale and rheology using a cup-and-bob technique would be used to find these.

Synthesis of PDCPD on a 2 g scale was found to be challenging to repeat without large sources of error. Despite this, it was shown that with a high temperature post-cure the adhesive strength of PDCPD can be increased by the addition of crosslinkers with 2 and 3 norbornene groups connected by ester linkages. These ester linkages increased the polarity, increasing the non-covalent interactions with the hydroxyl layer of the adherend, however provided weaknesses in the adhesive which lowered the degradation temperatures. Whilst these thermosets might not be suitable for adhesive applications as a room temperature cure was not achieved, they might provide strong materials for composites with increased polarity to enhance bonding to an adhesive layer. For these applications, reaction injection moulding (RIM) would be used to manufacture the composite with control over the properties.

In chapter 5, MF-ROMP was shown to be a method of producing unique norbornene and methacrylate copolymers. The catalyst efficiency was the factor limiting the conversion during the norbornene homopolymerisation however during the copolymerisation with methacrylate functionalised polymers there was remaining photocatalyst at the end of the reaction. Since the use of ethyl vinyl ether as an initiator gives a 0 % monomer conversion, an enol ether with a larger R group might be able to stabilise the radical cation better and lead to a greater conversion. This initiator could be synthesised through a Williamson etherification of an alkyl bromide and a secondary alcohol such as cyclohexanol.

7. References

1. I. Skeist, *Handbook of adhesives*, Chapman and Hall, New York, 3rd edn., 1990.
2. K. Balani, V. Verma, A. Agarwal and R. Narayan, *Biosurfaces: A Materials Science and Engineering Perspective*, John Wiley and sons, Hoboken, New Jersey, 2015.
3. B. E. Gdalin, E. V. Bermesheva, G. A. Shandryuk and M. M. Feldstein, *J. Adhes.* , 2011, **87**, 111-138.
4. C. Cui, B. Lui, T. Wu, C. Fan, Z. Xu, Y. Yao and W. Liu, *J.Mater. Chem. A*, 2022, **10**.
5. J. Comyn, *Adhesion Science*, RSC Publishing, 1st Edition edn., 1997.
6. E. P. Chang, *J. Adhes.*, 1997, **60**, 233-248.
7. T. Sugama and N. R. Carciello, *Int. J. Adhes. Adhes.*, 1993, **13**, 257-266.
8. Q. Quo, *Thermosets : Structure, Properties, and Applications*, 2nd edn., 2017.
9. E. Dolci, G. Michaud, F. Simon, B. Boulevin, S. Fouquay and S. Callol, *Polym. Chem.*, 2015, **6**, 7851-7861.
10. J. Beauson, B. Madsen, C. Toncelli, P. Brondsted and J. I. Bech, *Compos. A*, 2016, **90**, 390-399.
11. W. K. Chiang, E. Chassemieh, R. Lewis, J. Rowson and C. Thompson, *J. Adhes. Sci. Technol.*, 2012, **24**, 1949-1957.
12. H. S. Chung, G. H. Park, T. Kim, H. Ahn, D. H. Kim and I. Chung, *Mol. Cryst. Liq.*, 2013, **583**, 43-51.
13. E. Cohen, O. Binshtok, A. Dotan and H. Dodiuk, *J. Adhes. Sci. Technol.*, 2012, **27**, 1998-2013.
14. A. Higgins, *Int. J. Adhes. Adhes.*, 2000, **20**, 267-376.
15. M. S. Sohn, X. Z. Hu, J. K. Kim and M. Walker, *Compos. B Eng.*, 2000, **31**, 681-691.
16. L. F. M. da Silva, T. N. S. S. Rodrigues, M. A. V. Figueiredo, M. F. S. F. de Moura and J. A. G. Chousal, *J. Adhes.*, 2007, **82**, 1091-1115.

17. A. M. Pereira, J. M. Ferreira, F. V. Antunes and P. J. Bartolo, *J. Mater. Process. Technol.*, 2010, **210**, 610-617.
18. J. Kim, K. S. Kim and Y. H. Kim, *J. Adhes. Sci. Technol.*, 2012, **3**, 175-187.
19. M. D. Thouless and Q. D. Yang, *Int. J. Adhes. Adhes.*, 2008, **28**, 176-184.
20. R. J. C. Carbas, M. A. Dantas, E. A. S. Marques and L. F. M. da Silva, *J. Adv. Join. Process.*, 2021, **3**, 100061.
21. M. D. Banea and L. F. M. da Silva, *Proc. Inst. Mech. Eng. L: J. Mater.: Des. Appl.*, 2010, **224**, 51-62.
22. S. Kalpakijan, S. R. Schmid and K. S. V. Sekar, *Manufacturing Engineering and Technology*, Pearson Education LImited, Essex, 7th edn., 2014.
23. B. J. Holland and J. N. Hay, *Polym. Degrad. Stab.*, 2002, **77**, 435-439.
24. B. Bilyeu, W. Brostow and K. P. Menard, *J. Mater. Edu.*, 2000, **22**, 107-129.
25. S. V. Hoa, P. Ouellette and T. D. Ngo, *J. Compos. Mater.*, 2009, **43**, 783-803.
26. J. P. Bell, *J. Polym. Chem. A. Polym. Chem.*, 1970, **6**, 417-436.
27. R. A. Pethrick, *Proc. Inst. Mech. Eng. L: J. Mater.: Des. Appl.*, 2015, **229**, 349-379.
28. S. K. Ooi, W. D. Cook, G. P. Simon and C. H. Such, *Polymer*, 2000, **41**, 3639-3649.
29. R. J. C. Carbas, E. A. S. Marques, L. F. M. da Silva and A. M. Lopes, *J. Adhes.*, 2013, **90**, 104-119.
30. J. C. Moller, R. J. Berry and H. A. Foster, *Polym. J.*, 2020, **12**.
31. K. Horie, H. Hiura, M. Sawada, I. Mita and H. Kambe, *J. Polym. Sci. A. Polym. Chem.*, 1970, **8**, 1357-1372.
32. O. Lunder, F. Lapique, B. Johnsen and K. Nisancioglu, *Int. J. Adhes. Adhes.*, 2004, **24**, 107-117.
33. G. Ceylan, S. Emik, T. Yalcinyuva, E. Sumbuoglu, E. Bozdag and F. Unalan, *Polymers*, 2023, **15**, 2387-2402.
34. P. J. Flory, *J. Am. Chem. Soc.*, 1941, **63**, 3083-3090.
35. P. A. Lovell and R. Young, *Introduction to Polymers*, CRC Press, 3rd edition edn., 2011.

36. G. Moad and D. H. Soloman, *The Chemistry of Radical Polymerization, 2nd Edition*, Elseiver, 2nd edn., 2005.
37. M. J. Gibian and R. C. Corley, *Chem. Rev.*, 1973, **73**, 441-454.
38. J. C. Bevington, H. W. Melville and R. P. Taylor, *J. Polym. Sci.*, 1954, **12**, 449-459.
39. D. Walton and P. Lorimer, *Polymers*, Oxford Science Publishers, Great Britain, 2000.
40. B. O'Shaughnessy, *Macromolecules*, 1994, **27**, 3875-3884.
41. T. J. Tulig and M. Tirrell, *Macromolecules*, 1981, **14**, 1501-1511.
42. H. B. Lee and D. T. Turner, *Macromolecules*, 1977, **10**, 226-231.
43. D. T. Turner, *Macromolecules*, 1977, **10**, 221-226.
44. Y. Suzuki, R. Mishima and A. Matsumoto, *Int. J. Chem. Kinet.*, 2022, **54**, 361-370.
45. J. Chiefari, Y. K. Chong, F. Ercole, J. Krstina, J. Jeffery, T. P. T. Le, R. T. A. Mayadunne, G. F. Meijis, C. L. Moad, G. Moad, E. Rizzardo and S. H. Thang, *Macromolecules*, 1998, **31**, 5559-5562.
46. J. S. Wang and K. Matyjaszewski, *J. Am. Chem. Soc.*, 1995, **117**, 5614-5615.
47. J. Nicolas, Y. Guillaneuf, C. Lefay, D. Bertin, D. Gigmes and B. Charleux, *Prog. Polym. Sci.*, 2013, **38**, 63-235.
48. E. Sprick, J. Becht, B. Graff, J. Salomon, T. Tigges, C. Weber and J. Lalevee, *Dent. Mater.*, 2021, **37**, 382-390.
49. D. S. Achilias and I. D. Sideridou, *Macromolecules*, 2004, **37**, 4254-4265.
50. K. Kangmin, N. R. Singstock, K. K. Childress, J. Sinha, A. M. Salazar, S. N. Whitfield, A. M. Holder, J. W. Stansbury and C. B. Musgrave, *J. Am. Chem. Soc.*, 2019, **141**, 6279-6291.
51. M. P. Patel, M. Braden and K. W. M. Davy, *Biomaterials*, 1987, **8**, 53-56.
52. B. A. M. Venhoven, A. J. De Gee and C. L. Davidson, *Biomaterials*, 1993, **14**, 871-875.
53. C. S. Pfeifer, N. D. Wilson, Z. R. Shelton and J. W. Stansbury, *Polymer*, 2011, **52**, 3295-3303.

54. Y. Kinomoto, M. Torii, F. Takeshige and S. Ebisu, *J. Dent.*, 1999, **27**, 383-389.

55. J. Rychly and J. Pavlinec, *Polym. Degrad. Stab.*, 1990, **28**, 1-15.

56. Y. Hu and C. Chen, *Polym. Degrad. Stab.*, 2003, **82**, 81-88.

57. J. Pavlinec, M. Lazar and I. Janigova, *J. Macromol. Sci. A*, 1997, **34**, 81-90.

58. Y. Suzuki, D. S. Cousins, Y. Shinagawa, R. T. Bell, A. Matsumoto and A. P. Stebner, *Polym. J.*, 2019, **51**, 423-431.

59. T. Kashiwagi, A. Inaba, J. E. Brown, K. Hatada, T. HKitayama and E. Masuda, *Macromolecules*, 1986, **19**, 2160-2168.

60. Y. Hu, C. Chen and C. Wang, *Polym. Degrad. Stab.*, 2004, **84**, 545-553.

61. F. Laoutid, R. Sonnier, D. Francois, L. Bonnaud, N. Cinausero, J. Lopez Cuesta and P. Dubois, *Polym. Adv.*, 2009, **22**, 1713-1719.

62. N. Calderon, H. Y. Chen and K. W. Scott, *Tetrahedron Lett.*, 1967, **34**, 3327-3329.

63. A. K. Chatterjee, T. L. Choi, D. P. Sanders and R. H. Grubbs, *J. Am. Chem. Soc.*, 2002, **125**, 11360-11370.

64. K. B. Wagener, J. M. Boncella and J. G. Nei, *Macromolecules*, 1991, **24**, 2649-2687.

65. O. Fujimura and R. H. Grubbs, *J. Am. Chem. Soc.*, 1996, **118**, 2499-2500.

66. R. H. Grubbs, P. L. Burk and D. D. Carr, *J. Am. Chem. Soc.*, 1975, **97**, 3265-3267.

67. J. L. Herisson and Y. Chauvin, *Macromol. Chem. Phys.*, 1971, **141**, 161-176.

68. J. C. Mol, *J. Mol. Catal. A Chem.*, 2004, **213**, 39-45.

69. P. H. Deshmukh and S. Blechert, *Dalton Trans.*, 2007, 2479-2491.

70. J. S. Murdzek and R. R. Schrock, *Organometallics*, 1987, **6**, 1373-1374.

71. R. R. Schrock, J. S. Murdzek, G. C. Bazan, J. Robbins and M. DiMare, *J. Am. Chem. Soc.*, 1990, **112**, 3875-3886.

72. P. Schwab, M. B. France, J. W. Ziller and R. H. Grubbs, *Angew. Chem. Int. Ed.*, 1995, **34**, 2039-2041.

73. S. T. Nguyen, L. K. Johnson and R. H. Grubbs, *J. Am. Chem. Soc.*, 1992, **114**, 3974-3975.

74. M. S. Sanford, M. Ulman and R. H. Grubbs, *J. Am. Chem. Soc.*, 2001, **123**, 749-750.
75. E. L. Dias, S. T. Nguyen and R. H. Grubbs, *J. Am. Chem. Soc.*, 1997, **119**, 3887-3897.
76. T. L. Brown and K. J. Lee, *Coord. Chem. Rev.*, 1993, **128**, 89-116.
77. T. Weskamp, F. J. Kohl and W. A. Herrmann, *J. Organomet. Chem.*, 1999, **582**, 362-365.
78. M. Scholl, T. M. Trnka, J. P. Morgan and R. H. Grubbs, *Tetrahedron Lett.*, 1999, **40**, 2247-2250.
79. J. Huang, E. D. Stevens, S. P. Nolan and J. L. Peterson, *J. Am. Chem. Soc.*, 1999, **121**, 2674-2678.
80. M. Scholl, S. Ding, C. W. Lee and R. H. Grubbs, *Org. Lett.*, 1999, **1**, 953-956.
81. C. Slugovc, S. Demel and F. Stelzer, *Chem. Commun.*, 2002, 2572-2573.
82. J. A. Love, J. P. Morgan, T. M. Trnka and R. H. Grubbs, *Angew. Chem. Int. Ed.*, 2002, **41**, 4035-4037.
83. S. Maechling, M. Zaja and S. Blechert, *Adv. Synth. Catal.*, 2005, **347**, 1413-1422.
84. V. Forcina, A. García-Domínguez and G. C. Lloyd-Jones, *Faraday Discuss.*, 2019, **220**, 179-195.
85. M. G. Hyatt, D. J. Walsh, R. L. Lord, J. G. Andino Martinez and D. Guironnet, *J. Am. Chem. Soc.*, 2019, **141**, 17918-17925.
86. S. E. Blosch, M. Alaboalirat, C. B. Eades, S. J. Scannelli and J. B. Matson, *Macromolecules*, 2022, **55**, 3522-3532.
87. J. Louie and R. H. Grubbs, *Organometallics*, 2002, **21**, 2153-2164.
88. P. V. R. Schleyer, J. E. Williams and K. R. Blanchard, *J. Am. Chem. Soc.*, 1970, **92**, 2377-2386.
89. A. Hejl, O. A. Scherman and R. H. Grubbs, *Macromolecules*, 2005, **38**, 7214-7218.

90. I. Njoroge, P. A. Kempler, X. Deng, S. T. Arnold and G. K. Jennings, *Langmuir*, 2017, **33**, 13903-13912.

91. T. A. Davidson, K. B. Wagener and D. B. Priddy, *Macromolecules*, 1996, **29**, 786-788.

92. T. A. Davidson and K. B. Wagener, *J. Mol. Catal.*, 1998, **133**, 67-74.

93. Z. Yao, L. W. Zhou, B. B. Dai and K. Cao, *J. Appl. Polym. Sci.*, 2012, **125**, 2489-2493.

94. D. G. Ivanoff, J. Sung, S. M. Butikofer, J. S. Moore and N. R. Sottos, *Macromolecules*, 2020, **53**, 8360-8366.

95. M. R. Kessler and S. R. White, *J. Polym. Chem. A. Polym. Chem.*, 2002, **40**, 2373-2383.

96. R. S. Phatake, A. Masarwa, N. G. Lemcoff and O. Reany, *Polym. Chem.*, 2020, **11**, 1742-1751.

97. X. Liu, X. Sheng, J. K. Lee and M. R. Kessler, *J. Therm. Anal. Calorim.*, 2007, **89**, 453-457.

98. T. R. Long, R. M. Elder, E. D. Bain, K. A. Masser, T. W. Sirk, J. H. Yu, D. B. Knorr and J. L. Lenhart, 2018, **14**, 3344-3360.

99. L. Matejka and C. W. Mascosko, *J. Appl. Polym. Sci.*, 1985, **30**, 2787-2803.

100. L. Matejka and M. C. W., *J. Appl. Polym. Sci.*, 1985, **30**, 2787-2803.

101. T. J. Cuthbert, T. Li and J. E. Wulff, *ACS Polym. Mater.*, 2019, **1**, 2460-2471.

102. H. G. Kim, H. J. Son, D. K. Lee, D. W. Kim, H. J. Park and D. H. Cho, *Korean J. Chem. Eng.*, 2017, **34**, 2099-2109.

103. G. O. Wilson, M. M. Caruso, S. R. Schelkopf, N. R. Sottos, S. R. White and J. S. Moore, *ACS Appl. Mater. Interfaces*, 2011, **3**, 3072-3077.

104. G. O. Wilson, J. S. Moore, S. R. White, N. R. Sottos and H. M. Andersson, *Adv. Funct. Mater.*, 2008, **18**, 44-52.

105. S. R. White, N. R. Sottos, P. H. Geubelle, J. S. Moore, M. R. Kessier, S. R. Sriram, E. N. Brown and S. Viswanathan, *Nature*, 2001, **409**, 794-817.

106. A. J. Boyer, N. T. Tran and D. B. Knorr, *J. Adhes. Sci. Technol.*, 2023, **37**, 1806-1821.

107. J. G. Martin and R. K. Hill, *Chemical Reviews*, 1961, **61**, 537-562.

108. R. Xu, J. N. Jocz, L. K. Wiest, S. C. Sarngadharan, M. Milina, J. S. Coleman, L. L. Iaccino, P. Pollet, C. Sievers and C. L. Liotta, *Ind. Eng. Chem. Res.*, 2019, **58**, 22516-22525.

109. J. Clayden, S. Waren and N. Greeves, *Organic Chemistry*, Oxford University Press, Oxford, 2nd edn., 2012.

110. L. Rulisek, P. Sebek, Z. Havlas, R. Hrabal, P. Capek and A. Svatos, *J. Org. Chem.*, 2005, **70**, 6295-6302.

111. D. Huertas, M. Florscher and V. Dragojlovic, *Green Chem.*, 2009, **11**, 91-95.

112. N. Miyasko, S. Matsuoka and Y. Suzuki, *Macromol. Rapid. Commun.*, 2021, **42**.

113. J. D. Rule and J. S. Moore, *Macromolecules*, 2002, **35**.

114. Y. Nishihara, Y. Inoue, Y. Nakayama, T. Shiono and K. Takagi, *Macromolecules*, 2006, **39**, 7458-7460.

115. Z. M. Dong, X. H. Liu, X. L. Tang and Y. S. Li, *Macromolecules*, 2009, **42**, 4596-4603.

116. M. Kanao, A. Otake, K. Tsuchiya and K. Ogino, *Int. J. Org. Chem.*, 2012, **2**, 26-30.

117. A. Li, M. Jun and K. L. Wooley, *Macromolecules*, 2009, **42**, 5433-5436.

118. G. Zou, A. Zheng, D. Wei, Z. Li, S. Ling, T. Zhang, X. Xu and Y. Guan, *Chin, J. Chem.*, 2018, **36**, 934-938.

119. D. Khandelwal, S. Hooda, A. S. Brar, R. Shankar and *J. Polym. Chem. A. Polym. Chem.*, 2012, **50**, 3350-3362.

120. R. M. E. Schitter, D. Jocham, F. Stelzer, N. Moszner and T. H. Volkel, *J. Appl. Polym. Sci.*, 2000, **78**, 47-60.

121. B. G. Shin, M. S. Jang, D. Y. Toon and W. Heitz, *Macromol. Rapid. Commun.*, 2004, **25**, 728-732.

122. K. Tu, T. Xu, L. Zhang, Z. Cheng and X. Zhu, *RSC Adv.*, 2017, **7**, 24040.

123. K. A. Ogawa, A. E. Goetz and A. J. Boydston, *J. Am. Chem. Soc.*, 2015, **137**, 1400-1403.

124. T. Krappitz, K. Jovic, F. Feist, H. Frisch, V. P. Rigoglioso, J. P. Blinco, A. J. Boydston and C. Barner-Kowollik, *J. Am. Chem. Soc.*, 2019, **141**, 16605-16609.

125. R. F. Ohm and T. M. Vial, *J. Elastomers Plast.* , 1977, **10**, 150-162.

126. S. J. Scannelli, A. Paripati, J. R. Weaver, C. Vu, M. Alaboalirat, D. Troya and J. B. Matson, *Macromolecules*, 2023, **56**, 3848-3856.

127. J. Wang, J. Zhou, L. Fang, J. Sun and Q. Fang, *Mater. Chem. Front.*, 2018, **2**, 1467-1474.

128. B. R. Maughon, T. Morita, C. W. Bielawski and R. H. Grubbs, *Macromolecules*, 2000, **33**, 1929-1935.

129. B. R. Maughon and R. H. Grubbs, *Macromolecules*, 1996, **29**, 5765-5769.

130. A. Kumar, S. Y. Jang, J. Padilla, T. F. Otero and G. A. Sotzing, *Polymer*, 2008, **49**, 3686-3692.

131. C. Cheng and N. Yang, *Macromol. Rapid. Commun.*, 2005, **26**, 1395-1399.

132. C. Detrembleur, C. Jerome, M. Claes, P. Louette and R. Jerome, *Angew. Chem. Int. Ed.*, 2001, **40**, 1268-1271.

133. A. M. M. S. Medeiros, C. Le Coz and E. Grau, *ACS Sustainable Chem. Eng.*, 2020, **8**, 4451-4456.

134. D. J. Liaw, K. L. Wang and W. H. Chen, *Macromol. Symp.*, 2006, **245-246**, 68-76.

135. S. J. Scannelli, M. Alaboalirat, D. Troya and J. B. Matson, *Macromolecules*, 2023, **56**, 3838-3847.

136. S. E. Blosch, S. J. Scannelli, M. Alaboalirat and J. B. Matson, *Macromolecules*, 2022, DOI: 10.1021/acs.macromol.2c00338.

137. M. Naguib, L. K. Nixon and D. J. Keddie, *Polym. Chem.*, 2022, **13**, 1401-1410.

138. N. D. Ogbonna, M. Dearman, C. T. Cho, B. Bharti, A. J. Peters and J. Lawrence, *J. Am. Chem. Soc.*, 2022, **2**, 898-905.

139. S. C. Radzinski, J. C. Foster, R. C. Chapleski, D. Troya and J. B. Matson, *J. Am. Chem. Soc.*, 2016, **138**, 6998-7004.
140. A. B. Chang, T. Lin, N. B. Thompson, S. L. Luo, A. L. Liberman-Martin, H. Chen, B. Lee and R. H. Grubbs, *J. Am. Chem. Soc.*, 2017, **139**, 17683-17693.
141. T. L. Choi and R. H. Grubbs, *Angew. Chem. Int. Ed.*, 2003, **42**, 1743-1746.
142. W. J. Neary and J. G. Kennemur, *Macromolecules*, 2017, **50**, 4935-4941.
143. R. H. Lambeth, S. J. Pederson, M. Baranoski and A. M. Rawlett, *J. Polym. Sci. A. Polym. Chem.*, 2010, **48**, 5752-5757.
144. T. Ando, M. Kamigaito and M. Sawamoto, *Tetrahedron*, 1997, **53**, 15445-15457.
145. T. Ando, M. Kato, M. Kamigaito and M. Sawamoto, *Macromolecules*, 1996, **29**.
146. G. Szczepaniak, K. Urbaniak, C. Wierzbicka, K. Kosiński, K. Skowerski and K. Grela, *ChemSusChem*, 2015, **8**, 4139-4148.
147. R. P. Digby and D. E. Packham, *Int. J. Adhes. Adhes.*, 1995, **15**, 61-71.
148. Y. Li, X. Jia, X. Zhang, Y. Lu and H. Quian, *Soft Matter*, 2022, **19**, 128-136.
149. T. E. Pattern, J. Xia, T. Abernathy and K. Matyjaszewski, *Science*, 1996, **272**, 866-868.
150. W. Jakubowski and K. Matyjaszewski, *Macromolecules*, 2005, **38**, 4139-4146.
151. J. Chen, F. P. Burns, M. G. Moffitt and J. E. Wulff, *ACS Omega*, 2016, **1**, 532-540.
152. S. Saha, Y. Ginzburg, I. Rozenberg, O. Iliashevsky, A. Ben-Asuly and N. Gabriel Lemcoff, *Polym. Chem.*, 2016, **7**, 3071-3075.
153. C. G. Keck, J. L. Kendall and K. C. Caster, *Adv. Synth. Catal.*, 2007, **349**, 165-174.
154. X. Sheng, M. R. Kessler and J. K. Lee, *J. Therm. Anal. Calorim.*, 2007, **89**, 459-464.
155. H. Liu, H. Wei and J. S. Moore, *ACS Macro. Lett.*, 2019, **8**, 846-851.
156. T. J. Cuthbert, T. Li, A. W. H. Speed and J. E. Wulff, *Macromolecules*, 2018, **51**, 2038-2047.
157. J. Chen, B. Kilpatrick, A. G. Oliver and J. E. Wulff, *J. Org. Chem.*, 2015, **80**, 8979-8989.

158. J. Norman, S. C. Moratti, A. T. Slark, D. J. Irvine and A. T. Jackson, *Macromolecules*, 2002, **35**, 8954-8961.

159. V. Coessens and K. Matyjaszewski, *Macromol. Rapid. Commun.*, 1999, **20**, 66-70.

160. Sigma-Aldrich, Thermal Transitions of Homopolymers: Glass Transition & Melting Point, (accessed 8.09, 2023).

161. M. Hilmi Mahmood, Z. Abdullah, Y. Sakurai, K. Zaman and H. Mohd Dahlan, *Radiat. Phys. Chem.*, 2001, **60**, 129-137.

162. D. B. Knorr, K. A. Masser, R. M. Elder, T. W. Sirk, M. D. Hindenlang, J. H. Yu, A. D. Richardson, S. E. Boyd, W. A. Spurgeon and J. L. Lenhart, *Compos. Sci.*, 2015, **114**, 17-25.

163. G. C. Huang, J. K. Lee and M. R. Kessler, *Macromol. Mater. Eng.*, 2011, **296**, 965-972.

164. X. Liu, J. K. Lee, S. H. Yoon and M. R. Kessler, *J. Appl. Polym. Sci.*, 2006, **101**, 1266-1272.

165. J. Barkhimer, M. Erich, G. Nair, S. A. Tunick and K. C. Chen, California Polytechnic State University, 2015.

166. N. L. Reed and T. P. Yoon, *Chem. Soc. Rev.*, 2021, **50**, 2954-2967.

167. K. Ohkubo, K. Mizushima, R. Iwata and S. Fukuzumi, *Chem. Sci.*, 2011, **2**, 715-722.

168. S. Lin, M. A. Ischay, C. G. Fry and T. P. Yoon, *J. Am. Chem. Soc.*, 2011, **133**, 19350-19353.

169. A. E. Goetz, L. M. M. Pascual, D. G. Dunford, K. A. Ogawa, D. B. Knorr and A. J. Boydston, *ACS Macro. Lett.*, 2016, **5**, 579-582.

170. I. Polyzos, G. Tsigaridas, M. Fakis, V. Giannetas and P. Persephonis, *J. Phys. Chem. B*, 2006, **110**, 2593-2597.

171. A. E. Goetz and A. J. Boydston, *J. Am. Chem. Soc.*, 2015, **137**, 7572-7575.

172. P. Lu, N. M. Alrashdi and A. J. Boydston, *J. Polym. Sci. A. Polym. Chem.*, 2017, **55**, 2977-2982.

173. F. Wu, L. Wang, J. Chen, D. A. Nicewicz and Y. Huang, *Angew. Chem. Int. Ed.*, 2018, **57**, 2174–2178.

174. S. Song, Z. Fu and Z. Fan, *Polym. Chem.*, 2017, **8**, 5924-5933.

175. S. I. Subnaik and C. E. Hobbs, *Polym. Chem.*, 2019, **10**, 4524-4528.

176. D. J. Walsh, D. A. Schinski, R. A. Schneider, D. Guironnet and *Nat. Commun.*, 2020, **11**.

177. B. Wenn, M. Conradi, A. Demetrio Carreriras, D. M. Haddleton and T. Junkers, *Polym. Chem.*, 2014, **5**, 3053-3060.

178. J. Van Herck and T. Junkers, *Chemistry Methods*, 2022, **2**, e202100090.

179. M. H. Reis, T. P. Varner and F. A. Leibfarth, *Macromolecules*, 2019, **52**, 3441-3557.

180. M. Li, Y. Zhang, J. Zhang, M. Peng, L. Yan, Z. Tang and Q. Wu, *Ind. Eng. Chem. Res.*, 2021, **60**, 5451-5462.

181. Y. Zhou, Y. Gu, K. Jiang and M. Chen, *Macromolecules*, 2019, **52**, 5611-5617.

182. S. Lu and K. Wang, *React. Chem. Eng.*, 2019, **4**, 1189-1194.

183. J. Song, S. Zhang, K. Wang and Y. Wang, *J. Taiwan Inst. Chem. Eng.*, 2019, **98**, 78-84.

184. A. M. Bello and L. P. Kotra, *Tetrahedron Lett.*, 2003, **44**, 9271-9274.

185. P. K. Bhowmik, C. I. Lee, J. J. Koh, H. Han, A. Jubair, V. Kartazaev and S. K. Gayen, *J. Mol. Struct.*, 2020, **1202**, 127325.

186. M. Martiny, E. Steckhan, T. Esch, M. Martiny, E. Steckhan and T. Esch, *Chem. Ber.*, 1993, **126**, 1671-1682.

187. J. P. Bishop and R. A. Register, *Polymer*, 2010, **51**, 4121-4126.

188. A. J. Perkowski, W. You and D. A. Nicewicz, *J. Am. Chem. Soc.*, 2015, **137**, 7580-7583.

189. M. A. Esteruelas, F. González, J. Herrero, P. Lucio, M. Oliván and B. Ruiz-Labrador, *Polym. Bull.*, 2007, **58**, 923-931.

190. M. Rubens, J. Van Herck and T. Junkers, *ACS Macro. Lett.*, 2019, **8**, 1437-1441.

8. Appendix

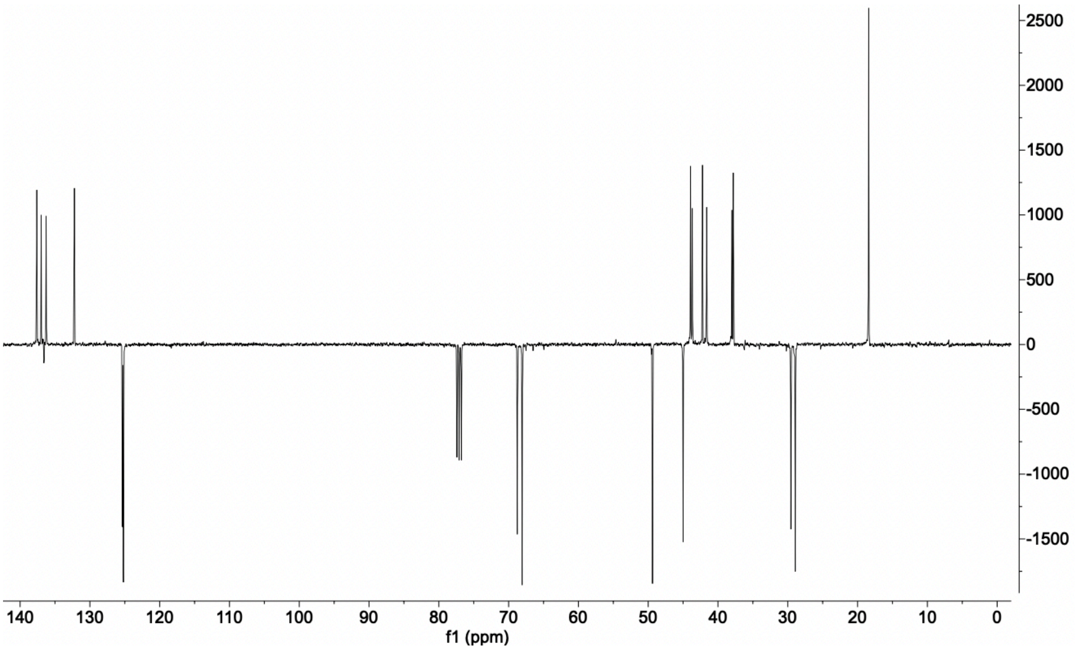

Appendix 1: DEPT ^{13}C NMR of NBMMA ($CDCl_3$)

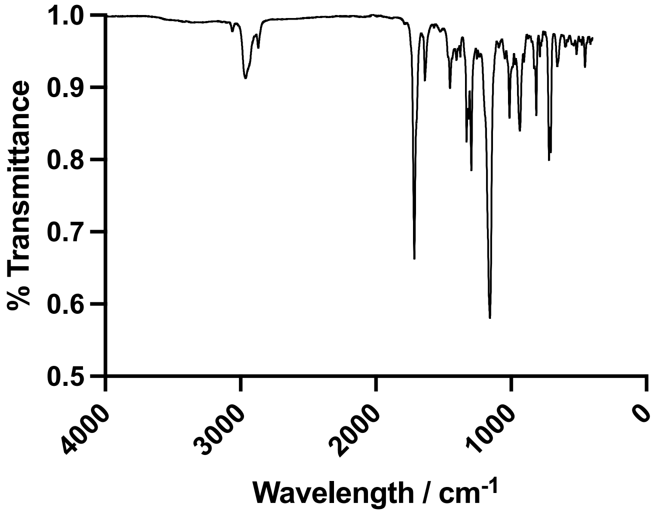

Appendix 2: FTIR of NBMMA

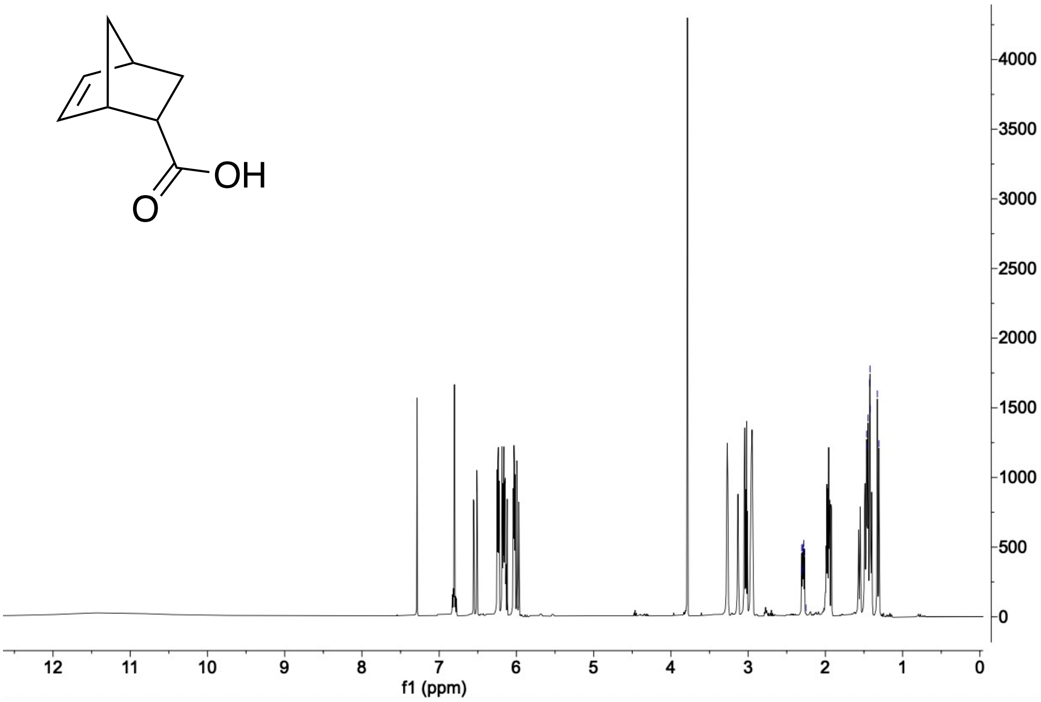

Appendix 3: ^1H NMR of NBOOH ($CDCl_3$)

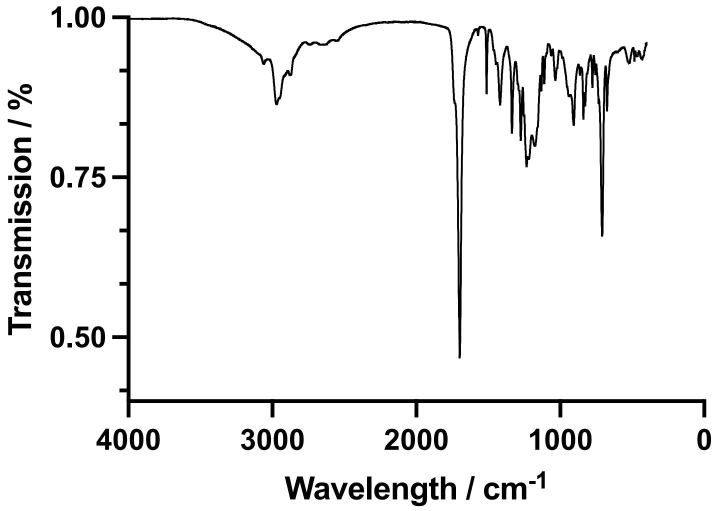

Appendix 4: FTIR of NBOOH

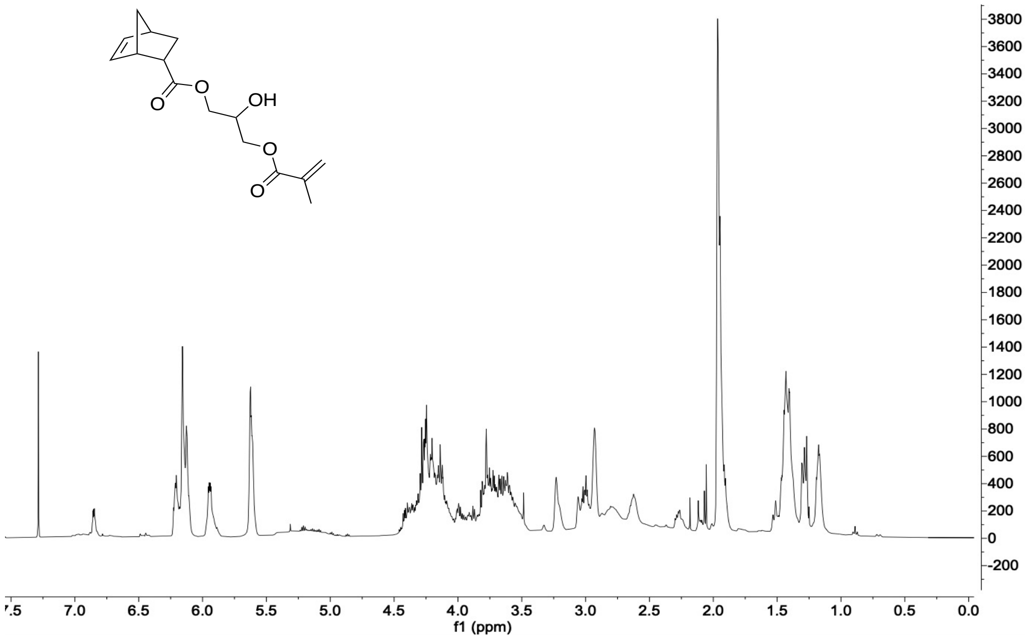

Appendix 5: ^{1}H NMR of NBGMA ($CDCl_3$)

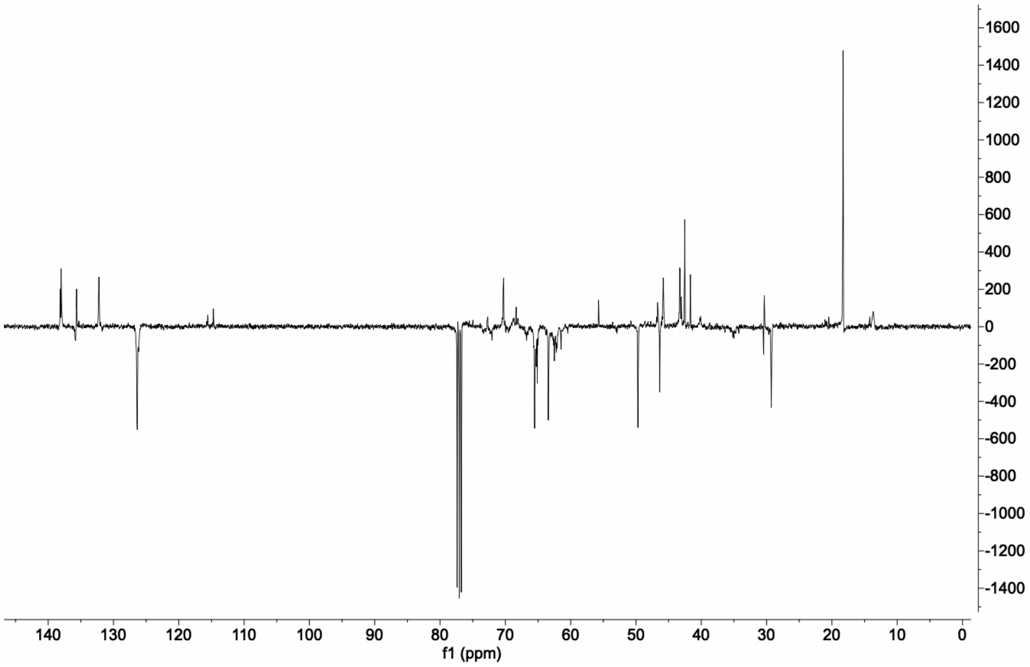

Appendix 6: DEPT ^{13}C NMR of NBGMA ($CDCl_3$)

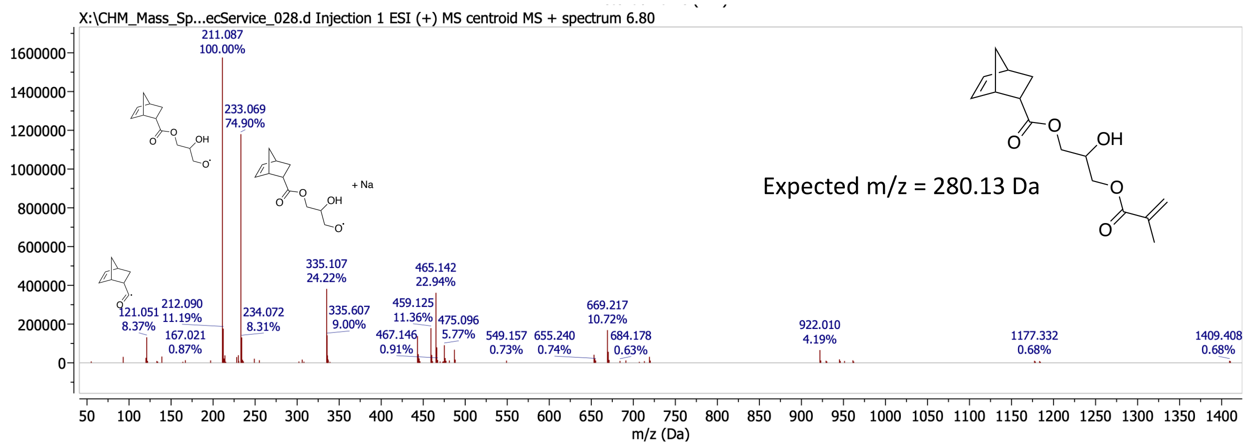

Appendix 7: MS of NBGMA

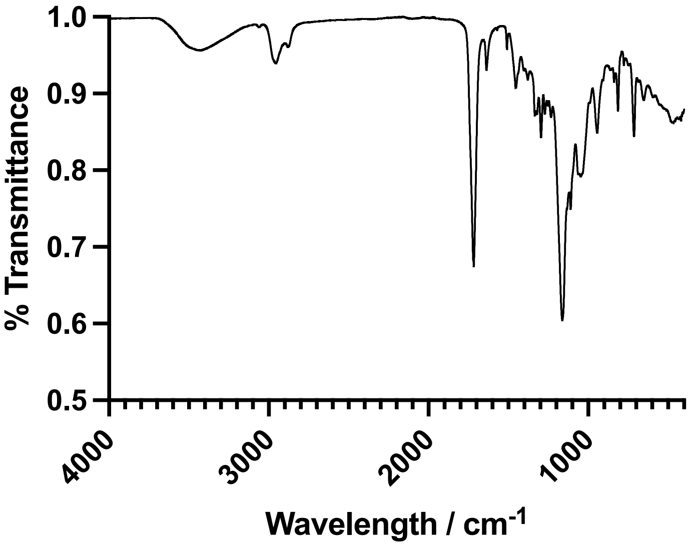

Appendix 8: FTIR of NBGMA

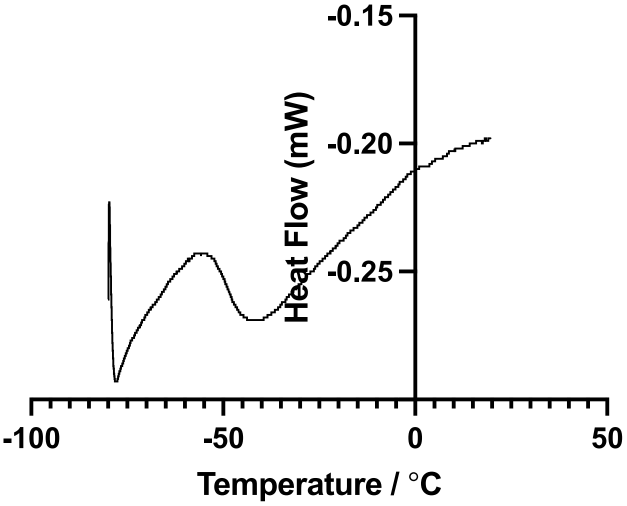

Appendix 9: Melting point of NBGMA

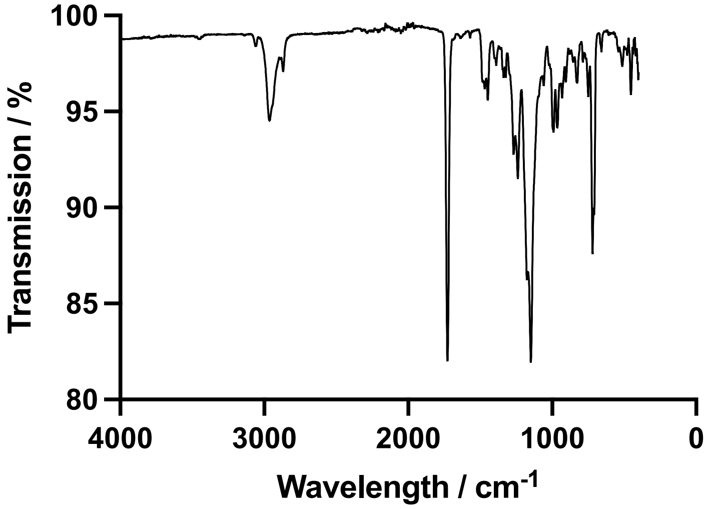

Appendix 10: FTIR of A-PNBMMA

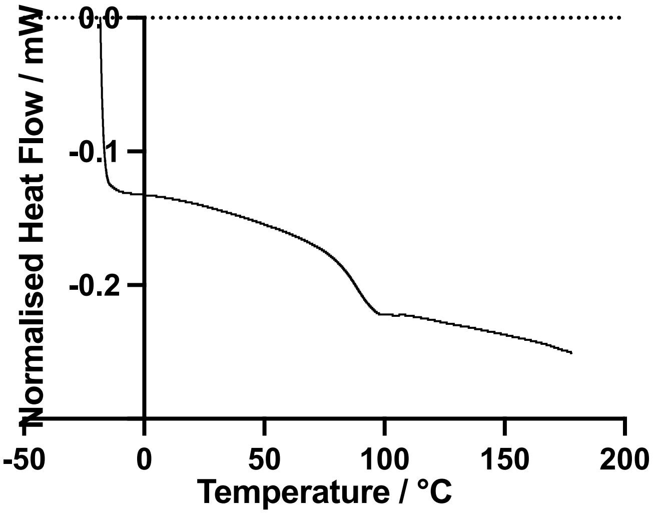

Appendix 11: DSC thermogram to show the *T*$_g$ of A-PNBMMA

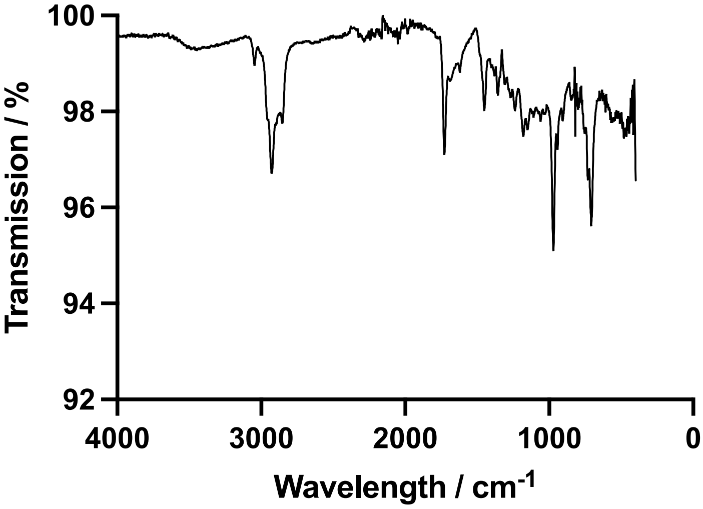

Appendix 12: FTIR of PIBMA

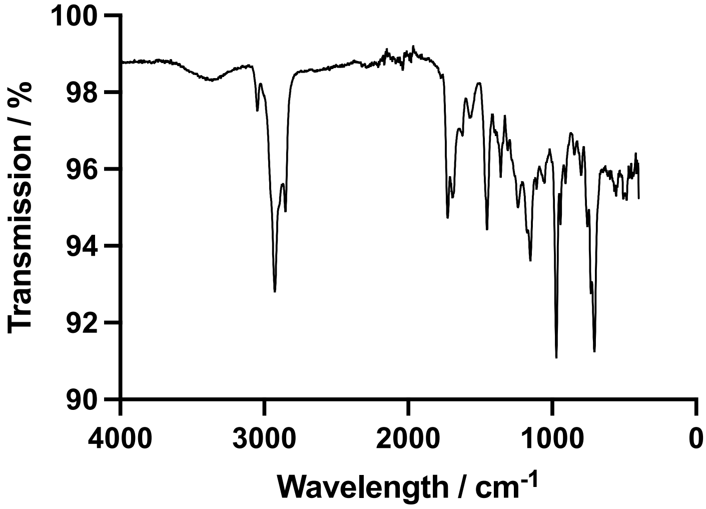

Appendix 13: FTIR of P(IBMA-*co*-NBMMA)

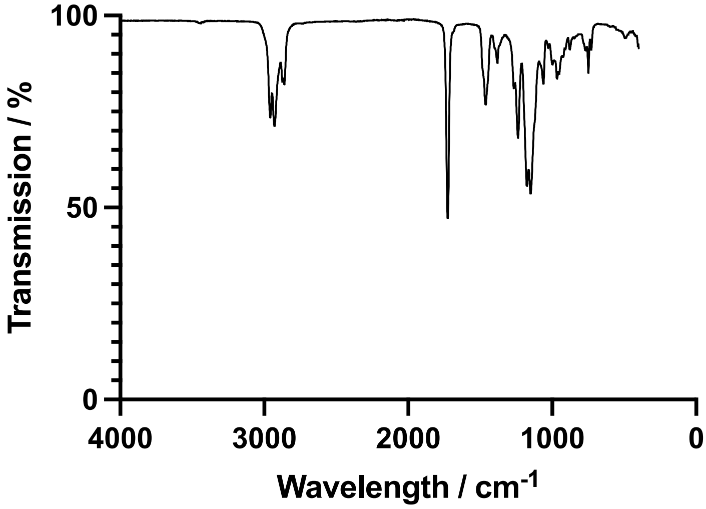

Appendix 14: FTIR of PEHMA

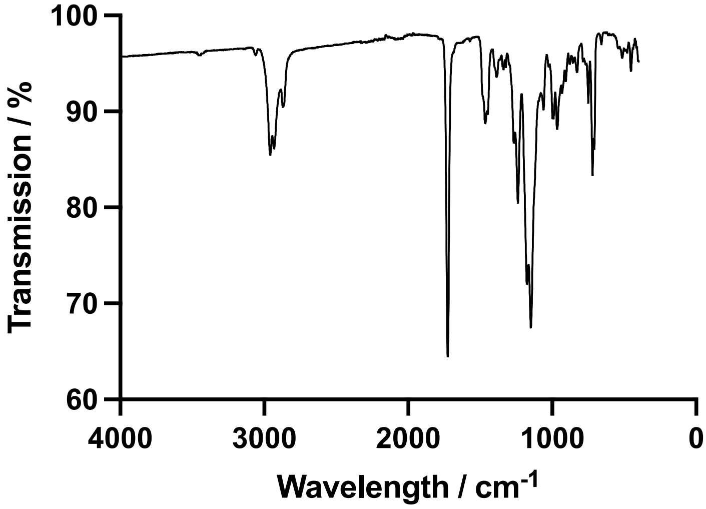

Appendix 15: FTIR of P(EHMA-*co*-NBMMA)

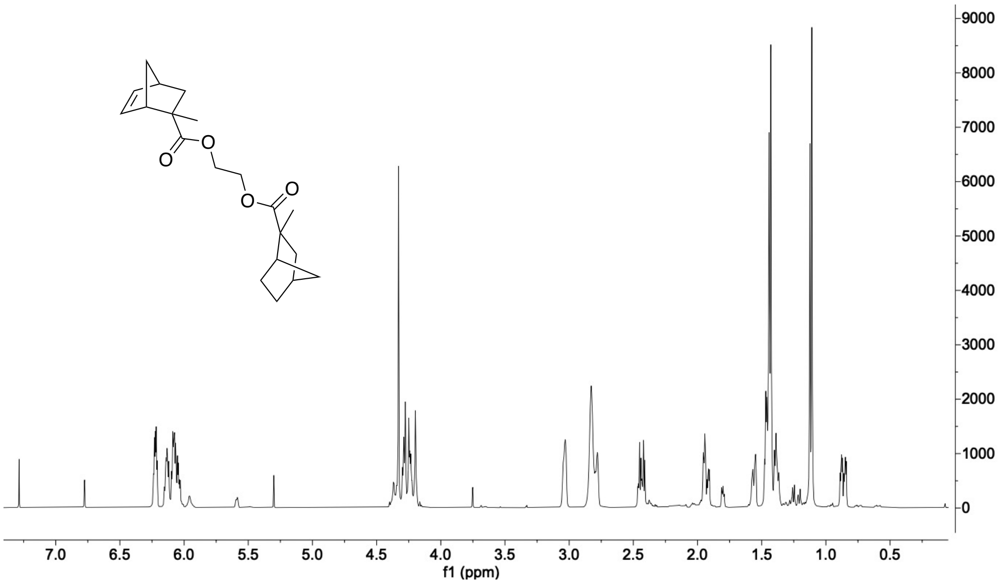

Appendix 16: ^{1}H NMR ($CDCl_3$) of EGDNB (CL2)

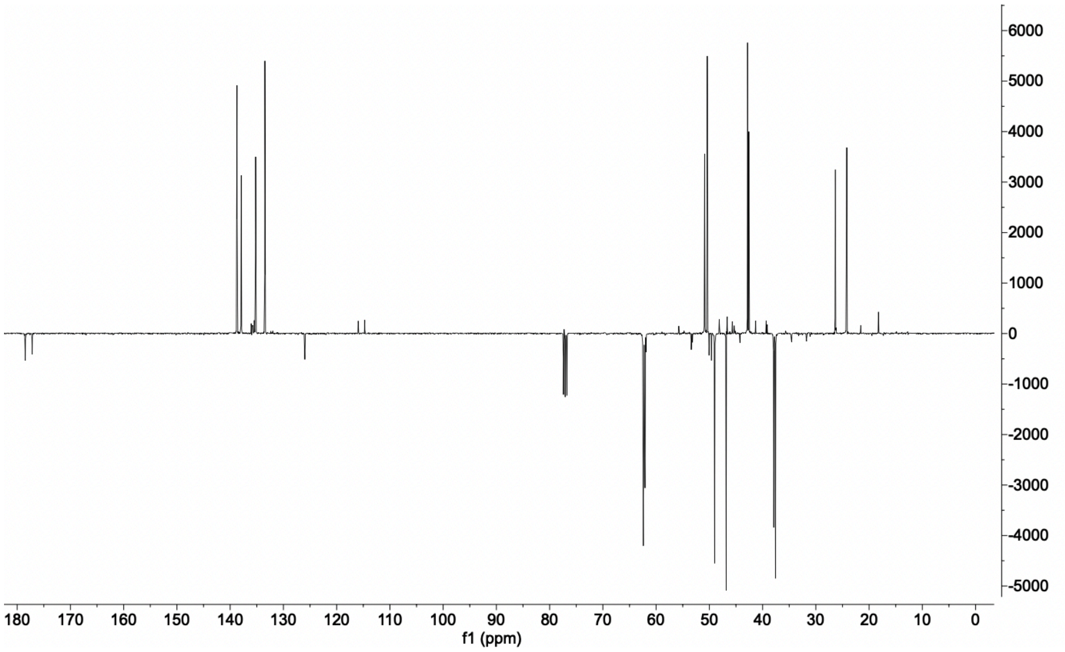

Appendix 17: DEPT ^{13}C NMR ($CDCl_3$) of CL2

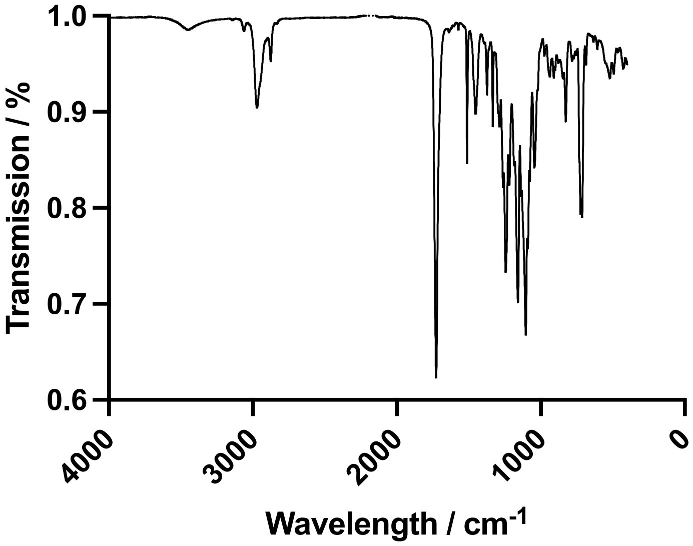

Appendix 18: FTIR spectrum of CL2

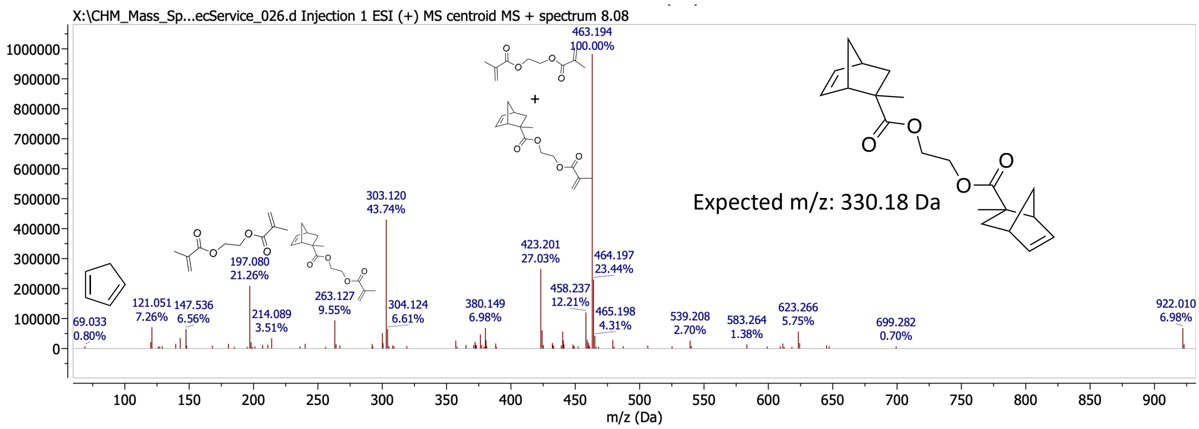

Appendix 19: Mass spectrum of CL2

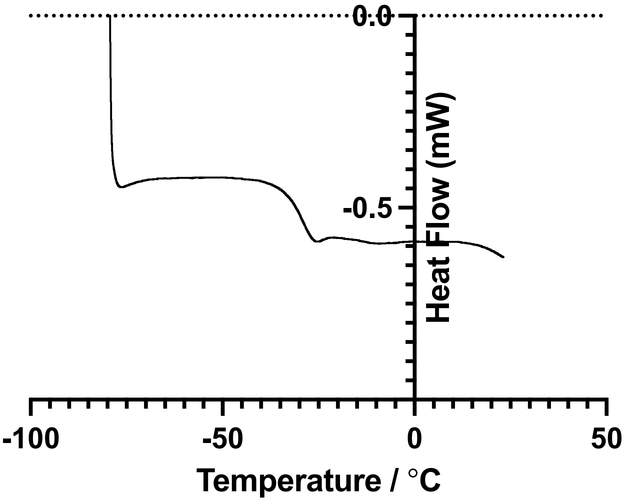

Appendix 20: DSC thermograph of CL2 showing the melting point

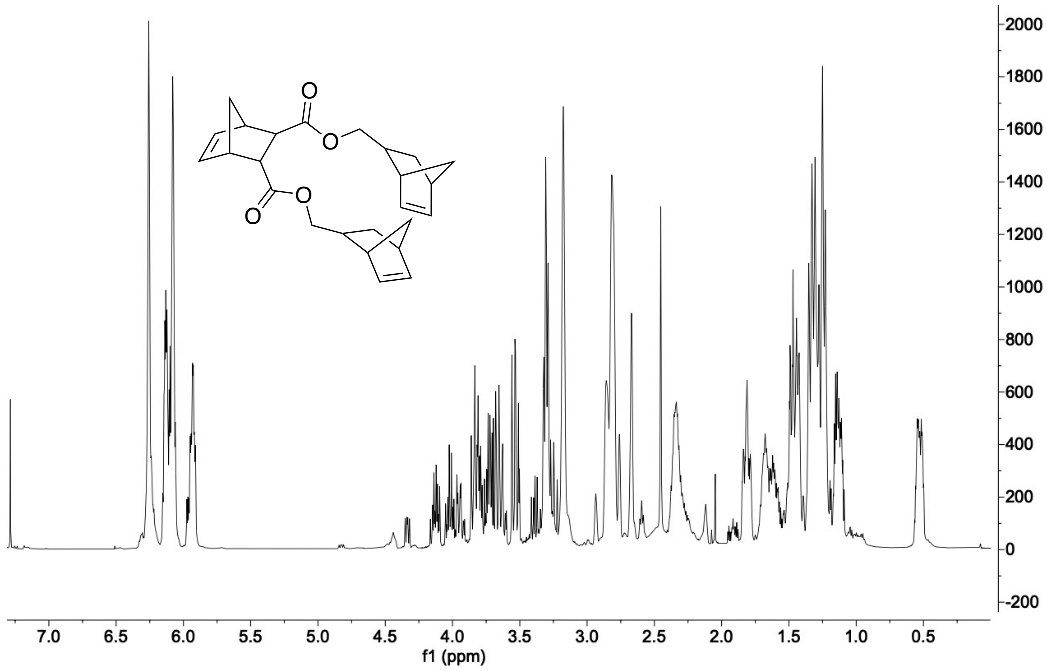

Appendix 21: ^{1}H NMR ($CDCl_3$) of 5-Norbornene,2,3-(di-5-norbornene-2-methanyl) (CL1)

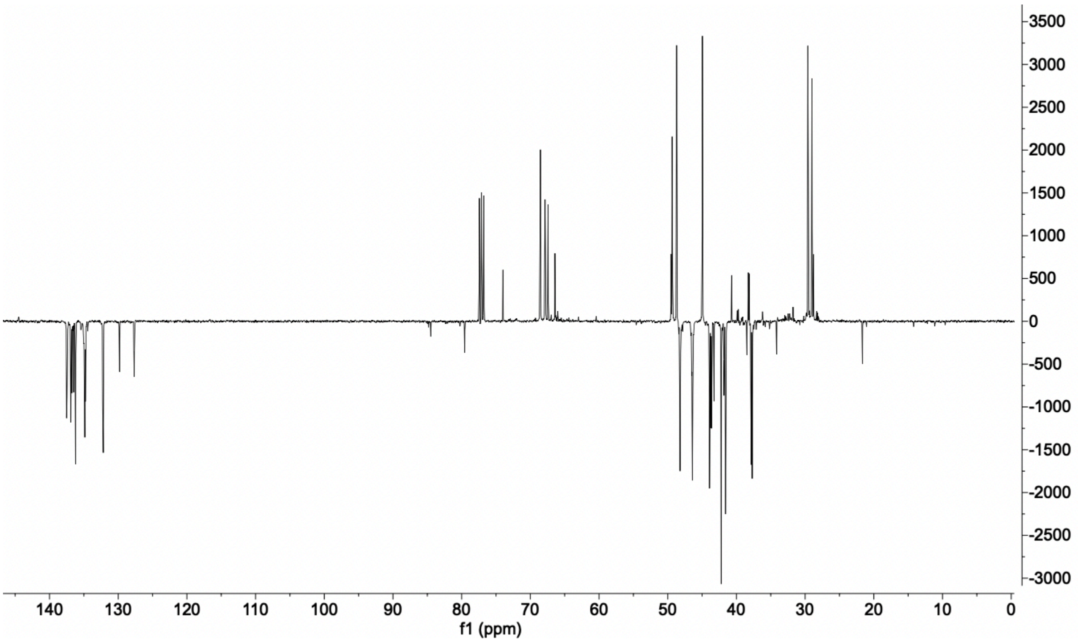

Appendix 22: DEPT^{13}C NMR ($CDCl_3$) of 5-Norbornene,2,3-(di-5-norbornene-2-methanyl) (CL1)

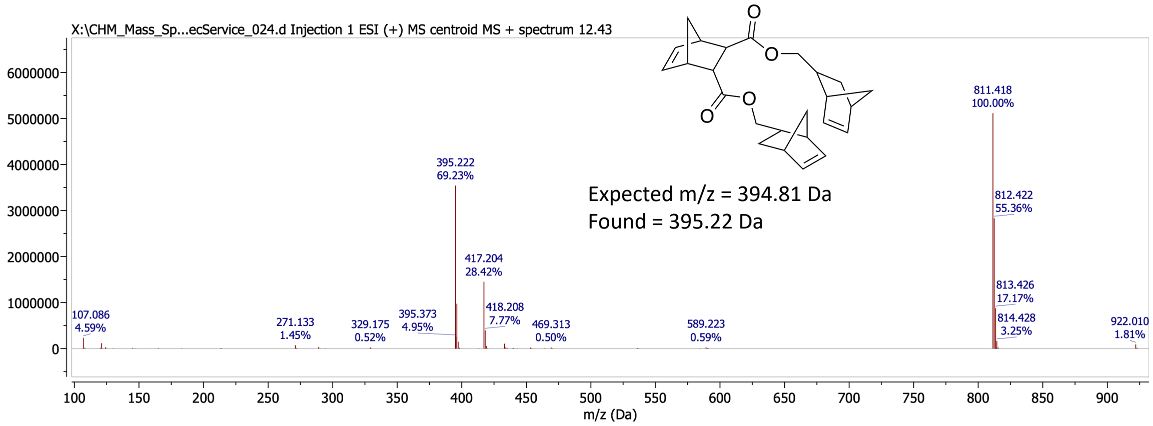

Expected m/z = 394.81 Da
Found = 395.22 Da

Appendix 23: Mass Spec of CL1

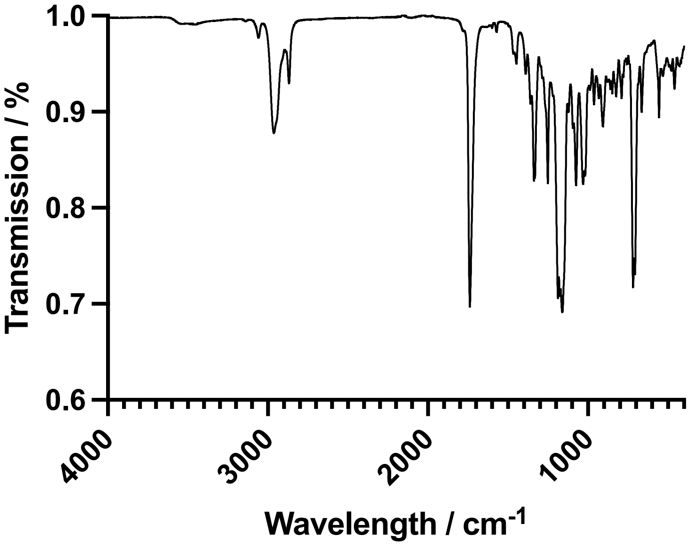

Appendix 24: FTIR of CL1

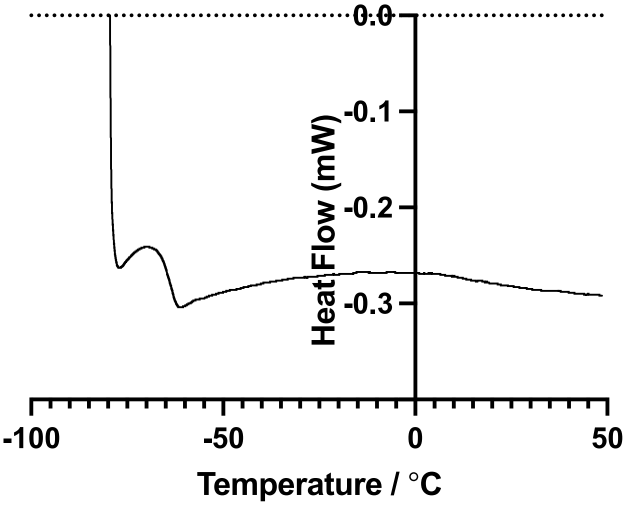

Appendix 25: DSC thermogram showing the melting point of CL1

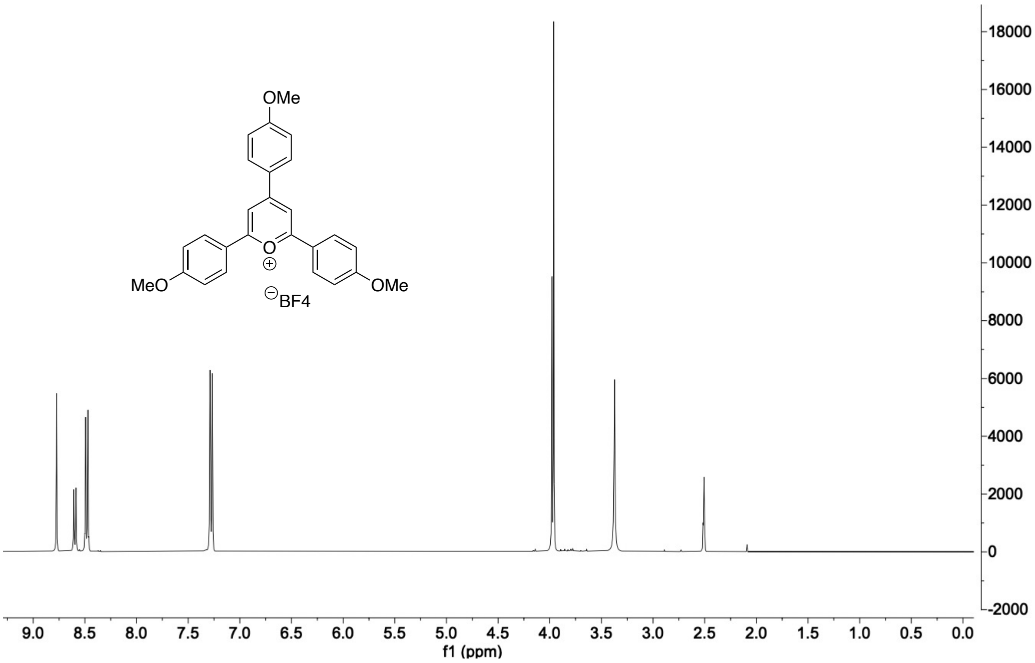

Appendix 26: ^{1}H NMR (DMSO) of *p*OMeTPT

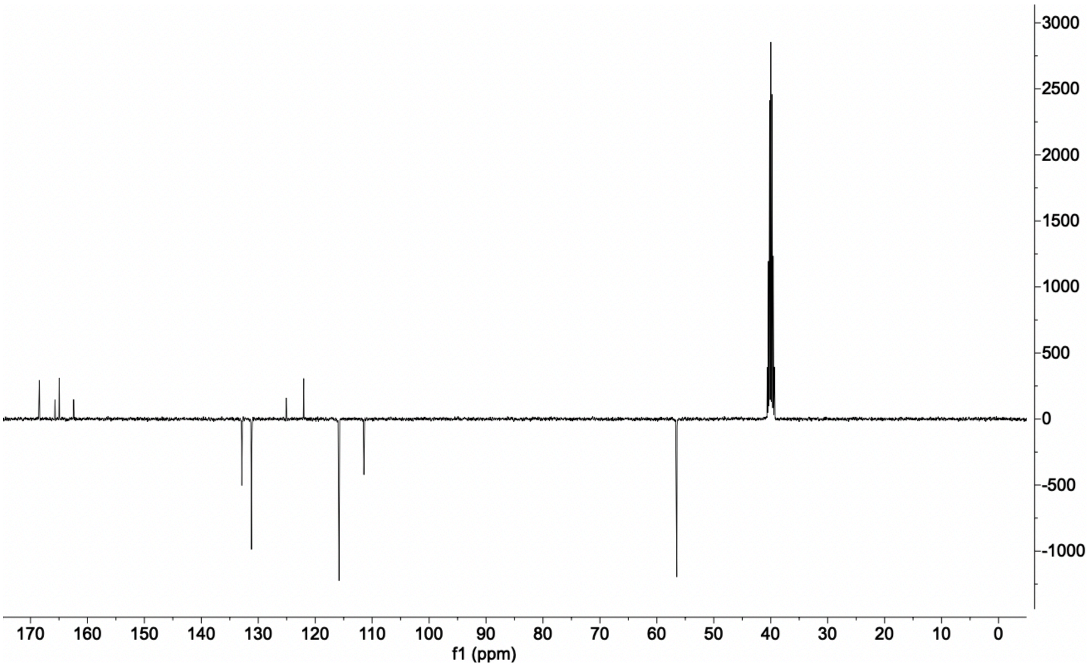

Appendix 27: DEPT ^{13}C NMR (DMSO) of *p*OMeTPT

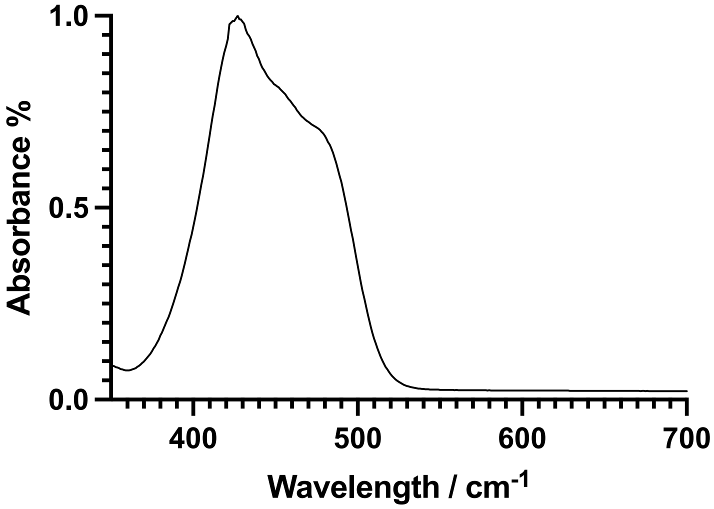

Appendix 28: UV/vis spectrum of *p*OMeTPT

Appendix 29: Hybrid MF-ROMP and radical copolymerisation of NB and MMA under dry air, [a] determined by ^{1}H NMR, [b] determined by SEC, [c] determined by DSC, [d] the yield was too low

Polymer	f_1 **(NB)**	f_2 **(MMA)**	F_1[a]	F_2[a]	**NB Conversion**[a] **/ %**	**MMA Conversion**[a] **/ %**	M_n **/ g mol**$^{-1}$ [b]	M_w **/ g mol**$^{-1}$ [b]	$Đ_M$[b]	T_g[c] **/ °C**
a	100	0	100	-	95.1	-	9890	36700	3.65	40.0
b	90	10	99.7	0.3	79.6	6	19100	31400	1.64	34.0
c	80	20	98.0	2.0	72.2	9.17	14900	27200	2.75	30.4
d	70	30	97.6	2.4	66.3	5.81	10200	25800	2.52	28.0
e	60	40	96.8	3.2	48.9	5.47	9800	21900	2.23	25.3
f	50	50	94.8	5.2	39.3	6.25	5372	17492	3.26	22.9
g	40	60	94.5	5.5	28.3	5.53	4990	10800	2.18	19.0
h	30	70	90.1	9.9	23.0	3.0	5960	9520	1.60	—[d]

Appendix 30: Hybrid MF-ROMP and radical copolymerisation of NB and MMA under dry air, [a] determined by ^{1}H NMR, [b] determined by SEC, [c] determined by DSC

Polymer	f_1 **(NB)**	f_2 **(MMA)**	F_1[a]	F_2[a]	**NB Conversion**[a] **/ %**	**MMA Conversion**[a] **/ %**	M_n **/ g mol**$^{-1}$ [b]	M_w **/ g mol**$^{-1}$ [b]	$Đ_M$[b]	T_g[c]**/ °C**
a	100	0	100	—	48.0	—	9891	36070	3.65	40.1
b	90	10	99.9	0.1	44.1	—	8650	29500	3.41	39.8
c	80	20	99.3	0.7	42.6	2.5	8963	20620	2.30	28.0
d	70	30	99.0	1.0	34.7	2.8	9540	27100	2.94	23.8
e	60	40	97.6	2.4	30.8	3.2	7930	25000	2.89	24.0
f	50	50	92.3	7.7	26.5	7.4	7536	21730	2.88	22.9

Appendix 31: Table to show the effect of the fraction of bifunctional monomer NBMMA on the properties of the copolymer

f_1 (NBE)	f_2 (NBMMA)	ROMP backbone / %	Radical backbone / %	NB *cis* / %	NB *trans* / %	MMA backbone *endo* / %	MMA backbone *exo* / %	Unreacted NB from NBMMA *endo* / %	Unreacted NB from NBMMA *exo* / %	NBMMA with unreacted MMA / %
0.9	0.1	95.7	4.3	21.5	78.5	48.8	51.2	8	18.5	74.5
0.8	0.2	92.0	8.0	22.9	77.1	38.6	61.4	6.1	25.6	70.3
0.7	0.3	87.3	12.7	24.8	75.2	37.1	62.9	5.4	28.6	42.1
0.6	0.4	84.1	15.9	22.3	77.7	54.9	45.1	12.8	36.7	39.8
0.5	0.5	78.5	21.5	22.4	77.6	51.7	48.3	20.8	40.1	29.4
0.4	0.6	61.9	38.1	21.9	78.1	50.5	49.5	21.3	42.0	24.9
0.3	0.7	53.1	46.9	25.0	75.0	49.1	50.9	25	46.4	16.1

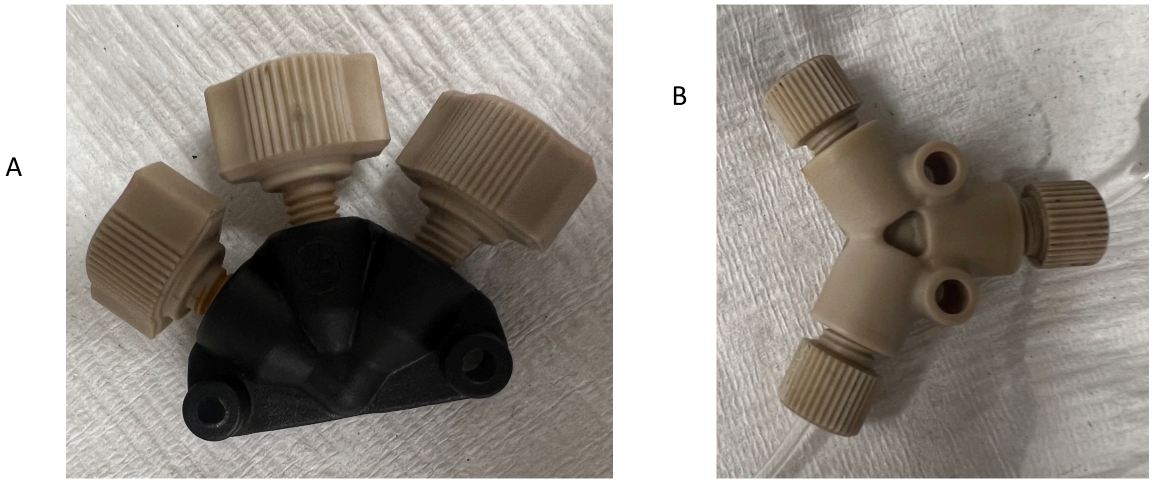

Appendix 32: Photos of the A) ball mixer and B) T-mixer for the MF-ROMP droplet-flow set-up